



**FRIEDRICH-SCHILLER-
UNIVERSITÄT
JENA**

**Inter-kingdom communication in the marine
environment.
Bacterial modulation of growth, sexual reproduction
and biofilm formation of marine microalgae**

Dissertation

zur Erlangung des akademischen Grades doctor rerum naturalium
(Dr. rer. nat.)

vorgelegt dem Rat der Chemisch-Geowissenschaftlichen Fakultät der
Friedrich-Schiller-Universität Jena

von M. Sc. Emilio Cirri
geboren am 22.01.1990 in Florenz (IT)

Gutachter:

1. Prof. Dr. Georg Pohnert
2. Prof. Wim Vyverman
3. Prof. Dr. Maria Mittag

Tag der öffentlichen Verteidigung: 21/08/2019

*To the ones,
who gave and give
love and support
unconditionally*

E' chiaro
Che il pensiero dà fastidio
Anche se chi pensa
E' muto come un pesce
Anzi un pesce
E come pesce è difficile da bloccare
Perchè lo protegge il mare
Com'è profondo il mare

Lucio Dalla – Com'è profondo il mare

Table of Contents

Table of Contents	I
List of Figures	V
List of Tables	IX
Abbreviations	XI
Zusammenfassung	XV
Summary	XV
1. Introduction	1
1.1 Chemical ecology of microalgae.....	1
1.1.1 Pheromones in algae	2
1.1.2 Sexual reproduction and pheromones in diatoms	6
1.1.3 The pheromone system of <i>Seminavis robusta</i>	11
1.2 Chemical interactions between microalgae and bacteria	14
1.2.1 The phycosphere: a marketplace for aquatic microbial interactions.....	14
1.2.2 Metabolic hotspots around algal cells.....	17
1.2.3 Cross-kingdom exchange of resources and its influence on elemental cycling.....	19
1.2.4 Speak to me: signaling and response in bacteria-microalgae interactions.....	21
1.2.5 Inter-kingdom signaling shapes marine microbial communities	24
1.3 Omics techniques in chemical ecology and marine research.....	31
1.3.1 The omics approach in chemical ecology	31
1.3.2 Transcriptomics approaches to study diatoms and other microalgae	33
1.3.3 From genes to molecules: metabolomics in microalgal research.....	35
1.3.4 Two is better than one: metabolomics and transcriptomics integration in microalgal research.....	38
2. Thesis Objective	41
3. Co-cultivation of a diatom with associated bacteria – a metabolomic approach	43
3.1. Introduction.....	43
3.2 Results.....	44
3.2.2 Endometabolome of <i>S. robusta</i> is changing in presence of bacteria	46
3.2.3 Bacteria modulate sexual inducing pheromone (SIP ⁺) from <i>S. robusta</i>	48
3.3 Discussion	49
4. Bacterial modulation of sexual efficiency of the diatom <i>Seminavis robusta</i>	53

4.1	Introduction.....	53
4.2	Results.....	55
4.2.1	Sexual reproduction efficiency of <i>S. robusta</i> in presence and absence of bacteria.....	55
4.2.2	Production of diproline by <i>S. robusta</i> and degradation by bacteria.....	59
4.2.3	Degradation of synthetic diproline by isolated strains.....	60
4.3.	Discussion.....	60
5.	Molecular insights into the bacterial effect on sexual reproduction of <i>S. robusta</i>.....	65
5.1	Introduction.....	65
5.2	Results.....	67
5.2.1	Bacterial exudates do not influence cell cycle arrest during sexual reproduction	67
5.2.2	Bacterial medium does not drastically influence expression of known sexual reproduction genes.....	68
5.2.3	<i>Maribacter</i> sp. causes major transcriptional changes in <i>S. robusta</i>	73
5.2.4	Both bacteria trigger detoxification and oxidative stress responses	79
5.2.5	Comparative metabolomics reflects the different effects of <i>Roseovarius</i> and <i>Maribacter</i>	82
5.2.6	The oxylipin precursor arachidonic acid is produced in response to both bacteria	85
5.3.	Discussion.....	86
6.	From ecology to applied research: effect of bacteria on a commercial microalga	93
6.1.	Introduction.....	93
6.2.	Results.....	95
6.2.1	Growth of <i>Nannochloropsis</i> sp. in co-cultivation with isolated bacteria from <i>S. robusta</i>	95
6.2.2	Bacteria are changing the endometabolome of <i>Nannochloropsis</i> sp.	96
6.2.3	Bacteria isolated from <i>S. robusta</i> enhance biofilm formation of <i>Poseidonocella</i> sp. on <i>Nannochloropsis</i> sp.	100
6.3.	Discussion.....	102
7.	A SPE-based, non-disruptive method to investigate macroalgal surface chemistry	107
7.1	Introduction.....	107
7.2	Results.....	109
7.2.1	Development of the extraction procedure.....	109
7.2.2	Microscopic observation.....	110
7.2.3	UPLC-MS measurements of extracted metabolites	112

7.2.4	Quantification of surface metabolites	112
7.2.5	GC-MS detection of free fatty acids	114
7.4	Discussion	116
8.	Conclusive discussion and perspectives	117
8.1	New methodologies and –omics techniques to study signalling between marine microorganism	117
8.2	Understanding metabolic interactions between microalgae and bacteria	120
8.3	Physiological and molecular insights into the bacterial effect on sexual reproduction of diatoms.....	122
8.4	From nature to application: microalgae-bacteria interactions in biotechnology	125
9.	Materials and methods	127
9.1.	Strains and growth conditions.....	127
9.1.1	Strains and general culture conditions	127
9.2.	Co-cultivation of microalgae with isolated bacteria – a metabolomic approach: materials and methods.....	129
9.2.1.	Growth of <i>S. robusta</i> in co-cultivations with isolated bacteria.....	129
9.2.2.	Sample preparation for endo- and pheromone analysis of <i>S. robusta</i>	130
9.2.3.	Endometabolite extraction, derivatization and GC-HR-MS measurements	131
9.2.4.	GC-HR-MS data analysis	132
9.2.5.	SIP ⁺ extraction and UHPLC-HR-MS targeted analysis.....	133
9.3.	Bacterial modulation of sexual efficiency of the diatom <i>Seminavis robusta</i> : materials and methods.....	134
9.3.1.	Bioassay to determine the influence of bacteria on sexual reproduction of <i>S. robusta</i>	134
9.3.2.	Targeted analysis of degradation of natural diproline	134
9.3.3.	Degradation of synthetic diproline by isolated bacterial strains	135
9.3.4.	GC-MS measurements of diproline	136
9.3.5.	Data analysis, statistics and quantification	136
9.4	Molecular insights into bacterial effect on sexual reproduction of <i>Seminavis robusta</i> : materials and methods.....	137
9.4.1	Cultivation of <i>S. robusta</i> and associated bacteria	137
9.4.2	Harvesting of MT ⁺ medium.....	137
9.4.3	Induction of sexuality in <i>S. robusta</i> and treatment with bacterial medium	138
9.4.4	Cell harvesting for RNA extraction	138
9.4.5	Cell cycle analysis using flow cytometry	139

9.4.6	RNA extraction and quality assessment.....	139
9.4.7	RNA sequencing and transcriptomic analysis	140
9.4.8	Exometabolome extraction	142
9.4.9	UHPLC-MS measurements	142
9.4.10	LC-HR-MS data analysis.....	143
9.4.11	Oxylipins measurements.....	144
9.5.	From ecology to applied research: effect of bacteria on a commercial microalga: materials and methods	145
9.5.1.	<i>Nannochloropsis</i> sp. cultivation and co-cultivation with isolated bacteria from <i>S. robusta</i>	145
9.5.2.	Sample preparation for endometabolomics of <i>Nannochloropsis</i> sp.....	146
9.5.3.	Extraction, derivatization, GC-HR-MS measurements and data analysis	146
9.5.4.	<i>Nannochloropsis</i> sp. biofilm formation assay.....	146
9.6.	A SPE based non-disruptive method to investigate macroalgal surface chemistry: materials and methods	147
9.6.1.	Materials	147
9.6.2.	Method development	147
9.6.3.	UPLC-MS measurements	148
9.6.4.	Calibration curve for UPLC-MS measurements.....	149
9.6.5.	GC-MS measurements.....	149
References		XXIV
Appendix		LXVII
Acknowledgments		LXXXV
Curriculum vitae		XCI
Selbstständigkeitserklärung		XCIV

List of Figures

Figure 1: Algae tree of life.....	2
Figure 2: Bombykol.	2
Figure 3: Pheromones from brown and green algae.	6
Figure 4: Structure of diatom cell walls.....	7
Figure 5: Diatom mitosis (a) and life cycle (b) of a centric (<i>Thalassiosira punctigera</i> , on the left) and a pennate diatom (<i>Seminavis robusta</i> , on the right).	8
Figure 6: Sexual life cycle of a centric (<i>Thalassiosira pseudonana</i> , top) and a pennate diatom (<i>Pseudo-nitzschia multistriata</i> , bottom).	9
Figure 7: <i>Seminavis robusta</i> life cycle.....	11
Figure 8: Microalgae-bacteria interactions and their effects on the biogeochemical cycle.	15
Figure 9: Molecules exchange in microalgae-bacteria interactions.	18
Figure 10: Interaction network between a diatom (<i>Pseudo-Nitzschia multiseriata</i>) and a bacterium (<i>Sulfitobacter sp.</i>).....	22
Figure 11: System biology workflow.....	32
Figure 12: Illumina® sequencing by synthesis (SBS) technology.....	34
Figure 13: Untargeted metabolomics workflow.....	37
Figure 14: Co-cultivation of a diatom with associated bacteria – a metabolomics approach: experimental setup.	44
Figure 15: <i>S. robusta</i> growth curve in presence of <i>Croceibacter sp.</i> (a), <i>Maribacter sp.</i> (b) and <i>Roseovarius sp.</i> (c).	45
Figure 16: PCA plot of bacterial effect on <i>S. robusta</i> endometabolome.	46
Figure 17: PCA loadings plots for <i>S. robusta</i> axenic cultures vs co-cultivations with <i>Roseovarius</i> (a) and <i>Maribacter</i> (b).	47
Figure 18: Heatmaps of <i>S. robusta</i> axenic cultures vs co-cultivations with <i>Roseovarius</i> (a) and <i>Maribacter</i> (b). t-Test, $\alpha=0.05$	47
Figure 19: SIP+ degradation by the bacteria isolated <i>S. robusta</i>	48
Figure 20: Target diproline analysis: general experimental setup.....	53
Figure 21: Sexual efficiency bioassay: general experimental setup	54

Figure 22. Mating efficiency of <i>S. robusta</i> in presence of different bacteria at different optical densities (OD).....	57
Figure 23. Mating efficiency of <i>S. robusta</i> in the presence of spent medium of different bacteria.....	58
Figure 24. Diproline degradation by the microbial community associated to <i>S. robusta</i>	59
Figure 25. Degradation of synthetic diproline by bacteria isolated from <i>S. robusta</i>	60
Figure 26. Molecular insights into bacterial effect on sexual reproduction of <i>Seminavis robusta</i> : experimental setup.....	65
Figure 27: Cell cycle arrest measurements.....	67
Figure 28: Multi-dimensional scaling plot for transcriptomic data.	69
Figure 29: Venn diagrams of up- (a) and downregulated (b) <i>S. robusta</i> genes under SIP+ influence.	69
Figure 30: Venn diagrams of up- (a and c) and downregulated (b and d) <i>S. robusta</i> genes under bacterial influence.	74
Figure 31: PCA of exometabolome samples of SIP+-induced cultures and bacteria spent medium.....	83
Figure 32: Heatmaps of up- and downregulated <i>S. robusta</i> exometabolites in presence or absence of <i>Maribacter</i> spent medium after subtraction of <i>Maribacter</i> sp. features	84
Figure 33: Heatmaps of up- and downregulated <i>S. robusta</i> exometabolites in presence or absence of <i>Maribacter</i> spent medium and up- and downregulated exometabolites from <i>Maribacter</i> sp.	85
Figure 34: a) Arachidonic acid (AA) and b) diproline relative concentration.	86
Figure 35: Overview of metabolic changes in <i>S. robusta</i> when exposed to SIP+ and <i>Maribacter</i> sp. exudates.	91
Figure 36: Experimental design of biofilm formation of <i>Nannochloropsis</i> sp. in presence of different bacteria.	95
Figure 37: <i>Nannochloropsis</i> sp. growth curves.....	96
Figure 38: PCA plot of bacterial effect on <i>Nannochloropsis</i> endometabolome.....	98
Figure 39: Heatmaps of <i>Nannochloropsis</i> endometabolites abundance under different treatments.	99
Figure 40: Biofilm formation of <i>Nannochloropsis</i> sp. in presence of different bacteria.....	101

Figure 41: Schematic workflow of the C18 method.....	109
Figure 42: Evaluation of surface damage by different extraction methods.....	108
Figure 43: Quantification of extracted compounds from macroalgae.....	114
Figure 44: GC-MS run of a C18 extract of <i>F. vesiculosus</i> performed with the C18 method and with MeOH as elution solvent.	115
Figure S1. a) Axenic culture b) non-axenic culture of <i>S. robusta</i> 5 days after inoculation.....	LXXII
Figure S2. Assessment of axenicity with agar plates	LXXII
Figure S3. Assessment of axenicity via flow cytometry	LXXIII
Figure S4: Mean-difference plot of log₂ fold change versus the average log₂-count per millions in different comparisons of different treatments.....	LXXI
Figure S5: Venn diagrams of up- (a and b) and downregulated (b and c) <i>S. robusta</i> genes under bacterial influence.....	LXXI
Figure S6: PCA of exometabolome samples of SIP⁺-induced cultures and bacteria spent medium.....	LXXII
Figure S7: PCA of exometabolome samples of non-induced cultures and bacteria spent medium.....	LXXII
Figure S8: Heatmaps of up- and downregulated exometabolites from <i>Maribacter</i> sp. spent medium and <i>Roseovarius</i> sp. spent medium.	LXXIII
Figure S9: Microscopic prove of non-distruptive effect of C18 material on <i>Caulerpa taxifolia</i> surface.	LXXXI
Figure S10: GC/MS profiles of C18 material (non endcapped) blank a) before and b) after conditioning with eluting solvent.	LXXXI
Figure S11: GC/MS profiles of silica Gel 100. a) blank b) extract of <i>Fucus vesiculosus</i>.	LXXXII
Figure S12: GC/MS profiles of silica Gel 90.....	LXXXII

List of Tables

Box 1: Chemical communication glossary.....	3
Box 2: Sexual reproduction glossary.....	10
Box 3: Algae-bacteria interactions glossary	16
Table 1: Example of signaling molecules and exchanged nutrients in aquatic microbial communities.....	30
Box 4: -Omics glossary	31
Table 2: Summary of the differentially expressed genes in different comparisons.....	68
Table 3: Upregulated pathways shared by all SIP⁺-induced cultures compared to non-induced controls (SIP vs C, SIP+M vs M, SIP+R vs R).....	72
Table 4: Upregulated genes involved in sexual reproduction and diproline production shared by all SIP⁺-induced cultures compared to non-induced controls (SIP vs C, SIP+M vs M, SIP+R vs R).	72
Table 5: Upregulated pathways induced by <i>Maribacter sp.</i> medium in SIP⁺-induced cultures (SIP+M vs SIP).	75
Table 6: Downregulated pathways shared by control and SIP⁺-induced cultures treated with <i>Maribacter sp.</i> medium (SIP+M vs SIP, M vs C).	76
Table 7: Downregulated pathways in SIP⁺-induced cultures treated with <i>Maribacter sp.</i> medium (SIP+M vs SIP).	77
Table 8: Upregulated pathways elicited by bacterial medium in SIP⁺-induced cultures (SIP+M vs SIP, SIP+R vs R).	81
ST1: Statistical evaluation of the bacterial effect on <i>S. robusta</i> sexual reproduction efficiency.....	LXIX
ST2: Statistical evaluation of bacterial medium effect on <i>S. robusta</i> sexual reproduction efficiency.....	LXX
ST3: Downregulated pathways shared by all SIP⁺-induced cultures compared to non-induced controls (SIP vs C, SIP+M vs M, SIP+R vs R).	LXXIV
ST4: Upregulated pathways elicited by <i>Roseovarius sp.</i> medium in SIP⁺-induced cultures (SIP+R vs SIP).	LXXV
ST5: Downregulated pathways triggered by <i>Roseovarius sp.</i> medium in SIP⁺-induced cultures (SIP+R vs SIP).	LXXV

ST6: Upregulated genes elicited by <i>Maribacter</i> sp. medium in SIP⁺-induced cultures (SIP+M vs SIP, SIP+R vs R).....	LXXVII
ST7: Upregulated genes elicited by <i>Roseovarius</i> sp. medium in SIP⁺-induced cultures (SIP+R vs SIP).....	LXXVIII
ST8: Upregulated genes elicited by bacterial medium in SIP⁺-induced cultures (SIP+M vs SIP, SIP+R vs R).....	LXXIX
ST9: Downregulated genes elicited by <i>Maribacter</i> sp. medium in SIP⁺-induced cultures (SIP+M vs SIP).	LXXX

Abbreviations

15-HETE	Hydroxyeicosatetraenoic acid
AA	arachidonic acid
ACG	automatic gain control
AHL	N-acyl homoserine lactone
ANOVA	analysis of variance
cAMP/cGMP	cyclic adenine/guanosine monophosphate
CCN	cloud condensation nuclei
CPM	counts-per-million
CV	coefficient of variation
DC	direct current
DE	differential expression
DHPS	2,3-dihydroxypropane-1-sulfonate
DKP	diketopiperazine
DMS	dimethylsulfide
DMSP	dimethylsulfoniopropionate
DNA	deoxyribonucleic acid
DOC	dissolved organic carbon
EI	electron impact
EPI	enhanced product ion scan
EPS	exopolymeric substances
ESI	electrospray ionization
FAME	fatty acid methyl ester
FCP	fucoxanthin-chlorophyll a-c binding proteins
FDR	false discovery rate
FMN	flavin mononucleotide
FT-ICR	Fourier transform ion cyclotron resonance
FWHM	full width at half maximum
GABA	γ -aminobutyric acid
GC	gas chromatography

GLM	generalized linear model
GO	gene ontology
GSEA	gene set enrichment approach
GST	glutathione S-transferase
GTA	gene transfer agent
HET	(4-methyl-5-(β -hydroxyethyl)thiazole)
HMP	(4-amino-5-hydroxymethyl-2-methylpyrimidine)
HPLC	high pressure liquid chromatography
HRSM	High-Resolution mass spectrometry
IAA	indole-3-acetic acid
IAM	indole-3-acetamide
IDA	information dependent acquisition
IS	internal standard
LFC	log fold-change
LHC	light harvesting complex
LRR	leucine rich repeat
LTQ	linear triple quadrupole
MDS	multidimensional scaling
MRM	multiple reaction monitoring
MS	mass spectrometry
MT	mating type
NGS	next generation sequencing
NMR	nuclear magnetic resonance
NO	nitric oxide
NPQ	non-photochemical quenching
OD	optical density
OPR	12-oxophytodienoate reductase
PAM	Pulse-Amplitude-Modulation
PBR	closed photobioreactor
PCA	principal component analysis
PDE	phosphodiesterase

Ppm	part per million
PR-IP	protoplast-release-inducing pheromone
QC	quality control
QS	quorum sensing
RF	radio frequency
RNA	ribonucleic acid
ROS	reactive oxygen species
SIP	sexual inducing pheromone
SPE	solid phase extraction
SPME	solid phase microextraction
SST	sexual size threshold
TAM	tryptamine
TCA	tricarboxylic acid cycle
TMM	trimmed mean of M-values
ToF	time of flight
UHPLC	ultra-high pressure liquid chromatography

Zusammenfassung

Mikroalgen, und insbesondere Kieselalgen, spielen eine grundlegende ökologische Rolle und haben ein breites Feld von industriellen und technologischen Anwendungen.

In den letzten Jahren hat sich die Forschung in der chemischen Ökologie und Biotechnologie auf molekulare Mechanismen, die die Wechselwirkung zwischen Algen und Bakterien regulieren, fokussiert. Die Beziehungen zwischen Algen und Bakterien beeinflussen das Leben von beiden interagierenden Organismen. Sie bestimmen damit die Dynamik von mikrobiellen Gemeinschaften, welche wiederum die globalen Elementzyklen und das Nahrungsnetz in den Meeren beeinflussen. Darüber hinaus ist das Verständnis dieser Wechselwirkungen auch für angewandte Forschung wichtig geworden, beispielsweise zur Verbesserung der Biomassequalität und -Produktivität in Algenreaktoren oder zur Stabilisierung von Artengemeinschaften und zur Verringerung des Biofouling.

Diese Dissertation untersucht die bakterielle Beeinflussung der sexuellen Fortpflanzung der pennaten Modelldiatomee *Seminavis robusta* durch die Verwendung verschiedener Techniken, wie physiologische Bioassays, mit GC/LC-MS durchgeführte gezielte chemische Analysen und einen kombinierten Metabolomics-Transcriptomics-Ansatz. Außerdem wird beschrieben, wie Bakterien sich auf das Wachstum und den Metabolismus von *S. robusta* und einer weiteren, wirtschaftlich relevanten Mikroalge (die ölhaltige Eustigmatales *Nannochloropsis* sp.), sowie auf die Biofilmbildung in einem Bioreaktor auswirken. Weiterhin entwickelte ich eine neue, zerstörungsfreie Methode für die Extraktion von primär- und Sekundärmetaboliten von Algenoberflächen.

Gezielte Analysen mittels GC-MS zeigten, dass die mit *S. robusta* Paarungstyp $\bar{}$ (MT $\bar{}$) assoziierten Bakterien das von der Kieselalge produzierte Attraktionspheromon (Diprolin) innerhalb von 24 Stunden nach der Freisetzung abbauen. Falls keine andere Kohlenstoffquelle zur Verfügung stand konnte für vier, aus *S. robusta* Kulturen isolierten Bakterien (*Croceibacter* sp., *Roseovarius* sp., *Marinobacter* sp. und *Maribacter* sp.) der Pheromonabbau dokumentiert werden. Interessanterweise zeigten diese Bakterien verschiedene Einflüsse auf die sexuelle Fortpflanzung von Diatomeen. Ich beobachtete die Entwicklung von unterschiedlichen sexuellen Zellphasen nach der Paarung der zwei Paarungstypen und ich konnte beobachten, dass der Prozentsatz der Zellen, die sich sexuell fortpflanzen, von *Maribacter* sp. stark reduziert wurde, während der Anteil der Paare in Gegenwart von *Roseovarius* sp. etwas erhöht war. Dieser Effekt wurde selbst dann

beobachtet, wenn nur das überstehende bakterielle Medium verwendet wurde, was klar die Beteiligung chemischer Signale zeigt. Zusätzlich reduzierten *Roseovarius* sp. und insbesondere *Maribacter* sp. die von *Seminavis robusta* MT⁺ produzierte sex-induzierende Pheromone (SIP⁺)-Konzentration.

Motiviert durch diese Ergebnisse führte ich ein komplexes Experiment durch, um die molekularen Gründe hinter diese Bakterien / Algen Interaktion aufzuklären. Axenischen MT⁻-Kulturen, sowohl sexuell induziert als auch nicht induziert, wurden unter verschiedenen Bedingungen inkubiert (axenisch, mit verbrauchtem Medium von *Maribacter* sp. und mit verbrauchtem Medium von *Roseovarius* sp.). Ich verwendete einen kombinierten Metabolomics-Transcriptomics-Ansatz sowie physiologische Bioassays, um die Auswirkungen der abgegebenen bakteriellen Metabolite auf sexuell induzierte *S. robusta* zu untersuchen. Durchflusszytometrie-Experimente zeigten, dass bakterielle Exsudate keinen Einfluss auf den Zellzyklus in SIP⁺-induzierten MT⁻-Zellen haben, und Transcriptomics-Daten zeigten, dass Bakterien den Wechsel von Mitose zu Meiose nicht beeinträchtigen. Bakteriell verbrauchtes Medium löst allerdings eine Oxidative Stressreaktion in Diatomeen aus, die zur Produktion von Fettsäuren und Oxylipinen als Abwehrmetaboliten führen kann. *Maribacter* sp. hat von allen getesteten Bakterien den größten Einfluss sowohl auf die Proteinexpression als auch auf die Metabolitenabgabe: die bakteriellen Exometabolite wirken sich auf die Photosysteme von *S. robusta* aus und beeinflussen den Sterol-, Fettsäure- und vor allem der Aminosäuremetabolismus. Die gleichzeitige Reduktion von Diprolin Abgabe von MT⁻ Zellen, die *Maribacter* sp. Medium ausgesetzt waren, stützt die Hypothese, dass der Einfluss von Aminosäurebiosynthesewegen den Pool des Prolins, das an der Diprolinsynthese beteiligt ist, verändert und somit indirekt die sexuelle Vermehrung beeinträchtigen kann. Diese Ergebnisse stellen eine neuartige Wechselbeziehung zwischen Algen und Bakterien dar.

Neben der Untersuchung der Auswirkungen von Bakterien auf die sexuelle Fortpflanzung von Kieselalgen, erforschte ich auch deren Einfluss auf das Wachstum und die metabolische Aktivität von *S. robusta*. *Roseovarius* sp. unterstützte das Diatomeenwachstum, während *Croceibacter* sp. und *Maribacter* sp. im Vergleich zur axenischen Kontrolle keine signifikante Wirkung zeigten. Alle Bakterien leiteten eine Hochregulierung der Produktion von Aminosäuren und Disacchariden und eine Verringerung von Squalen, Alditolen und einfachen Zuckern ein. *Roseovarius* sp. führte zu einer Verringerung der Konzentration von Tocopherol und vergrößerte die Produktion von Arabinose.

In Zusammenarbeit mit einem belgischen Privatunternehmen (Proviron®) wurde mit dem gleichen Ansatz der Effekt der Bakterien aus *Seminavis robusta* auf eine andere, kommerziell relevante Mikroalge, den ölhaltigen Eustigmatophyten *Nannochloropsis* sp., untersucht. Im Gegensatz zu den bereits vorgestellten Ergebnissen, verbesserte *Maribacter* sp. das Wachstum der Mikroalge stärker als *Roseovarius* sp., während *Poseidonocella* sp., ein biofilm induzierendes Bakterium, welches aus einer *Nannochloropsis* sp. Bioreaktorprobe isoliert wurde nur einen kleinen Einfluss auf das *Nannochloropsis* Wachstum zeigte.

Maribacter sp. und *Roseovarius* sp. beeinflussten außerdem das Metabolom der Mikroalge, so kam es zu einer Verringerung der intrazellulären Konzentration von Tocopherol und mehreren Aminosäuren und zu einer Erhöhung der Konzentration von Sterolen und insbesondere von Stressmarkern wie Spermidin und Putrescin.

Außerdem wurde die Einwirkung von Bakterien auf die Biofilmbildung, eine nicht erwünschte Nebenerscheinung in geschlossenen, nicht-axenischen Bioreaktoren für Algenkultivierung, geprüft. *Roseovarius* sp. und *Maribacter* sp. induzierten keine Biofilmentwicklung, aber ihre Kombination mit dem biofilmbildenden Bakterium *Poseidonocella* sp. erhöhte bezeichnenderweise den Biofilm im Vergleich mit der Kontrolle. Diese Erkenntnisse sind wichtig, um die herausragende Bedeutung der Algen-Bakterien-Kommunikation unter der Perspektive der Algenkultivierung und -produktion zu verstehen. Diese könnte den Einsatz von mikrobiologischen Gemeinschaften mit erhöhter Produktivität in Bioreaktoren fördern.

Schließlich entwickelte ich eine neue Technik, um Metaboliten von Algenoberflächen zu extrahieren. Die Moleküle, die aus Algen freigesetzt werden, prägen die Wechselwirkungen mit anderen Organismen, aber die bisher entwickelten Methoden (wie die „Dipping-Methode“) verletzen häufig die Oberfläche der Algen, was zu einer unbeabsichtigten Freisetzung von Endometaboliten führt. Ich habe die Festphasenextraktion (SPE) angewendet, um eine zerstörungsfreie Methode zu entwickeln, die nur ausgeschiedene Metaboliten erfasst. Durch das Aufbringen von einem C18-SPE-Extraktionsmaterial auf die Oberfläche der Braunalge *Fucus vesiculosus*, das folgende Waschen und die Extraktion des SPE Materials konnte ich mehrere Fettsäuren und Fucoxanthin, ein Pigment mit Antifouling-Eigenschaften, reproduzierbar extrahieren. Das Verfahren wurde auch erfolgreich auf die Oberflächenextraktion der Grünalge *Caulerpa taxifolia* und der Rotalge *Gracilaria vermiculophylla* angewendet. Das zeigt das breite Potenzial der Technik zeigt, die leicht auf andere feuchte Oberflächen, z.B. mit Biofilmen bedeckte Felsen, Korallen oder Schwämme,

angewendet werden kann, um Metaboliten, die eine wichtige Rolle bei chemisch vermittelten Interaktionen, zu extrahieren.

Die Ergebnisse dieser Doktorarbeit zeigen neue Erkenntnisse in dem relativ jungen Gebiet der Mikroalgen-Bakterien-Wechselwirkungen, indem verschiedene Ansätze (-omische Techniken, physiologische Bioassays, innovative analytische Verfahren) in einen breiten interdisziplinären Ansatz angewendet und miteinander verknüpft wurden.

Summary

Microalgae, and especially diatoms, have a fundamental ecological role and they have also a broad range of industrial applications.

In recent years, chemical ecology and biotechnology have started to focus on the molecular mechanisms behind the inter-kingdom communication between microalgae and bacteria. These interactions influence the life of both interacting organisms and shape community dynamics, which can, in turn, affect global elemental cycling and the marine food web. Furthermore, the understanding of this communication has become important for applied research, for example to improve biomass quality and productivity or to stabilize communities and reduce biofouling.

This thesis focuses on the effect of bacteria on the sexual reproduction of the model pennate diatom *Seminavis robusta* using different techniques, such as physiological bioassays, targeted chemical analysis and a combined metabolomics-transcriptomics approach. In addition, the effect of bacteria on the growth and the metabolism of *S. robusta* was tested. A metabolomics approach was used to investigate the impact of bacteria on the metabolism of an economically important microalga, the oleaginous estigmatophyte *Nannochloropsis* sp. The bacteria were also tested in a bioassay to study if they can induce biofilm in a bioreactor. Finally, I have developed a new, non-disruptive method for extracting primary and secondary metabolites released from algal surfaces, which could be applied for aqueous biofilms as well as for other wet surfaces.

Targeted analysis performed with GC-MS demonstrates that the bacterial community associated to *S. robusta* mating type $-$ (MT $-$) is able to degrade the diatom's attraction pheromone diproline during the 24h after its release. Four bacteria isolated from *S. robusta* MT $+$ cultures (*Croceibacter* sp., *Roseovarius* sp., *Marinobacter* sp. and *Maribacter* sp.) consume diproline, but only when they do not have any other carbon source available. Interestingly, these bacteria have different effects on the sexual efficiency of the diatom. I followed the development of different sexual stages after mating of the two MT and I could see that in the presence of *Maribacter* sp. the percentage of cells undergoing sexual reproduction was reduced, while in the presence of *Roseovarius* sp. it was slightly increased. This effect was observed even when only spent medium of the bacteria was present, thus showing that excreted molecules are involved as signals. *Roseovarius* sp. and especially *Maribacter* sp. reduce also the concentration of sexual inducing pheromone (SIP $+$) produced by *S. robusta* MT $+$.

I set up a complex experiment to elucidate the molecular reasons behind the observed bacteria / alga interaction. Axenic cultures of MT⁻, both sexually induced and not, were incubated in different conditions (axenic, with spent medium from *Maribacter* sp. and with spent medium from *Roseovarius* sp.). I used a combined metabolomics-transcriptomics approach, as well as physiological assays and targeted analysis, to understand the impact of bacterial-derived exuded metabolites on sexually-induced *S. robusta*. Flow cytometry experiments showed that bacterial exudates do not have any effect on cell cycle arrest in SIP⁺-induced MT⁻ and transcriptomics data demonstrated that they do not interfere with the switch from mitosis to meiosis. However, bacterial spent medium triggers an oxidative stress response in diatoms, which may involve fatty acids and oxylipins as mediators of defensive mechanisms. *Maribacter* sp. has the higher impact on both transcriptomic expression and metabolites released by the diatom if compared to the control. The bacterial exudates are affecting diatoms' photosystems and causing a rewiring of the biosynthetic pathways that lead to sterols, fatty acids and especially amino acids synthesis. The concomitant reduction of diproline in the medium of MT⁻ cells exposed to *Maribacter* sp. medium supports the hypothesis that the influence of amino acid biosynthetic pathways may alter the pool of proline, a molecule believed to be involved in diproline synthesis. This could reduce diproline levels, thus indirectly interfering with the sexual reproduction cycle. These results introduce a novel inter-kingdom interaction mechanism that can raise new, interesting questions about the life cycle of marine benthic organisms.

Besides studying the effect of bacteria on sexual reproduction, I studied their influence on the growth and metabolic response of *Seminavis robusta* to bacterial presence. *Roseovarius* sp. strongly supports diatom growth, while *Croceibacter* sp. and *Maribacter* sp. do not significantly affect *S. robusta* growth if compared to axenic controls. All of the tested bacteria induce an upregulation of amino acid and disaccharides production and a reduction of squalene, alditols and simple sugars. *Roseovarius* sp. also reduces the concentration of tocopherol and increases the production of arabinose.

In collaboration with a private company from Belgium (Proviron®), I used a metabolomics approach to study the effect of bacteria from *S. robusta* on a different, commercially relevant microalga, the oleaginous eustigmatophyte *Nannochloropsis* sp. In contrast to what observed in diatom-bacteria co-cultivations, *Maribacter* sp. sustains the growth of the microalga better than *Roseovarius* sp., while *Poseidonocella* sp., a bacterium isolated from a bioreactor sample able to induce biofilms, only slightly increases *Nannochloropsis* sp. growth. Bacteria affect *Nannochloropsis* sp. metabolome, reducing the endocellular concentration of

tocopherol and several amino-acids, and increasing the concentration of sterols and stress markers, like spermidine and putrescine. I also tested the influence of bacteria on biofilm formation, an undesired effect of algal cultivation in closed, non-axenic bioreactors. *Roseovarius* sp. and *Maribacter* sp. do not induce biofilm formation, but their combination with the biofilm forming bacterium *Poseidonocella* sp. increases significantly this phenomenon. These results are important to understand the relevance of inter-kingdom communications under the perspective of algal cultivation and production, and can contribute to the engineering of communities that can increase productivity.

To monitor exudation of metabolites that might play a role in chemical communication in the water, I developed a new technique to extract metabolites from algal surfaces. Molecules released from algae shape the interaction with other organism, but methods currently employed (like the “dipping” method) often wound the surface cells of algae, leading to an accidental release of endometabolites. I applied the principle of solid phase extraction (SPE) to create a non-disruptive method to obtain only exuded metabolites. By powdering the surface of the brown alga *Fucus vesiculosus* with a C18 SPE extraction powder and subsequently washing and extracting it, I was able to reproducibly extract several fatty acids and fucoxanthin, a pigment with antifouling properties. The method was successfully applied to the green alga *Caulerpa taxifolia* and the red alga *Gracilaria vermiculophylla*, demonstrating the broad potential of the technique which could be easily applied to other wet surfaces, e.g. rock covered with biofilms, corals or sponges, to extract metabolites that play a role in inter-species interactions.

The results of this thesis introduce knowledge in the relatively young field of microalgae-bacteria interactions by applying and connecting several different approaches (-omics techniques, physiological bioassays, innovative chemical techniques), a broad interdisciplinary methodology that is becoming crucial in both the fields of chemical ecology and of applied biotechnology.

1. Introduction

1.1 Chemical ecology of microalgae

The study and understanding of natural products that are mediating interactions among organisms and their environment is the core interest of chemical ecology (Bergström, 2007). Understanding chemical communication is a complex and fascinating field of research that strongly interconnects biology, chemistry and physics: organisms require a sophisticated biological machinery to produce and recognize many different molecules, from DNA to RNA, proteins and smaller metabolites, which are released into the environment and can therefore mediate interactions with the surroundings. The study of this complexity presents many theoretical and technological challenges, which depend on both the organisms that are studied and the environment in which they live (Schulz, Kubanek and Piel, 2015). The comprehension of chemical communication is not only important for ecological reasons, but it has motivated huge investments in applied research, for example to develop strategies for pest control (Cook, Khan and Pickett, 2007; Begg *et al.*, 2017), conservation biology (Leal, 2017) or antibiotic production (Van der Meij *et al.*, 2017). In the last years, marine chemical ecology provided a fundamental contribution to this research, as explained in many extensive and insightful reviews (Paul and Ritson-Williams, 2008; Paul, Ritson-Williams and Sharp, 2011; Blunt *et al.*, 2013; Schwarzer *et al.*, 2016), and algae play a key role in this field (Amsler, 2008). This polyphyletic group comprises diverse eukaryotic, photoautotrophic as well as some mixotrophic organisms, both unicellular and multicellular, from different taxa that live in water (Figure 1). Due to their high abundance in aquatic ecosystems, they are major global primary producers (Longhurst *et al.*, 1995) and they influence biogeochemical cycles (Andreae, 1990; Falkowski, 1994). In addition to their ecological role, algae have attracted more and more attention from the industrial sector because of their high nutritional value both for animal feeding and human nutrition (Brown, 2002; Duarte *et al.*, 2009; Loureiro, Gachon and Rebours, 2015), for their potential in biofuels production (Jones and Mayfield, 2012) and high value compounds (Chew *et al.*, 2017). Studying algal life cycles and algal natural products is therefore of great importance for ecological and applied purposes. In this framework, research on algal pheromones play a pivotal role, presenting stimulating challenges and opportunities to expand the knowledge in aquatic chemical ecology research.

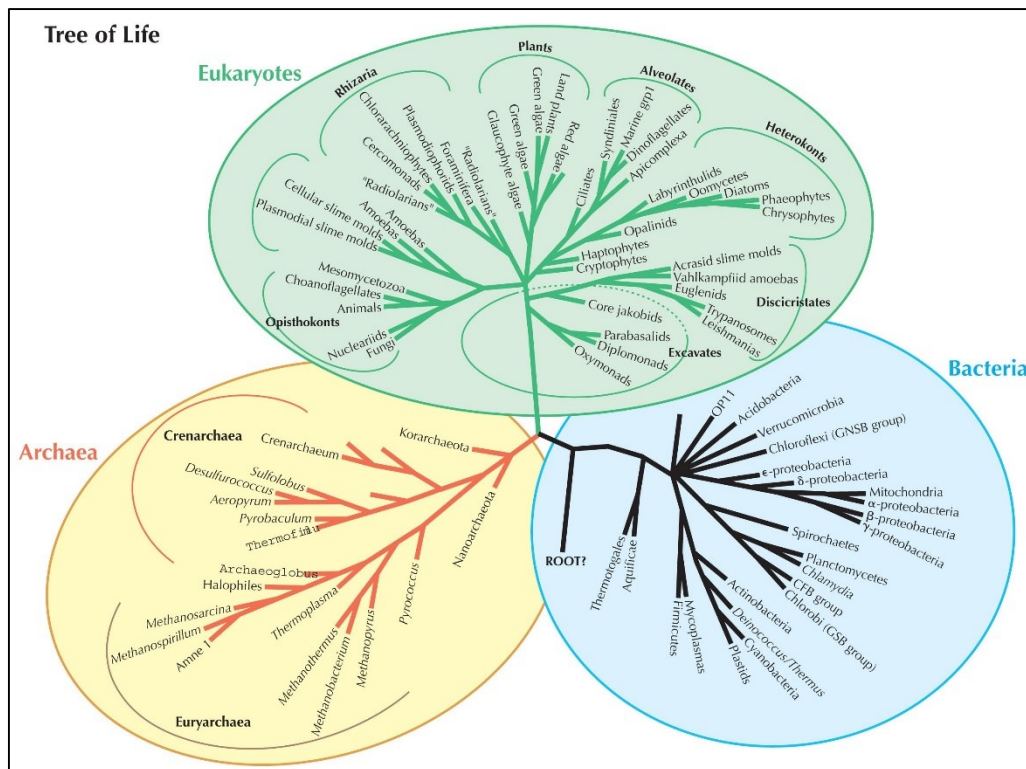


Figure 1: Algae tree of life. (Barton *et al.*, 2007).

1.1.1. Pheromones in algae

The interest in chemical communication between organisms has a long history (Fabre, 1918), but if we have to find a birthdate for chemical ecology, that would be 1959. In this year, Adolf Butenandt, a pioneer in human hormone research, published the identification of bombykol, the mate attractant chemical compound from the female silk moth, *Bombyx mori* (Figure 2). After 20 years of research, extraction of up to 500'000 specimens by classical organic methods, chemical synthesis of geometrical isomers, and behaviour experiments, his research group was able to confirm the structure of the molecule to be (10*E*,12*Z*)-10,12-Hexadecadiene-1-ol.

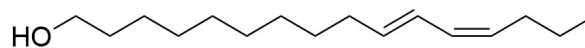


Figure 2: Bombykol. The first identified sex pheromone extracted from the female silk moth *Bombyx mori* (Butenandt *et al.*, 1959).

Based on these findings, Karlson and Lüscher (1959) proposed the term pheromone (from ancient Greek, *pherein* = carry and *hormon* = set in motion, excite, see Box 1) for all those molecules, which are produced by an organism and elicit a certain reaction or behaviour in another organism of the same species. Since then the terminology of molecules involved in chemical communication has evolved (Nordlund and Lewis, 1976): while metabolites that

Hormone:	a regulatory substance produced in an organism and transported in tissue fluids to stimulate specific cells or tissues into action.
Pheromone:	substance secreted to the outside by an individual and received by a second individual of the same species, in which it triggers a specific response.
Semiochemical:	chemical involved in the interaction between organisms. Semiochemicals include nutrients and toxins (which are beneficial or detrimental to the interacting organisms per se) and infochemicals (which are beneficial or detrimental to the organisms through the response they evoke in the receiver)
Infochemical:	A chemical that conveys information from an emitter to a receiver and elicits a behavioral or physiological response in the receiver.
Allelochemical:	compound involved in interspecific interactions, which is produced by a donor organism and elicits a response in a receiver organism belonging to a different species.

Box 1: Chemical communication glossary.

mediate chemical interactions within the same individual are called hormones (Starling, 1905, Box 2), semiochemicals are involved in inter- and intraspecies communications between different individuals. Semiochemicals (Box 2) comprise different kinds of infochemicals, defined as chemical cues used by organisms to get information about their environment (Dicke and Sabelis, 1985); allelochemicals (Box 2) facilitate interspecific interactions and they can be further divided into allomones (favorable response only for the donor organism), kairomones (favorable response only for the receiver organism) and synomones (favorable for both) (Box 1). This section of the introduction will focus on pheromone chemistry in algae and especially microalgae, while allelochemicals interactions between microalgae and bacteria will be in focus in the next section.

Pheromone research is complicated by many factors. The low amount and dilution of pheromones complicate their detection and structural elucidation. Chemical instability and fast uptake rates can cause additional difficulties. Since 1959, pheromone research has rapidly evolved and many hundreds of compounds involved in intraspecific interactions were discovered. Research on insects provided the best insights in pheromone chemistry (Yew and Chung, 2015) and perception (Ha, 2009), and these findings were efficiently exploited in commercial and industrial applications (Howse, Stevens and Jones, 2013).

Pheromones were also found in fungi (Bahn *et al.*, 2007), bacteria (Kell, Kaprelyants and Grafen, 1995) and mammals (Dulac and Torello, 2003). They are not only guiding mate finding, but they are also regulating social behaviour, as in ant trail formation (David Morgan, 2009), aggregation in arthropods (Wertheim *et al.*, 2005), or alarming and defensive signaling in many animals (Verheggen, Haubruge and Mescher, 2010).

Marine chemical ecology has also given a strong contribution to pheromone research. Several new molecules and interaction mechanisms have been found in e.g. fishes (Sorensen and Wisenden, 2015), arthropods (Titelman *et al.*, 2007) and amphibians (Woodley, 2010), and profuse efforts have been made to apply this knowledge to aquaculture (Hubbard 2015) and to understand how human activities interfere with these interactions (Lüring and Sheffer, 2007).

Only few algal pheromones have been identified so far (Pohnert and Boland, 2002; Frenkel *et al.*, 2014a; Venuleo, Raven and Giordano, 2017). According to Frenkel *et al.* (2014a) there are several reasons behind the slow identification of new pheromones and infochemicals from algae. First of all, lack of knowledge in algal life cycle and coordination of sexual induction mechanisms prevents the application of traditional bioactivity-guided fractionation assays. In addition, while high local concentrations around the producing cells can be reached, the average concentration in the sea water is sometimes particularly low (Ziegler and Forward, 2007). It is therefore necessary to concentrate a high volume of water to collect enough of these cues, thus leading to the increase of interfering inorganic salts concentrations, cue degradation and contamination with plasticizers and co-occurring organisms. Furthermore, the physical properties of water facilitate the distribution of highly diverse compounds, ranging from volatile molecules to unpolar fatty acid derivatives to highly polar macromolecules (Poulin *et al.*, 2018a), therefore requiring advanced analytical methodologies for a proper identification. New –omics technologies and their combinations will help to overcome these challenges, as will be briefly explained in the third part of this introduction.

The first brown algal pheromone was identified in *Ectocarpus siliculosus* as the volatile ectocarpene (Figure 3, Müller *et al.*, 1971), which is produced by female gametes to attract male gametes. Further studies demonstrated that the true pheromone is the thermolabile pre-ectocarpene (Figure 3), which is converted to the up to 10.000-fold less bioactive ectocarpene in a thermally controlled rearrangement (Boland, Pohnert and Maier 1995, Pohnert and Boland, 1997).

Since then, other pheromones from brown algae were found (Pohnert and Boland 2002). Some species, like *Laminaria digitata*, release epoxid (lamoxirene in Figure 3, Maier *et al.*, 1988), while *Fucus serratus* and *Fucus vesiculosus*, as well as the microscopic diatom *Asterionella formosa*, release an unsaturated and unfunctionalized hydrocarbon (fucoserratene in Figure 3, Müller, 1972; Jüttner and Müller, 1979). Brown algae usually release a blend of several hydrocarbons that act both as inducer of male gamete release and attraction of these gametes, thereby promoting mate finding at different levels.

Green algae use different strategies for sexual reproduction, which rarely include pheromone secretion and perception (Sekimoto *et al.*, 2017). The model unicellular green alga *Chlamydomonas reinhardtii* develops gametes under nitrogen starvation. Gametes release a mating-type (MT, see definition in Box 2)-specific hydroxyproline-rich glycoprotein (agglutinin) which promotes attachment of cells after random encounters (Ferris *et al.*, 2005). However, the closely related *Chlamydomonas allensworthii* produces two pheromones (lurlenic acid and lurnelol, Figure 3) that attract MT⁺ towards MT⁻ (Coleman, Jaenicke and Starr, 2001).

Another green alga, *Volvox carteri*, is able to release a glycoprotein under heat-stress. This molecule act as an inducer for production of eggs in female cells and sperm packs in male cells (Gilles *et al.*, 1984). The activity of this pheromone is highly potent: one single male gamete is able to convert all other individuals in a 1000 L culture from asexual to sexual cells by releasing the pheromone at a femtomolar (fM) concentration. The high activity is due to a signaling cascade, produced by additional proteins, called pherophorins, that is believed to amplify the sex-inducing pheromone (Hallmann *et al.*, 1998; Hallmann, 2011).

A complex multi-step pheromone system has been described for the green alga *Closterium peracerosum-strigosum-littorale* complex (Tsuchikane *et al.*, 2003; Tsuchikane *et al.*, 2005). Here, the MT⁻ cells produce a glycoprotein that induces production of another glycoprotein, the protoplast-release-inducing pheromone (PR-IP), in MT⁺ cells. After PR-IP perception, MT⁻ cells release their protoplasts and cell fusion becomes possible.

Besides these examples and the importance of algae pheromones, there is a lack of knowledge especially about microalgae sexual life cycle and pheromone systems. The study of diatoms provided the best insight in this topic, as it will be explained in the next two sections.

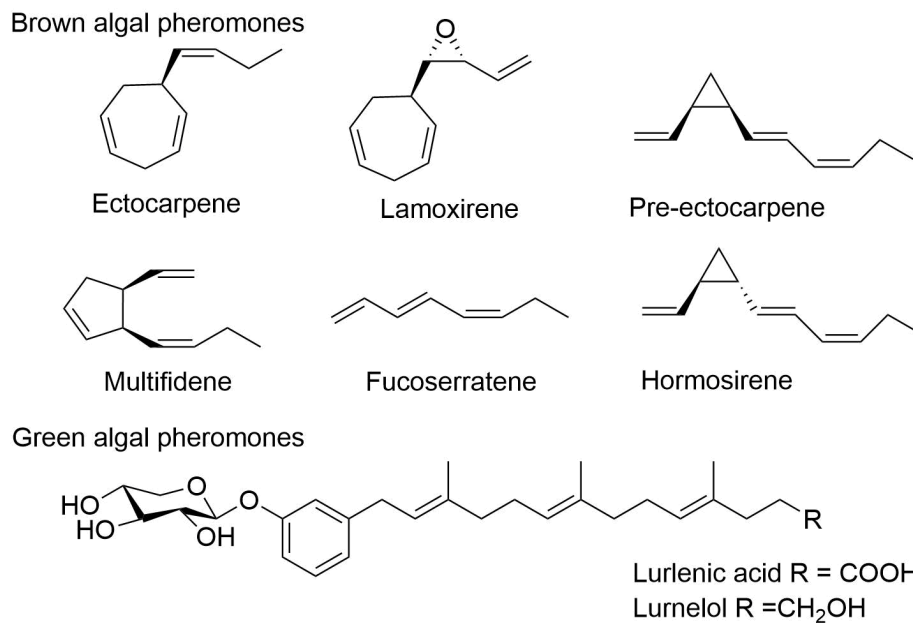


Figure 3: Pheromones from brown and green algae. Figure adapted from Frenkel *et al.*, 2014a.

1.1.2 Sexual reproduction and pheromones in diatoms

Among microalgae, diatoms represent a fascinating groups. They contribute up to 20 % of global carbon fixation (Armbrust, 2009) and they have a huge genetic variability within the group (Mann and Vanormelingen, 2013) that allows them to adapt to light and nutrient stress (Malviya *et al.*, 2016). Their morphology distinguishes them in two different groups, centric (radially symmetric) and pennate (bilaterally symmetric) (Armbrust, 2009). Despite this high genetic and morphological variability, they all share the same unique characteristic of having a robust, silicified, porous cell wall, called frustule (Figure 4, Tréguer and De La Rocha, 2013), a hydrated glass house (SiO₂·H₂O) that protects them from predators and mechanical stress (Hamm *et al.*, 2003). Because of this feature, they have a deep impact on the silicon cycling in the ocean (Nelson *et al.*, 1995). Many diatoms are planktonic and float in open waters, where their interactions are random. Benthic pennate diatoms who developed a raphe (a microscopic slit in the biomineralized silica cell wall) are able to glide over surfaces by the extrusion of exopolymeric substances (EPS) that can form pseudopods (Wang *et al.*, 2013).

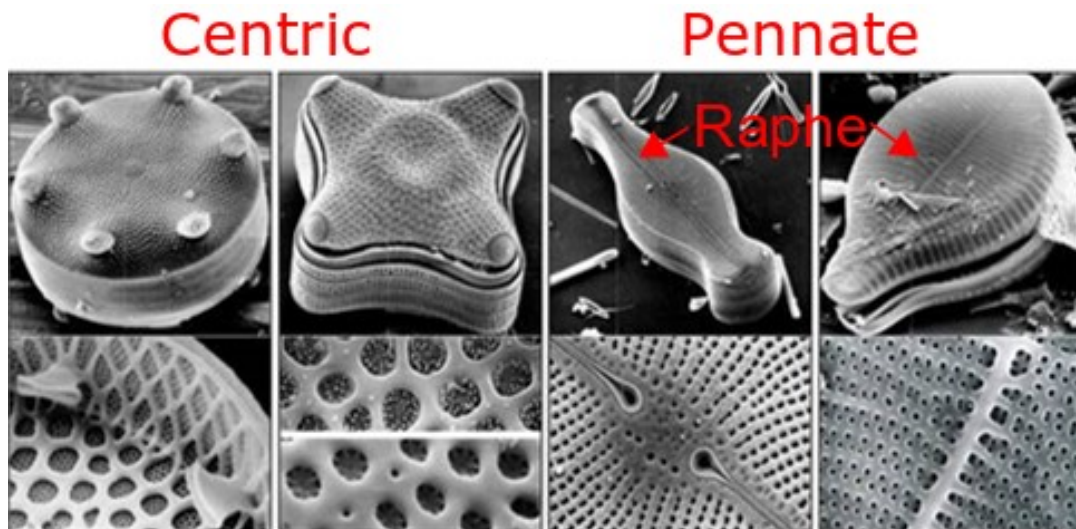


Figure 4: Structure of diatom cell walls. Scanning electron microscopy (SEM) images of overviews (top row) and details (bottom row) of the frustule from four different diatom species (from left to right): *Aulacodiscus* sp. (marine), *Amphitertras* sp. (freshwater), *Didymosphenia* sp. (freshwater) and *Podocystis* sp. (marine). Most of the diatoms, despite their morphological differences and the different environment in which they live, possess a porous cell wall made of silica. (Figure taken from Round, Mann and Crawford, 1990).

A crucial characteristic of the diatom frustule is its “box-and-lid”-like structure (Figure 4 and 5). The frustule consists out of two overlapping halves, an upper and a lower theca (epitheca and hypoteca), that are connected by girdle bands (Chepurnov *et al.*, 2002). During vegetative growth, the daughter cells are forming within the parent cells. This leads to a decrease of the average cell size within diatom populations until a critical minimal size (a phenomenon known as McDonald-Pfitzer rule, Drebes, 1977). To avoid cell death, cells below this limit called sexual size threshold (SST), switch their life cycle from vegetative (mitosis) to sexual reproduction (meiosis) and restore their cell size (Figure 5). Hence, sexual reproduction is a pivotal step in the life cycle of diatoms.

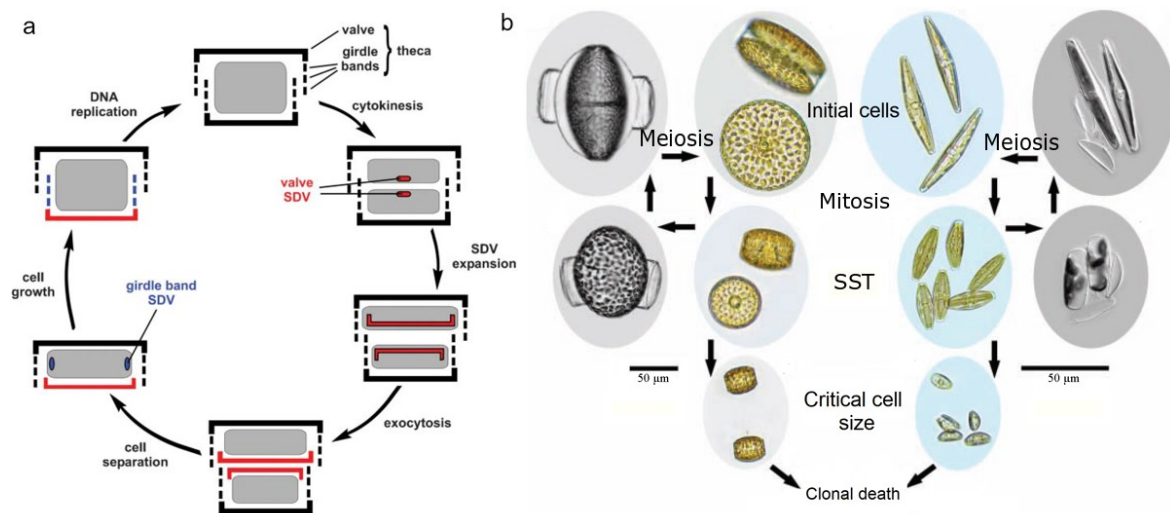


Figure 5: Diatom mitosis (a) and life cycle (b) of a centric (*Thalassiosira punctigera*, on the left) and a pennate diatom (*Seminavis robusta*, on the right). Silica deposition vesicles (SDV) are necessary to form two new thecae within the parent cell during mitotic cell division. Doing so, cell size decreases until a critical cell size. The initial cell size can be restored by sexual reproduction when the diatom crosses the sexual size threshold (SST). Diatoms have different sexual reproduction strategies: while only one daughter cell is produced from *T. punctigera*, a pair of auxospores is produced from *S. robusta* after gametogenesis. Figure modified from Sumper and Kröger (2004) and Chepurnov *et al.*, (2008).

After gamete production, the gametes fuse to form zygotes and after auxosporulation they form new initial cells (Figure 5). While vegetative growth can proceed for months to years, sexual reproduction lasts from some hours up to one week (Chepurnov *et al.*, 2004, Figure 6). However, not all diatoms show sexual reproduction: a famous example of non-sexual species is the model pennate diatom *Phaeodactylum tricornutum* (Bowler *et al.*, 2010). Moreover, the mechanisms are different between centric and pennate species: centric diatoms are mostly oogamic and have a homothallic system (Box 2), with vegetative cells developing in either non-motile eggs or flagellated sperm cells after abiotic induction, such as by light intensity, temperature or concentration of specific nutrients, like NH_4^+ for *Thalassiosira pseudonana* (Moore *et al.*, 2017). Pennate diatoms, on the other hand, show a multifaceted sexual reproduction behavior including isogamy, anisogamy and oogamy (Box 2) with both heterothallic and homothallic mating systems (Chepurnov *et al.*, 2004, Box 2).

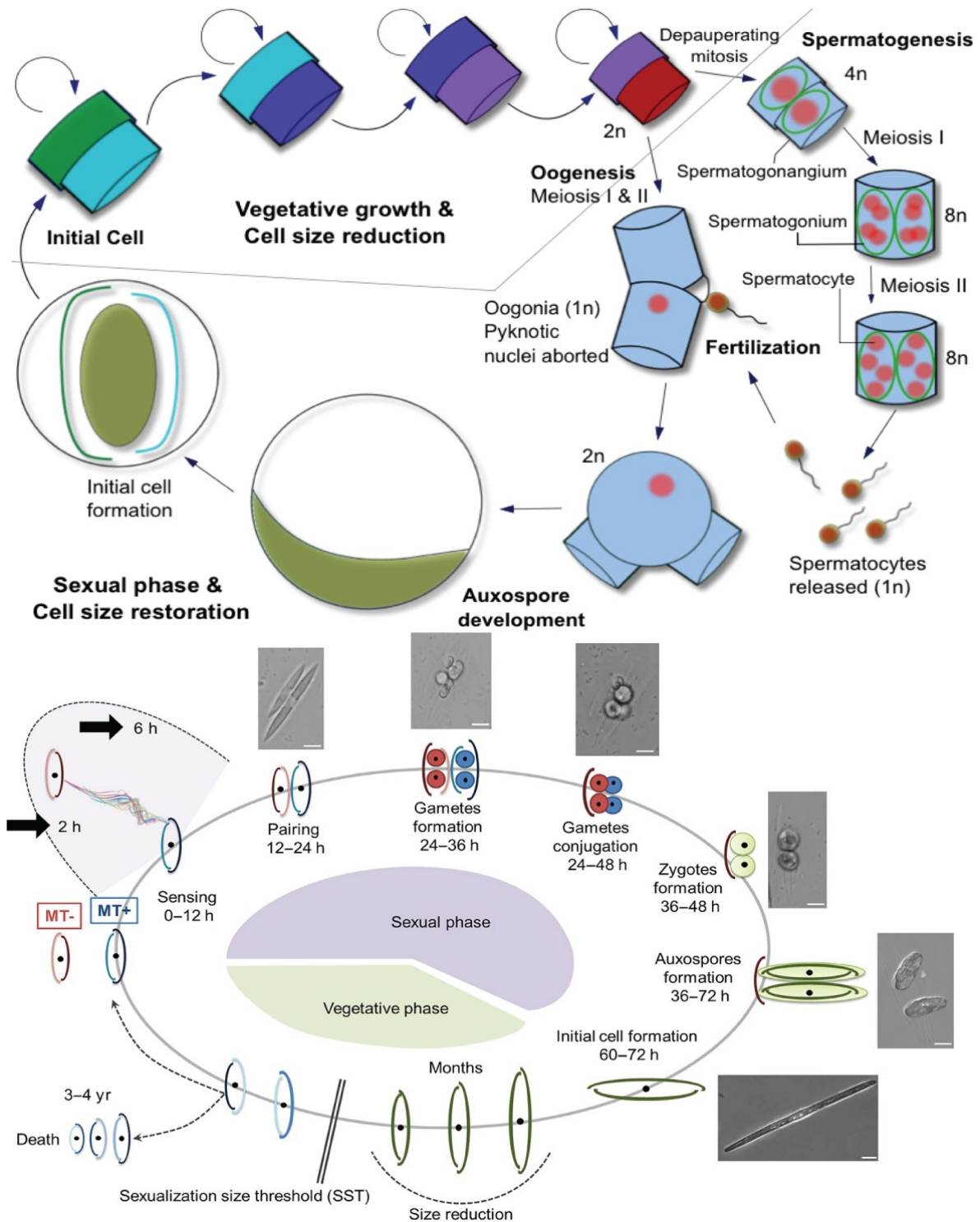


Figure 6: Sexual life cycle of a centric (*Thalassiosira pseudonana*, top) and a pennate diatom (*Pseudo-nitzschia multistriata*, bottom). For centric diatoms sexual reproduction starts with the production of haploid motile spermatocytes and a non-motile oocyte. After fertilization, auxosporulation takes place and restores initial cells. Although no pheromones were found for centric diatoms so far, Moore *et al.*, (2017) showed that abiotic factors (NH_4^+ availability) can trigger sexual reproduction (Figure from Moore *et al.*, 2017). For some pennate diatoms, sexual reproduction involves pheromone release and active recognition cascades, such as in *Seminavis robusta* (Gillard *et al.*, 2013, Moeys *et al.*, 2016) and *Pseudo-nitzschia multistriata* (Basu *et al.*, 2018, Figure from Basu *et al.*, 2018).

Heterothallic:	having male and female reproductive organs on different thalli.
Homothallic:	having both male and female reproductive organs on the same thallus, which can be self-fertilizing.
Oogamous:	reproducing by the fusion of a large, non-motile egg and a small, motile sperm.
Anisogamous:	reproducing by the fusion of dissimilar gametes or individuals, usually differing in size.
Isogamous:	reproducing by the fusion of similar gametes in which no differentiation can be observed.
Mating type (MT):	depend on molecular mechanisms that regulate compatibility in sexually reproducing eukaryotes.

Box 2: Sexual reproduction glossary.

The regulation of this complex and variegated sexual life has been earlier studied using different perspectives, and chemical mediators have been proposed for few diatoms. In *Pseudostaurosira trainorii* some vegetative cells with a specific “sexual size range” release an unspecified chemical mediator (called ph-1) that induces meiosis in other vegetative cells (Sato *et al.*, 2011). The induced cells release two motile, amoeboid male gametes able to release another unknown pheromone (ph-2) that triggers the formation of female gametes in the initial vegetative cells. Finally, the female gametes excrete an attraction pheromone (ph-3), which triggers movement in the amoeboid male gametes towards the female gametes. The study of *Pseudo-nitzschia multistriata* provided additional interesting insights into sexual reproduction regulation. *P. multistriata* requires not only the right cell size, but also a specific cell density, absence of turbulences in the medium, and optimal growth conditions to mate (Scalco *et al.*, 2014). Scalco *et al.*, (2016) described in detail chloroplast arrangement and important timepoints during sexual reproduction. Recent studies (Basu *et al.*, 2018) elucidated a molecular mechanism involved in the sexual reproduction processes of *P. multistriata*, specifically the upregulation of several meiosis-related genes, soluble guanylate cyclase and G protein-coupled receptors, as well as downregulation of genes encoding nutrient transporters during the onset of the sexual phase. However, no pheromone from *P. multistriata* has been identified thus far.

1.1.3 The pheromone system of *Seminavis robusta*

The sexual reproduction system of the pennate diatom *Seminavis robusta* has been intensively studied in the last years and it represents the best characterized among diatoms, both from a genetic and a chemical point of view (Figure 7).

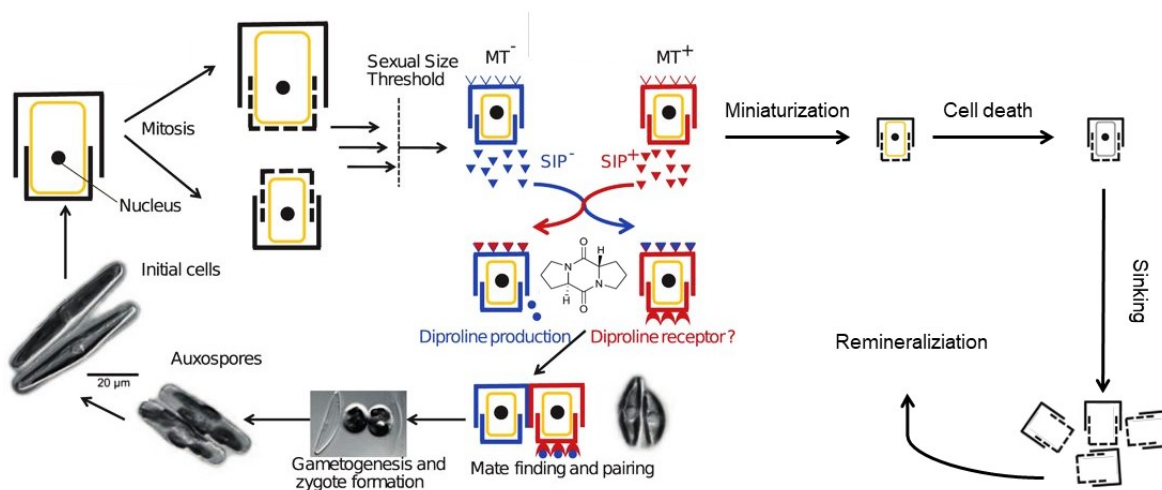


Figure 7: *Seminavis robusta* life cycle. *S. robusta* is a model organism to study the life cycle of pennate diatoms. Its sexual life is regulated by a multistep pheromone system (center). After crossing sexual size threshold (SST), *S. robusta* cells differentiate in two morphologically identical and genetically different mating types (MT) and both mating types start to produce sexual inducing pheromones (SIP). SIP⁺ from MT⁺ arrests the cell cycle of MT⁻ and triggers the production of an attraction pheromone (diproline). Diproline is perceived by MT⁺ and elicits motility towards MT⁻. Afterwards, cells can pair, form zygotes, auxospores and restore initial cell dimensions.

This benthic pennate diatom was first identified by Danieliedis and Mann in 2002: they realized that the previously identified *Amphora ventricosa* (Gregory, 1857) was indeed more similar to diatoms belonging to the genus *Seminavis* and named it *Seminavis robusta*. *S. robusta* possesses all the characteristics to be used as a model system. Its cultivation is highly controllable, and cells can be cryopreserved (Stock *et al.*, 2018). Monoclonal strains of each mating type are available, have a known pedigree (De Decker *et al.*, 2018) and reproducible protocols for dark synchronization of the diatoms' cell cycle exist (Gillard *et al.*, 2008). Furthermore, their cell size (between 20 and 100 μm) and their ability to settle on surfaces make microscopic observations with standard microscope equipment feasible (Chepurnov *et al.*, 2008).

This diatom shows a heterothallic isogamous (Box 2) mating behavior, with two morphologically identical mating types (MT) that are genetically different (Vanstechelmann *et al.*, 2013). After vegetative cells reach the sexual size threshold (SST), they differentiate into two mating types (MT⁺ and MT⁻). MT⁺ cells have the ability to glide towards MT⁻ cells.

Once the cells are paired, two auxospores are produced, resulting in two initial cells from one pair of mating cells (Chepurnov *et al.*, 2002). In the last years, the complex pheromone system regulating the attraction process has been elucidated by means of metabolomics and transcriptomics. Comparative metabolomics assays, fractionations, bioassays, and subsequent structural identification revealed that the attraction of MT^+ towards MT^- is due to the production by the latter of a diketopiperazine (DKP) made by two proline molecules, which was therefore called diproline (Figure 7, Gillard *et al.*, 2013). Interestingly, diproline production is light-dependent and its production is induced by the addition of spent medium of the opposite partner. Furthermore, pheromone perception is only possible if MT^- medium is added to MT^+ cultures, thus suggesting the presence of additional pheromones released by both mating types. Further studies proved that both mating types release sexual inducing pheromones (SIP^+ and SIP^-) (Moeys, Lembke, Frenkel *et al.*, 2016, Lembke, 2018). Although the full chemical characterization is still open, it has been proven that SIP^+ induces cell cycle arrest and synchronization, thus causing a shift from mitosis-related genes to meiosis-related genes (similar to those found by Basu *et al.*, 2018) and it triggers diproline production. Moreover, the sexual inducing pheromone is prompting the expression of genes involved in cGMP biosynthesis (guanylate cyclase, GC) and breakdown (phosphodiesterases, PDE) (Moeys, Lembke, Frenkel *et al.*, 2016). These genes were also upregulated in sexually induced cells of *P. multiseriis*, thus hinting to a possible pathway of pheromone recognition in diatoms. However, information on the specificity and the mechanism of pheromone recognition in diatoms is still scarce. Gillard *et al.*, (2013) found that both the natural (*S,S*)-diproline and its enantiomer (*R,R*)-diproline have a comparable bioactivity. Also a diketopiperazine made of two pipecolic acid molecules tested in attraction bioassays has an effect comparable to diproline, while other open-ring DKP showed no effect (Lembke *et al.*, 2018). Further studies on the structure-activity relationship with labeled diproline and its analogs may reveal the mechanism of perception in *Seminavis robusta*.

The established attraction assay protocol for *S. robusta* (Gillard *et al.*, 2013) provided a great tool to study motility and decisional behavior in diatoms. Recently, Bondoc *et al.*, (2016) found that *S. robusta* moves towards the pheromones via a biased random walk that is a mixture of chemotaxis (directed orientation towards chemical gradients) and chemokinesis (change in motility parameters such as turning frequency and speed in response to the presence of signal molecules in sufficient concentrations) (Amsler and Iken, 2001). *S. robusta* uses the same mechanism to move towards aluminum beads loaded with $Si(OH)_4$

(Bondoc *et al.*, 2016) and towards phosphate (Bondoc *et al.*, 2018a) under nutrient starvation. More interestingly, *S. robusta* demonstrated an unexpected ability of decision making under different stimuli: when cells are below the SST and nutrients are available, mate finding behavior is initiated. However, when silica levels are too low, *S. robusta* diverts all its efforts towards the search for nutrients. When the critical cell size is reached (Figure 5), *S. robusta* will search for a partner even if nutrients levels are low, thus preferring mating over nutrition (Bondoc *et al.*, 2018b).

The microphytobenthos, defined as the diverse assemblages of photosynthetic diatoms, cyanobacteria, flagellates, and green algae that inhabit the surface layer of sediments in marine systems, is one of the most productive marine ecosystems (Smith and Underwood, 1998) and fundamentally contributes to biogeochemical cycles (Paerl and Pinckney, 1996; Bhaskar and Bhosle, 2005; Dang and Lovell, 2016).

Biofilm formation by diatoms is not only important from an ecological point of view (Stal and De Brouwer, 2003), but it is becoming more important in industrial applications (Grozea and Walker, 2009; Schnurr and Allen, 2015), as it will be discussed in Chapter 6.

1.2 Chemical interactions between microalgae and bacteria¹

1.2.1. The phycosphere: a marketplace for aquatic microbial interactions

In recent decades our understanding of microalgae interactions has undergone fundamental changes. Until the 1990s the notion prevailed that the observed species richness in plankton is a result of fluctuating biotic and abiotic resources available to the plankton community (Vanni and Findlay, 1990). Locally and temporally limited favorable conditions of e.g. nutrients concentration, temperature, light and other resources, set the stage for the transient dominance of selected phytoplankton species (algal blooms) and an accompanying complex array of microbial community members (Sommer, 1989). Early observations of single metabolites from microalgae that act as regulators of the growth of competitors or as defense metabolites paved the way for the concept of chemically mediated plankton interactions (Gross, 2003). This predicts that interactions by means of the production, storage and release of chemical mediators can influence the growth and prevalence of phytoplankton as well as their associated microorganisms (Pohnert, 2004). Selected compound classes were studied in great detail, revealing that single metabolites can exhibit a multitude of cascading effects in the plankton. For example, oxylipins (for structures, see Table 1) produced by marine diatoms are used as an activated chemical defense against grazers, for antibacterial effects and even for the regulation of cell death within diatom blooms (Ianora *et al.*, 2011). Given these complex roles of chemical mediators it is not surprising that signaling in water can shape and balance entire communities, including phytoplankton populations.

Microalgae are responsible alone for almost 50% of global photosynthesis (Falkowski , 1994), while associated heterotrophic bacteria (mainly *Proteobacteria* and *Bacteroidetes*, Amin *et al.*, 2012) are able to metabolize most of the dissolved organic carbon (DOC) and particulate organic carbon (POC), helping the oceanic nutrient circulation and carbon sinking (Azam *et al.*, 2007) by establishing the so called “microbial loop” (Buchan *et al.*, 2014, Figure 8). Interactions between these two groups contribute to stabilize the aquatic food web (Cole, 1982) and regulate the fluxes of climatically crucial chemicals (Carpenter *et al.*, 2012), not only in the pelagic zone but also in the benthic environment (Haynes *et al.*, 2007).

¹ This chapter is adapted from: Cirri, E., & Pohnert, G. Algae-bacteria interactions that balance the planktonic microbiome. *The New Phytologist*. Under revision.

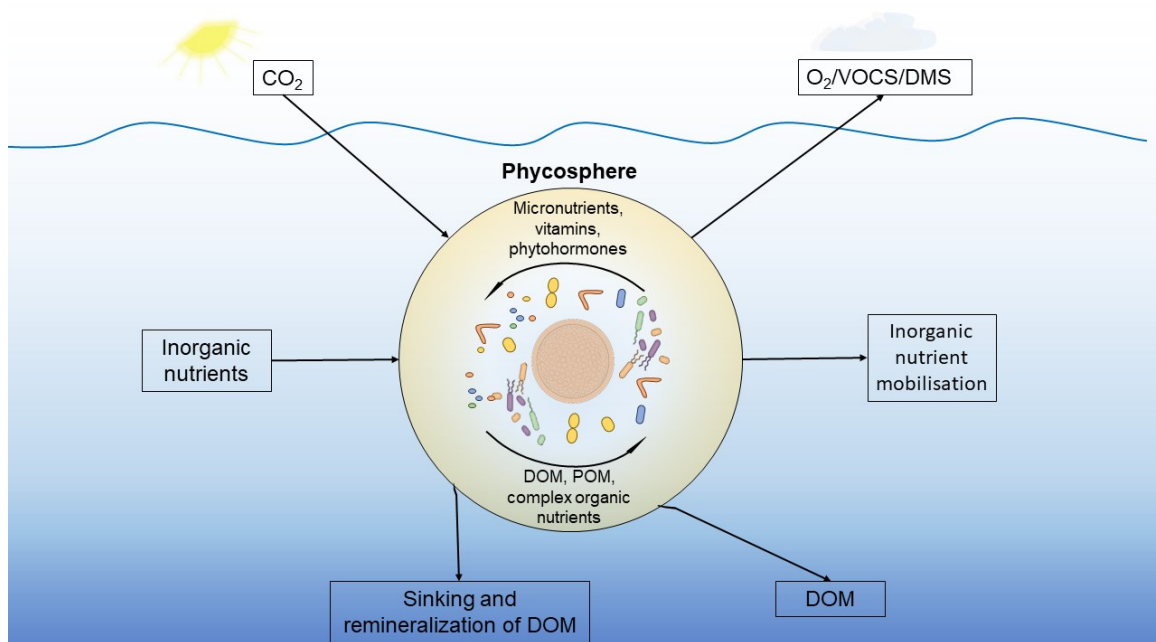


Figure 8: Microalgae-bacteria interactions and their effects on the biogeochemical cycle. The complex interactions in the phycosphere surrounding the algal cell (Bell and Mitchell 1972) are deeply influencing the biogeochemical composition of oceans, air and soil. For example, microalgae use CO₂, sun energy and inorganic nutrient (e.g. sulfur or silicate) to produce several compounds, like the widespread osmolyte dimethylsulfoniopropionate (DMSP), which is produced and excreted by many algae (Thume *et al.*, 2018). Bacteria are able to degrade it and release dimethylsulfide (DMS), a volatile organic compound (VOC) that is escaping to the atmosphere where it acts, after transformation to sulfuric acid, as cloud condensation nuclei (CCN, Andreae, 1990). POM= Particulate organic matter, DOM = dissolved organic matter, DOC = Dissolved organic carbon.

A pre-requisite for such association and exchange networks is the spatial assembly of interacting organisms. Inspired by the seminal work of Lonz Hiltner, who coined the word rhizosphere (Hiltner, 1904) to refer to the microbial community living in close proximity to plants' rhizoids, in 1972 Bell and Mitchell coined the term phycosphere, defining a microscopic region rich in organic molecules surrounding algal cells (Bell and Mitchell, 1972). This chemically enriched zone around the algal cells represents the first interface where interactions between algae and bacteria are controlled by exuded chemicals (Seymour *et al.*, 2017). Such persistent zones allow for the formation of tight associations that forged the evolutionary history of algae and bacteria, leading to microbes with streamlined genomes that benefit from reduced reproduction costs, but face challenges due to the loss of metabolic functions which have to be overcome by random, symbiotic, mutualistic or parasitic interactions (Box 3 for glossary, Kazamia *et al.*, 2016; Ramanan *et al.*, 2016). The complex orchestration of microalgae-bacteria interactions mediates resource (re)cycling, inter-kingdom signaling and community dynamics (Figure 8). Many extensive reviews explored

this field the field (Azam and Malfatti, 2007; Amin *et al.*, 2012; Seymour *et al.*, 2017). Broad reviews also explored the potential of these interactions in industrial context, such as biomass production (Fuentes *et al.*, 2016), wastewater treatment (Gonçalves, Pires and Simões, 2017) and biofuels production (Yao *et al.*, 2019).

Marine food web:	Trophic linkages between all living organisms found in the marine environment.
Chemical mediators:	Small molecules that play a role in regulating the composition and interactions of species in communities.
Algal bloom:	The increase and dominance of algal taxa within the plankton community.
Benthos:	The community of organisms that live on, in, or near the seabed, also known as the benthic zone.
Phycosphere:	The region surrounding a (unicellular) alga or an aquatic bacterium in which gradients of exuded metabolites are maintained.
Heterotroph:	An organism that must acquire organic carbon from an external source to produce energy and sustain growth.
Phototroph:	An organism capable of using the energy of light to carry out cellular metabolic processes.
Metallophores:	Compounds secreted by bacteria to chelate a metal and to ease its transport across cell membranes. Siderophores are specific for iron transport.
Mutualism:	Association between two organisms belonging to different species in which both benefit.
Commensalism:	Association between two organisms belonging to different species in which one benefits from the other without harming or benefiting the latter.
Quorum sensing:	Population density dependent mechanism whereby bacteria communicate and coordinate population behavior and gene expression (QS).

Box 3: Algae-bacteria interactions glossary.

1.2.2. Metabolic hotspots around algal cells

Marine bacteria have evolved strategies to use resources released from living and decaying microalgae (Figure 8). Algicidal species are capable of controlling entire algal blooms by inducing algal lysis, facilitating the uptake of released metabolites (reviewed in Meyer *et al.*, 2017). One example is the interaction between *Kordia algicida* and *Skeletonema costatum* (Paul and Pohnert, 2011): the release of a protease from the bacteria leads to cell lysis of the alga and the subsequent outflow of organic compounds sustains bacterial growth. Another diatom, *Chetoceros didymus*, is able to protect itself from this bacterium by exuding a protease that interferes with the lytic enzyme from the bacteria (Paul and Pohnert, 2013). Such interactions can go beyond random associations as this is strikingly shown for antagonistic bacteria that have evolved group hunting strategies (Aiyar *et al.*, 2017). In this scenario, the bacteria (*Pseudomonas protegens*) accumulate around the initially motile algal cells (*Chlamydomonas reinhardtii*) and immobilize the prey by deflagellation. This process, triggered by the lipopeptide orfamide A (Table 1), leads also to the disruption of algal Ca²⁺-homeostasis and to subsequent cell lysis (Aiyar *et al.*, 2017).

In closely-coupled associations, mutual support of algae and associated bacteria has been also observed. The phycosphere with associated bacteria can thereby be considered as a marketplace where cross kingdom interactions are mediated by the release and uptake of organic compounds (Wienhausen *et al.*, 2017). Gradients within this sphere guide chemoattraction of bacteria in microscale interactions (Seymour and Raina, 2018). For example, bacteria of the class of *Marinobacter* have shown chemoattraction towards the diatom *Thalassiosira weissflogi* (Sonnenschein *et al.*, 2012), while *Vibrio alginolyticus* is attracted by the exudates of the toxic phytoplankton species *Heterosigma akashiwo* (Seymour *et al.*, 2009). To date no spatially resolved chemical imaging of the phycosphere around a microalga is available. Calculations based on growth rates and physical principles of molecular diffusion suggest that the phycosphere is strongly related to microalgal dimensions (Seymour *et al.*, 2017). Raman microscopy on macroalgal surfaces suggests that the phycosphere extends several hundreds of micrometers into the water and a steep build-up of gradients with up to millimolar concentrations of chemical mediators directly above the algal surface can be observed (Grosser *et al.*, 2012). The phycosphere is not a static environment, rather a dynamic entity as revealed in time-lapse video recordings (Smriga *et al.*, 2016): motile bacteria isolated from an enriched ocean community (especially bacteria from the *Roseobacter* clade) form clusters around lysed phytoplankton cells that

subsequently rapidly dissipate. The whole process lasts less than 10 minutes and movement pattern analysis suggests that the phycosphere extends to ca. 2 mm around a lysed diatom (Smriga *et al.*, 2016).

Very recently the concept of chemical communication was extended beyond the mere diffusion-limited exchange of metabolites. In an elegant study, Schatz *et al.*, (2017) found that extracellular vesicles, produced by virus infected microalga *Emiliania huxleyi* enable cell-cell communication. Vesicles carry small RNAs that target sphingolipid metabolism and cell cycle pathways. The internalization by *E. huxleyi* promotes a faster infection of the population. This mechanism might very well be relevant beyond this first example and further studies might extend it to other microorganisms, since bacteria are also known to produce extracellular vesicles with different substances (DNA, antimicrobial peptides, quorum sensing molecules) (Schatz and Vardi 2018).

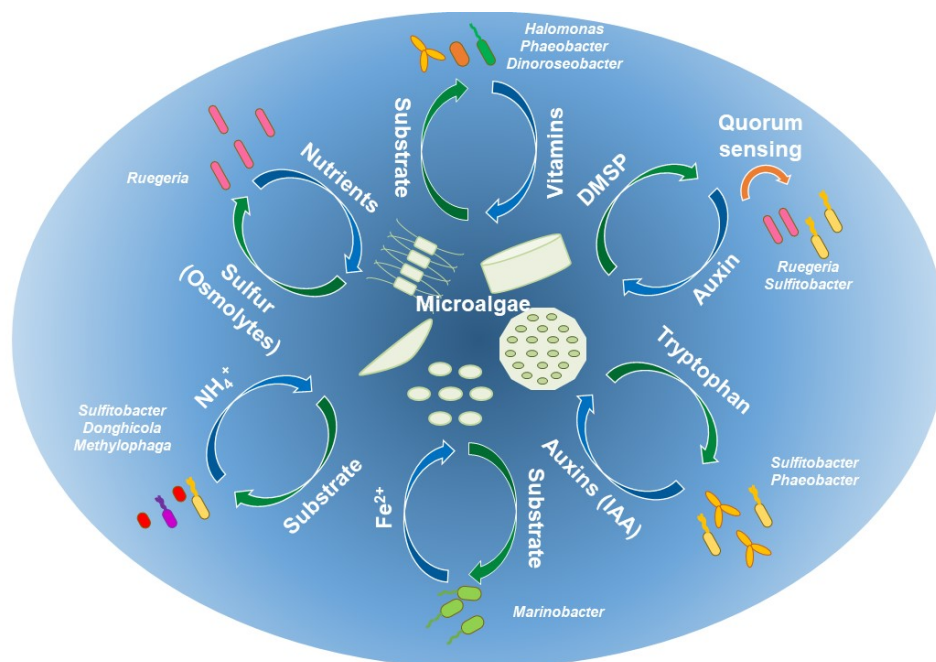


Figure 9: Molecules exchange in microalgae-bacteria interactions. Interactions between microalgae and bacteria involve many different chemical compounds. Vitamins (B12 and B1) are often produced by bacteria and taken up by microalgae that are not able to produce them de-novo (Croft *et al.*, 2005). Also sulfur containing metabolites (e.g. DMSP) are important exchanged nutrients. Bacteria can metabolize it and release nutrients or phytohormones (auxins) to sustain microalgal growth (Segev *et al.*, 2016) or quorum sensing molecules to improve further bacterial colonization (Johnson *et al.*, 2016). Also amino acids play a crucial role in inter-kingdom interactions: for example, *Sulfitobacter* sp. is taking up tryptophan produced by diatom and releasing indole-3-acetic acid (IAA) to sustain algal growth (Amin *et al.*, 2015). Some bacteria, like *Marinobacter algicola*, are enhancing the bioavailability of nutrients, for example by complexing Fe^{2+} with a photolabile siderophore (Amin *et al.*, 2009).

1.2.3. Cross-kingdom exchange of resources and its influence on elemental cycling

Element cycling is a long-standing topic in ocean sciences and exchange of carbon, sulfur, nitrogen and iron were recognized early as factors that determine species composition. With the notion of closely associated algae/bacteria interactions our understanding of such element cycling expanded substantially. Especially with the advent of elaborate analytical techniques the concept could be significantly expanded from simple “element exchange” to the specific interaction by means of defined metabolites that is briefly highlighted in the following paragraph and in Table 1.

The release of vitamins (especially vitamin B12) by bacteria is one of the most common and well-studied means mediating algae-bacteria interactions. An estimated 50% of algal species require exogenous sources of vitamin B12 due to the lack of pathways to synthesize this essential component *de novo* (Croft *et al.*, 2005). In addition, algal supply of vitamin B1 is often dependent on precursors provided by bacteria (Paerl *et al.*, 2017). An untargeted exometabolome survey of two strains of the widely-distributed *Roseobacter* clade (*Phaeobacter inhibens* and *Dinoroseobacter shibae*) revealed that bacteria release plant growth hormone (IAA), nitrogen sources (amino acids) and vitamin precursors (Wienhausen *et al.*, 2017). Among them, two vitamin B1 precursors, 4-methyl-5-(β -hydroxyethyl)thiazole (HET) and 4-amino-5-hydroxymethyl-2-methylpyrimidine (HMP), stimulated the growth of the diatoms *Thalassiosira pseudonana* and *Leptocylindrus danicus*. This can be considered as a cultivation strategy of algae as suppliers of organic resources, which they can consume with up to 82% efficiency (Hornák *et al.*, 2017). Vice versa, algal metabolites can stimulate the production of quorum sensing molecules in bacteria (Johnson *et al.*, 2016), thereby further promoting mutualistic associations.

An intensively studied example of a metabolite that structures the marine environment is the omnipresent sulfur-containing dimethylsulfoniopropionate (DMSP), a compound produced by algae (Sunda *et al.*, 2002). DMSP and its degradation products carry essential physiological functions as osmoregulators and antioxidants in the producing algae (Johnston *et al.*, 2016). Leaked DMSP is a chemoattractant, guiding bacteria and predators towards phytoplankton cells (Seymour *et al.*, 2010). In recent years, DMSP chemistry served as a platform for striking methodological and conceptual developments that led to a substantially refined understanding of the ecological consequences of bacterial competition for organic matter in the phycosphere. A study providing unprecedented spatial information in plankton

ecology focused on the distribution of DMSP down to a subcellular resolution (Raina *et al.*, 2017). Secondary-ion mass spectrometry was used to trace sulfur in the form of its stable isotope ^{34}S in co-cultivation of the DMSP-producing alga *Symbiodinium* sp. and the DMSP-degrading bacterium *Pseudovibrio* sp. The steps from the initial incorporation over the biosynthesis of DMSP, the intracellular storage, release and degradation were visualized. DMSP is localized in the vacuoles, cytoplasm and chloroplasts of the dinoflagellates. The key role of DMSP is supported by the notion that sulfur incorporation is seven times higher for DMSP-degrading bacteria compared to those that lack DMSP-degrading enzymes. In another study, it has been shown that the bacterium *Phaeobacter inhibens* attaches to the cells of the coccolithophore *Emiliana huxley* and exploits released DMSP as a source of carbon and sulfur (Segev *et al.*, 2016). Recently the concept of DMSP as essential metabolite in sulfur cycling has been expanded by the description of the structurally related oxidized metabolite dimethylsulfoxonium propionate (DMSOP). This metabolite, that is formed by algae and bacteria can serve as precursor for oceanic dimethylsulfoxide and is expanding the oceanic sulfur cycle driven by the connected metabolism of algae and bacteria (Thume *et al.*, 2018). Another sulfur metabolite, 3-dihydroxypropane-1-sulfonate (DHPS), is released in high amounts by *Thalassiosira pseudonana* (Durham *et al.*, 2015) and it is influencing *Reugeria pomeroyi* gene expression, which is adapting to the presence of diatom exudates in order to grow better (Durham *et al.*, 2017).

With the ongoing discovery of other widely-distributed organic osmolytes containing reduced sulfur, including gonyol, dimethylacetate and DHPS, the field of algal / bacterial sulfur shuttling is now expanding (Gebser and Pohnert, 2013; Durham *et al.*, 2015). Initial studies investigating the orchestrated regulation of these metabolites under osmotic stress already suggest a novel degree of complexity (Gebser and Pohnert, 2013).

Another essential nutrient for both algae and bacteria is the inorganic nutrient iron. Iron is one limiting factor in the formation of algal blooms (Coale *et al.*, 1996). Its low solubility in water and the resulting small concentration reduces its bioavailability. Consequently, large regions of the oceans are depleted in iron and phytoplankton growth is limited in these areas. Eukaryotic phytoplankton access iron via ferrireductases and Fe(II) transporters, while bacteria excrete small organic molecules (siderophores) that bind iron with high affinity and serve as shuttles into cells. Based on the contrasting requirements of algae and bacteria, a “carbon for iron” mutualism evolved, in which algae release organic matter that supports the growth of heterotrophic bacteria. In return, bacteria in the phycosphere produce siderophores that make iron available to both partners (Amin *et al.*, 2009). Among siderophores,

vibrioferrin (Table 1) represents the best example for this function. It is produced by *Marinobacter algicola* and shows a comparably low affinity for iron but a high sensitivity to light. After complexation of Fe(III) with vibrioferrin, photolysis of the resultant complex leads to the release of Fe(II) that can be readily taken up by algae (Amin *et al.*, 2009).

Nitrogen in its different chemical species, both organic (e.g. amino acids) and inorganic (e.g. nitrate and ammonium), is a fundamental nutrient for both for bacteria and microalgae. Most microalgae, including diatoms, cannot directly acquire nitrogen from N₂, but need inorganic forms such as nitrate or ammonium that are delivered by nitrogen fixing bacteria and cyanobacteria (Foster *et al.*, 2011). In accordance, associations of algae with nitrogen fixing bacteria or those that are able to transform other (in)organic nitrogen sources are observed. For example, *Methylobacterium* sp. is able to break down amino acids, producing ammonium that can be assimilated by *Chlamydomonas* sp. and in exchange exploit the glycerol released from the microalga (Calatrava *et al.*, 2018). A similar mechanism involves methylamines. These compounds are typical degradation products of proteins that are abundant in surface waters, but methylamines are not accessible for e.g. the benthic diatom *Phaeodactylum tricornutum* (Suleiman *et al.*, 2016). To overcome this limitation, a mutualistic interaction with the methylamine-degrading alphaproteobacterium *Donghicola* sp. is established. It degrades methylamine to ammonium that is readily taken up by the alga. The bacterium benefits from the diatom exudates and grows faster. In other cases, bacteria farm microalgae and exploit their production of amino acids, as in the case of *Croceibacter atlanticus*, which is attaching to diatom cells and is able to block cell cycle progression and rewire diatom metabolism towards production of amino acid biosynthesis (Van Tol *et al.*, 2016).

1.2.4. Speak to me: signaling and response in bacteria-microalgae interactions

All molecular exchanges described in the previous section establish a chemical communication between species which influences their genetic and metabolic expression, causing a molecular response cascade that can trigger the production of several infochemicals.

The best example of a response cascade involving infochemicals is the system *Sulfitobacter-P. multiseriis* (Amin *et al.*, 2015). Tryptophan produced by the diatom triggers the expression of bacterial transcripts associated to indole and tryptamine pathways (IAM and TAM), inducing the synthesis and release of the phytohormone IAA. IAA sustains diatom

growth and influences its metabolic gene expression. Cysteine dioxygenase, responsible for taurine biosynthesis, is upregulated and the metabolite is taken up by the bacterium, metabolized, and its byproducts are incorporated in the Calvin cycle. In addition, *Sulfitobacter* increase nitrate import and degradation to ammonia, which is then used by *P. multiseriis* to grow (Figure 10).

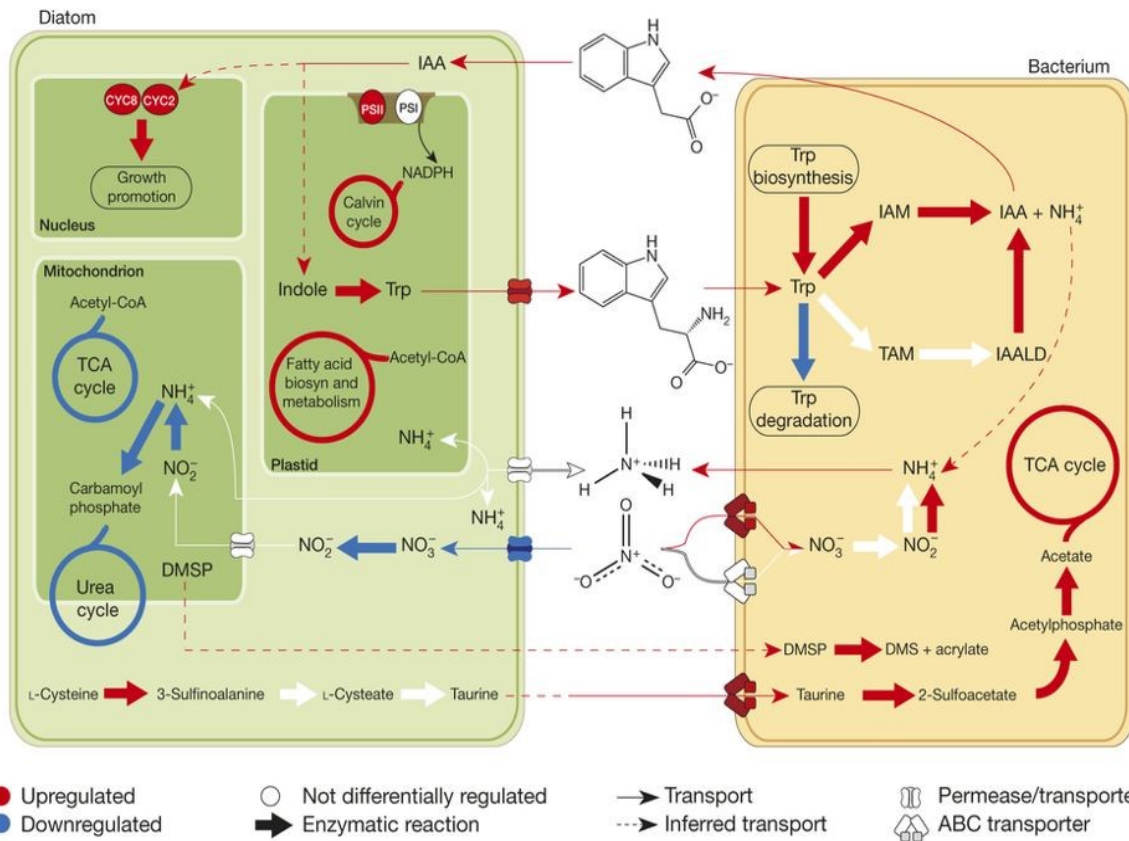


Figure 10: Interaction network between a diatom (*Pseudo-Nitzschia multiseriis*) and a bacterium (*Sulfitobacter sp.*). Depicted metabolites were measured in the medium. Genes/transports/metabolic cycles are shown as upregulated (red), downregulated (blue), or not differentially regulated (white) in co-culture relative to monocultures. IAA potentially regulates expression of two cyclins that typically regulate the cell cycle. Trp, tryptophan; DMS, dimethyl sulfide; PSI, PSII, photosystem I, II; CYC2, CYC8, cyclins 2 and 8; IAALD, indole-3-acetaldehyde. (From Amin *et al.*, 2015, Copyright © 2015, Springer Nature).

A similar mechanism was found for *E. huxleyi* co-cultivated with *P. inhibens* (Segev *et al.*, 2017). Interestingly, this interaction changes during the growth of the microalga: the bacterium can perceive microalgal senescence and increase the levels of IAA to cause cell death by activation of oxidative stress pathways. A similar “Jekyll and Hyde” mechanism, with a switch from a mutualistic to a pathogenic relationship, was also observed in *P. gallaeciensis* / *E. huxleyi* interactions (Seyedsayamdost *et al.*, 2011). Initially, *P. gallaeciensis* produces phenylacetic acid to sustain algal growth and metabolize its exudates. When *E. huxleyi* reaches senescence and starts releasing *p*-coumaric acid (Table 1), the

bacterium responds with the production of algicidal roseobactin (Table 1) to trigger algal cell death.

Several studies also suggested that bacterial quorum sensing (QS), a well understood and common bacterial signaling mechanism (Miller and Bassler, 2001), may play a role in inter-kingdom signaling. Algal metabolites can stimulate bacteria QS molecule production (Johnson *et al.*, 2016). QS compounds can induce biofilm formation in diatoms (Yang *et al.*, 2016) or kill algae, as in the case of *Alteromonas* sp. that produces several quinolone derivatives that act as algicidal compounds towards dinoflagellates, like the harmful-bloom-forming dinoflagellate *Alexandrium tamarense* (Cho *et al.*, 2012). Moreover, microalgae could mimic the quorum sensing molecular family of N-acyl homoserine lactones (AHLs) to influence their microbiome. *Chlamydomonas reinhardtii* secretes a set of compounds (riboflavin and its derivative lumichrome) that are interfering with quorum sensing of bacteria and induce them to produce antibacterials to kill possible pathogens (Teplitski *et al.*, 2004).

The low concentrations and rapid uptake of several info- and allelochemicals (Box 1) complicate their detection via standard analytical methods. However, genomics and transcriptomics experiments allow for the detection of changes in genetic expression upon inter-kingdom interactions and to understand inter-species signaling pathways.

Transcriptomics analysis of a co-cultivation of three different microalgal strains with their natural bacterial consortium showed that many signaling pathways governing higher plant-bacteria interactions are also present in algae-bacteria interactions such as secretion systems type IV and V, flagellin, vitamin B12 and B1 synthetic pathways (Krohn-Molt *et al.*, 2017). In the presence of *Ruegeria pomeroyi*, *T. pseudonana* responds by upregulating the genes for leucine-rich repeat (LRR) receptors, protein kinase systems, calcium-binding proteins and cell cycle regulators (Durham *et al.*, 2017). All these genes are known for immune response and developmental signaling in plant-bacteria interactions. In addition, chitin-binding and chitin metabolism were stimulated. Diatoms synthesize chitin as part of their cell walls, while marine bacteria attach to chitinous regions of diatom cells. *R. pomeroyi* proved to be a flexible, fast-adapting bacterium able to remodel its genomic expression under different conditions thanks to a quick response to signaling molecules. In a co-cultivation experiment with the dinoflagellate *Alexandrium tamarense* and the diatom *T. pseudonana*, *R. pomeroyi* changed its metabolic requirements following a population shift from a dinoflagellate dominated culture to a diatom one (Landa *et al.*, 2017). The response cascade involved phosphorelay genes, flagellar assembly genes and gene transfer agent (GTA) genes

when the dinoflagellate is present. This cascade triggered a metabolic response in the bacterium that involves degradation of DMSP, transport and catabolism of taurine and N-acetyltaurine, xanthine and purine metabolism and transporters for polyamines. Also *Marinobacter adhaerens* can change its protein pattern to reduce amino acid synthetic pathways and to facilitate the uptake of amino acids released by the diatom *T. weissflogii* (Stahl and Ulrich, 2016). These results are supported by the evidence that some algae change their proteome to produce more proteins and amino acids in the presence of bacteria, establishing a mutualistic relationship in exchange of e.g. vitamin B12 (Helliwell *et al.*, 2018) or iron (Beliaev *et al.*, 2014). All these mechanisms are not only found in the pelagic environment, but also have an important role in biofilm formation in benthic environments. A *Roseobacter* strain able to grow on secreted diatom exopolymers as a sole source of carbon influenced the aggregation of *Phaeodactylum tricornutum* by inducing a morphotypic transition from planktonic, fusiform cells to benthic, oval cells and by triggering the production of mucin-like proteins involved in biofilm formation (Buhmann *et al.*, 2016). Other bacteria are necessary for biofilm formation and exopolymeric substances (EPS) release in the freshwater diatom *Achnanthydium minutissimum* (Windler *et al.*, 2015).

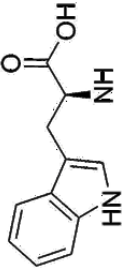
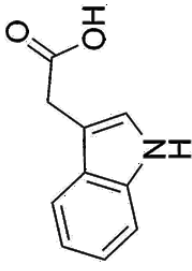
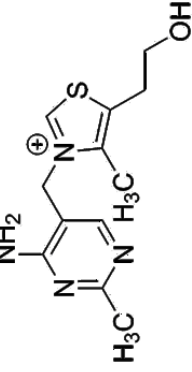
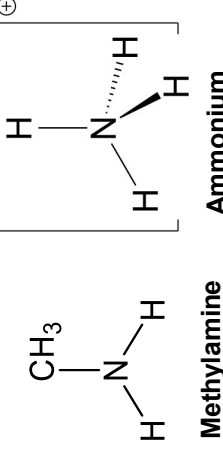
1.2.5. Inter-kingdom signaling shapes marine microbial communities

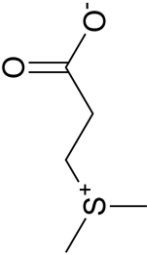
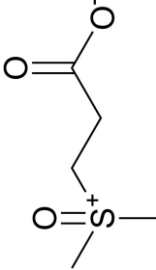
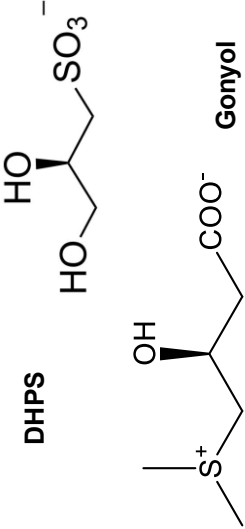
All the above-mentioned interactions between microalgae and bacteria have a crucial role in shaping aquatic microbial communities. The diversity of phytoplankton and the specialization in substrate utilization resulted in the diversification of the bacteria associated to microalgae. Early mesocosm experiments first provided important insights into the dynamics of natural bacteria populations during phytoplankton blooms (Riemann *et al.*, 2000) that were further tested in other experimental setups, for example by documenting community shifts in bacterioplankton after addition of organic matter derived from different phytoplankton species (Tada *et al.*, 2017). Laboratory experiments demonstrated that bacterial colonization strongly depends on the host and that bacterial communities change over time (Crenn, Duffieux and Jeanthon, 2018; Behringer *et al.*, 2018). Besides short term associations, different diatoms establish on the long term specific relationships with selected bacteria, creating a community that is stable across strains and unique for each species, thus suggesting a careful choice of the microbiome based on chemical signaling (Behringer *et al.*, 2018). The involvement of chemical compounds in this process was further demonstrated by documenting community shifts in bacterioplankton after addition of organic matter

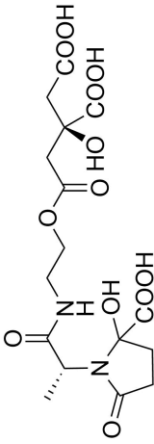
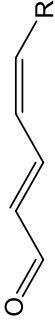
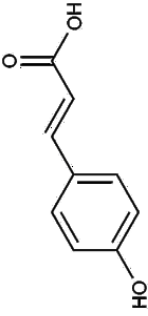
derived from different phytoplankton species (Tada *et al.*, 2017). Lab findings were confirmed by monitoring species- and functional diversity during spring phytoplankton blooms (Landa *et al.*, 2016). The observed succession of bacterial clades was indeed largely explained by specific substrate availability. Remarkably, this succession pattern remained consistent despite considerable inter-annual variation between spring phytoplankton blooms (Teeling *et al.*, 2016). Similar concepts emerged from the study of naturally iron fertilized regions in the Southern Oceans, where the input of iron from island run offs initiates phytoplankton blooms of variable composition (Landa *et al.*, 2016). Heterotrophic bacteria rapidly respond to these blooms and process a substantial fraction of primary production with consequences for the entire pelagic ecosystem. Changes in algal primary production thereby create ecological niches for distinct bacterial populations. This control by substrate delivery leads to a succession of specialized bacteria that utilize different organic components and influence carbon recycling (Landa *et al.*, 2016; Teeling *et al.*, 2016).

Beyond the aspect of succession, nutrient recycling also facilitates the stability of algal-bacterial communities. The phototrophic picocyanobacterium *Synechococcus* sp. allocates more resources to carbon and energy production when co-cultivated with *R. pomeroyi*. In return, the bacterium switches to the preferential use of the photosynthate as a source of organic phosphate, nitrogen and carbon, and re-mineralizes the leaked photosynthate to maintain a feedback of inorganic nutrients to the photosynthetic producer (Christie-Oleza *et al.*, 2017). The phenomenon of fluctuating community compositions with defined annual species successions in plankton was recognized early and motivated a series of theoretical considerations as to how the homeostasis of the system is maintained (Hutchinson, 1961). With the recognition of the close link between phytoplankton and microbial communities, of functional species associations and of chemical factors mediating interactions we have made enormous progress in the understanding of marine species richness and plankton ecosystem functioning at a given time. However, we still lack fundamental knowledge of how the observed annually re-occurring community patterns emerge, how they are stabilized and how succession is triggered. Surveys such as the Tara Oceans expedition (Lima-Mendez *et al.*, 2015) that provide a comprehensive inventory of life in the ocean will surely contribute substantially facilitating pattern recognition and correlations. High resolution time series surveys will as well expand the knowledge on this rapidly changing microbial landscape by monitoring the fast expansion and decline of short-lived communities that display a high level of cohesion (Needham *et al.*, 2017; Martin-Platero *et al.*, 2018). However, the metabolic landscape will also have to be documented in time and space providing an exciting

challenge to link community dynamics directly with chemical mediators of interactions. The metabolic complexity of microbial systems, coupled with the low concentrations of molecules in water, their hitherto poorly documented steep gradients within the phycosphere and open waters, and their rapid uptake pose interesting challenges that must be overcome to take the next step in the understanding of ocean functioning.

Molecules/Molecular class	Example for molecular structure	Ecological function	Reference
Amino acids	 <p style="text-align: center;">Tryptophan</p>	<p>Nutrients and signaling molecules.</p> <p>Tryptophan produced by microalgae serves as precursor for the biosynthesis of auxins in bacteria and promotes mutualism.</p>	Amin <i>et al.</i> 2014 Segev <i>et al.</i> 2014
Auxins	 <p style="text-align: center;">Indole-3-acetic acid (IAA)</p>	<p>Growth promoting molecules in plants and algae.</p> <p>IAA is produced by different bacteria and shows an hormetic effect: at low concentration it promotes algal growth, at high concentration it reduces it and leads to cell death.</p>	Amin <i>et al.</i> 2014 Segev <i>et al.</i> 2016
Vitamins	 <p style="text-align: center;">Thiamine</p>	<p>Nutrients and growth promoters.</p> <p>Microalgae cannot synthesize some vitamins de novo, so they are exploiting bacteria that can produce these vitamins or their precursors.</p>	Croft <i>et al.</i> 2005 Wienhausen <i>et al.</i> 2017
Other N-containing metabolites	 <p style="text-align: center;">Methylamine Ammonium</p>	<p>Nutrients and signaling molecules.</p> <p>Nitrogen fixing bacteria and methylamine degrading bacteria release ammonium, increasing nitrogen availability for microalgae</p>	Amin <i>et al.</i> 2014 Suleiman <i>et al.</i> 2016

Molecules/Molecular class	Example for molecular structure	Ecological function	Reference
DMSP		<p>Osmolytes, nutrients, regulators, signaling molecule.</p> <p>Algal derived DMSP stimulates chemotaxis in certain marine bacteria, which can metabolize it as sulfur and carbon source.</p>	<p>Seymour <i>et al.</i> 2010 Amin <i>et al.</i> 2014 Johnson <i>et al.</i> 2016 Smirga <i>et al.</i> 2016</p>
DMSOP		<p>Osmolytes, nutrients (?).</p> <p>DMSOP from algae is metabolized by bacteria to form oceanic dimethylsulfide</p>	<p>Thume <i>et al.</i> 2018</p>
Other S-containing osmolytes		<p>Transfer of reduced sulfur to bacteria.</p> <p>In addition to DMSP, an entire family of algal S-containing osmolytes (such as DHPS) contributes to S-shuttling between algae and bacteria.</p>	<p>Gebser <i>et al.</i> 2013 Durham <i>et al.</i> 2015</p>

Molecules/Molecular class	Example for molecular structure	Function	Reference
Vibrioferriin		<p>Binding and uptake of iron ions.</p> <p>The iron-complex with bacterial derived vibrioferrin can be photolyzed, thereby releasing Fe^{2+} that can be taken up by algae.</p>	Amin <i>et al.</i> 2009
Oxylipins		<p>Defense metabolites, antibiotics, and regulators of algae.</p> <p>Algal oxylipins are metabolites derived from the oxidative transformation of polyunsaturated fatty acids. They can have multiple structures (given here are the diatom derived $\alpha, \beta, \gamma, \delta$-unsaturated aldehydes) and functions</p>	lanora <i>et al.</i> 2011
Organic acid	 <p style="text-align: center;">p-coumaric acid</p>	<p>Signaling molecules.</p> <p>Some algae release p-coumaric acid during senescence that can be recognized by bacteria, inducing pathogenic responses.</p>	Segev <i>et al.</i> 2017 Wang <i>et al.</i> 2017

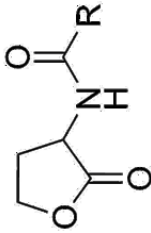
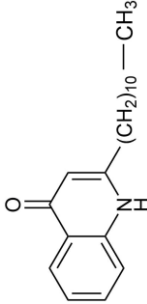
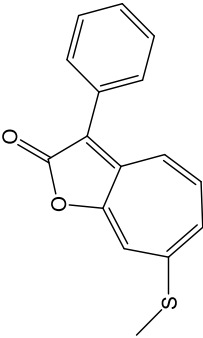
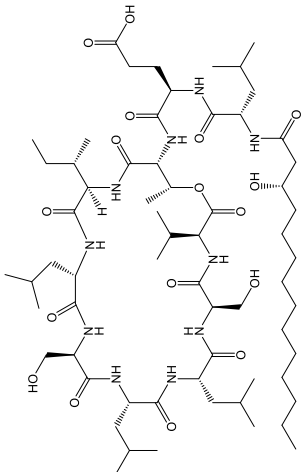
Molecules/Molecular class	Example for molecular structure	Function	Reference
N-Acyl homoserine lactones (AHL)	 <p>AHL (R=acyl chain or fatty acid chain)</p>	<p>Quorum sensing molecules in bacterial communities.</p> <p>AHLs production is promoted by degradation of DMSP produced by microalgae, stimulating bacterial settling.</p>	Johnson et al. 2016
Quinolones	 <p>2-undecyl-4-quinolone</p>	<p>Quorum sensing molecules in bacterial communities.</p> <p><i>Alteromonas</i> sp. uses for quinolones for QS but also as algicidal compounds.</p>	Cho et al. 2012
Algicidal compounds	 <p>Roseobactin B</p>	<p>Induce algal death.</p> <p><i>Phaeobacter inhibens</i> releases roseobactins when <i>E. huxleyi</i> reaches senescence and promotes algal lysis</p>	Seyedsayamdost et al. 2011
Orfamide A		<p>Hunting and killing of algal prey.</p> <p>The lipopeptide is produced by the bacterium <i>Pseudomonas protegens</i> and induces deflagellation and disruption of Ca²⁺ homeostasis in the motile microalga <i>Chlamydomonas reinhardtii</i></p>	Aiyar et al. 2017

Table 1: Example of signaling molecules and exchanged nutrients in aquatic microbial communities.

1.3 Omics techniques in chemical ecology and marine research

1.3.1 The omics approach in chemical ecology

In biology and life sciences, the suffix omics comprises all those approaches that aim to universally detect molecules such as genes, transcripts, proteins or metabolites in a specific biological sample in a non-targeted, non-biased and holistic manner (Horgan and Kenny, 2011). This suffix was first introduced in biology in 1986 by Thomas H. Roderick, a geneticist at the Jackson Laboratory in Bar Harbor: starting from the word genome, which was coined by Hans Winkler in 1920, he suggested the word “genomics” to describe the global study of a genome, a term that was later adopted for a whole new science (McKusick and Ruddle, 1987). Since then, the application of “omics” in biology and life science research has grown exponentially and many new omics approaches were introduced (Yadav, 2007). The integration of different techniques, such as genomics, transcriptomics, proteomics and metabolomics (see Box 4 and workflow Figure 11), is the foundation of system biology (Westerhoff and Palsson, 2004).

Systems biology and omics experiments differ from traditional studies for their holistic nature: while traditional approaches are largely hypothesis-driven or reductionist, systems biology experiments consider a complex system as a whole, acquiring all the data with different technologies without prior knowledge to generate a hypothesis that can be further tested (Horgan and Kenny, 2001).

Genome:	the total DNA of a cell, tissue or organism.
Genomics:	the study of a genome.
Transcriptome:	the total mRNA in a cell, tissue or organism and the template for protein synthesis during translation.
Transcriptomics:	the study of mRNA that is expressed in a precise moment under a precise condition.
Proteome:	the total proteins in a cell, tissue or organism
Proteomics:	the study of proteins, including their structure and function, within a cell, tissue or organism.
Metabolome:	the total low molecular weight compounds (< 1kDa) present in a cell, tissue or organism that participate in metabolic reactions.
Metabolomics:	the study of all metabolites produced by an organism under a given set of conditions.

Box 4: -Omics glossary. Table adapted from Horgan and Kenny 2001.

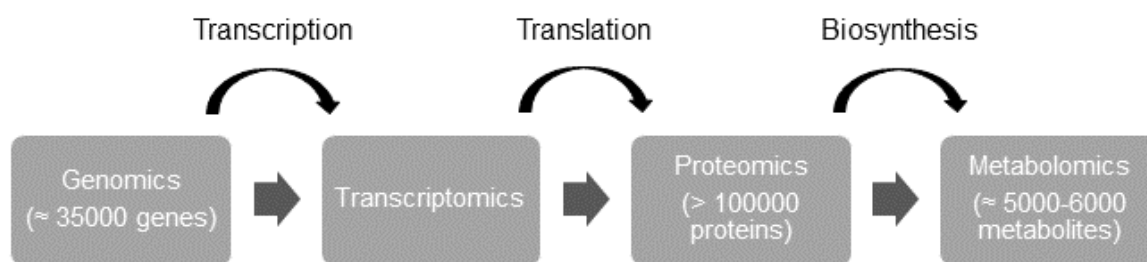


Figure 11: System biology workflow. The numbers in each box indicate the average number of genes, proteins or molecules found in each step for human studies. (Adapted from Horgan and Kenny 2001).

In the last thirty years this discipline made giant steps thanks to the fast-paced development of technologies in different fields. DNA and RNA sequencing has been revolutionized by further development of microarray methods (Rosa, De Leon and Rosa, 2017), introduction of next-generation sequencing (NGS) technologies (Wang, Gerstein and Snyder, 2009; Morozova and Marra, 2008) and single cell investigation approaches (Shapiro, Biezuner and Linnarsson, 2013). Proteomics and metabolomics rapidly evolved especially thanks to the introduction of novel, high-resolution mass spectrometry technologies (Bantscheff *et al.*, 2007; Liu, Ser and Locasale 2014; Schubert *et al.*, 2017; Fuhrer and Zamboni, 2015). Moreover, new methods for data analysis, such as machine learning approaches for data mining, are constantly improving the way to analyze the huge amount of data coming from omics experiments (Larranaga *et al.*, 2006; Libbrecht and Noble, 2015; Yi *et al.*, 2016).

One of the research fields that benefitted greatly from systems biology and omics approaches is chemical ecology (Kuhlisch and Pohnert, 2015; Baudino, Lucas and Smadja, 2016). Systems biology helped to describe chemical communication systems of different organisms, like insects (Boerjan *et al.*, 2012), fungi (Keller, Turner and Bennet, 2005) and bacteria (Güell *et al.*, 2011). Especially in plant chemical ecology, the integration of proteomics, genomics, transcriptomics and ecology allowed for a deep understanding in plant responses to abiotic stress (Urano *et al.*, 2010), plant-fungi interactions (Peršoh, 2015), plant-insect communications (Zebelo and Maffei, 2014) and defenses against predators (Barah and Bones, 2014). Also, the rhizosphere, defined as the narrow region of soil that is directly influenced by root secretions and associated soil bacteria, has been extensively studied with –omics approaches (Badri *et al.*, 2009; Mendes, Garbeva and Raaijmakers, 2013). The knowledge gathered in plant science has been successfully applied to algal chemical ecology, helping to understand the reaction of algae to abiotic stress (Jamers, Blust and De Coen., 2009; Holzinger and Pichrtová, 2016) and the interactions between algae and bacteria (Hollants *et al.*, 2014; Singh and Reddy, 2016), thereby paving the way to

application of omics technologies in an industrial context (Guarnieri and Pienkos, 2015; Arora *et al.*, 2018).

In this thesis, transcriptomics and metabolomics were used to understand the interaction between a diatom (*Seminavis robusta*) and its associated bacteria. I will therefore focus the rest of this part of introduction on recent advances in transcriptomics and metabolomics in microalgal research.

1.3.2 Transcriptomics approaches to study diatoms and other microalgae

The introduction of RNA sequencing and the development of next generation sequencing technologies (NGS) (Morozova and Marra, 2008) has propelled transcriptomics application in different scientific fields, from cancer research (Maher *et al.*, 2009) to molecular ecology (Ekblom and Galindo, 2011). RNA sequencing is a technique that uses parallel sequencing platforms to sequence an entire transcriptome with high sensitivity, allowing for the detection of both known and novel features in a single assay by the detection of transcript isoforms, gene fusions, single nucleotide variants and other features without the limitation of prior knowledge. It is therefore a fundamental technique for the study of non-model species (species that do not have a sequenced and annotated genome). NGS technologies allow the acquisition of huge amounts of reads with high speed and low costs, making transcriptomics affordable for many laboratories. In particular, Illumina[®] sequencing-by-synthesis technology (see Figure 12 for details) offers a broad dynamic range for more sensitive and accurate measurements of gene expression and high throughput data.

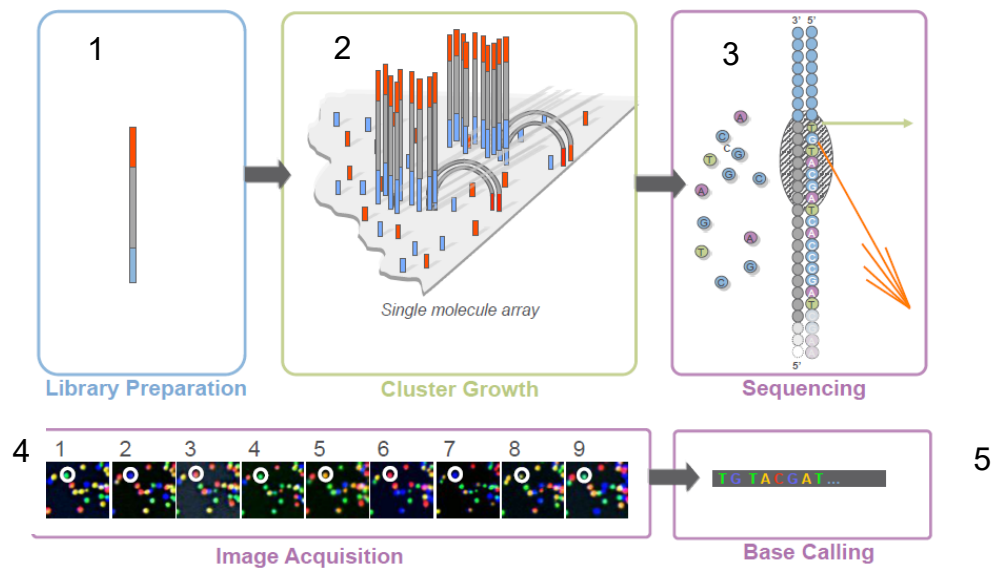


Figure 12: Illumina® sequencing by synthesis (SBS) technology. 1) Small fragment of RNA is converted to cDNA by translation and random universal primer are attached. 2) cDNA is loaded into a glass flowcell and each separated cDNA is amplified by PCR bridge amplifications generating millions of isolated clonal cDNA clusters. 3) Each segregated clonal cluster is sequenced by synthesizing a complementary DNA strand. SBS is a cyclic process where fluorescent, reversible-terminated nucleotides are added in each cycle. 4) At each cycle, a fluorescent nucleotide is read by laser-imaging, one channel for each nucleotide type. 5) Finally, all intensity quadruplets for each cluster are processed by a base-caller, which determines the most probable nucleotide that was added during each cycle. (Copyright Illumina 2015 ®)

The increase in the number of microalga genomes, starting from those of the model diatoms *T. pseudonana* (Armbrust *et al.*, 2004) and *P. tricornutum* (Bowler *et al.*, 2008) and the unicellular green alga *Ostreococcus lucimarinus* (Palenik *et al.*, 2007), paved the way for sophisticated transcriptomics experiments that were used to elucidate different aspects of microalgal life.

Especially diatoms have been extensively investigated with transcriptomic approaches and many aspects have been elucidated. Many studies focused on nutrient uptake and pathways for nutrient limitation in order to understand how this could affect their physiology and life cycle, and therefore their ecological repercussion. Besides studies on carbon fixation (Chauton *et al.*, 2013), nitrogen starvation (Levitan *et al.*, 2015) and phosphorous limitation (Dyhrman *et al.*, 2012), efforts were directed towards understanding the mechanism behind iron uptake, a crucial nutrient to understand diatom blooms (Lommer *et al.*, 2012; Cohen *et al.*, 2018) and silicon metabolism, a unique and fascinating feature of diatoms that was elucidated with extensive studies in *T. pseudonana* and *P. tricornutum* (Mock *et al.*, 2008; Sapriel *et al.*, 2009; Shrestha *et al.*, 2012). Cell cycles of diatoms have been deeply investigated in the model diatom *S. robusta* and in *P. multiseriis* (see first section of this

introduction and Huysman, Vyverman and Veylder, 2013), while light acclimation was studied in *P. tricornutum* (Nymark *et al.*, 2009). Transcriptomics plays an important role in understanding how diatoms cope with global warming (Toseland *et al.*, 2015), the increase of CO₂ (Hennon *et al.*, 2015) and water pollution (Hook and Osborn, 2012). All the data taken from *T. pseudonana* and *P. tricornutum* contributed to the “Diatom Expressed Sequence Tag”, an online database containing differentially expressed genes under different conditions. This database is a useful resource for *in silico* gene prediction and comparative studies using non-model organism grown in the same conditions (Maheswari *et al.*, 2008). Also the coccolithophore *Emiliana huxleyi*, an ecologically relevant calcifying phytoplankton, has been subjected to intensive transcriptomics studies (Read *et al.*, 2013; Feldmesser *et al.*, 2014): they provided important information on the genetic differences between the haploid and diploid cells of this microalga (Von Dassow *et al.*, 2009) as well as on acclimation to changing climate conditions, especially regarding the calcifying mechanism of this haptophyte (Bach *et al.*, 2013). Apart from diatoms and *E. huxleyi*, several transcriptomics studies have been performed on dinoflagellates (for an extensive review, see Akbar *et al.*, 2018), organisms that play a key role in marine ecology, especially in harmful algal blooms.

In addition to its crucial contribution to ecological studies, transcriptomics is also a fundamental approach in biotechnology. Hundreds of studies focused on unraveling the mechanisms behind accumulation of lipids and high-value compounds, especially in green algae belonging to *Chlamydomonas* (Merchant *et al.*, 2012; Lu, 2013), *Nannochloropsis* (Liu, Song and Qiu., 2017) and *Haematococcus* (Cheng *et al.*, 2017) species and in the oleaginous diatom *Fistulifera solaris* (Tanaka *et al.*, 2015).

All these studies provided important insights into alga metabolism that will help metabolic engineering of algae for oil accumulation (Goncalves *et al.*, 2016), high-value compounds (Harun *et al.*, 2010) and other more unusual but fascinating applications, like silver nanoparticles production from diatoms (Wishkerman and Arad, 2017).

1.3.3 From genes to molecules: metabolomics in microalgal research

In the last years, metabolomics provided important insights into algae and microalgae, shedding light on molecules involved in defining different growth stages and intra- and interspecific interactions (Kuhlich and Pohnert, 2015).

Endometabolite profiling studies expanded the knowledge of how algal metabolism changes during different stages of their life (Barofksy, Vidoudez and Pohnert, 2009; Vidoudez and Pohnert, 2012; Mausz and Pohnert, 2015) or when exposed to abiotic stresses (Jamers, Blust and De Coen, 2009; Wördenweber *et al.*, 2018). Development in metabolomics investigation of microalgae were exploited in applied research (Liu, Pohnert and Wei, 2016), for example to discover new biomarkers useful for industrial bio-processes (Courant *et al.*, 2013) or to improve the production of high valuable compounds, such as carotenoids (Lee *et al.*, 2014; Su *et al.*, 2014), nutraceuticals (Li *et al.*, 2014) and lipids for biofuels (Martin *et al.*, 2014).

Metabolic fingerprinting:	screening tool to differentiate among samples of different origin or treatment. It is a high throughput qualitative screening of the metabolic composition of the system (no identification or quantitation).
Metabolic footprinting:	as above but monitoring metabolites secreted into extracellular growth medium.
Metabolic profiling:	identification and quantification of a group of related compounds (frequently belonging to a specific metabolic pathway or sharing common chemical features).
Target metabolite analysis:	analysis of few metabolites related to a specific metabolic reaction by using optimized extraction and separation/detection techniques.

Box 3: Metabolomics glossary. (Goodacre *et al.*, 2004, Scognamiglio *et al.*, 2015).

Metabolomics also helped expand marine and algal chemical ecology research, although several technical challenges are present. Fresh- and seawater represent a rather complex matrix to detect waterborne signals that are often released in small concentrations and additionally diluted by the aqueous environment. Salts from seawater constitutes one of the major interfering compounds, especially affecting electrospray ionization (ESI) in liquid chromatography (LC) (Goulitquer, Potin and Tonon 2012). Pre-selection of specific compounds for enrichment and extraction, as done with volatiles mediating insect communications, is not a suitable approach either, because, as seen in the previous chapters, the physical nature of aquatic infochemicals can range from polar substances, like zwitterionic metabolites (Wang *et al.*, 2014), to hydrophobic hydrocarbons, like fatty acids or oxylipins (Pohnert and Boland, 2002). In addition, the molecular weight of signaling compounds can vary from gases (Vanellander *et al.*, 2012) to big polar molecules (Seyedsayamdost *et al.*, 2011), thus requiring very different extraction and detection methods. A lot of research has therefore been done to optimize metabolomics experiments

applied to marine chemical ecology, from sample preparation, especially solid phase extraction (SPE) and solid phase microextraction (SPME), to analytical measurements, mainly done with chromatographic techniques (liquid or gas chromatography) coupled to mass spectrometry (MS) or nuclear magnetic resonance (NMR) spectroscopy (Figure 13).

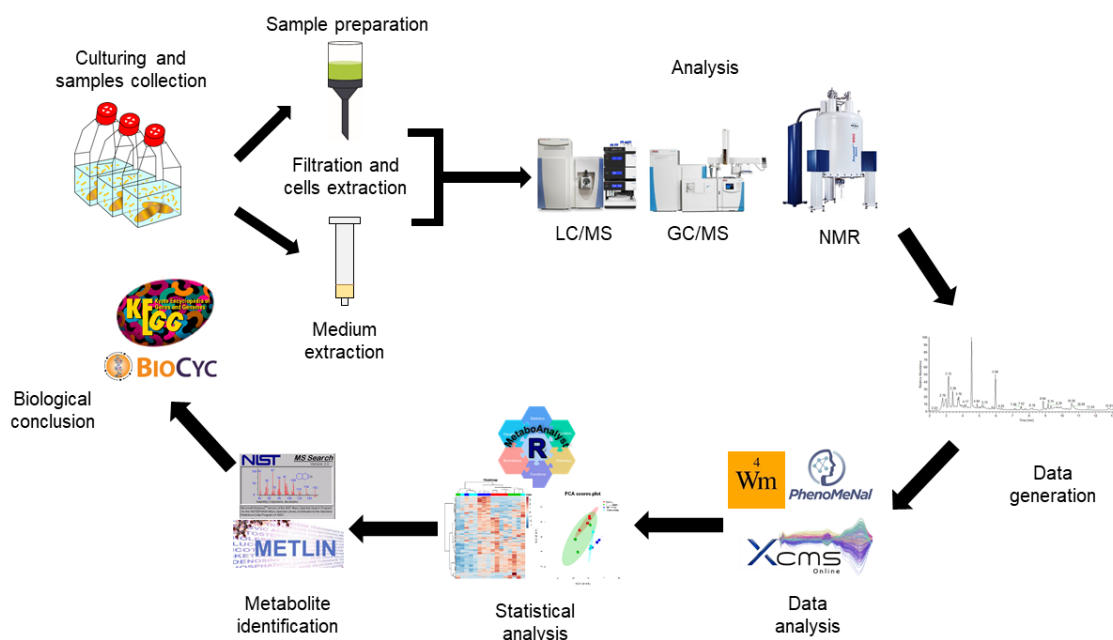


Figure 13: Example of untargeted metabolomics workflow.

Comparative metabolomics allowed the exploration of several interaction mechanisms between algae, for example allelopathy, a biological phenomenon by which an organism produces one or more biochemicals that influence the germination, growth, survival, and reproduction of other organisms (Legrand, 2003). A co-cultivation experiment using special chambers separated by a permeable membrane showed that *S. costatum* promotes *T. weissflogii* growth by releasing metabolites that are changing the endo- and exometabolome of both diatoms (Paul *et al.*, 2009). The harmful-algal-bloom (HAB) forming dinoflagellate *Karenia brevis*, which releases potent neurotoxins known as brevetoxins (Prince *et al.*, 2010), also produces compounds that negatively affect diatom competitors (Kubanek *et al.*, 2005). NMR-based metabolomics allowed to associate these effects to the presence of yet unknown metabolites that could produce spectral features common to fatty acid-derived lipids or polyunsaturated compounds. (Poulin *et al.*, 2018b) and a lipidomic approach revealed that thylakoid-associated lipids and cell membranes of the diatoms *T. pseudonana* are affected by the presence of the dinoflagellate exudates (Poulin *et al.*, 2018c). Interactions between microalgae and grazers, a mechanism that is fundamental to understand microalgal bloom regulation in the ocean, has also been explored by metabolomics approaches. The changes

of the exometabolome during the life cycle of the bloom forming diatom *S. marinoi* influence the feeding behavior of copepods, which prefer to eat cells in the late stationary phase (Barofsky *et al.*, 2009), when higher concentrations of carbohydrates and lipids are available (Ray *et al.*, 2016). Other copepods feed on young cells from the benthic diatom *S. robusta* and this preference might be connected both to the exudates from the diatom itself and from the bacteria composition (De Troch *et al.*, 2012). On the other hand, grazers induced strain-specific exometabolomic responses in the coccolitophore *E. huxleyi* (Poulson-Ellestad *et al.*, 2016) suggesting a broader range of interactions between predators and prey. Metabolomics approaches also contributed to understanding of interactions between microalgae and bacteria. Using dual co-cultivation chambers separated by a membrane, Paul *et al.* (2012) used an untargeted metabolomics approach to study the effect of exuded chemicals from *D. shibae* on *T. pseudonana*, finding out that the medium from *D. shibae* only increased the amino acid production in the diatom. Another untargeted metabolomics approach proved that *Pseudomonas sp.* is changing the nutrient removal behavior of *Chlorella sorokiniana* in a wastewater treatment system (Chen *et al.*, 2017b). On the other hand, bacteria release putative molecules that increase algal growth in the diatom *Haslea ostrearia* (Lepinay *et al.*, 2018) and in other microalgae (Wienhausen *et al.*, 2017).

All these examples show that metabolomics plays a central role among the omics techniques employed in microalgal research and the rapid evolution of sample preparation, especially single-cell sampling (Sun, Yang and Wawrik, 2018), analytical technologies, as well as data analysis, with the introduction of new pipelines (Chong *et al.*, 2018; Liggi *et al.*, 2018) and programs to identify unknown features in LC/MS and GC/MS datasets (Misra and van der Hoof, 2016; Barupal, Fan and Fiehn, 2018; Blaženović *et al.*, 2018), will increase our ability to explore the life of algae and will rise new, exciting research questions.

1.3.4 Two is better than one: metabolomics and transcriptomics integration in microalgal research

Although transcriptomics and metabolomics are self-defined and self-sustaining approaches, their integration enables one to combine biology and chemistry to have a broader and more complete picture of inter-organism interactions. So far, few studies joining transcriptomics and metabolomics are available for algal chemical ecology, despite this joint approach having already proven to be useful both for ecological and applied research.

A combined metabolomics-transcriptomics approach applied on the model diatom *P. tricornutum* under iron starvation showed that the photosynthetic activity is dramatically altered, with a higher production of chlorophyll, as proved both by upregulation of several pathways connected to its biosynthesis and high concentration of intracellular glutamate (Allen *et al.*, 2008). The concomitant increase of tocopherol and amino acids like valine, leucine and alanine and a steep increase in glycolysis and protein lysis suggested a big rewiring of energy and protein metabolism, as well as a strong oxidative stress response (Allen *et al.*, 2008). A similar approach untangled the diatom reaction towards low nitrogen uptake: under this condition, *P. tricornutum* increases nitrogen fixation, decreases photosynthesis and changes its lipid metabolism by increasing triacylglycerol content (Remmers *et al.*, 2018).

-Omics approach provided interesting information on diatoms' response to grazers. The chain forming diatom *S. marinoi* reacted to the presence of copepods by reducing chain length, changing cell cycle and division rate (Amato *et al.*, 2018). Moreover, the presence of predators trigger stress response mechanisms that increase the expression of transcripts connected to NO production and heat-shock proteins (Amato *et al.*, 2018). The downregulation of lipoxygenase in the transcriptomic data and of its products in the metabolomic data also indicate an involvement of oxylipins in this process (Amato *et al.*, 2018). The authors suggest that G-proteins coupled receptors may be involved in diatom recognition of copepods.

Combined transcriptomics-metabolomics approaches allowed to elucidate the mechanism of interaction between microalgae and bacteria or viruses (Cooper and Smith, 2015; Ramanan *et al.*, 2016). The effect viral infection on the metabolism of the coccolithophore *E. huxleyi* were reconstructed with a combined weighted correlation network analysis that linked clusters from transcriptomics to metabolite levels (Rosenwasser, Mausz *et al.*, 2016). Especially during the early stages of viral infection a dynamic modulation of the host metabolism was observed. A viral up regulation of algal fatty acid biosynthesis to help viral assembly, and a down regulation of host sphingolipid biosynthesis was observed, thus proving that the virus is exploiting sphingolipids to propagate the infection. The alga responded to this infection by reducing terpenes, as confirmed by the decrease in the concentration of several terpenes and the concomitant reduction of all host genes related to the production of isopentenyl-pyrophosphate in the mevalonate pathway. Targeted metabolic analyses revealed that the suppression of steroid formation interferes with viral

replication. Viral replication in *E. huxleyi* thus depends on the host metabolism to provide sterols, fatty acids and sphingolipids as building blocks for infection propagation.

Evaluation of *R. pomeroyi* in co-culture with *T. pseudonana* revealed that in exchange for vitamin B12 released by the bacterium the alga produced the sulphur-containing compound C3-sulfonate 2,3-dihydroxypropane-1-sulfonate (DHPS), which in turn could be metabolised by *R. pomeroyi*, as shown by the upregulation, found both in transcriptomics and metatranscriptomics data, of genes connected to transport and catabolism of this compound and by the concentration of it both in lab cultures and in environmental samples. The joint use of transcriptomics and metabolomics therefore provided a possible explanation for the previously cryptic role for this molecule, which is produced in large amounts by many marine algae (Duhram *et al.*, 2015).

Moreover, the combination of metabolomics and transcriptomics contributed to commercial research on several economically relevant species. A recent study on the heterotrophic microalga *Cryptothecodinium cohnii*, a species that accumulates lipids with a high fraction of docosahexaenoic acid (DHA), reconstructed the major part of the DHA biosynthetic pathways and allowed to find the best growth condition to increase DHA production (Pei *et al.*, 2017). Similar experiments elucidated the lipid accumulation mechanisms of the oleaginous microalgae *Nannochloropsis oceanica* (Li *et al.*, 2014) and *Chlamydomonas* (Winck, Melo and Barrios, 2013) and the reprogramming of fatty acid production under low and high temperature of *Auxenochlorella protothecoides* (Xing *et al.*, 2018).

All these works are an example of the successful integration of transcriptomics and metabolomics approaches, showing that multiomics approaches are a necessary tool to further understand the complex and fascinating world of microalgae.

2. Thesis Objective

Understanding inter-kingdom communication between microalgae and bacteria is a key element to understand the ecological role, as well as the potential industrial application, of these organisms. These interactions are chemically mediated and they take place in the phycosphere, a region surrounding a (unicellular) alga or an aquatic bacterium in which gradients of exuded metabolites are maintained (Bell and Mitchell, 1972). Such relationships influence the life of both interacting organisms and shapes community dynamics. In consequence, these processes are affecting the marine food web and global elemental cycling. Furthermore, the understanding of these relationships has become important for algal aquaculture applied research in a sustainable development perspective.

This thesis aims at in-depth analysis of interspecific chemical communication between microalgae and bacteria. A combination of targeted analytical chemistry, untargeted metabolomics approaches, physiological bioassays and transcriptomic analysis shall be used to disentangle mechanism underlying inter-kingdom relationships and to discover novel signaling strategies. The benthic pennate diatom *Seminavis robusta* is selected as the model organism used to investigate the effect of bacterial on an ecologically relevant algal species. Moreover, the oleaginous microalga *Nannochloropsis* sp. is selected to test the influence of bacteria on a commercially relevant species.

The following research questions will be addressed.

Effect of bacteria on pheromone chemistry and sexual reproduction of a benthic diatom

A fundamental characteristic of diatom's life cycle is the short phase of sexual reproduction, which is crucial to avoid population cell death. The benthic diatom *Seminavis robusta* uses a complex system of pheromones to support synchronization of sexuality and mate finding (Gillard et al., 2013; Moeys et al., 2016). The attraction pheromone diproline is stable in water but nevertheless its concentration decreases over time (Frenkel *et al.*, 2014b). Targeted analysis of the concentration of this compound in presence and absence of *S. robusta* associated bacteria will prove if they are directly involved in the degradation of this signal molecule (Chapter 4). Furthermore, a bioassay on mating cultures of *S. robusta* will be used to see what are the effect of isolated bacteria and of their spent medium on the sexual efficiency of the diatoms. The spent medium of the bacteria with the highest positive or negative effect on *S. robusta* sexual reproduction will be then selected for further experiments, using a combination of physiological tests, targeted chemical analysis and a

joint metabolomics-transcriptomics approach (Chapter 4). This will elucidate the molecular mechanisms and potential molecules involved in bacteria-diatom communication in the context of diatom sexual reproduction (Chapter 5), and thus provide fundamental knowledge for the understanding of the behavior of benthic diatoms and the organization of intertidal environments.

Bacterial impact on microalgal growth, metabolome and biofilm formation

Growth and metabolism of microalgae can be strongly influenced by bacteria. These interactions have deep repercussions on the natural communities' organization and on their ecological role. Selected bacteria will be investigated to assess their impact on *S. robusta* growth. Moreover, an untargeted metabolomics approach will be used to study bacteria impact on the diatom metabolism and understand how bacteria can impact the life and organization of benthic biofilms (Chapter 3).

Apart from their ecological relevance, the communication between bacteria and algae can be used in algal aquaculture to increase yield, product quality and in the same time reduce negative side effects, such as biofouling.

In collaboration with the private company Proviron® (Antwerp, Belgium), the effect of bacteria isolated from *S. robusta* on the commercially relevant *Nannochloropsis* sp. will be investigated with bioassays and an untargeted metabolomics approach in order to evaluate the potential of microbial community engineering to increase biomass and high value compounds productivity and decrease the formation of biofilm in a closed photobioreactor system (Chapter 6).

Development of a non-disruptive method for extracting algal surface metabolites

Metabolites released from algal surfaces or other underwater surfaces, such as biofilms, mediate interactions with many organisms. The extraction of such metabolites is a delicate and challenging procedure. The methods developed so far provide for direct contact of the surface with organic solvents that may damage the surface and lead to the release of intracellular metabolites. Using the principles of solid phase extraction (SPE), we will develop a fast and non-disruptive method that can extract only metabolites that are present at surface of macroalgae (Chapter 7). The method could be adapted to different species of algae as well as to other underwater surfaces, and it will allow to get more realistic concentrations of signaling molecules at the interface where interactions between algae and other organisms are taking place.

3. Co-cultivation of a diatom with associated bacteria – a metabolomic approach²

3.1. Introduction

Interactions between microalgae and bacteria cover a wide range of relationships, going from mutualism (Seymour *et al.*, 2017) to pathogenicity (Meyer *et al.*, 2017) (Chapter 1.2). These interactions are fundamental for the co-evolution of phytoplankton and bacteria (Ramanan *et al.*, 2016); they are shaping population dynamics in the oceans (Azam and Malfatti, 2007; Teeling *et al.*, 2012) and are affecting biogeochemical cycles (Grossart and Simon, 2007; Worden *et al.*, 2015).

Such relationships are important not only for the pelagic zone but also for the benthic environment (Haynes *et al.*, 2007), where the high primary production is mainly due to the formation of biofilm constituted by epipellic diatoms and bacteria (Smith and Underwood, 1998).

As explained in chapter 1.2, bacteria influence algal growth and metabolism in different ways. This chapter focuses on the influence of bacteria on growth, endo- and exometabolome of the biofilm-forming benthic pennate diatom *Seminavis robusta* (Chepurnov *et al.*, 2004). *S. robusta* was co-cultivated for 7 days with *Roseovarius* sp., *Maribacter* sp. or *Croceibacter* sp., bacteria isolated from this diatom (MT⁺ 85A, BCCM: DCG0105) (Figure 16). Diatom growth was monitored daily by counting cells under the microscope and at the end of the growth period the diatom cells were extracted and the obtained samples were analyzed with a gas-chromatography high-resolution mass spectrometry (GC-HR-MS) untargeted metabolomics approach to investigate changes in the endometabolome (Figure 16). Additionally, since MT⁺ cells are producing a sexual inducing pheromone (SIP⁺) which is causing cell cycle arrest and diproline production in MT⁻ cells (Moeys *et al.*, 2016), the spent medium of MT⁺ cells was extracted and pheromone chemistry was examined with a liquid chromatography mass spectrometry (LC-MS) targeted analysis to understand if bacteria can modulate SIP⁺ concentration in the medium (Figure 14).

² This chapter is adapted from: Cirri, E., Vyverman, W., & Pohnert, G. (2018). Biofilm interactions-bacteria modulate sexual reproduction success of the diatom *Seminavis robusta*. *FEMS microbiology ecology*, 94(11). And from: Cirri, E.*, Giraldo, J.*, Neupane, S., Willems, A., Mangelinckx, S., Roef, L., Vyverman, W., Pohnert, G Bacteria isolated from *Seminavis robusta* influence growth, biofilm production and the metabolome of *Nannochloropsis* sp. Submitted to *Algal Research*.

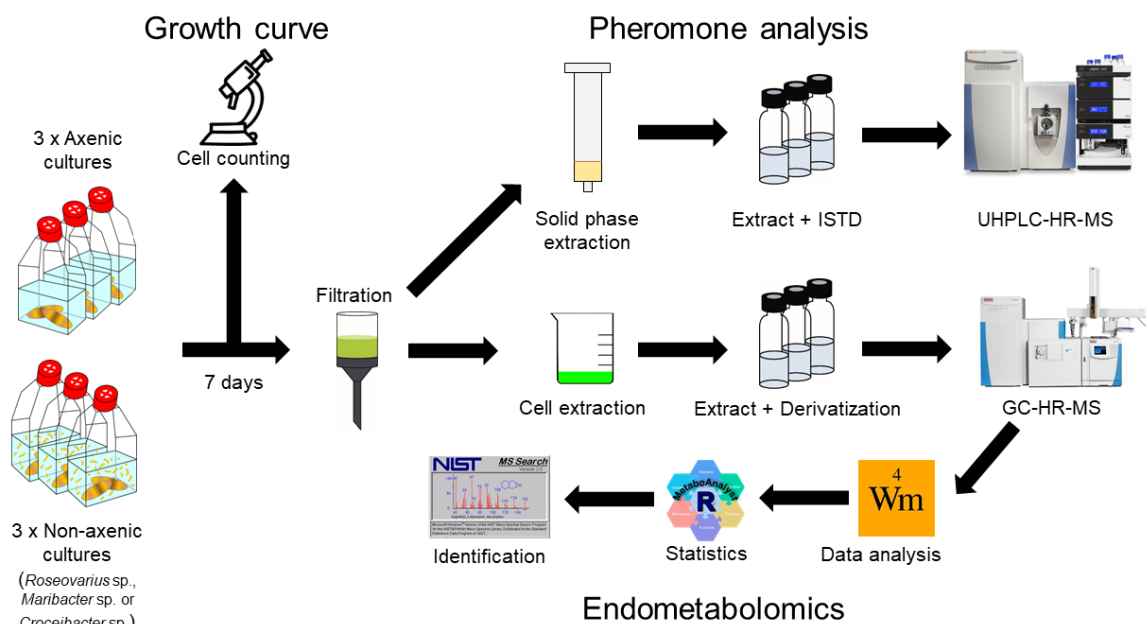


Figure 14: Co-cultivation of a diatom with associated bacteria – a metabolomics approach: experimental setup. Cultures of *S. robusta* strain 85A (MT⁺) were grown for 7 days in presence of absence of bacteria. Each day the cell number was evaluated under the microscope. At the end of the growth period, cells were extracted with organic solvents, samples were derivatized and measured with a GC-HR-MS. Data were analyzed with an untargeted metabolomics approach. For pheromone analysis, medium from the different co cultivations was extracted on SPE cartridges and samples were analyzed with UHPLC-HR-MS.

3.2 Results

3.2.1 Growth of *S. robusta* in co-cultivation with isolated bacteria

Axenic *S. robusta* MT⁺ (strain 85A, cell size = 22.4 μm) was co-cultivated with *Croceibacter* sp., *Roseovarius* sp. and *Maribacter* sp. for seven days (Figure 15). All cultures and the control started from an identical cell density (10^4 cells/ml for both bacteria and diatoms). *Roseovarius* sp. significantly supports algal growth already after two days of co-cultivation ($p = 0.0021$ compared to the control) and this effect is increasing over the days ($p = 0.00029$ at day 7). The culture reaches a cell density 1.5 times higher compared to axenic conditions at day 7. These effects are supported by ANOVA analysis ($P < 0.0001$). *Maribacter* sp. is promoting algal growth as well, although not as consistent as *Roseovarius* (significant up-regulation at 3 out of 7 days, ANOVA interaction $P = 0.0047$). *Croceibacter* sp. does not significantly affect growth of *S. robusta*, since both the multiple comparison and the ANOVA interaction ($P = 0.1847$) are not significant. *Marinobacter* was not used in these co-cultivation experiments due to problems in maintaining *f/2* medium cultures for more

than 12 days and due to frequent contaminations when co-cultivated with *S. robusta* for 7 days.

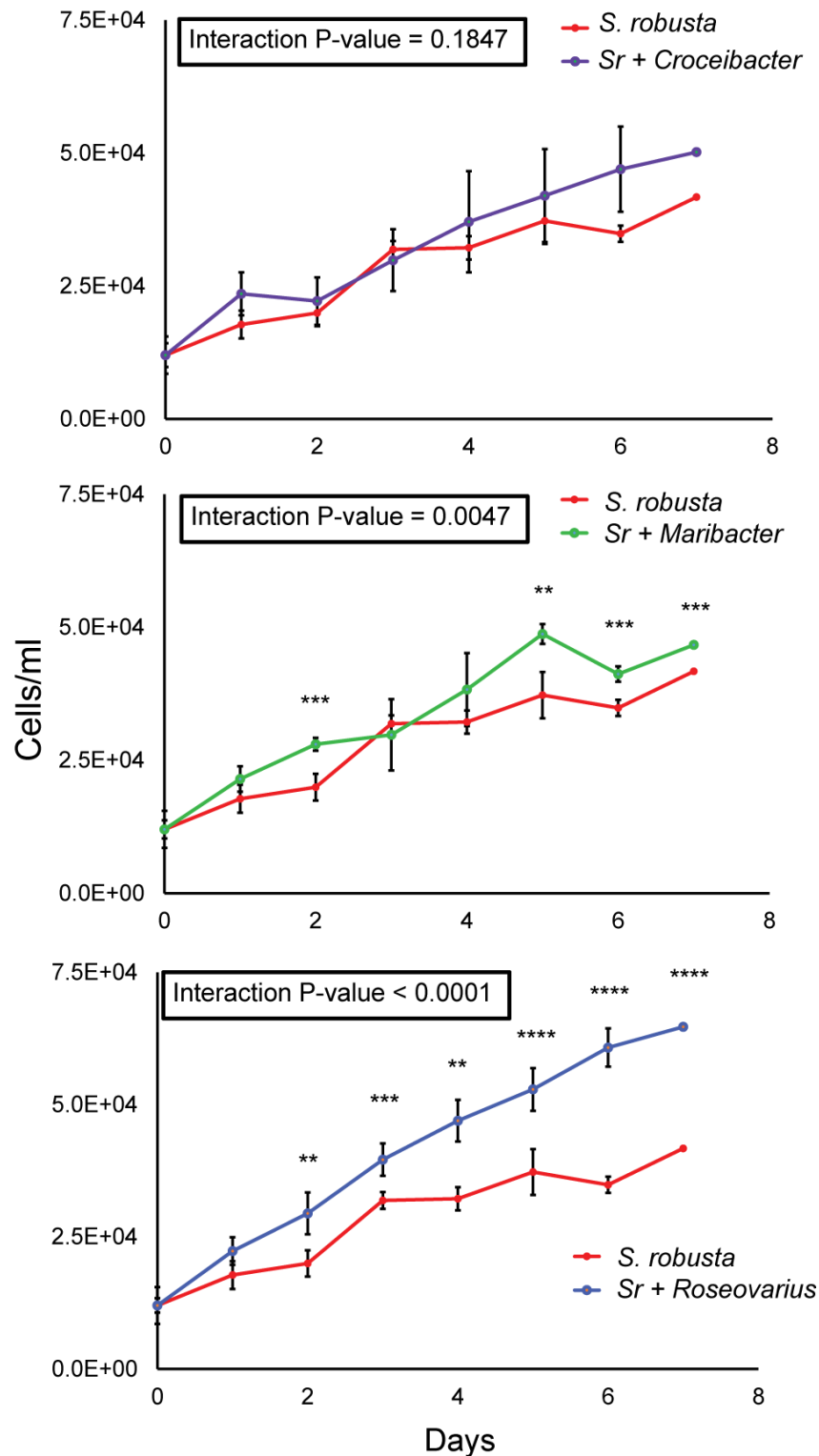


Figure 15: *S. robusta* growth curve in presence of *Croceibacter* sp. (a), *Maribacter* sp. (b) and *Roseovarius* sp. (c). Two-way ANOVA, $\alpha=0.05$, Bonferroni's correction for multiple comparisons. Asterisks refer to multiple comparisons; boxes give results from the two-way ANOVA. *Sr* is an abbreviation for *Seminavis robusta*.

3.2.2 Endometabolome of *S. robusta* is changing in presence of bacteria

After seven days of growth, intracellular extracts of different bacteria-*S. robusta* co-cultivations were prepared and analyzed with an untargeted metabolomics approach to highlight changes in the metabolome of diatoms grown in presence of bacteria. It is important to point out that data were normalized to cell number before statistical analysis, thus preventing biomass difference bias in the evaluation of potential biomarkers. PCA analysis (Figure 16) allows visualization of these changes: cultures treated with *Roseovarius* sp. and *Maribacter* sp. have a different endometabolome than axenic cultures, while *Croceibacter* sp. is causing minor changes and samples from this treatment are overlapping with the control. This result is in line with the observation from the growth of *S. robusta* under different treatments (Figure 15). We therefore focused on the first two bacteria to search for endometabolites that are influencing the separation. PCA loadings plots (Figure 17) show some common features of the two treatments: in both cases, squalene (a precursor of sterols in diatoms (Rampen *et al.*, 2010)), sugars, alditols and a putative ornithine are among the most upregulated metabolites in axenic treatment, while bacterial presence is enhancing the concentration of several disaccharides, some amino acids (in particular alanine) and amino acids derivatives.

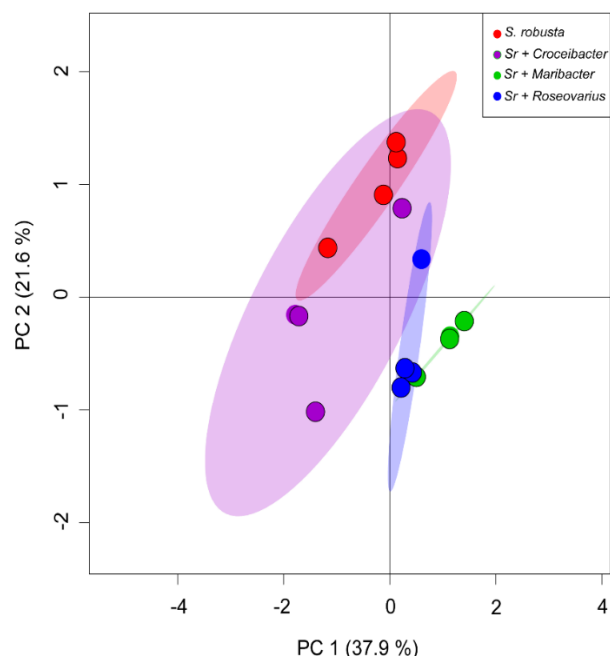


Figure 16: PCA plot of bacterial effect on *S. robusta* endometabolome. Cultures co-cultivated with *Croceibacter* don't show a clear separation from axenic control cultures. *Roseovarius* and *Maribacter* have a more pronounced influence on *S. robusta* endometabolome, grouping similarly and away from the controls. *Sr* is an abbreviation for *Seminavis robusta*.

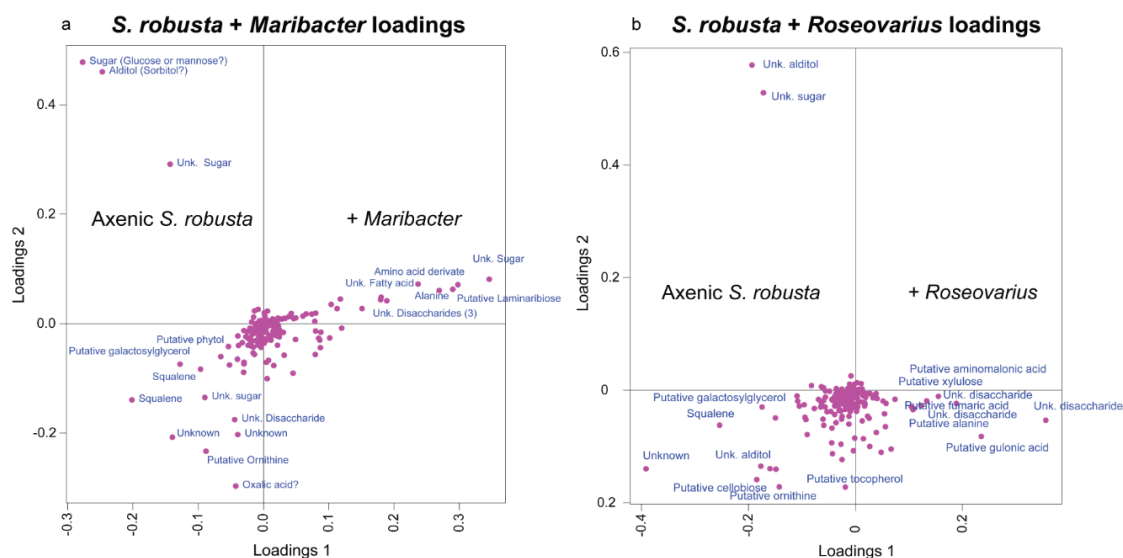


Figure 17: PCA loadings plots for *S. robusta* axenic cultures vs co-cultivations with *Roseovarius* (a) and *Maribacter* (b).

A t-Test ($\alpha = 0.05$) confirmed the significance of these results, which are visualized by heatmaps (Figure 18, only the 25 most significant analytes are reported). When *Roseovarius* sp. is co-cultivated with *S. robusta*, the diatom produces less α -tocopherol (vitamin E) and increases the production of arabinose and a putative aminomalonic acid, while *Maribacter* sp. is stimulating the production of more disaccharides, as for example a putative laminaribiose, and a reduction in phytol and oxalic acid concentrations.

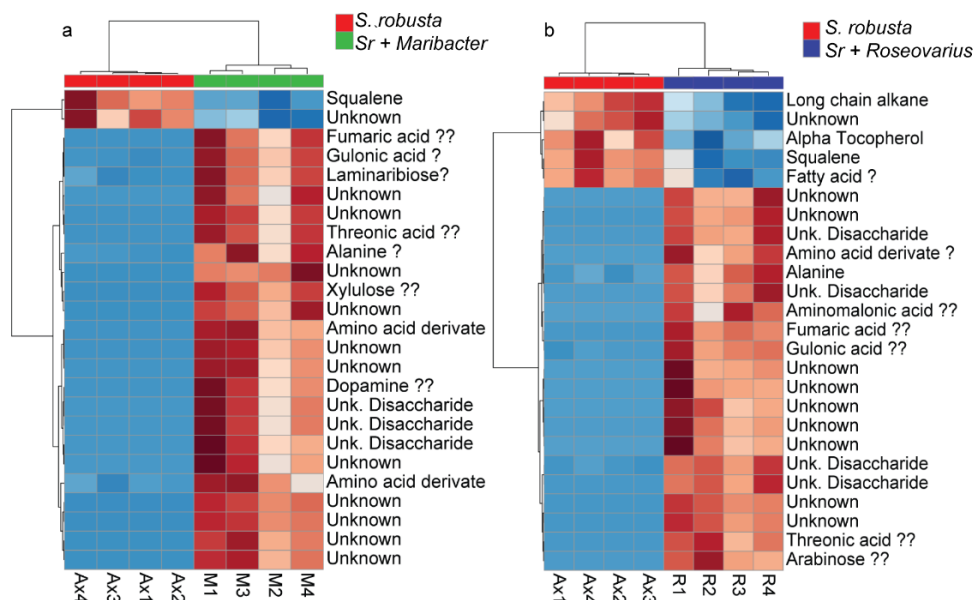


Figure 18: Heatmaps of *S. robusta* axenic cultures vs co-cultivations with *Roseovarius* (a) and *Maribacter* (b). t-Test, $\alpha=0.05$. Mass spectra with a reverse match factor (R Match) > 800 were considered to suggest a reliable structure, tagged with "?" if the R Match was between 800 and 700, with "???" if the RM was between 700 and 600 and "?????" if below 600. Red are upregulated features, blue are downregulated features. *Sr* is an abbreviation for *Seminavis robusta*.

3.2.3 Bacteria modulate sexual inducing pheromone (SIP⁺) from *S. robusta*

During sexual reproduction, *Seminavis robusta* MT⁺ under sexual size threshold (SST=22.4 μ m) is known to release a sexual inducing pheromone (SIP⁺) which is triggering cell cycle arrest and attraction pheromone production in *S. robusta* MT⁻ cells (Moeys *et al.*, 2016). We evaluate the relative concentration of SIP⁺ in different culture conditions to study the effect of bacteria on this pheromone. As figure 19 shows, after 7 days of co-cultivation, the relative concentration of SIP⁺ is higher in axenic conditions if compared to non-axenic conditions. *Maribacter* sp. shows the most important effect on SIP⁺ relative concentration, reducing it significantly ($p = 0.0068$). *Roseovarius* sp. has also a significant influence on SIP⁺ concentration, even if lower than *Maribacter* sp. ($p = 0.0180$), while *Croceibacter* sp. ($p = 0.0650$) has a reduced, non-significant impact on it.

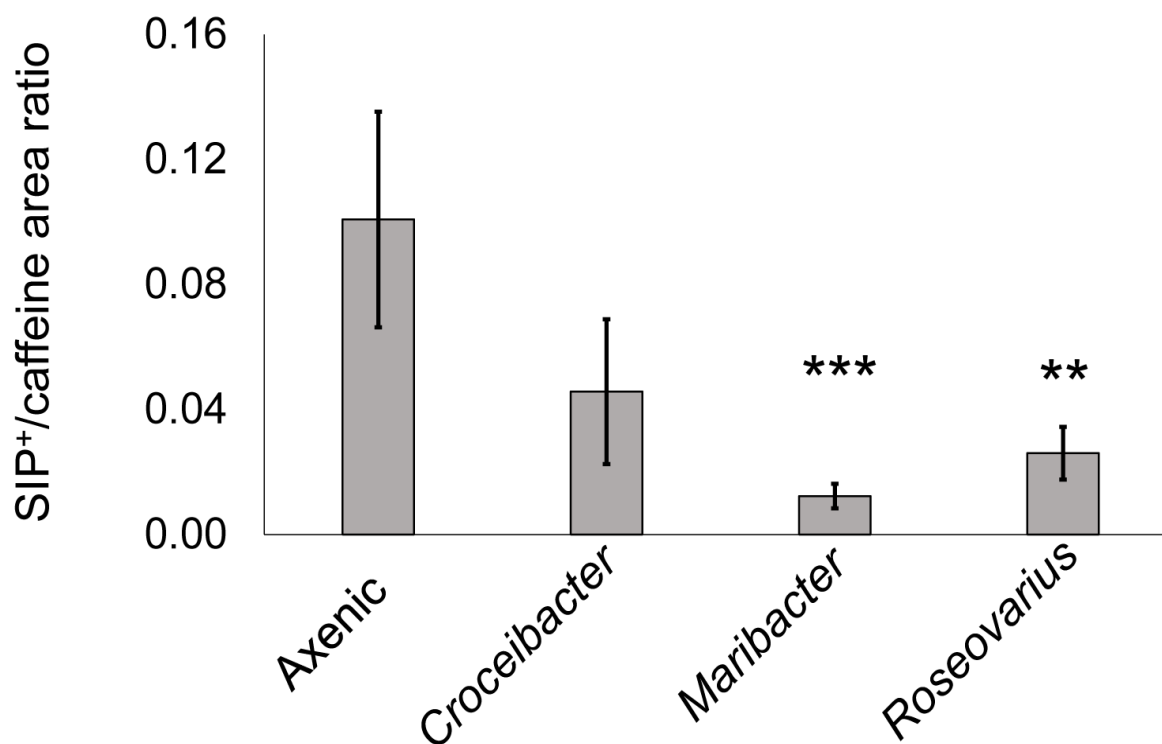


Figure 19: SIP⁺ degradation by the bacteria isolated *S. robusta*. Relative quantities of SIP⁺ are normalized to the internal standard caffeine are given. For each bacterium, three biologically independent treatments are evaluated ($n=3$). Data are normalized to cell count. Significance was evaluated with t-test (unequal variance, $\alpha=0.05$).

3.3 Discussion

In recent years, the crucial role of diatom-bacteria interactions in the balancing of benthic and pelagic ecosystems has become manifest (Amin *et al.*, 2012).

As explained in the introduction to this thesis, these inter-kingdom communications can be based on nutrient and growth factor exchange (Haines and Guillard, 1975; Cooper and Smith, 2015) that take place in the so-called phycosphere (Seymour *et al.*, 2017) and facilitates algal-bacteria mutualism. These interactions have an impact on both players in this relationship: bacteria can influence the phenotype of associated diatoms (Sison-Magnus *et al.*, 2014), stimulating changes in diatom metabolism (Paul, Mausz and Pohnert, 2013) and inducing the production of substrates for attachment and proliferation, for example exopolymeric substances (EPS) in biofilms (Bruckner *et al.*, 2011, Moerdijk-Poortvliet *et al.*, 2018). The host, on the other hand, can deeply affect its microbial environment under different environmental conditions (Grossart *et al.*, 2005; Sapp *et al.*, 2007) by releasing different exudates (Paul *et al.*, 2009).

These microscopic communications control population dynamics (Dang *et al.*, 2016) and organic carbon fluxes (Grossart and Simon, 2007), therefore reverberating on the macroscopic world by affecting biogeochemical cycles (Falkowski, 1994).

Different bacteria have a wide range of effect on *S. robusta* growth over seven days of co-cultivation. *Roseovarius* sp. is considerably supporting diatom growth, *Maribacter* sp. is slightly enhancing it, while *Croceibacter* sp. is not affecting it significantly. Bacteria from the *Roseobacter* clade are known to be associated with diatoms (Amin *et al.*, 2012) and to release metabolites that support algal growth and fitness (Wienhausen *et al.*, 2017). Also *Bacteroidetes* are often associated with diatoms (Bennke *et al.*, 2013) and they are major players in algal blooms thanks to their ability to degrade polysaccharides (Unfried *et al.*, 2018). Their effects on algal growth is species dependent: for example, a *Bacteroidetes* from the benthic freshwater diatom *Cymbella microcephala* supports algal proliferation (Bruckner *et al.*, 2008), while *Croceibacter atlanticus* is responsible for the decrease of cell division and for major physiological changes in the pelagic diatom *T. pseudonana* (Van Tol *et al.*, 2016). A *Maribacter* strain isolated from the Western English Channel showed algicidal effect towards the diatom *Skeletonema* sp. and not towards other species (Wang *et al.*, 2016a), but no other information is available on the effects of this bacterium on microalgae. It has been demonstrated that another *Maribacter* strain is releasing a morphogenetic compound that is essential for the development of the green macroalga *Ulva mutabilis*

(Weiss, Costa and Wichard, 2017), thus confirming its yet underestimated and potentially species-specific importance in algae-bacteria interactions.

Bacteria are also affecting the endometabolome of *S. robusta*. The lower abundance of squalene in comparison to axenic conditions, an important precursor of sterols in diatoms (Fabris *et al.*, 2014), suggests that sterol chemistry is rewired by the presence of bacteria, probably as a response to stress.

The upregulation of many disaccharides may support the hypothesis of an oxidative stress response caused by bacteria. This class of molecules could be an indication polysaccharides breakdown, as it was already observed in the declining phase of some microalgae, like the coccolitophore *E. huxleyi* (Mausz and Pohnert, 2015). The higher concentration of threonic acid in presence of bacteria might result from the breakdown of ascorbic acid (Helsper and Loewus, 1982), a cofactor in de-epoxidation steps of the xanthophyll cycle further functioning in removal of free radicals and their precursors (Raven and Beardall, 2003). However, the presence in axenic cultures of several unknown sugars and alditols could hint to a stress response of the diatom during stationary phase, when glycolysis is activated due to scarcity of resources (Allen *et al.*, 2006.; Vidoudez and Pohner, 2012; Mausz and Pohnert, 2015). Also the presence of galactosylglycerol (Figure 19), a compounds derived from lipid mobilization of galactolipids that occur in photosynthetic tissue of algae and higher plants (van Hummel, 1975), supports this hypothesis. Furthermore, isoprenes like a putative phytol and a putative tocopherol (see Figure 19) have a lower concentration in presence of bacteria. An increased presence of tocopherol is usually correlated to an oxidative stress response during stationary phase of microalgae (Mausz and Pohnert, 2015). These data seem to be contradictory and a biological interpretation that matches the enhancing growth effect of bacteria is not straightforward. Since glycolysis is active in diatoms under starvation or when exposed to toxic substances, bacteria could have a beneficial effect in rewiring the mechanisms that microalgae use to cope with stress. It can also be possible that bacteria are releasing nutrients that reduce or slow down stress response during stationary phase, therefore sustaining algal growth. However, these are highly speculative hypothesis that would need additional experiments and more data to be supported.

Amino acids are only marginally affected by bacterial presence: a putative ornithine was found upregulated in axenic conditions, while alanine and other unknown amino acids derivate were upregulated in presence of bacteria. Ornithine, in particular, plays an important role in diatoms' urea cycle and proline biosynthesis (Bromke, 2013), which is also involved in stress response mechanisms in many plants and some algae (Dar *et al.*, 2016).. Proline is

a fundamental amino acid in diatoms, since it is supposed to be involved in synthesis of the attraction pheromone diproline (Moeys *et al.*, 2016) and it is an important osmoregulator (Krell *et al.*, 2007). The function of these amino acids, however, has not been yet connected to inter-kingdom communications between microalgae and bacteria.

Finally, investigation on *S. robusta* exometabolome and in particular on its pheromone chemistry give us more insights on bacteria effect on diatom's metabolome. Using high resolution mass spectrometry (HR-MS), we observed that cultures co-inoculated with *Maribacter* sp. contain significantly less SIP⁺ in comparison with axenic cultures. Also *Roseovarius* sp. has a strong impact on pheromone concentration, while *Croceibacter* sp. do not have any effect on it. Pheromone signaling is a target of interference and mimicry strategies used by predators to attract or find their preys, or by plants to attract pollinators (Bohman *et al.*, 2016) or to mislead predators (Pregitzer *et al.*, 2012). So far, no form of such interference mechanisms has been found in algae-predators or algae-bacteria interactions. These results, together with the findings of the two following chapters, present for the first time the effect of bacteria on diatoms life cycle and introduce a novel inter-kingdom chemical communication system that could explain complex biofilm organization in aquatic environment.

4. Bacterial modulation of sexual efficiency of the diatom *Seminavis robusta*³

4.1 Introduction

Many species rely on pheromones to synchronize and optimize sexual reproduction. These chemical signals are also frequent targets for interference strategies and guide predators to their prey or help to misguide competitors (Haynes *et al.*, 1999). Such sexual deception strategies are most commonly known from the insect world where mainly attraction and social synchronization pheromones serve as targets (Lehtonen *et al.*, 2014).

In this chapter, we extend the concept of sexual deception to biofilm interactions, in which pheromones play a central role in diatoms' sexual reproduction. In chapter 1.1 the unique features of diatom morphology and physiology have been discussed, in particular their rigid biomineralized silica cell wall with a "lid and box" structure, and their necessity to undergo sexual reproduction in order to survive (Drebes, 1977). A well-studied system is the complex pheromone chemistry of the model species *Seminavis robusta* (Chapter 1.1.3, Gilliard *et al.*, 2013; Moeys *et al.*, 2017). A remarkable feature of one of this pheromones, the attraction pheromone diproline, is its stability in the aqueous medium where there is no sign of pheromone degradation (Gilliard *et al.*, 2013). Nevertheless, in non-axenic cultures of the diatoms a daily rhythm in pheromone concentration is observed. The diatoms only produce diproline within the first hours after the onset of light and subsequently its concentration decreases. As a result, no further attraction of the opposite mating type occurs few hours after daybreak (Gilliard *et al.*, 2013).



Figure 20: Target diproline analysis: general experimental setup. Medium of axenic and non-axenic MT-cultures under different conditions at different time points (see paragraphs 9.3.2-9.3.5) were extracted on SPE cartridges and the samples were measured with a single quadrupole GC-MS (Thermo Scientific® ISQ). Diproline was normalized to the internal standard caffeine.

³ This chapter is adapted from: Cirri, E., Vyverman, W., & Pohnert, G. (2018). Biofilm interactions-bacteria modulate sexual reproduction success of the diatom *Seminavis robusta*. *FEMS microbiology ecology*, 94(11).

In this chapter, we follow up the hypothesis that the cause of the decreasing pheromone concentration is the metabolic activity of bacteria co-existing in the biofilm that modulate pheromone signaling. Bacteria could utilize the pheromones as nutrient source or target the reproductive chemistry to interfere with the proliferation of competing algae. Alternatively, the degradation of an otherwise stable pheromone could support algal mate finding by creating steeper gradients and by avoiding misguidance towards aged pheromone sources. To explore the effect of bacteria on pheromone chemistry and sexual reproduction, different experiments were performed. The concentration of diproline in MT⁻ (strain 84A, BCCM: DCG0104) *S. robusta* medium in presence and absence of bacteria over time (6h, 10h, 13h and 24h), as well as the ability of specific isolated bacteria to degrade the synthetic pheromone were determined with GC-MS targeted analysis (Figure 20). Furthermore, a bioassay to explore the effect of bacteria and bacterial medium on sex efficiency of *S. robusta* was implemented. Briefly, axenic MT⁺ and MT⁻ from *S. robusta* were co-inoculated in well plates and mixed with different concentrations of bacteria or bacteria spent medium. After 24h, the number of cells in different sexual stages were counted under the microscope and percentages of sexual efficiency were calculated (Figure 21).

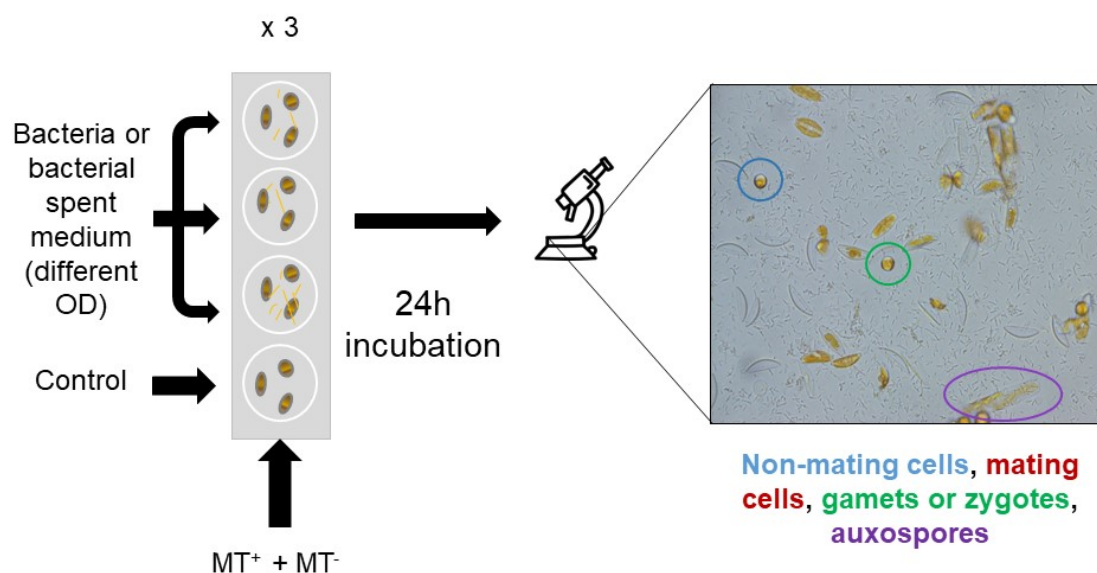


Figure 21: Sexual efficiency bioassay: general experimental setup. Axenic MT⁺ and MT⁻ were mixed together and then bacteria or bacterial medium at different concentrations (OD= 0.1-0.05-0.01-0.005, see paragraph 9.3.1) were added to the mating cultures. Assessment of sexual reproduction efficiency was done by counting the number of cells at different sexual stages under the microscope after 24 hours of incubation. 3 replicates are done for each treatment.

4.2 Results

4.2.1 Sexual reproduction efficiency of *S. robusta* in presence and absence of bacteria

Dark-synchronized MT⁺ (strain 85A) and MT⁻ (strain 84A) cultures below the sexual size threshold SST (cell size: MT⁺ = 22.4 μm, MT⁻ = 23.5 μm) were paired by inoculation in 24 well plates and treated with four different bacteria (*Croceibacter* sp., *Roseovarius* sp., *Maribacter* sp. and *Marinobacter* sp.). Each bacterium was administered in different concentrations with optical densities in the range of 0.005 to 0.1. The effect on sexual reproduction was evaluated after 24 h incubation by counting the number of cells in different stages of reproduction (non-mating cells, mating cells, gametes/zygotes, auxospores) (Chepurnov, 2002). Mating axenic cultures served as controls. The results are reported as percentage of different reproductive stages normalized to the total number of cells (Figure 22 and 23). All treatments were done in triplicate and a two-way ANOVA ($\alpha=0.05$, Bonferroni's correction for multiple comparison, see table ST1 and ST2 in the appendix for statistical evaluation) was performed in order to test the significance of each treatment. All bacterial strains affect sexual reproduction at an OD = 0.1, where the concentration of bacterial cells exceeds that of *S. robusta* 1000 times (Figure 22, table ST1 in the Appendix). In these cases, a significant reduction of auxospores and gametes / zygotes ($P < 0.01$) was observed and the proportion of non-mating cells was increased. At lower bacterial concentrations their different effects on *S. robusta* reproduction manifested. *Maribacter* sp. is the strain with the strongest effect on sexual reproduction, causing significantly less auxospores production ($P < 0.01$ at all concentrations down to OD = 0.01) and higher percentages of non-mating cells ($P < 0.01$ at OD=0.05 at OD=0.01). *Marinobacter* sp. and *Croceibacter* sp. also significantly impair sexual reproduction at OD=0.05 ($P < 0.05$ for all mating stages for both bacteria), but these effects were not observed at lower bacterial concentrations. *Roseovarius* sp. shows no significant negative effect on sexual reproduction at an OD of 0.05. Surprisingly, this strain exhibits significant positive effect on auxospores formation at OD=0.01 and OD=0.005 ($P = 0.0211$ and $P = 0.0312$). No activity was observed in any strain at OD of 0.005, corresponding to cell concentrations below 10^4 cells/mL. To evaluate if physical contact is required for the manifestation of the mating interference or if exuded metabolites or dissolved enzymes mediate the interaction, we conducted an additional set of experiments using bacterial spent medium. Therefore, bacteria were grown in minimal medium to an OD \approx 0.1-0.3 and subsequently the medium was separated from

the cells by sterile filtration, the filtered medium was diluted to obtain concentrations corresponding to the ODs that were used for the experiments described above. These medium preparations were added to *S. robusta* cultures after crossing them in 24-wells plates as described above. The spent medium of three out of the four tested bacteria also inhibits sexual reproduction of the diatoms (Figure 23 and Table ST2). As in the incubations with bacterial cells, *Croceibacter* sp. and *Marinobacter* sp. medium resulted in a significant negative effect at a concentration equivalent to an OD = 0.05 ($P < 0.01$ for all sexual mating stages). The negative effect of *Maribacter* sp. medium on sexual reproduction is highly significant as well at an OD = 0.05 ($P = 0.0022$ for auxospore formation, $P = 0.00210$ for non-mating cells), but it is not observed at the lower OD of 0.01, where activity is still evident for incubations with cells. As in the incubations with cells, *Roseovarius* sp. has a significant positive effect on auxospore-formation observed in the incubation with cells at OD = 0.01 ($P = 0.0012$).

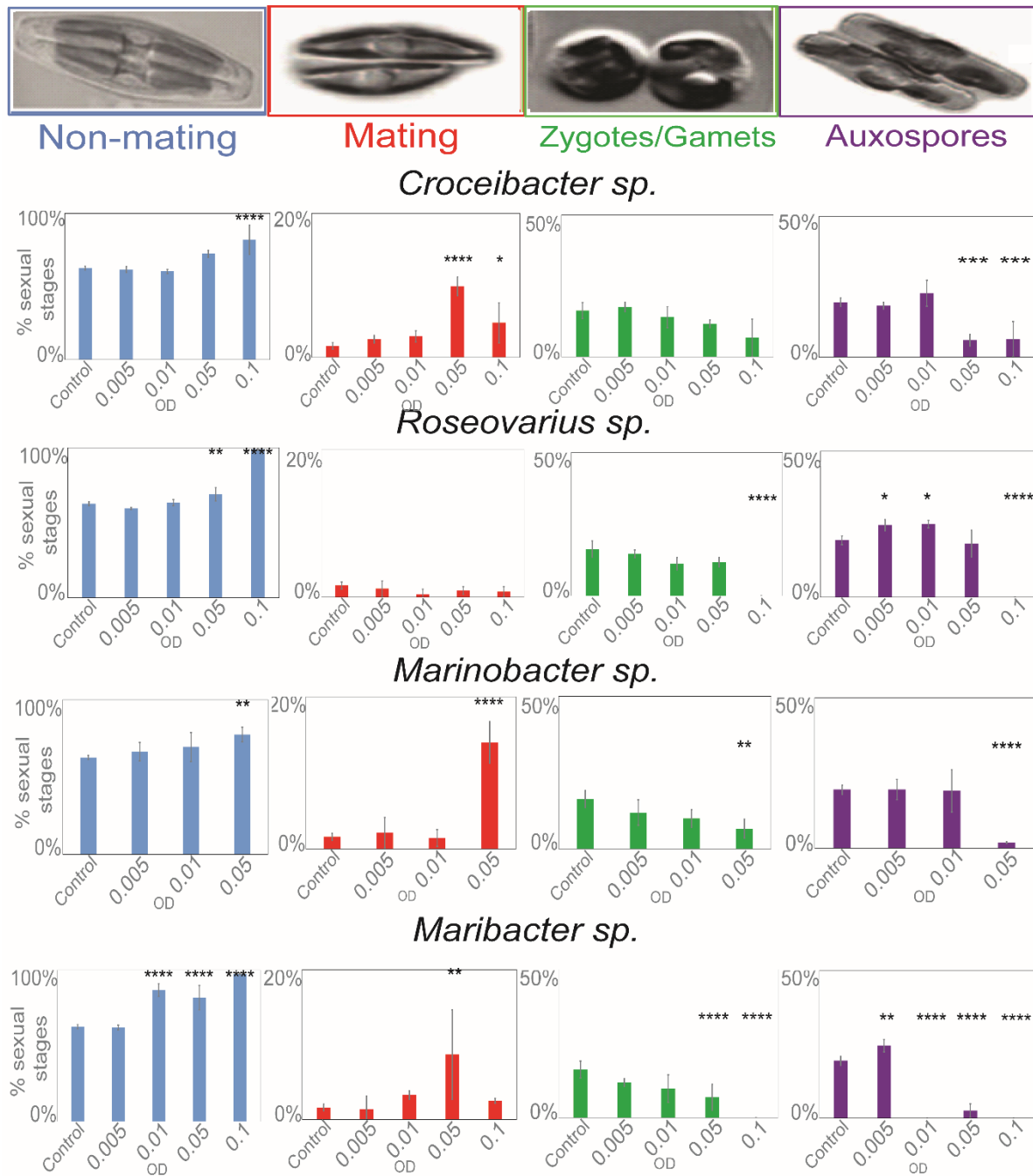


Figure 22. Mating efficiency of *S. robusta* in presence of different bacteria at different optical densities (OD). Ca. 2,000 diatom cells/mL were exposed to 10^4 - 10^6 bacteria cells/mL, Results are based on three independent replicates, 9 pictures for each replicate were evaluated and counted. Different colors indicate different stages in sexual reproduction: blue = non mating cells, red = mating cells, green = gametes / zygotes, purple = auxospores. Results are expressed as percentage of the total counted cells. Significance was evaluated with two-way ANOVA ($\alpha = 0.05$, Bonferroni's correction for multiple comparisons, complete statistical information including error ranges are found in Supporting Table ST1).

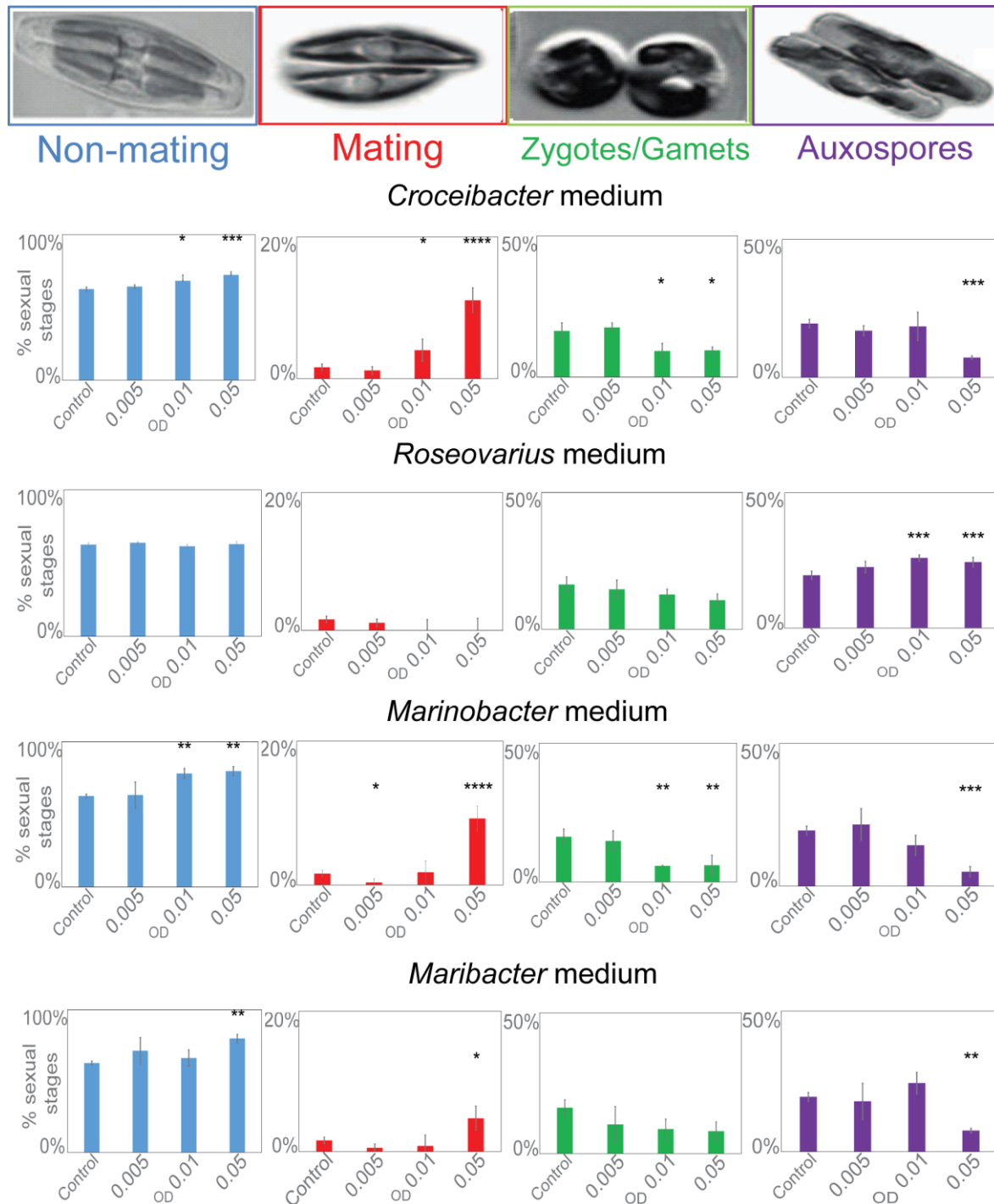


Figure 23. Mating efficiency of *S. robusta* in the presence of spent medium of different bacteria. Ca. 2,000 diatom cells/mL were exposed to 10^4 - 10^6 bacteria cells/mL. Results are based on three independent replicates, 9 pictures for each replicate were evaluated and counted. Different colors indicate different stages in sexual reproduction: blue = non mating cells, red = mating cells, green = gametes / zygotes, purple = auxospores. Results are expressed as percentage of total counted cells. Significance was evaluated with two-way ANOVA ($\alpha=0.05$, Bonferroni's correction for multiple comparisons, complete statistic information including error ranges are found in Supporting Table ST2).

4.2.2 Production of diproline by *S. robusta* and degradation by bacteria

A possible target for bacterial interference of *S. robusta* sexual reproduction is the attraction pheromone diproline, which can be taken up as a nutrient. To elucidate the impact of bacteria on pheromone mediated mate finding, we compared the concentrations of diproline in axenic and non-axenic cultures. Therefore, axenic and non-axenic cultures of *S. robusta* MT⁺ and MT⁻ below the SST were darkness-synchronized at comparable cell densities and combined. The supernatant was extracted at different time points (8 h, 10 h, 13 h, 24 h) after the onset of light and the pheromone was quantified with GC-MS relative to the internal standard caffeine. The concentration of diproline is always higher under axenic conditions compared to non-axenic cultures of similar cell densities (Figure 24a), and the difference between the two treatments is significant from 13 h after the onset of light (Figure 24a). In presence of bacteria, the concentration of diproline is decreasing over time while it is stable or even increasing in axenic cultures. To exclude possible degradation of diproline by the diatoms, we repeated the experiments after removing diatom cells by filtration 6 h after the onset of light. Diproline concentration in these treatments is decreasing even more markedly with an almost complete degradation after 24 h (Figure 24b). Diproline itself is stable in the medium in the absence of bacteria (Gillard *et al.*, 2013, Frenkel *et al.*, 2014b). *S. robusta* associated bacteria are thus efficient degraders of the algal attraction pheromone.

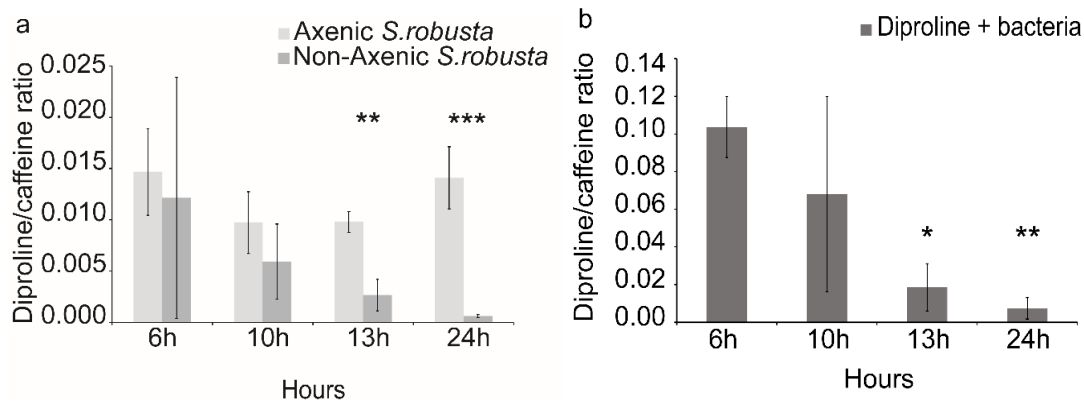


Figure 24. Diproline degradation by the microbial community associated to *S. robusta*. Relative quantities of diproline normalized to the internal standard caffeine are given. For each time point, three biologically independent treatments are evaluated (n=3): a) naturally produced diproline is stable or increasing in the presence of axenic diatom cells (light grey); naturally produced diproline in non-axenic conditions is readily degraded (dark grey). b) Naturally produced diproline is degraded in presence of bacteria and absence of diatom cells (light black). Data are normalized to cell count. Significance was evaluated with t-test (unequal variance, $\alpha=0.05$).

4.2.3 Degradation of synthetic diproline by isolated strains

Selected bacteria isolated from *S. robusta* 85A cultures were tested for their ability to degrade diproline. Bacteria were incubated in nutrient free *f/2* medium containing 300 nM diproline as sole carbon source (Figure 25a) and in modified *f/2* medium supplemented with 300 nM diproline (Figure 25b). After 72 h, bacteria were removed and the culture medium was extracted on solid phase and analyzed by GC/MS as described above. Significant diproline degradation was observed when this diketopiperazine was administered as only carbon source. Given the fact that racemic diproline was administered the ca. 50% consumption could be explained with the metabolization of the natural stereoisomer. If other carbon sources are available in excess as it was the case in cultures in full medium (Figure 25b), the diproline consumption was not significant, indicating preferred or simultaneous use of alternative carbon sources. This experiment indicates that our isolates could metabolize diproline, if limited in alternative carbon sources.

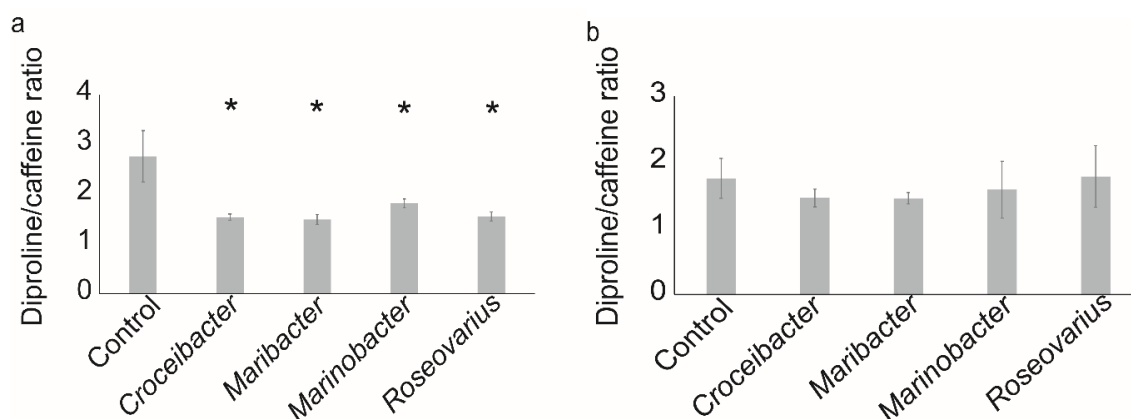


Figure 25. Degradation of synthetic diproline by bacteria isolated from *S. robusta*. Bacterial strains were grown in *f/2* medium (a) or minimal medium (b) ($OD \approx 0.1-0.3$). Diproline was added to a final concentration of 300 nM and incubated for 72 h ($n=3$). Relative quantities of diproline normalized to the internal standard caffeine are given. As a control, minimal medium and *f/2* with 300 nM of diproline were quantified. Significance was evaluated with a t-test (unequal variance, $\alpha=0.05$).

4.3. Discussion

Interactions between diatoms and bacteria are crucial in the balancing of benthic and pelagic communities, as they can regulate entire population dynamics (Dang *et al.*, 2016). Studies revealed that mutual support based on nutrient exchange takes place in mixed communities (Haines and Guillard, 1975; Kazamia *et al.*, 2012; Segev *et al.*, 2016; Suleiman *et al.*, 2016). Vitamins and growth factor exchange also facilitates mutualism between diatoms and bacteria (Amin *et al.*, 2015; Johnson *et al.*, 2016; Seymour *et al.*, 2017). But bacteria can

also negatively influence diatom performance as is most strikingly demonstrated in the case of algicidal bacteria (Meyer *et al.*, 2017). These cause the collapse of entire algal blooms thereby directly controlling the marine food web in a bottom up process (Wang *et al.*, 2014). Here we demonstrate that also the subtler mechanism of signaling interference has evolved in this cross-kingdom interaction with bacteria that inhibit or promote algal sexual reproduction.

We studied the benthic pennate diatom *S. robusta* as model organism for marine biofilm inhabiting diatoms, since we can reliably synchronize its sexual reproduction by sex-inducing pheromones (SIPs) (Moeys *et al.*, 2017). Further, it is the only diatom for which the chemical structure of the attraction pheromone is known (Gillard *et al.*, 2013), thereby enabling a targeted analytical monitoring of pheromone chemistry in the presence and absence of bacteria.

In order to observe ecologically relevant interaction partners we obtained and purified bacterial strains from a *S. robusta* field isolate.

By supplying the four different isolated bacteria to axenic, mating *S. robusta* in a controlled set-up we could show that all four bacterial isolates tested affected *S. robusta* sexual reproduction. In high concentrations (1:1000 ratio of diatom:bacteria cells) all isolates blocked sexuality and nearly exclusively vegetative algal cells were observed in the cultures while efficient mating occurred in controls. If diluted (1:100-1:10 ratio of diatom:bacteria cells), three of the four tested bacteria still inhibited sexuality with *Maribacter* sp. having the strongest, most significant effect. The reduced efficiency of sexual reproduction manifested in an increase in non-sexual cells and a decrease of gametes and auxospores. When the diatom:bacteria cell ratio was below 1:1000, an increased proportion of pairing cells was observed (red bars in Figure 22), indicating that mate finding is still active, but all further stages of the sexual cycle are inhibited. *Croceibacter* sp. and *Marinobacter* sp. show similar but less pronounced activities compared to *Maribacter* sp., causing small shifts in sexual behavior as shown by the higher number of mating diatom cells at higher bacterial concentration and reduced amounts of auxospores and zygotes / gametes only in the case of very high bacterial densities.

Roseovarius sp. represents a remarkable exception. Like all other bacteria it inhibits reproduction at the high OD of 0.1 ($\geq 10^6$ cells/mL) but surprisingly, a significant increase of the proportion of auxospores was induced at lower bacterial concentrations. The bacteria thus specifically promote a sexual state, which indicates a direct influence on the diatom life cycle. The fact that the effects of bacteria on *S. robusta* are species dependent suggests that

complex networks within natural biofilms are established where competition, mutual support and antagonism are driven by chemical communication (Leach *et al.*, 2017). In addition to the diversity of species specific effects also cell densities determine the outcome of the interaction. However, it is difficult to estimate the bacterial densities in diatom dominated biofilms, the actual habitat of *S. robusta*. It was estimated that up to 20 % of the biomass of the biofilms can be attributed to bacteria, thereby cell concentrations of up to 10^6 cells/mL as utilized in our study are plausible (Barranguet *et al.*, 2005).

Algal bacterial interactions can be classified into two major categories. The direct attachment of bacteria on the algae can cause contact interactions mediated by physical as well as (bio)chemical signals. Alternatively, a chemically mediated interaction caused by diffusible factors can mediate the interaction. To distinguish these modes of action, we performed a set of experiments with spent bacterial medium containing the chemical mediators but excluding the cells. Similar effects compared to those caused by the bacterial cultures were observed in all cases, supporting the concept of a chemically mediated mechanism of interaction.

An additional mode of interference could involve the degradation of the attraction pheromone diproline that supports the mate finding process in diatoms. In fact, the concentration of diproline was always higher in axenic conditions compared to co-cultures with bacteria. Analytical quantification revealed that bacteria reduce the concentration of naturally produced as well as of synthetic diproline over time while the compound is stable over 24 hours in axenic cultures. The microbiome associated to *S. robusta* thus actively degrades signaling metabolites from the co-occurring algae. It is likely that bacteria metabolize diproline and use it as carbon and/or nitrogen source since bacterial isolates from *S. robusta* degrade synthetic diproline only in the absence of alternative carbon sources. In accordance, diketopiperazine metabolism and utilization of the liberated amino acids is generally known from bacteria (Tamura *et al.*, 1964; Adams *et al.*, 1978; Kanzaki *et al.*, 1997; Perzborn *et al.*, 2012). This is also supported by the fact that only ca. 50% of the added racemic diproline is degraded (Figure 25a). The remaining D-amino acid derived diproline would not feed the canonical amino acid metabolism as it would be the case for the natural L-proline derived diproline (Figure 25a). It is thus evident that bacteria target both, the attraction pheromone itself as well as the production of sexual cells, thereby affecting diatom sexual reproduction on multiple levels.

Interference with signaling molecules from co-occurring species is well understood for bacterial communication where quorum sensing mediators from competing species are

degraded enzymatically to interfere with the signal mediated synchronization of the competitors (Grandclément *et al.*, 2015). Inter-kingdom signal interference, as it is observed here, is however rather poorly documented. Especially for the highly vulnerable pheromone communication of algae that relies on release, diffusion and perception of chemical signals, interference strategies are not reported.

Our study clearly documents that bacteria play a substantial role in the life cycle of diatoms, especially on sexual reproduction. We further demonstrate that the involved mechanisms are triggered by chemical mediators that most likely contribute to the delicate balance of species in the often highly complex biofilms.

5. Molecular insights into the bacterial effect on sexual reproduction of *S. robusta*⁴

5.1 Introduction

The previous chapter was showed that two bacteria associated with *S. robusta* are able to modulate the concentration of SIP⁺ and the attraction pheromone diproline and the spent medium of both bacteria have different effects on the reproductive success of *S. robusta*. Medium of *Maribacter* sp. negatively affects sexual reproduction, while *Roseovarius* sp. medium slightly enhances it. This novel cross-kingdom interaction adds to the already multifaceted aspects of diatom - bacteria interactions (Amin *et al.*, 2012; Seymour *et al.*, 2017). In order to gain mechanistic insights into the effect of these two bacteria on *S. robusta*, a combination of physiological, metabolomics and transcriptomic approaches was employed (Figure 26).

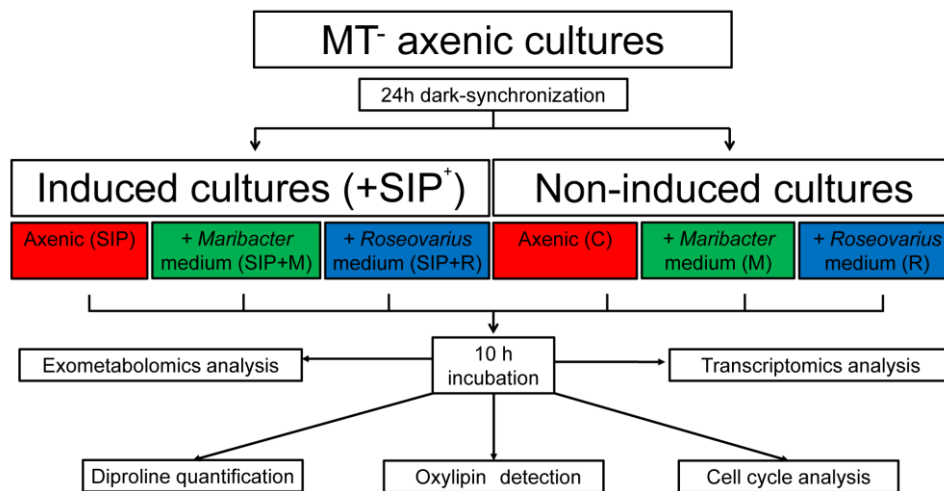


Figure 26. Molecular insights into the effect of bacteria on sexual reproduction of *Seminavis robusta*: experimental setup. Axenic MT⁻ cells were dark-synchronized for 24h and then half of them were induced to sexuality by replacing their medium with 10-times diluted medium from MT⁺ (containing sexual inducing pheromone SIP⁺). A third of the cultures was left axenic as a control, a third treated with *Roseovarius* sp. medium and a third with *Maribacter* sp. medium. Each treatment was done in five replicates. After 10 h of incubation, samples were harvested for different analyses (see section 9.5 for the specifics).

⁴ This chapter is based on: Cirri, E.*, De Decker, S.*, Bilcke, G., Osuna, C., Werner, M., Werz, O., Van Delpoole, K., De Veylder, L., Vyverman, W., Pohnert, G. Associated bacteria affect sexual reproduction by altering gene expression and metabolic processes in a biofilm inhabiting diatom. Submitted to *Molecular Ecology*.

Axenic MT⁻ (84A, BCCM: DCG0104) *S. robusta* cells were dark synchronized for 24 hours prior to undergo different treatments (Gillard *et al.*, 2013; Moeys *et al.*, 2016). Some cultures were induced to sexuality using spent MT⁺ medium containing SIP⁺, while others remained untreated. Two different bacterial media were added to some cultures, leading to a total of six different treatments (Figure 26). After 10 hours of incubation, different analyses were performed.

To investigate the effect of bacterial exudates on the cell cycle, we measured aliquots of each culture with flow cytometry to assess changes in cell cycle progression. A temporary cell cycle arrest is fundamental for a synchronized switch to meiosis in both mating partners (Frenkel *et al.*, 2014a) and sex-inducing pheromones (SIPs) play a pivotal role in this mechanism in *S. robusta*. After 24 h dark-synchronization, control cultures that are not treated with SIP of the opposite mating type (MT) show a peak in the number of cells in S/G2 phase 8-10 h after re-illumination. In cultures treated with SIP of the opposite MT, the cell cycle is temporarily arrested in G1-phase and cultures do not show this peak (Moeys *et al.*, 2016).

Furthermore, RNA was extracted from diatom cells and sequenced. Moeys *et al.*, (2016) identified several genes that might be involved in the early switch from mitosis to meiosis and in cell signaling (especially guanylate cyclase signals). Moreover, they found an upregulation in the proline biosynthetic pathway, which might be connected to the yet unknown process of diproline biosynthesis. In the present experiments, sequences were analyzed with a transcriptomic approach to confirm these genes and to check if bacteria are influencing them, as well as to find new up- and downregulated pathways corresponding to the bacterial treatments.

In parallel, spent medium from the cultures was extracted on SPE cartridges and the samples were analyzed both with targeted analysis to measure the concentration of diproline and of stress markers, like oxylipins, and with an untargeted UHPLC-HR-MS metabolomics approach to unravel putative signaling molecules and unknown compounds released both from *S. robusta* and from the bacteria.

Given the fundamental importance of sexual reproduction in diatoms, unravelling the molecular mechanism laying behind this cross-kingdom interplay is highly relevant to better understand the effect of bacterial presence on diatom performance and how diatoms react to the presence of other organisms during a delicate phase of their life cycle.

5.2 Results

5.2.1 Bacterial exudates do not influence cell cycle arrest during sexual reproduction

We first tested if the effect of the bacterial exudates on sexual reproduction is due to an interference with the regulation of the cell cycle during the initial sexual stages.

The relative number of MT⁻ cells in G1- and S/G2-phase of the cell cycle in six different, all dark-synchronized, treatments (Figure 28): control (not SIP⁺-treated, axenic, C), SIP⁺-treated cultures (axenic, SIP), *Roseovarius* sp.-treated cultures (not SIP⁺-treated, R), *Maribacter* sp.-treated cultures (not SIP⁺-treated, M), *Roseovarius* sp.+ SIP⁺-treated cultures (SIP+R) and *Maribacter* sp.+ SIP⁺-treated cultures (SIP+M).

Ten hours after re-illumination, the percentage of cells in S/G2 phase was significantly lower ($p < 0.001$) in the SIP⁺-treated cultures compared to controls, confirming that SIP⁺ is indeed blocking cell cycle progression (Figure 27). The presence of bacterial spent medium only (without SIP⁺ induction) does not reduce the peak in S/G2-phase cells, suggesting that the exudates do not affect the cell cycle progression in mitotic cells. Most importantly, the presence of the bacterial medium does not influence the SIP⁺-induced cell cycle arrest. This is supported by post-hoc multiple contrasts (SIP vs SIP+M and SIP vs SIP+R) that do not show significant effects of bacterial medium on cell cycle progression compared with SIP⁺-treated cultures ($p=0.8$ and $p=0.91$, respectively).

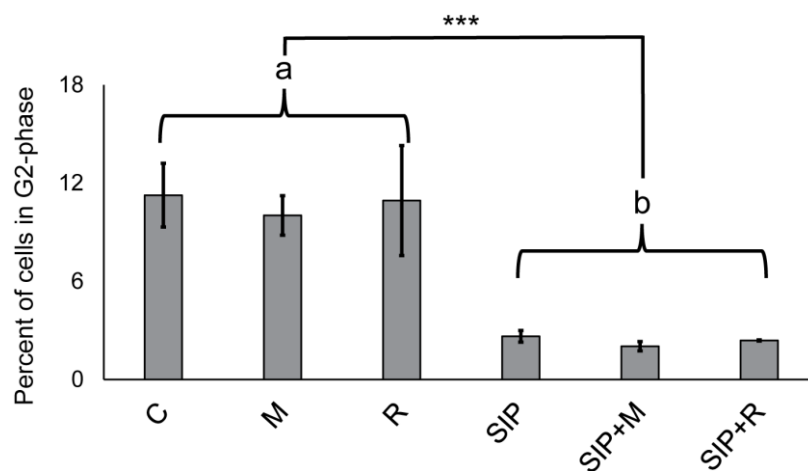


Figure 27: Cell cycle analysis. Flow cytometry measurements of the percentages of cells that have progressed through S-phase for all six experimental treatments. C is the axenic, non-induced control, M is non-induced control + *Maribacter* sp. medium, R is non-induced control + *Roseovarius* sp. medium, SIP is induced axenic control, SIP+M is induced culture + *Maribacter* sp. medium, SIP+R is induced control + *Roseovarius* sp. medium. Proportion post-S-phase cells differed significantly between all non-conditioned cells (“a”) and SIP+-conditioned cells (“b”).

5.2.2 Bacterial medium does not drastically influence expression of known sexual reproduction genes

To study the bacteria-induced transcriptional changes in sexualized MT⁻ cells, we extracted mRNA of SIP⁺-induced and non-induced cultures; both untreated and treated with bacterial spent medium after 24h dark-synchronization followed by 10h of illumination (Figure 28). We obtained expression data for 25.557 genes. 4.225 unique genes (16,6% of the expressed genes) were differentially expressed (DE) in at least one treatment (Table 2, $|\log_2$ fold change $| > 1$, FDR < 0.05) and more than half of these genes were functionally annotated ($> 59\%$ in each comparison).

	SIP vs C	SIP+M vs M	SIP+R vs R	M vs C	SIP+M vs SIP	R vs C	SIP+R vs SIP
Up	983	484	613	268	406	105	180
Not Sign.	22305	23716	23344	25226	25027	25450	25367
Down	2269	1357	1600	63	124	2	10

Table 2: Summary of the number of significantly differentially expressed genes in different comparisons.

A multidimensional scaling (MDS) plot of all RNAseq libraries (Figure 28) shows that the biggest separation between samples is caused by the induction of sexuality (SIP⁺-treatment). This was confirmed by the high number of DE genes in induced cultures compared to non-induced cultures (Table 2 and Appendix Figure S4, SIP vs C: 983 up-regulated and 2269 down-regulated genes; SIP+M vs M: 484 up-regulated and 1357 down-regulated genes; SIP+R vs R: 613 up-regulated and 1600 down-regulated genes).

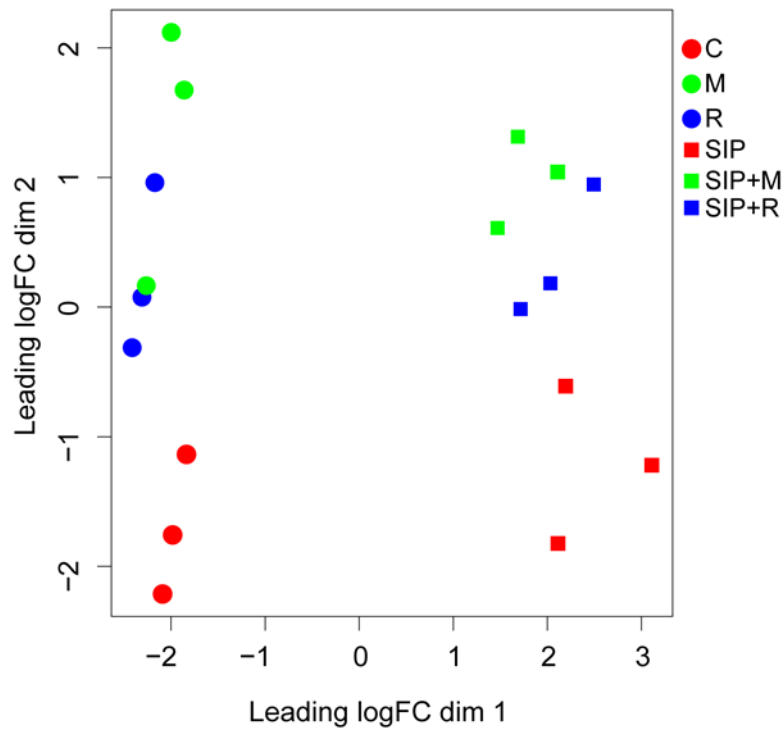


Figure 28: Multi-dimensional scaling plot for transcriptomic data. Distance between samples is calculated with based on \log_2 fold changes. C is axenic non-induced control, M is non-induced control + *Maribacter* sp. medium, R is non-induced control + *Roseovarius* sp. medium, SIP is induced axenic control, SIP+M is induced culture + *Maribacter* sp. medium, SIP+R is induced control + *Roseovarius* sp. medium.

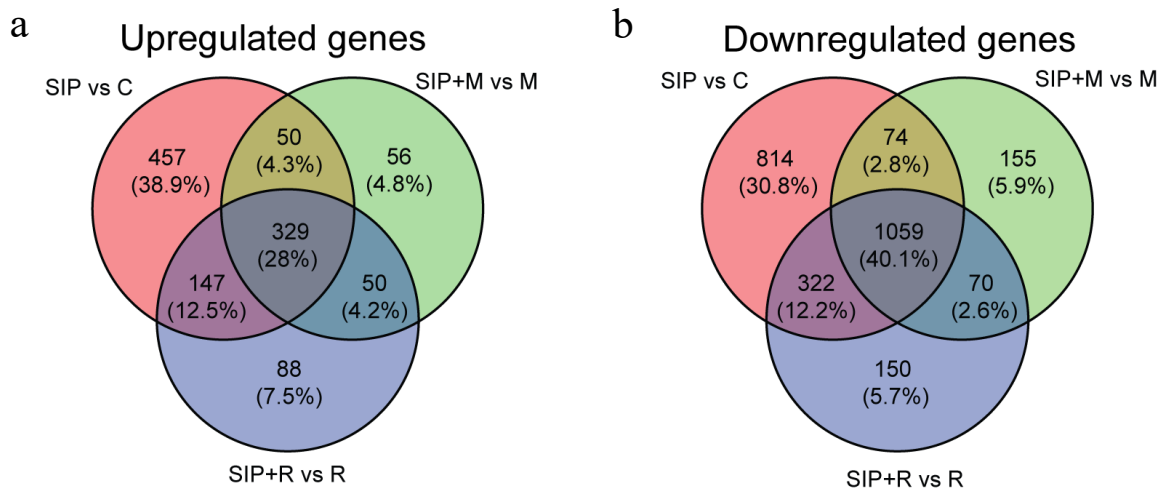


Figure 29: Venn diagrams of up- (a) and downregulated (b) *S. robusta* genes under SIP+ influence. The up- and downregulated genes thresholds are: \log_2 fold change (LFC)= 1, false discovery rate (FDR)= 0.05

Moreover, comparisons of control cultures (C), *Maribacter*-treated cultures (M) and *Roseovarius*-treated cultures (R) with their SIP⁺-treated equivalents (SIP, SIP+M and SIP+R, respectively) showed that a high amount of genes that are up- or downregulated in the presence of SIP⁺ are shared in all three comparisons (329 upregulated genes, 28% of the total upregulated genes and 1059 downregulated genes, 40.1% of the total downregulated

genes) (Figure 29). Of this shared set of 329 genes that are SIP⁺-upregulated despite bacterial presence, some are related to early meiosis-related processes (Table 3), especially dsDNA break repair, DNA duplex unwinding and DNA replication. We also found upregulation of cAMP/cGMP signaling and phosphodiesterase activity (PDE) (Table 3). It has been shown that cGMP signaling likely plays an important role during the onset of sexual reproduction in pennate diatoms (Moeys *et al.*, 2016; Basu *et al.*, 2018). The upregulation of these genes was not unambiguous, with some GC/PDE genes showing higher upregulation in axenic conditions (Sro991_g228730, LFC=4.09, Table 4) while others being more upregulated either in presence of *Roseovarius* sp. (Sro1233_g254830) or in presence of *Maribacter* sp. (Sro218_g090200, Sro1656_g289030). The transcriptional patterns of these genes suggest a complex involvement of different cGMP-related signaling pathways during sexual reproduction and the perception of bacterial presence.

Interestingly, expression of several receptor-type guanylate cyclase with PDE activities was triggered by the bacteria, especially by *Maribacter* sp. spent medium (upregulation of 8 guanylate cyclase SIP⁺M vs SIP, two of which containing a PDE domain in, Appendix Table ST6). This bacteria-elicited receptor-type guanylate cyclase are different from those involved in SIP⁺-induced signaling in *S. robusta* MT⁻, thus hinting to a broader and bacteria-specific response of *S. robusta* receptor-type guanylate cyclase towards compounds of bacterial origin.

Moreover, the proline biosynthetic pathway was strongly upregulated in all SIP⁺-induced treatments (Table 3). Moreover, the proline biosynthetic pathway was strongly upregulated in all SIP⁺-induced treatments, despite the presence of either bacterial exudate. Interestingly, the upregulation was stronger in the presence of *Roseovarius* sp. A Δ 1-pyrroline-5-carboxylate synthetase (*P5CS*, Sro2012_g310890), a key enzyme in proline biosynthesis (Hu, Delauney, & Verma, 1992), was upregulated in SIP vs C, SIP+M vs M and SIP+R vs R, but the strongest upregulation was observed in presence of *Roseovarius* sp. medium (LFC = 6.89, FDR < 10⁻⁶), while upregulation was less strong in axenic conditions (LFC = 3.64, FDR < 10⁻⁴) and in presence of *Maribacter* sp. medium (LFC = 4.94, FDR < 10⁻⁵). Another gene of this pathway, Δ 1-pyrroline-5-carboxylate reductase (*PC5*, Sro216_g089310), was upregulated in SIP vs C, SIP+M vs M and SIP+R vs R. Also here, upregulation was stronger in the presence of *Roseovarius* sp. medium (LFC = 4.46, FDR < 10⁻⁵) than in presence of *Maribacter* sp. medium (LFC = 3.15, FDR < 10⁻³) or in axenic conditions (LFC= 3.84, FDR < 10⁻⁴).

In conclusion, of the known SIP⁺-triggered processes, early meiosis and cGMP signaling are not significantly affected by either bacterium, while proline synthesis is more strongly induced in presence of *Roseovarius* sp. exudates. Expression of proline biosynthesis genes is less affected by *Maribacter* sp. exudates.

GO ID	GO Function	Genes	p-value
Biological function			
GO:0006561	proline biosynthetic process	2	0.0002
GO:0032508	DNA duplex unwinding	4	6.10E-04
GO:0007535	donor selection	2	6.80E-04
GO:0009154	purine ribonucleotide catabolic process	12	2.50E-03
GO:0061028	establishment of endothelial barrier	8	2.69E-03
GO:0019933	cAMP-mediated signaling	8	3.48E-03
GO:0006302	double-strand break repair	5	5.25E-03
GO:0002109	maturation of SSU-rRNA from tricistronic rRNA transcript	1	5.83E-03
GO:0045005	DNA-dependent DNA replication maintenance of fidelity	2	7.76E-03
GO:0000718	nucleotide-excision repair, DNA damage removal	2	0.00914
GO:0010777	meiotic mismatch repair involved in reciprocal meiotic recombination	1	1.16E-02
GO:0006284	base-excision repair	2	1.30E-02
Molecular function			
GO:0030552	cAMP binding	8	2.80E-03
GO:0004115	3',5'-cyclic-AMP phosphodiesterase activity	8	2.80E-03
GO:0004735	pyrroline-5-carboxylate reductase activity	1	5.90E-03
GO:0004505	phenylalanine 4-monooxygenase activity	1	5.90E-03
GO:0034617	tetrahydrobiopterin binding	1	5.90E-03
GO:0008094	DNA-dependent ATPase activity	3	8.00E-03
GO:0017084	delta1-pyrroline-5-carboxylate synthetase activity	1	1.18E-02
GO:0004147	dihydroliipoamide branched chain acyltransferase activity	1	1.18E-02
GO:0004528	phosphodiesterase I activity	1	1.77E-02
Cellular component			
GO:0000795	synaptonemal complex	2	0.0023
GO:0043073	germ cell nucleus	2	0.0044
GO:0005856	cytoskeleton	11	0.0154

Table 3: Upregulated pathways shared by all SIP+-induced cultures compared to non-induced controls (SIP vs C, SIP+M vs M, SIP+R vs R).

Function	Gene ID	Description	SIP ⁺	SIP ⁺ + M	SIP ⁺ + R
Proline biosynthesis	Sro2012_g310890	Δ 1-pyrroline-5-carboxylate synthetase	3.64	4.94	6.89
	Sro216_g089310	Pyrroline-5-carboxylate reductase	3.84	3.15	4.46
Mitotic-related genes	Sro371_g128600	MCM8	2.00	NF	2.06
	Sro552_g165070	MSH4	2.25	2.68	NF
	Sro13_g010240	Double-strand break repair protein MRE11	2.73	2.63	2.88
Guanylate cyclase	Sro931_g221400	Affinity cAMP-specific and IBMX-insensitive 3',5'-cyclic phosphodiesterase	5.91	4.62	5.05
	Sro382_g131010	Inhibited 3',5'-cyclic phosphodiesterase B	6.53	4.20	4.49
	Sro931_g221440	Receptor-type guanylate cyclase gcy	5.16	4.44	4.28
	Sro218_g090200	Guanylate cyclase type - natriuretic peptide receptor 2	4.12	4.81	3.22
	Sro1656_g289030	Receptor-type guanylate cyclase gcy	5.44	6.73	4.25
	Sro1233_g254830	Receptor-type guanylate cyclase gcy	2.21	2.25	3.06
	Sro804_g204860	Receptor-type guanylate cyclase gcy	7.02	7.53	7.40
	Sro141_g065940	Receptor-type guanylate cyclase gcy	3.85	3.24	3.49
	Sro109_g054500	Receptor-type guanylate cyclase gcy	3.35	3.43	3.15
Sro991_g228730	Receptor-type guanylate cyclase gcy	4.09	NF	NF	

Table 4: Upregulated genes involved in sexual reproduction and diproline production shared by all SIP+-induced cultures compared to non-induced controls (SIP vs C, SIP+M vs M, SIP+R vs R). Mitotic-related genes explanation: *MRE11* (Sro13_g010240) is part of the Mre11-Rad50-Nbs1 complex involved in repairing DNA double-strand breaks and homologous recombination during meiosis (Ajimura *et al.*, 1993). *MSH4* (Sro552_g165070) is a meiosis-specific mismatch repair protein (Kolas and Cohen, 2004). *MCM8* (Sro371_g128600) is involved in meiotic recombination (Blanton *et al.*, 2005).

5.2.3 *Maribacter* sp. causes major transcriptional changes in *S. robusta*

The second major separation observed in the MDS plot corresponds to the presence or absence of bacterial medium in MT⁻ cultures (Figure 28). Interestingly, the replicates of SIP⁺-induced samples treated with bacterial medium (SIP+M and SIP+R) cluster together more closely compared to the replicates of non-induced samples (M and R), suggesting that the transcriptional changes induced by the bacterial exudates are more coherent when SIP⁺ is present. Additionally, the number of DE genes was higher when bacterial spent medium was added to SIP⁺-treated cultures compared to when the bacterial medium was added to non-sexualized cultures (M vs C: 331 DE genes; SIP+M vs SIP: 530 DE genes; R vs C: 107 DE genes; SIP+R vs SIP: 190 DE genes). Moreover, there is only limited overlap between genes that are DE in response to bacterial exudates in presence and absence of SIP⁺ (Appendix Figure S5).

Since *Maribacter* sp. and *Roseovarius* sp. affect sexual reproduction of *S. robusta*, we focused on transcriptional changes induced by these bacteria in sexualized cultures (SIP+M vs SIP and SIP+R vs SIP). Venn diagrams showing the numbers of shared and unique up- and downregulated genes between SIP+M vs SIP and SIP+R vs SIP are respectively shown in Figure 32 a and b, while Venn diagrams in Figure 32 c and d display up- and downregulated genes in M vs C and R vs C, respectively.

Both in sexualized and non-sexualized cultures, *Maribacter* spent medium triggered significantly more transcriptional changes compared to *Roseovarius* sp. spent medium (Table 2, Figure 32 and Appendix Figure S4 and S5). This confirms the stronger negative effect of *Maribacter* sp. on both the physiology and sexuality of *S. robusta* compared to the mild positive effect of *Roseovarius* sp. (Chapter 4). GO enrichment of a set of genes that is only upregulated by *Maribacter* sp. exudates in the presence of SIP⁺ (SIP+M vs SIP) showed induction of a number of redox processes involving sterols and fatty acids, as well as sulfite reductase NHDP dependent functions (Table 5). These processes were not induced by *Maribacter* sp. in the absence of SIP⁺ (M vs C).

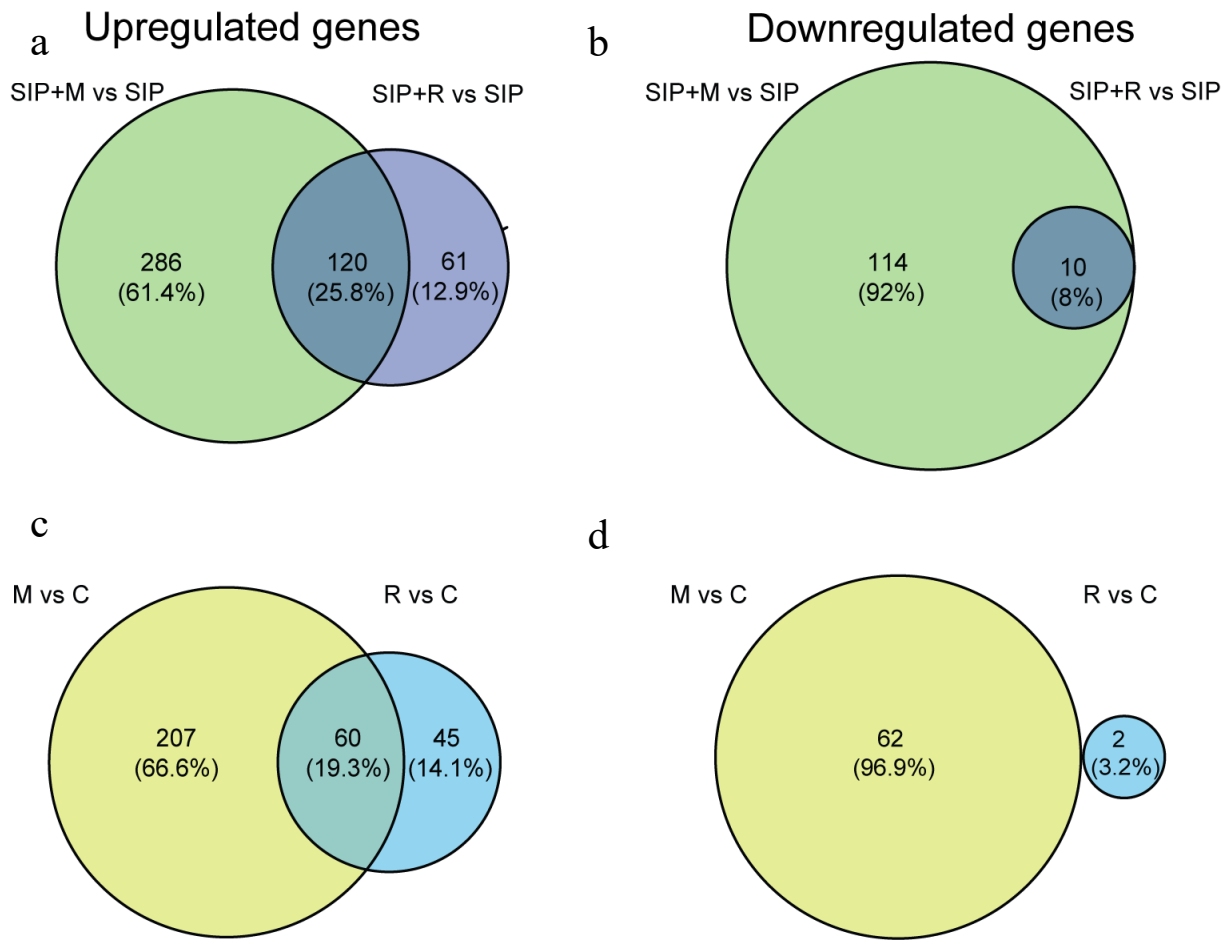


Figure 30: Venn diagrams of up- (a and c) and downregulated (b and d) *S. robusta* genes under bacterial influence. a) and b) refers to SIP⁺ induced treatment, c) and d) refer to non-induced conditions. The up- and downregulated genes thresholds are: log₂ fold change (LFC)= 1, false discovery rate (FDR)= 0.05

GO ID	GO Function	Genes	p-value
Biological functions			
GO:0006779	porphyrin-containing compound biosynthetic process	9	8.40E-09
GO:0009768	photosynthesis, light harvesting in photosystem I	4	2.50E-05
GO:0015994	chlorophyll metabolic process	5	2.70E-05
GO:0010218	response to far red light	4	4.60E-04
GO:0010114	response to red light	4	8.40E-04
GO:0016116	carotenoid metabolic process	3	1.44E-03
GO:0055114	oxidation-reduction process	23	1.79E-03
GO:0009637	response to blue light	4	2.43E-03
GO:0042374	phyloquinone metabolic process	2	3.43E-03
GO:0070127	tRNA aminoacylation for mitochondrial protein translation	2	6.27E-03
GO:0000103	sulfate assimilation	2	7.98E-03
GO:0031388	organic acid phosphorylation	1	1.55E-02
GO:0019424	sulfide oxidation, using siroheme sulfite reductase	1	1.55E-02
GO:0007225	patched ligand maturation	1	1.55E-02
GO:0042049	cellular acyl-CoA homeostasis	1	1.55E-02
GO:0009704	de-etiolation	1	1.55E-02
GO:0006427	histidyl-tRNA aminoacylation	1	1.55E-02
GO:1900160	plastid DNA packaging	1	1.55E-02
Molecular Functions			
GO:0004783	sulfite reductase (NADPH) activity	2	0.00023
GO:0042286	glutamate-1-semialdehyde 2,1-aminomutase activity	2	2.30E-04
GO:0016634	oxidoreductase activity, acting on the CH-CH group of donors, oxygen as acceptor	2	2.22E-03
GO:0010181	FMN binding	2	3.30E-03
GO:0004500	dopamine beta-monoxygenase activity	2	1.15E-02
GO:0050311	sulfite reductase (ferredoxin) activity	1	1.52E-02
GO:0004853	uroporphyrinogen decarboxylase activity	1	1.52E-02
GO:0015390	purine-specific nucleoside:sodium symporter activity	1	1.52E-02
GO:0050561	glutamate-tRNA(Gln) ligase activity	1	1.52E-02
GO:0004631	phosphomevalonate kinase activity	1	1.52E-02
GO:0004821	histidine-tRNA ligase activity	1	1.52E-02
GO:0030248	cellulose binding	1	1.52E-02
GO:0004160	dihydroxy-acid dehydratase activity	1	1.52E-02
GO:0015389	pyrimidine- and adenine-specific:sodium symporter activity	1	1.52E-02
GO:0016162	cellulose 1,4-beta-cellobiosidase activity	1	1.52E-02
GO:0047012	sterol-4-alpha-carboxylate 3-dehydrogenase (decarboxylating) activity	1	1.52E-02
GO:0008685	2-C-methyl-D-erythritol 2,4-cyclodiphosphate synthase activity	1	1.52E-02
GO:0016002	sulfite reductase activity	1	1.52E-02
GO:0009976	tocopherol cyclase activity	1	1.52E-02
GO:0003864	3-methyl-2-oxobutanoate hydroxymethyltransferase activity	1	1.52E-02
GO:0003854	3-beta-hydroxy-delta5-steroid dehydrogenase activity	1	1.52E-02
GO:0000252	C-3 sterol dehydrogenase (C-4 sterol decarboxylase) activity	1	1.52E-02
GO:0050421	nitrite reductase (NO-forming) activity	1	1.52E-02
Cellular component			
GO:0044434	chloroplast part	55	6.6E-29
GO:0009337	sulfite reductase complex (NADPH)	2	0.00027
GO:0048046	apoplast	7	0.00028
GO:0020011	apicoplast	8	0.00093
GO:0009509	chromoplast	2	0.00389

Table 5: Upregulated pathways induced by *Maribacter sp.* medium in SIP⁺-induced cultures (SIP+M vs SIP).

GO ID	GO Function	Genes	p-value
Biological function			
GO:1902000	homogentisate catabolic process	2	8.50E-07
GO:0006572	tyrosine catabolic process	2	4.20E-06
GO:0006527	arginine catabolic process	2	4.20E-06
GO:0006559	L-phenylalanine catabolic process	2	7.90E-06
GO:0008205	ecdysone metabolic process	1	6.10E-04
GO:0008210	estrogen metabolic process	1	4.29E-03
GO:0008209	androgen metabolic process	1	6.13E-03
GO:0033327	Leydig cell differentiation	1	8.57E-03
GO:0019433	triglyceride catabolic process	1	1.04E-02
GO:0009083	branched-chain amino acid catabolic process	1	1.47E-02
Molecular function			
GO:0004334	fumarylacetoacetase activity	2	1.20E-06
GO:0008709	cholate 7-alpha-dehydrogenase activity	1	7.40E-04
GO:0047022	7-beta-hydroxysteroid dehydrogenase (NADP+) activity	1	7.40E-04
GO:0001540	amyloid-beta binding	1	1.48E-03
GO:0004303	estradiol 17-beta-dehydrogenase activity	1	1.48E-03
GO:0018454	acetoacetyl-CoA reductase activity	1	3.71E-03
GO:0003857	3-hydroxyacyl-CoA dehydrogenase activity	1	6.67E-03
GO:0004806	triglyceride lipase activity	1	1.04E-02
Cellular component			
GO:0012511	monolayer-surrounded lipid storage body	1	2.00E-03

Table 6: Downregulated pathways shared by control and SIP⁺-induced cultures treated with *Maribacter sp.* medium (SIP+M vs SIP, M vs C).

GO ID	GO Function	Genes	p-value
Biological function			
GO:0009083	branched-chain amino acid catabolic process	7	5.20E-12
GO:0006559	L-phenylalanine catabolic process	4	2.20E-08
GO:0006570	tyrosine metabolic process	4	1.00E-07
GO:0051262	protein tetramerization	4	3.20E-05
GO:1902000	homogentisate catabolic process	2	5.70E-05
GO:0006637	acyl-CoA metabolic process	4	1.10E-04
GO:0006527	arginine catabolic process	2	2.80E-04
GO:0006567	threonine catabolic process	2	4.00E-04
GO:0033539	fatty acid beta-oxidation using acyl-CoA dehydrogenase	2	5.30E-04
GO:0000098	sulfur amino acid catabolic process	2	2.50E-03
GO:0010188	response to microbial phytotoxin	1	4.45E-03
GO:0044524	protein sulfhydration	1	4.45E-03
GO:0018272	protein-pyridoxal-5-phosphate linkage via peptidyl-N6-pyridoxal phosphate-L-lysine	1	4.45E-03
GO:0008205	ecdysone metabolic process	1	4.45E-03
GO:0007563	regulation of eclosion	1	4.45E-03
GO:0048830	adventitious root development	1	4.45E-03
GO:0009684	indoleacetic acid biosynthetic process	1	8.89E-03
GO:0002047	phenazine biosynthetic process	1	8.89E-03
GO:0019343	cysteine biosynthetic process via cystathionine	1	8.89E-03
GO:0046951	ketone body biosynthetic process	1	8.89E-03
GO:0001560	regulation of cell growth by extracellular stimulus	1	8.89E-03
GO:0019346	transsulfuration	1	1.33E-02
Molecular functions			
GO:0004485	methylcrotonoyl-CoA carboxylase activity	2	2.10E-05
GO:0016937	short-branched-chain-acyl-CoA dehydrogenase activity	2	2.10E-05
GO:0004085	butyryl-CoA dehydrogenase activity	2	6.20E-05
GO:0004334	fumarylacetoacetase activity	2	6.20E-05
GO:0004121	cystathionine beta-lyase activity	2	6.20E-05
GO:0016833	oxo-acid-lyase activity	2	1.20E-04
GO:0050897	cobalt ion binding	2	4.51E-03
GO:0044540	L-cystine L-cysteine-lyase (deaminating)	1	4.64E-03
GO:0047982	homocysteine desulfhydrase activity	1	4.64E-03
GO:0080108	S-alkylthiohydroximate lyase activity	1	4.64E-03
GO:0033855	nicotianamine aminotransferase activity	1	4.64E-03
GO:0047022	7-beta-hydroxysteroid dehydrogenase (NADP+) activity	1	4.64E-03
GO:0004505	phenylalanine 4-monooxygenase activity	1	4.64E-03
GO:0004490	methylglutaconyl-CoA hydratase activity	1	4.64E-03
GO:0034617	tetrahydrobiopterin binding	1	4.64E-03
GO:0004838	L-tyrosine:2-oxoglutarate aminotransferase activity	1	4.64E-03
GO:0008709	cholate 7-alpha-dehydrogenase activity	1	4.64E-03
GO:0001540	amyloid-beta binding	1	9.26E-03
GO:0004474	malate synthase activity	1	9.26E-03
GO:0004658	propionyl-CoA carboxylase activity	1	9.26E-03
GO:0004303	estradiol 17-beta-dehydrogenase activity	1	9.26E-03
GO:0009374	biotin binding	1	1.39E-02
GO:0008418	protein-N-terminal asparagine amidohydrolase activity	1	1.39E-02
GO:0004123	cystathionine gamma-lyase activity	1	1.39E-02
GO:0033938	1,6-alpha-L-fucosidase activity	1	1.39E-02
Cellular component			
GO:0005759	mitochondrial matrix	8	9.00E-06
GO:0012511	monolayer-surrounded lipid storage body	1	1.30E-02

Table 7: Downregulated pathways in SIP⁺-induced cultures treated with *Maribacter* sp. medium (SIP+M vs SIP).

Surprisingly, among the genes that are only upregulated in this specific treatment, forty are associated with photosynthetic functions and the light-harvesting complex (LHC) (Table 5, Appendix Table ST5). Twenty-two of these are fucoxanthin-chlorophyll a-c binding proteins (FCPs), intrinsic proteins of the thylakoid membrane that bind chlorophyll a and c and play a role in energy transfer for photosynthesis (Appendix Table ST6). In addition, we also found upregulation of genes involved in carotenoid biosynthesis (carotene desaturase, Sro536_g162170) and chlorophyll biosynthesis (one glutamate tRNA ligase: Sro20_g014070 and two glutamate-1-semialdehyde 2,1-aminomutases: Sro479_g151140 and Sro1597_g284880) (Appendix Table ST6). The latter two genes are involved in porphyrin biosynthesis, converting L-glutamate 1-semialdehyde to 5-aminolevulinate (Baele, 1990).

Several amino acid catabolic pathways were downregulated in presence of *Maribacter* spent medium (in SIP+M vs SIP and in M vs C), especially those of tyrosine (two genes), arginine (two genes) and phenylalanine (two genes) (Table 6). The downregulation of these pathways seems stronger in presence of SIP⁺ (SIP+M vs SIP, Table 7, four downregulated genes involved in tyrosine metabolism, four for phenylalanine catabolism and two for arginine catabolism). The strongest *Maribacter*-induced downregulation concerned a tyrosine aminotransferase (Sro379_g130480) and a fumarylacetoacetase (Sro341_g121520) (LFC < - 3.9 and LFC < - 3.4, respectively, in SIP+M vs SIP, Appendix ST8). Both are involved in phenylalanine catabolism: the former catalyzes the conversion of tyrosine to 4-hydroxyphenylpyruvate, the latter breaks down fumarylacetoacetate into fumarate and acetoacetate (Santucci *et al.*, 2017), thus influencing the citrate cycle. Interestingly, the phenylalanine-to-tyrosine pathway is one of the processes that is actively upregulated by SIP⁺ (Table ST8: phenylalanine 4-monooxygenase activity).

In addition to amino acid metabolism, fatty acid metabolism was also affected when *Maribacter* sp. medium was added to SIP⁺-treated cultures (SIP+M vs. SIP). The *Maribacter*-induced downregulation of fatty acid catabolism (fatty acid beta oxidation) and ketone body synthesis, combined with changes in acetyl-CoA metabolism (Table 7) and downregulation of fumarylacetoacetase activity (leading to a decreased fumarate pool, involved in the TCA cycle), all together suggest a shift from catabolism to intracellular accumulation of fatty acids (Shi and Tu, 2015). This observation is further supported by the downregulation of enoyl-CoA hydratase (Sro2125_g315680, LFC < - 3.3, ST9), an enzyme responsible for hydrating the double bond between the second and third carbons of Acyl-

CoA and involved in fatty acid catabolism to produce acetyl-CoA and energy (Bahnon *et al.*, 2002).

Compared to the changes induced by *Maribacter* sp., *Roseovarius* sp. medium triggers less radical transcriptional changes in *S. robusta*. Although *Roseovarius* sp. medium also induces downregulation of tyrosine, phenylalanine and fumarate synthesis (SIP+R vs SIP, Table ST5), these effects are less strong compared to what is triggered by *Maribacter* sp. and the number of total downregulated genes connected to these pathways is lower. Interestingly, several proteins localized at the cell surface were upregulated by addition of the *Roseovarius* sp. exudates in the presence of SIP⁺, which might hint to active perception of the bacteria by the diatom (Table ST4).

5.2.4 Both bacteria trigger detoxification and oxidative stress responses

Apart from bacteria-specific transcriptional changes, both *Maribacter* sp. and *Roseovarius* sp. exudates trigger an upregulation of metabolic processes related to oxidative stress responses, detoxification and defense mechanisms (appendix Table ST6, ST7, ST8).

Several genes that were upregulated in response to both *Roseovarius* sp. and *Maribacter* sp. treatments in the presence of SIP⁺ encode proteins that contain a flavodoxin-like fold, like a putative NADPH:quinone oxidoreductase (Sro481_g151580, LFC > 7) and a putative alcohol dehydrogenase (Sro989_g228490, LFC > 5). These proteins are involved in energy metabolism and in response mechanisms to reactive oxygen species (ROS)-induced stress (Sies, Berndt and Jones, 2017; Poirier *et al.*, 2018).

Moreover, both bacteria triggered strong upregulation of glutathione S-transferases (GST) (Sro1751_g295250 and Sro945_g223090) and glutathionyl-hydroquinone reductases (GS-HQR) (Sro596_g172810 and Sro2126_g315740) (Table ST8). These enzymes are important for detoxification reactions in plants. GSTs transfer GSH to electrophilic centers of toxic, hydrophobic compounds, and the resulting conjugates are more soluble and therefore less toxic (Sheenan *et al.*, 2001). GS-HQRs are a particular type of GSTs that reduce GS-hydroquinones and are believed to play a maintenance role for an array of metabolic pathways in photosynthetic organisms (Belchik and Xun, 2011).

Furthermore, sterol and fatty acid biosynthetic pathways are affected by both bacteria. A putative 12-oxophytodienoate reductase (OPR) (Sro250_g098890) was strongly upregulated in all bacterial treatments (LFC > 6) (Table ST6). OPRs are flavoprotein enzymes that regulate jasmonic acid biosynthesis from the fatty acid linolenic acid, a crucial mediator of

chemical defense mechanisms and plant-microbe interactions in plants (Erb, 2018, Koo, 2018). Diatoms are also known to produce different oxylipins, derivatives of fatty acids, as defense molecules (Pohnert, 2002). We detected a general upregulation in some acyl-CoA metabolic pathways different from those reported above, which are more consistent in presence of *Maribacter* sp., and can support the hypothesis of fatty acid derivatives as a defense mechanism against bacteria. Cholesterol catabolism and concomitant upregulation of tocopherol cyclase activity (Table 8) indicate an additional defensive mechanism against oxidative stress, employing Vitamin E as an antioxidant (Havaux and Garcia-Plazaola, 2014).

GO ID	GO Function	Genes	p-value
<i>Biological function</i>			
GO:0006805	xenobiotic metabolic process	3	6.80E-04
GO:0042049	cellular acyl-CoA homeostasis	1	3.84E-03
GO:0007225	patched ligand maturation	1	3.84E-03
GO:0015864	pyrimidine nucleoside transport	1	7.66E-03
GO:0090155	negative regulation of sphingolipid biosynthetic process	1	1.15E-02
GO:0090156	cellular sphingolipid homeostasis	1	1.15E-02
GO:0060539	diaphragm development	1	1.15E-02
GO:0015855	pyrimidine nucleobase transport	1	1.15E-02
GO:0006707	cholesterol catabolic process	1	1.15E-02
GO:0031024	interphase microtubule organizing center assembly	1	1.15E-02
GO:0031025	equatorial microtubule organizing center disassembly	1	1.15E-02
GO:0071397	cellular response to cholesterol	1	1.53E-02
GO:0042694	muscle cell fate specification	1	1.53E-02
GO:0021984	adenohypophysis development	1	1.53E-02
GO:0006863	purine nucleobase transport	1	1.53E-02
<i>Molecular functions</i>			
GO:0010181	FMN binding	2	1.90E-04
GO:0015390	purine-specific nucleoside:sodium symporter activity	1	3.71E-03
GO:0016162	cellulose 1,4-beta-cellobiosidase activity	1	3.71E-03
GO:0030248	cellulose binding	1	3.71E-03
GO:0009976	tocopherol cyclase activity	1	3.71E-03
GO:0015389	pyrimidine- and adenine-specific:sodium symporter activity	1	3.71E-03
GO:0050662	coenzyme binding	3	5.94E-03
GO:0008123	cholesterol 7-alpha-monooxygenase activity	1	7.41E-03
GO:0004064	arylesterase activity	1	1.11E-02

Table 8: Upregulated pathways elicited by bacterial medium in SIP⁺-induced cultures (SIP+M vs SIP, SIP+R vs R).

5.2.5 Comparative metabolomics reflects the different effects of *Roseovarius* and *Maribacter*

Spent medium of *S. robusta* cultures in different treatments was analyzed with a metabolomics approach to get insights into chemical responses of the induced *S. robusta* cells exposed to bacterial exudates. A principal component analysis (PCA) with all treatments in induced conditions (SIP+M, SIP+R, SIP) shows that the exometabolome of *S. robusta* is changing under the influence of bacterial medium, but the separation of the groups is small (Appendix Figure S6). We therefore decided to analyze the *Roseovarius* and *Maribacter* datasets separately, in order to highlight potential differences between the two bacterial treatments.

SIP+M and SIP+R samples are clearly separating from *S. robusta* induced axenic samples (SIP) and from bacterial spent medium (Figure 31a and 31c), thus confirming that both bacterial media affect the *S. robusta* exometabolome. To check if these differences were due to presence of molecules from bacterial exudates or in fact caused by *S. robusta* exometabolites, features found in bacterial media were removed from the feature list of SIP+M and SIP+R. The PCA plots in Figure 31b and 31d show a clear separation of *Maribacter* sp.-treated induced cultures (SIP+M) from the axenic controls (SIP), while cultures treated with *Roseovarius* sp. medium (SIP+R) are largely overlapping with SIP⁺ treated controls. When we compared the metabolome of non-induced cultures in presence of bacterial medium (R and M) to the axenic controls (C), both *Roseovarius*- (R) and *Maribacter*-treated cultures (M) are overlapping with the controls (Appendix Fig S7). These results corroborated the outcome of our transcriptomic analysis, with *Maribacter* sp. having a stronger effect on the metabolism of sexually induced MT⁻ *S. robusta* cells.

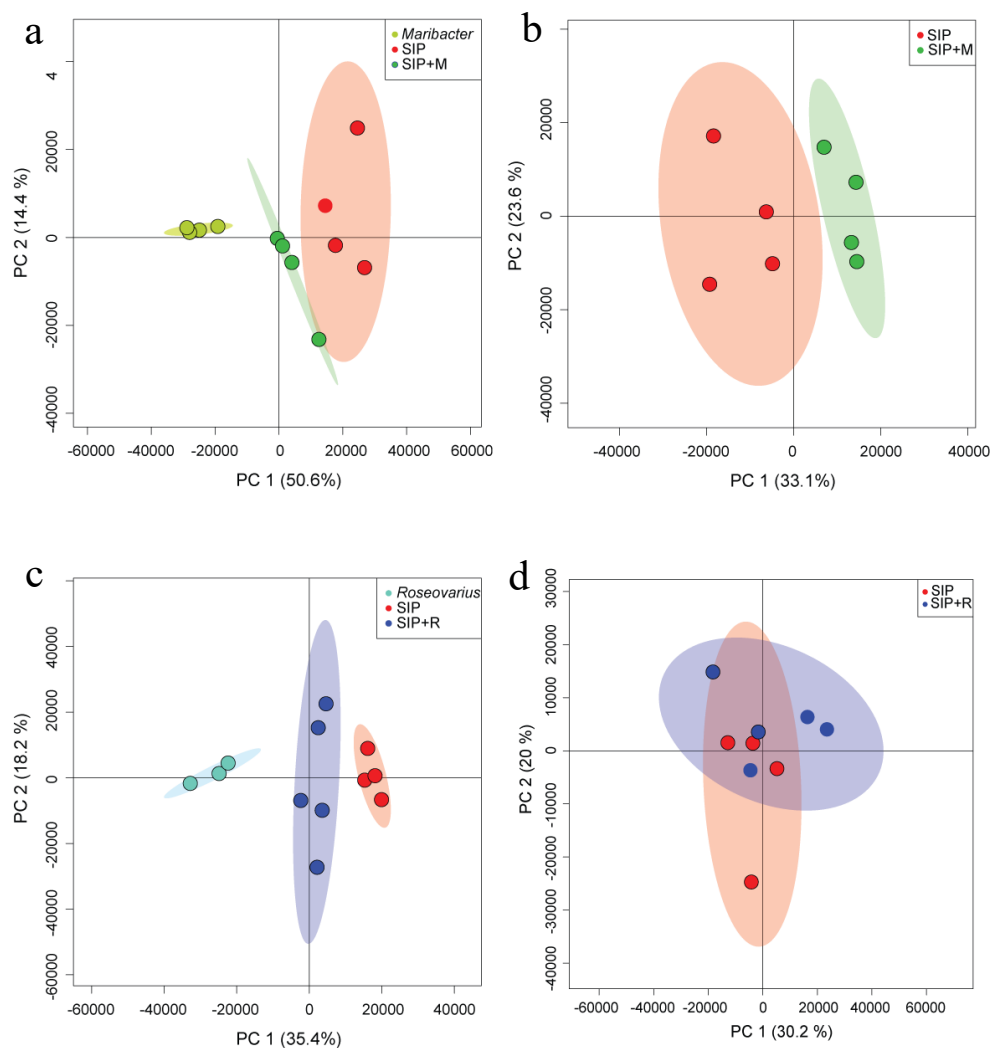


Figure 31: PCA of exometabolome samples of SIP+-induced cultures and bacteria spent medium. a) PCA of SIP axenic control, induced cultures + *Maribacter* sp. medium and *Maribacter* sp. exudates, b) PCA of SIP axenic control and induced cultures + *Maribacter* sp. medium with subtraction of features from *Maribacter* sp. exudates, c) PCA of SIP axenic control, induced cultures + *Roseovarius* sp. medium and *Roseovarius* sp. exudates, d) PCA of SIP axenic control and induced cultures + *Roseovarius* sp. medium with subtraction of features from *Roseovarius* sp. exudates.

We therefore used a comparative metabolomics approach to investigate the spent medium of *Maribacter* sp. and the exometabolome of sexualized *S. robusta* when exposed to *Maribacter* sp. exudates (SIP+M) to search for putative signaling molecules. We performed a one-way ANOVA (FDR cutoff = 0.05, Fisher LSD post-hoc analysis) to select for significant features and chose the top 25 among them (ranked by FDR). Although most of the molecules were identified as unknown, retention times helped us to classify them based on their polarity (Figure 32, upregulated metabolites in red and downregulated metabolites in blue). Most of the upregulated compounds in SIP+M treatment range from mid-polar to

unpolar, eluting between 4.5 and 9 minutes (from 45% of acetonitrile to 100% of acetonitrile solvent composition), while many of the upregulated molecules in SIP medium are unpolar, eluting after 9 minutes. If we include molecules from bacterial exudates in the analysis (Figure 33), several compounds released in the medium by *Maribacter* sp. show a high chromatographic peak intensity that is significantly decreased in SIP+M treatment, suggesting the potential involvement of a signaling mechanism in which the bacterial compound is degraded by the diatom. In particular, two compounds, eluting at 2.95 min. (MW= 165.06493 Da, putative chemical molecular formula C₆H₇N₅O) and at 8.45 min. (MW= 224.08345 Da, putative molecular formula C₁₅H₁₂O₂), are very intense in *Maribacter* spent medium (peak intensity=10⁶), while their intensities are respectively three and one order of magnitude lower in SIP+M treatments. Moreover, these compounds are not present in high amount in *Roseovarius* medium (Appendix, SF8). After obtaining a fragmentation tree from our MS/MS data and comparing it to public and in-house libraries, we obtained putative structure for the two compounds: the first one was annotated as a presumed methylguanamine, a methyl derivative of the nucleobase guanine, while the second one was annotated as a small weight flavanone (Figure 33).

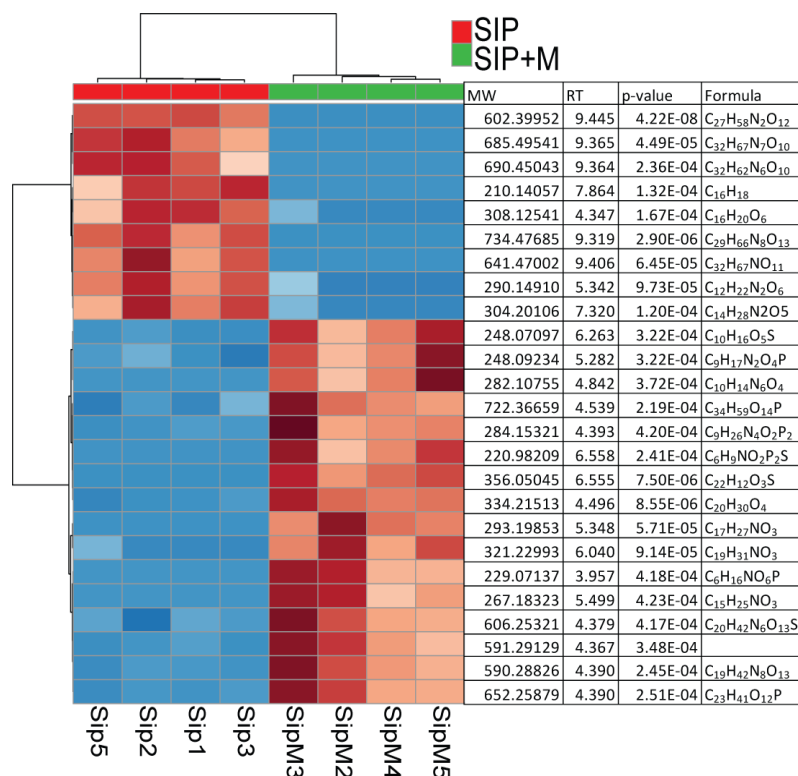


Figure 32: Heatmaps of up- and downregulated *S. robusta* exometabolites in presence or absence of *Maribacter* spent medium after subtraction of *Maribacter* sp. features. Significance evaluated with a t-Test ($\alpha=0.05$), hierarchical clustering is based on Euclidean distances and using Ward's method. Red is for upregulated metabolites, blue is for downregulated metabolites.

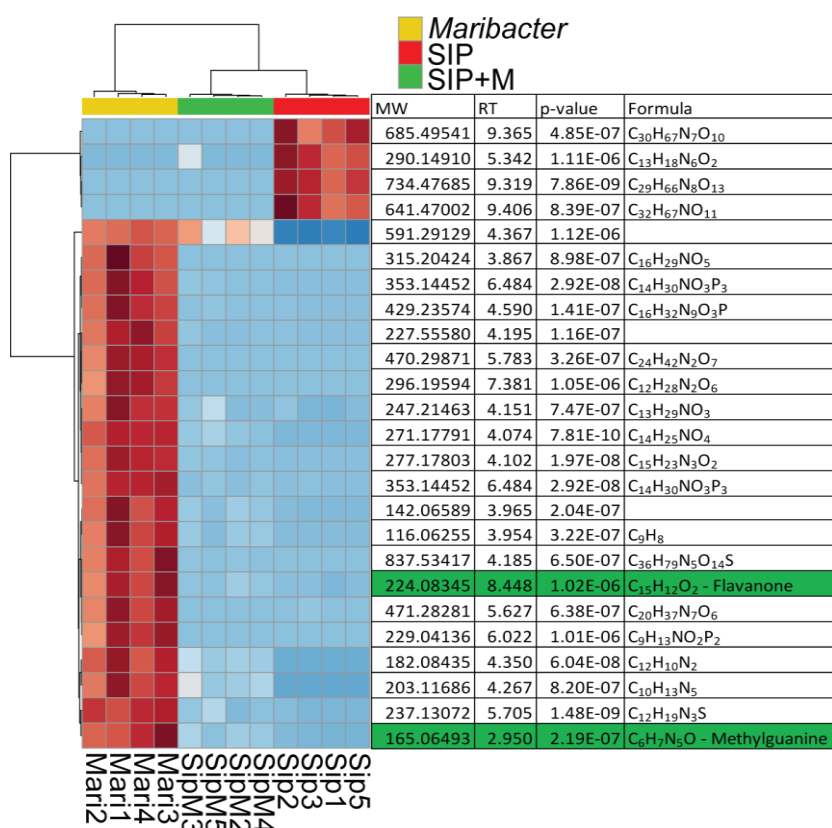


Figure 33: Heatmaps of up- and downregulated *S. robusta* exometabolites in presence or absence of *Maribacter* spent medium and up- and downregulated exometabolites from *Maribacter* sp. Significance evaluated with a One-Way Anova (adjusted p-value after Fisher LSD post-hoc test=0.05), hierarchical clustering is based on Euclidean distances and using Ward's method. Red is for upregulated metabolites, blue is for downregulated metabolites.

5.2.6 The oxylipin precursor arachidonic acid is produced in response to both bacteria

A targeted metabololipidomics analysis for fatty acids and oxylipins was performed to check if the production of these compounds was increased in presence of bacterial medium and oxidative stress conditions. The amounts of released arachidonic acid was significantly higher in both SIP+M and SIP+R when compared to induced axenic conditions (SIP) and also in the presence of *Roseovarius* spent medium without SIP⁺ (R) compared to the axenic control (C) (Figure 34a). polyunsaturated fatty acid involved in cell signaling (Piomelli, 1993) and inflammation (Calder, 2011). It is also synthesized by diatoms (Dunstan *et al.*, 2013) and it is a crucial precursor in oxylipin production involved in defenses mechanisms (Pohnert 2002; Rettner *et al.*, 2018). No other investigated oxylipin (the same investigate by Rettner *et al.*, 2018) was significantly upregulated in any treatment.

5.2.7 Diproline production is influenced by *Maribacter*, not by *Roseovarius*

Among the metabolites released by induced *S. robusta* MT⁻ cells, the attraction pheromone diproline plays a fundamental role in sexual reproduction (Gillard *et al.*, 2013). We measured its concentration in the medium of induced cultures to check if bacterial exudates could have an influence on its production (Figure 34b). These measurements confirm that only SIP⁺-induced cultures are producing diproline and bacteria are not triggering its production. More interestingly, we observed that the concentration of diproline in the presence of *Maribacter* sp. medium is significantly lower ($p < 0.012$) compared to axenic induced cultures and to *Roseovarius* sp. medium-treated cultures, which show no differences in diproline concentration in comparison to control cultures.

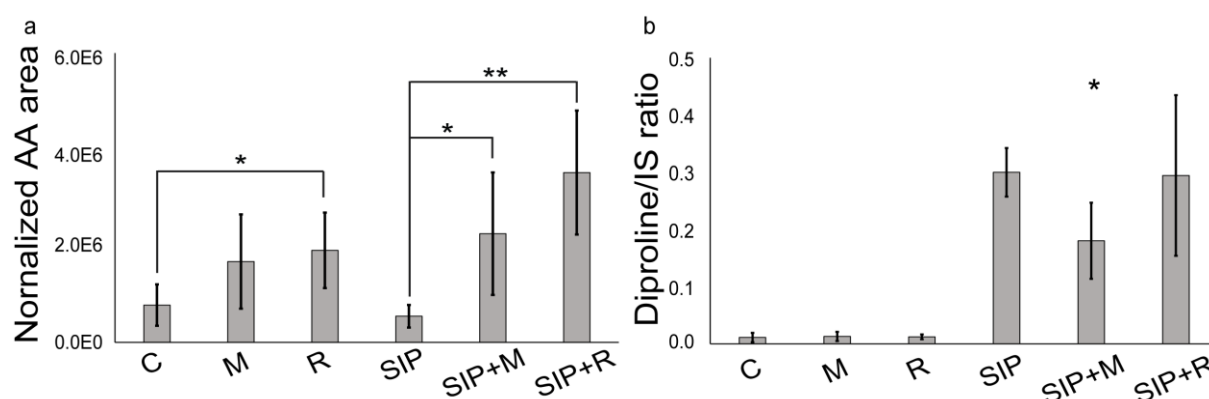


Figure 34: a) Arachidonic acid (AA) and b) diproline relative concentration. Arachidonic acid is normalized to cell number. Internal standard (IS) is caffeine (15 nmol). One-way ANOVA (adjusted p-value after Bonferroni's correction for multiple comparisons=0.05). SIP⁺ is taken as control for assessing significant differences in diproline concentration in SIP+M and SIP+R treatments. C is the axenic, non-induced control, M is non-induced control + *Maribacter* sp. medium, R is non-induced control + *Roseovarius* sp. medium, SIP is induced axenic control, SIP+M is induced culture + *Maribacter* sp. medium, SIP+R is induced control + *Roseovarius* sp. medium.

5.3. Discussion

Interactions between diatoms and bacteria cover a wide array of inter-kingdom relationships (Chapter 1.2). We showed that bacteria can not only influence diatom growth but can also interfere sexual reproduction (Chapter 4). Sex is an essential step in nearly all diatoms life cycles (Frenkel *et al.*, 2014a) and contributes to the often extraordinary genetic diversity of natural populations. *S. robusta* is a well-studied model due to the knowledge of the chemical signaling involved in mate finding (Gillard *et al.*, 2013; Moeys *et al.*, 2016). Bacteria associated to *S. robusta* are able to modulate diproline concentrations in the medium and two of them (*Roseovarius* sp. and *Maribacter* sp.) have an opposite effect on the sexual

efficiency of *S. robusta*, with *Maribacter* sp. reducing mating efficiency and *Roseovarius* sp. slightly improving it (Chapter 4). Following these findings, we now provide the first insights into the bacterial effect on sexual reproduction of *S. robusta* on a molecular level using a combination of physiological, metabolomic and transcriptomic approaches.

When a suitable mating partner is present, *S. robusta* cell cycle is temporarily arrested in G1 phase by the SIP of the opposite mating type to synchronize the switch to meiosis in both partners (Gillard *et al.*, 2014; Moeys *et al.*, 2016). A few studies reported that algicidal bacteria can have an effect on microalgal cell cycle progression (Pokrzywinski *et al.*, 2017). In this chapter, we show that bacterial exudates of *Maribacter* sp. or of *Roseovarius* sp. do not impede mitosis nor the temporary SIP⁺-induced cell cycle arrest of MT⁻ cells during mating (Figure 27). SIP⁺ triggers substantial changes in gene expression in *S. robusta*. Moeys *et al.* (2016) showed that SIP⁺ induces the switch from mitosis to early-meiotic processes. Here, we confirm this result and, more importantly, we show that upregulation of SIP⁺-induced early meiotic processes is not significantly influenced by bacterial exudates. Furthermore, our experiment corroborates the involvement of cGMP signaling during the initial phase of sexual reproduction (including one GC/PDE already found in 2016 by Moeys *et al.*). Interestingly, upregulation of a number of receptor-type guanylate cyclase was elicited by *Maribacter* sp. specifically, suggesting a role of cGMP signaling in the interaction of *S. robusta* with the bacterium. It has been shown that cyclic nucleotide signaling is crucial for an array of physiological processes in diatoms, from regulation of silicon cycle (Aline *et al.*, 1984; Smith *et al.*, 2015) to acclimation to CO₂ (Hennon *et al.*, 2015). Moreover, this mechanism was also suggested to be involved during the onset of the sexual reproduction also in the diatom *Pseudo-nitzschia multistriata* (Basu *et al.*, 2018). In plants, signaling by cyclic nucleotides (cGMP and cAMP) is well studied (Isner and Maathuis, 2018) and cAMPs was suggested to play a role in plant-bacteria interactions (Tian *et al.*, 2012). In diatoms or other algae, a similar role of cGMP in inter-kingdom crosstalk has not been described so far.

One of our main research questions is whether the positive effect of *Roseovarius* and negative effect of *Maribacter* on sexual reproduction is linked to a change in diproline production by the diatom. Moeys *et al.* (2016) hypothesized that the upregulation of proline biosynthesis is crucial for diproline synthesis, increasing the proline pool that can be used for diproline production. Our transcriptomic data revealed that the proline biosynthetic pathway was strongly upregulated in all SIP⁺-treated cultures. A slightly higher expression of $\Delta 1$ -pyrroline-5-carboxylate synthetase (Sro2012_g310890) and $\Delta 1$ -

pyrroline-5-carboxylate reductase (Sro216_g089310) was shown in the presence of *Roseovarius* sp. exudates while no substantial differences in gene expression between axenic cultures and cultures treated with *Maribacter* sp. spent medium were observed (Table 3). Targeted measurements of diproline in the medium of SIP⁺-treated cultures indicate that the pheromone concentration was significantly lower in presence of *Maribacter*. As suggested by the transcriptome data, an increase in diproline concentration after treatment with *Roseovarius* exudates was found, however, the increase is small and not significant (Figure 36b). Although this seems like a discrepancy between our transcriptomics and metabolomics data, one has to consider that the exact mechanism of diproline production remains unknown and that a significant amount of *S. robusta* genes lack a good annotation. Hence, it is possible that the lower diproline concentrations in *Maribacter*-treated samples are caused by up-or downregulation of other pathways that are directly related to diproline production but yet unknown or indirectly related to the synthesis of the attraction pheromone. As we will discuss in the following paragraphs, our transcriptomic data support this latter hypothesis.

In our experiments, phenylalanine and tyrosine catabolic pathways are slightly affected by *Roseovarius* medium and this effect is stronger in response to *Maribacter* (Table 6). Both processes are upregulated by SIP⁺ (in SIP vs C, SIP+M vs M and SIP+R vs R, Table 8), while they are downregulated compared to axenic conditions when *Maribacter* spent medium is present (SIP+M vs SIP and M vs C, Table 6), especially in presence of SIP⁺ (SIP+M vs SIP, Table 4). In higher plants, phenylalanine and tyrosine are produced via the shikimate pathway (Tzin and Galili, 2010) and it has been suggested that downstream products like tyramine are involved in defense responses (Trezza *et al.*, 1993). In diatoms, less is known about the importance of the metabolism of these two amino acids. However, their biosynthesis is strongly connected to the biosynthetic pathway of tryptophan (Bromke, 2013), an amino acid that has a fundamental role in algae-bacteria interactions (Amin *et al.* 2015).

Interestingly, in the presence of SIP⁺, *Maribacter* sp. (and not *Roseovarius* sp.) induces upregulation of several light-harvesting complex (*lhc*) genes (Table 5, Bailleul *et al.*, 2010a). Many of these encode fucoxanthin-chlorophyll a-c binding proteins (FCPs), thylakoid membrane-intrinsic proteins responsible for the absorption of the blue-green wavelengths in aquatic environments (Schellenberger Costa *et al.*, 2012; Kuczynska, Jemiola-Rzeminska, & Strzalka, 2015). FCPs are also involved in non-photochemical quenching (NPQ) (Kuczynska *et al.*, 2015), a mechanism that protects plants and algae

from high light stress (Horton and Ruban, 2004; Dong *et al.* 2016). So far, nothing was known about possible effects of bacteria on diatom FCPs or NPQ, and the biological significance of this observation requires more in-depth photophysiological studies. Regardless of the biological implications, we found that three enzymes involved in porphyrin synthesis (a glutamate tRNA ligase, Sro20_g014070, and two glutamate-1-semialdehyde 2,1-aminomutases, Sro479_g151140 and Sro1597_g284880, Table 5) are strongly upregulated in response to *Maribacter*. These enzymes are fundamental for the Baele cycle (Baele, 1990), which converts glutamate to 5-aminolevulinate that is afterwards used to synthesize the porphyrinic ring of chlorophyll. The strong upregulation of these enzymes, combined with the downregulation of the arginine catabolic pathway (Table 7), could diminish the availability of glutamate and arginine, two important substrates for proline biosynthesis in diatoms (Bromke, 2013).

Taken these results into account, we hypothesize that *Maribacter* sp. exudates do not negatively influence the sexual reproduction of *S. robusta* by directly targeting proline production. Instead, we suggest that the upregulation of photosynthetic pigment production, combined with the diminishing glutamate availability, reduces the intracellular pool of proline precursors (glutamate, arginine) and thereby indirectly influences diproline biosynthesis (Figure 33). In *Roseovarius* sp.-treated samples, we did not find upregulation of photosynthetic pigment production. Hence, the glutamate pool is not further reduced to produce these pigments and can be used for proline biosynthesis (which is upregulated in presence of *Roseovarius*, see ST4) and, eventually, diproline production. Our metabolomics shows only slightly higher extracellular diproline concentrations in *Roseovarius* sp.-treated samples, which is comparable to axenic cultures (Figure 34b). In addition to the annotated DE genes discussed here, several highly up- and downregulated genes in all treatments were lacking a functional annotation. Better annotations will provide future studies with more knowledge to unravel the influence of *Maribacter* sp. on diatom sexuality and metabolic regulation.

Despite our incomplete knowledge of the diproline biosynthesis pathway regulation, we hypothesize that the higher intracellular proline concentration in the presence of *Roseovarius* sp. could result in an increased or prolonged diproline production and release, explaining the enhancement of sexual efficiency observed in chapter 4 and the concentration of diproline comparable to that of axenic cultures. However, further investigation at different time points of both proline biosynthesis gene expression and diproline concentration in presence of *Roseovarius* are needed to support this hypothesis.

Besides the bacteria-specific responses of *S. robusta*, we also found that a general oxidative stress response is induced by both *Roseovarius* sp. and *Maribacter* sp. exudates, especially in SIP⁺-induced cultures (SIP+M vs SIP, SIP+R vs SIP) (Table 8 and ST8). Several of the upregulated genes encode flavin mononucleotide (FMN) binding proteins, which are generally involved in energy metabolism and electron transfer and act as important anti-oxidant species (Quijano *et al.*, 2016). Also glutathione-related enzymes, such as glutathione S-transferase (GST) and glutathionyl-hydroquinone reductase (GS-HQR), were upregulated in the presence of bacterial spent medium (Table ST8). Glutathione is a tripeptide acting as fundamental antioxidant in many eukaryotes, including phytoplankton (Vikoert *et al.*, 2018; Poirier *et al.*, 2018). A similar role is fulfilled by tocopherols, antioxidants that are present in plastids of all lineages of photosynthetic eukaryotes and that are involved in different stress responses in diatoms (Lauritano *et al.*, 2015). The increase of cholesterol catabolism and the simultaneous upregulation of tocopherol cyclase activity in response to *Maribacter* sp. and *Roseovarius* sp. (Table 8) suggests that also in *S. robusta* tocopherol may act as an anti-oxidant.

Fatty acid metabolism is also affected by the bacteria, especially by *Maribacter* sp. in presence of SIP⁺ (SIP+M vs SIP, Table 7). Reduction of the citric acid cycle by a decrease of the intracellular of fumarate pool, combined with downregulation of ketone bodies synthesis (Table 4) and of enoyl-CoA hydratase (Sro2125_g315680, Table ST9), an enzyme involved in fatty acid catabolism (Bahnon *et al.*, 2002), all hint to a shift from energy consumption by fatty acid degradation to an accumulation of these compounds for other purposes, such as defensive mechanisms. Interestingly, one gene, a putative 12-oxophytodienoate reductase (OPR) (Sro250_g098890), was upregulated in all bacterial treatments (SIP+M, SIP+R, M and R). OPR is a flavoprotein enzyme with a key function in the biosynthesis of jasmonic acid, a regulator of stress responses in plants (Koo, 2018). More generally, OPRs function in α -linolenic acid metabolism and oxylipin biosynthesis (Weber, 2002), well-studied derivatives of fatty acids known for their function as defense molecules in algae (Wasternack, 2007; Pohnert, 2002). In our study, targeted metabolic analysis showed that the concentration of arachidonic acid, an important intermediate in oxylipin production (Pohnert and Boland, 2002), was significantly higher in the exometabolome of cultures treated with bacterial spent medium (Figure 34a). Together with the transcriptomic evidence for fatty acid accumulation (Table 7, Table 8), this suggests that *S. robusta* increases production of sterols and fatty acids, probably as a defense mechanism, in response to *Maribacter* sp. and *Roseovarius* sp.

Arachidonic acid was the only detectable oxylipin in our metabolomics analysis. One possible explanation lies in the fact that arachidonic acid is an important precursor for a range of oxylipins (Fischer *et al.*, 2016). Significant differences in the levels of this precursor will eventually also lead to differences in the downstream products. Oxylipins were so far only detected from lysed or damaged diatom cells (Pohnert and Boland, 2002), but recently it was suggested that this compound could have a role in diatom resistance against algicidal bacteria (Meyer *et al.*, 2018). Further experiments performed on a longer time scale and targeted analysis on endometabolites from *S. robusta* cells are necessary to elucidate diatom defensive mechanism against bacteria and the actual involvement of oxylipins.

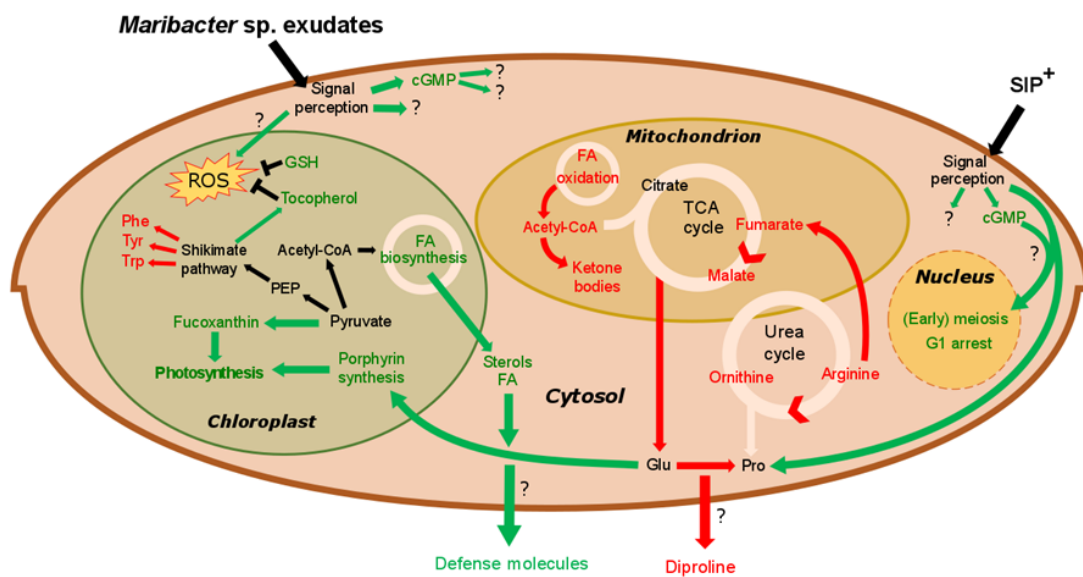


Figure 35: Overview of metabolic changes in *S. robusta* when exposed to SIP⁺ and *Maribacter sp.* exudates. In green are the upregulated processes, red the downregulated ones. *Maribacter sp.* exudates do not directly influence early meiotic processes. Stress induced by bacterial medium induces cGMP signalling cascades an upregulation of photosynthetic pigment production and an oxidative stress response (by tocopherol and glutathione biosynthesis). Flux through the urea- and TCA cycle is reduced, reducing intracellular arginine, fumarate, malate and glutamate pools. Glutamate, precursor for proline synthesis, is used for porphyrin synthesis, so the upregulated porphyrin synthesis could affect proline biosynthesis and thus also diproline production. Abbreviations: Phe: phenylalanine, Tyr: tyrosine, Trp: tryptophane, Glu: Glutamate, Pro: Proline, GSH: Glutathion, FA: Fatty acid, PEP: Phosphoenolpyruvate.

The effect of both bacterial exudates on sexually induced *S. robusta* cultures, and especially the stronger effect of *Maribacter sp.*, is confirmed by our exometabolome data. Among the bacterial treatments, cultures treated with *Maribacter sp.* medium show the clearest deviation from axenic control cultures. We compared the exometabolomes of SIP⁺-induced *S. robusta* cultures (SIP), induced cultures with *Maribacter* exudates (SIP+M) and

Maribacter spent medium only (M) and we found several unknown molecules, mostly non-polar (Figure 32). Some of these compounds have higher concentrations in the bacterial spent medium compared to co-cultivation treatments with diatoms and bacteria, suggesting potential degradation of the bacterial compound by *S. robusta*. Some other molecules are only present in co-cultivation treatments, suggesting they too are possible chemical responses of the diatom to the bacterial exudates. Unfortunately, the low concentration of many of these compounds prevented us to identify them by MS/MS and library matching. Interestingly, among the few identified molecules, a putative methylguanine (MW= 165.06493 Da, RT=2.95 min, C₆H₇N₅O) and a flavanone-like molecule (MW= 224.08345 Da, RT=7.35 min, C₁₅H₁₂O₂) were only found in *Maribacter* sp. medium and their concentration decreased in presence of the diatom (Figure 33 and S8). Methylguanines are naturally occurring modified purines from tRNA in humans but they are not known to be produced by bacteria as exometabolites. Flavanones are a type of flavonoids that often occur in plants and have several functions, from antioxidants to antimicrobial (Cushnie and Lamb, 2005), and were also found in a *Pseudovibrio* sp. (Crowley *et al.*, 2014). However, flavanone production by other marine bacteria as well as a function in inter-kingdom crosstalk has not yet been described. Further metabolomics experiments using large volumes of bacterial exudates and *S. robusta* are needed to better elucidate the nature of these compounds. Moreover, fractionated-guided bioassays may explain their biological function.

In conclusion, the present study provides first insights into the influence of bacteria on diatom sexual reproduction by combining physiological, transcriptional and metabolomics evidence. With the integration of different approaches, we were able to highlight several responses of the model benthic diatom *S. robusta* towards bacterial exudates from the naturally associated bacteria *Maribacter* sp. and *Roseovarius* sp. These results will pave the way to a better understanding of diatoms life cycle regulation in natural environments and more generally of the importance of inter-kingdom signaling diatom reproduction and survival.

6. From ecology to applied research: effect of bacteria on a commercial microalga⁵

6.1. Introduction

In recent years, the study of inter-kingdom communication between microalgae and bacteria has moved from a pure ecological interest to applied research for industrial purposes (Kouzuma and Watanabe, 2015). Microalgae-bacteria consortia have been fruitfully employed in several fields, from bioremediation (Abinandan *et al.*, 2018) to aquaculture and cultivation in photobioreactors (Lian *et al.*, 2018; Natrah *et al.*, 2014) for the production of high value compounds (Fuentes *et al.*, 2016) and biofuels (Wang *et al.*, 2016b). Also biofilms formed by these organisms can be successfully exploited for industrial purposes, for example in wastewater treatment (De-Bashan *et al.*, 2004; Ji *et al.*, 2018; Liu, Song, and Qiu, 2017). On the other hand, biofilm formation on technical surfaces, a phenomenon called biofouling, has a negative economic impact on many human activities (Schultz *et al.*, 2010; Fitrige *et al.*, 2012), since huge investments are needed to reduce and control fouling. Anti-fouling research has directed its efforts not only to the development synthetic products to counteract biofilm development (Almeida, Diamantino, and de Sousa, 2007; Yee *et al.*, 2016) but also to use interspecific natural interaction mechanisms to inhibit fouling using ecologically robust approaches (Dahms and Dobretsov, 2017). This research is particularly important in industrial microalgae production in closed bioreactors, as this is typically conducted in non-axenic conditions. Alteration in the algal microbiome may induce biofilm growth on solid surfaces of the bioreactors, leading to a reduced productivity due to reduction of light penetration and increasing contamination (Zerriouh *et al.*, 2017). Recent studies have employed high throughput analysis, such as genomics, transcriptomics, proteomics and metabolomics (Abinandan *et al.*, 2018; Chen *et al.*, 2017b; Krohn-Molt *et al.*, 2017; Lépinay *et al.*, 2018) to better understand the mechanism behind biofilm formation.

Giraldo *et al.* (submitted) isolated several bacteria associated to the oleaginous eustigmatophyte *Nannochloropsis* sp. from closed bioreactor samples and found out that the

⁵ This chapter is adapted from: Cirri, E.*, Giraldo, J.*, Neupane, S., Willems, A., Mangelinckx, S., Roef, L., Vyverman, W., Pohnert, G Bacteria isolated from *Seminavis robusta* influence growth, biofilm production and the metabolome of *Nannochloropsis* sp. Submitted to *Algal Research*.

alphaproteobacterium *Poseidonocella* sp. is strongly inducing biofilm formation on this microalga. In this project, we studied the effect of bacteria isolated from another Stramenopile, the model benthic pennate diatom *Seminavis robusta*, on growth, metabolome and biofilm formation of *Nannochloropsis* sp.

In chapter two, *Maribacter* sp., *Roseovarius* sp. and *Croceibacter* sp. were shown to have a different influence on the growth of *S. robusta*. Following this result, in this chapter their potential industrial application as a beneficial engineered microbiome was tested on *Nannochloropsis* sp., a commercially relevant microalga (Liu, Song and Qiu, 2017; Reboloso-Fuentes *et al.*, 2001). *Nannochloropsis* sp. is an industrially-promising candidate due to its high protein and lipid content – particularly eicosapentanoic acid (EPA) – (Hulatt, *et al.*, 2017) which makes it important to be used for aquaculture high quality feed (Yaakob *et al.*, 2014), as well as a promising candidate for replacing fish oil as eicosapentaenoic acid (EPA) source (Lenihan-Geels, Bishop, and Ferguson, 2013). This work has been done in collaboration with Proviron © (Antwerp, Belgium), a chemical company that, since many years, is investing in microalgal cultivation research and development, both from an engineering and biological point of view. Different combinations of bacteria were tested (*Poseidonocella* sp. alone, *Roseovarius* sp. alone, *Maribacter* sp. alone, *Poseidonocella* sp. and *Roseovarius* sp., *Poseidonocella* sp. and *Maribacter* sp.) to evaluate the effects on microalgal growth, on the endometabolome of *Nannochloropsis* sp. and their influence on biofilm development. For growth and endometabolomics analysis, *Nannochloropsis* sp. was co-cultivated with various bacterial strains for 7 days and each day algal growth was monitored with UV analysis. At the end of the growth period, algae were extracted and analyzed with a GC-HR-MS untargeted metabolomics approach. In parallel, biofilm formation was investigated in a bioassay. Algae were co-cultured with different bacteria at different OD₆₀₀ (for their combination see Figure 36) in 96 well plates for 10 days and at the end of this period absorption was measured to assess biofilm thickness.

<i>Nannochloropsis</i> + saline medium (Control)	<i>Nannochloropsis</i> + Minimal medium	<i>Nannochloropsis</i> + <i>Poseidonocella</i> sp.	<i>Nannochloropsis</i> + <i>Poseidonocella</i> sp.+ Minimal medium
<i>Nannochloropsis</i> + <i>Roseovarius</i> sp. (OD=0.1)	<i>Nannochloropsis</i> + <i>Roseovarius</i> sp. (OD=0.01)	<i>Nannochloropsis</i> + <i>Roseovarius</i> sp. medium (OD=0.1)	<i>Nannochloropsis</i> + <i>Roseovarius</i> sp. medium (OD=0.01)
<i>Nannochloropsis</i> + <i>Roseovarius</i> sp. (OD=0.1) + <i>Poseidonocella</i> sp.	<i>Nannochloropsis</i> + <i>Roseovarius</i> sp. (OD=0.01) + <i>Poseidonocella</i> sp.	<i>Nannochloropsis</i> + <i>Roseovarius</i> sp. medium(OD=0.1) + <i>Poseidonocella</i> sp.	<i>Nannochloropsis</i> + <i>Roseovarius</i> sp. medium(OD=0.01) + <i>Poseidonocella</i> sp.
<i>Nannochloropsis</i> + <i>Maribacter</i> sp. (OD=0.1)	<i>Nannochloropsis</i> + <i>Maribacter</i> sp. (OD=0.01)	<i>Nannochloropsis</i> + <i>Maribacter</i> sp. medium (OD=0.1)	<i>Nannochloropsis</i> + <i>Maribacter</i> sp. medium (OD=0.01)
<i>Nannochloropsis</i> + <i>Maribacter</i> sp. (OD=0.1) + <i>Poseidonocella</i> sp.	<i>Nannochloropsis</i> + <i>Maribacter</i> sp. (OD=0.01) + <i>Poseidonocella</i> sp.	<i>Nannochloropsis</i> + <i>Maribacter</i> sp. medium(OD=0.1) + <i>Poseidonocella</i> sp.	<i>Nannochloropsis</i> + <i>Maribacter</i> sp. medium(OD=0.01) + <i>Poseidonocella</i> sp.
<i>Nannochloropsis</i> + <i>Croceibacter</i> sp. (OD=0.1)	<i>Nannochloropsis</i> + <i>Croceibacter</i> sp. medium (OD=0.1)	<i>Nannochloropsis</i> + <i>Croceibacter</i> sp. (OD=0.1) + <i>Poseidonocella</i> sp.	<i>Nannochloropsis</i> + <i>Croceibacter</i> sp. medium (OD=0.1) + <i>Poseidonocella</i> sp.

Figure 36: Experimental design of biofilm formation of *Nannochloropsis* sp. in presence of different bacteria.

6.2. Results

6.2.1 Growth of *Nannochloropsis* sp. in co-cultivation with isolated bacteria from *S. robusta*

As seen in chapter 3, different bacteria from *S. robusta* showed a different effect on diatom sexuality and growth, with *Roseovarius* sp. enhancing it and *Maribacter* sp. only having a limited positive influence. We therefore tested these bacteria to check if they were able to enhance growth and induce metabolic changes in another organism belonging to the Stramenopiles phylum, the commercially relevant *Nannochloropsis* sp. *Nannochloropsis* sp. (initial $OD_{630}=0.620\pm 0.050$) was co-cultivated with different bacteria for seven days (Figure 37). Growth was monitored every day by measuring OD_{630} (chlorophyll maximum, Kandilian *et al.*, 2013) and OD_{750} (standard measurement for algal biomass, Griffiths *et al.*, 2011). Both measurements gave similar results, so only OD_{630} outcomes are reported. All bacteria are significantly supporting *Nannochloropsis* sp. growth at the end of the seven days' cultivation period (two-way ANOVA interaction p-value < 0.0001 in all conditions) but the extent of this positive effect on growth are different depending on bacterial species. *Poseidonocella* sp., an alphaproteobacterium isolated from *Nannochloropsis* sp. capable of inducing biofilm formation (Giraldo *et al.*, *subm.*), is significantly supporting *Nannochloropsis* sp. growth only after 7 days of co-cultivation (p < 0.0001 on the seventh day of co-incubation in comparison to the control) (Figure 37 c and d, orange line).

Bacteria isolated from *S. robusta* have different effects on *Nannochloropsis* growth if compared with the results observed in Chapter 4 (Figure 15): *Roseovarius* sp., which is supporting *S. robusta* growth, has on *Nannochloropsis* sp. an influence similar to

Poseidonocella, but the positive effect at day seven is slightly less significant if compared to the control ($p=0.001$). Also the combination of the two bacteria is not improving algal growth. On the contrary, *Maribacter* sp. is significantly enhancing *Nannochloropsis* sp. growth already after three days of co-cultivation ($p=0.001$) and it is constantly increasing until day seven. The presence of *Poseidonocella* sp. is partially reducing the *Maribacter* effect at the beginning of the growth curve, but the algal cell concentration at the end of the seven-day cultivation is the highest among the treatments ($OD_{630}=1.84\pm 0.12$).

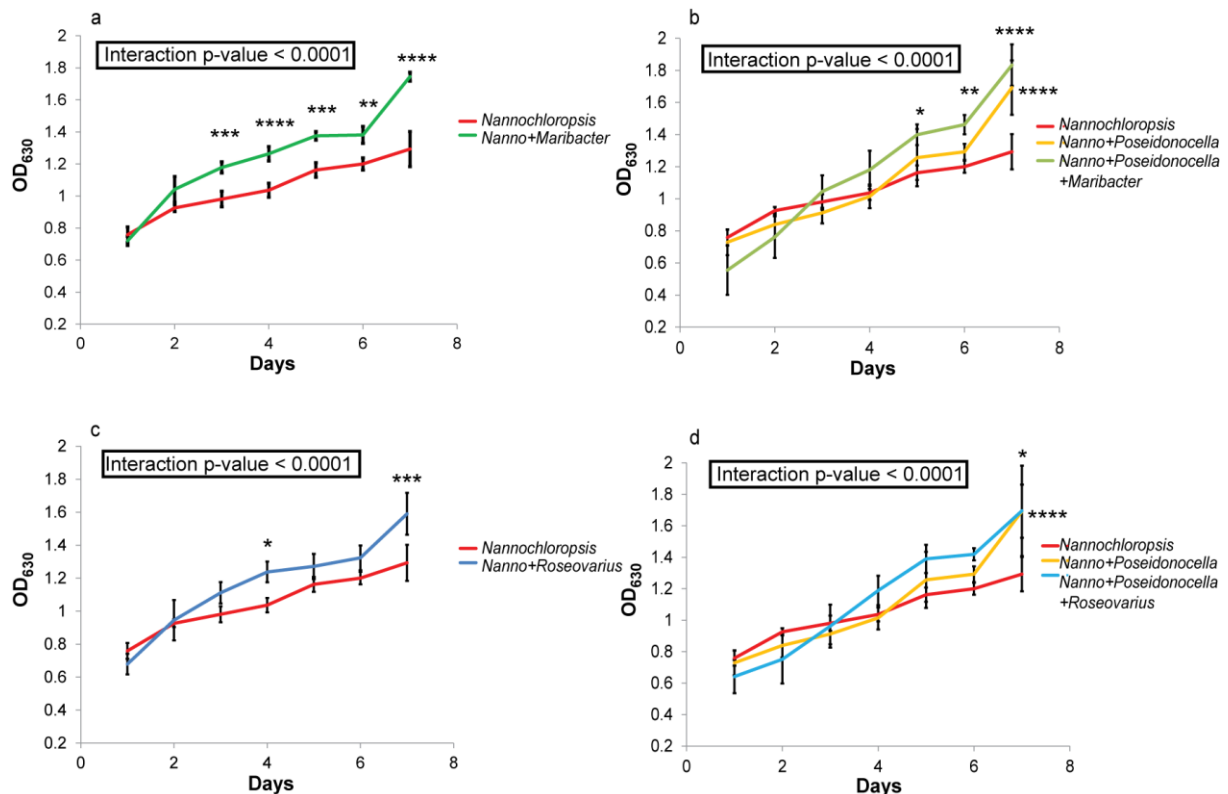


Figure 37: *Nannochloropsis* sp. growth curves. Co-cultivation with *Maribacter* sp. (a), *Maribacter* sp. and *Poseidonocella* sp. (b), *Roseovarius* sp. (c), *Roseovarius* sp. and *Poseidonocella* sp. (d). Two-way ANOVA, $\alpha=0.05$, Bonferroni's correction for multiple comparisons. Asterisks refer to multiple comparisons to the control cultures (red line); boxes give results from the two-way ANOVA.

6.2.2 Bacteria are changing the endometabolome of *Nannochloropsis* sp.

After seven days of growth, extracellular extracts of *Nannochloropsis* sp. under different treatments were prepared and analyzed with an untargeted metabolomics approach to highlight changes in the metabolome in presence or absence of bacteria. Figure 38a shows a PCA plot with all the treatments. Principal component one and 2 explains over the 70 % of the total variation of the features. However, the separation between the different treatments is not significant, especially because of the effect of *Roseovarius* sp. co-cultivation, which is showing a big spread between the samples, thus dominating the samples variation. We

therefore decided to divide the analysis in sub-groups in order to better visualize potential separation between treatments. The PCA plot in figure 38b displays the changes in the metabolome of *Poseidonocella* - *Nannochloropsis* co-cultivation: the samples are partially overlapping, thus confirming that the mild effect of *Poseidonocella* sp. alone on *Nannochloropsis* sp. growth.

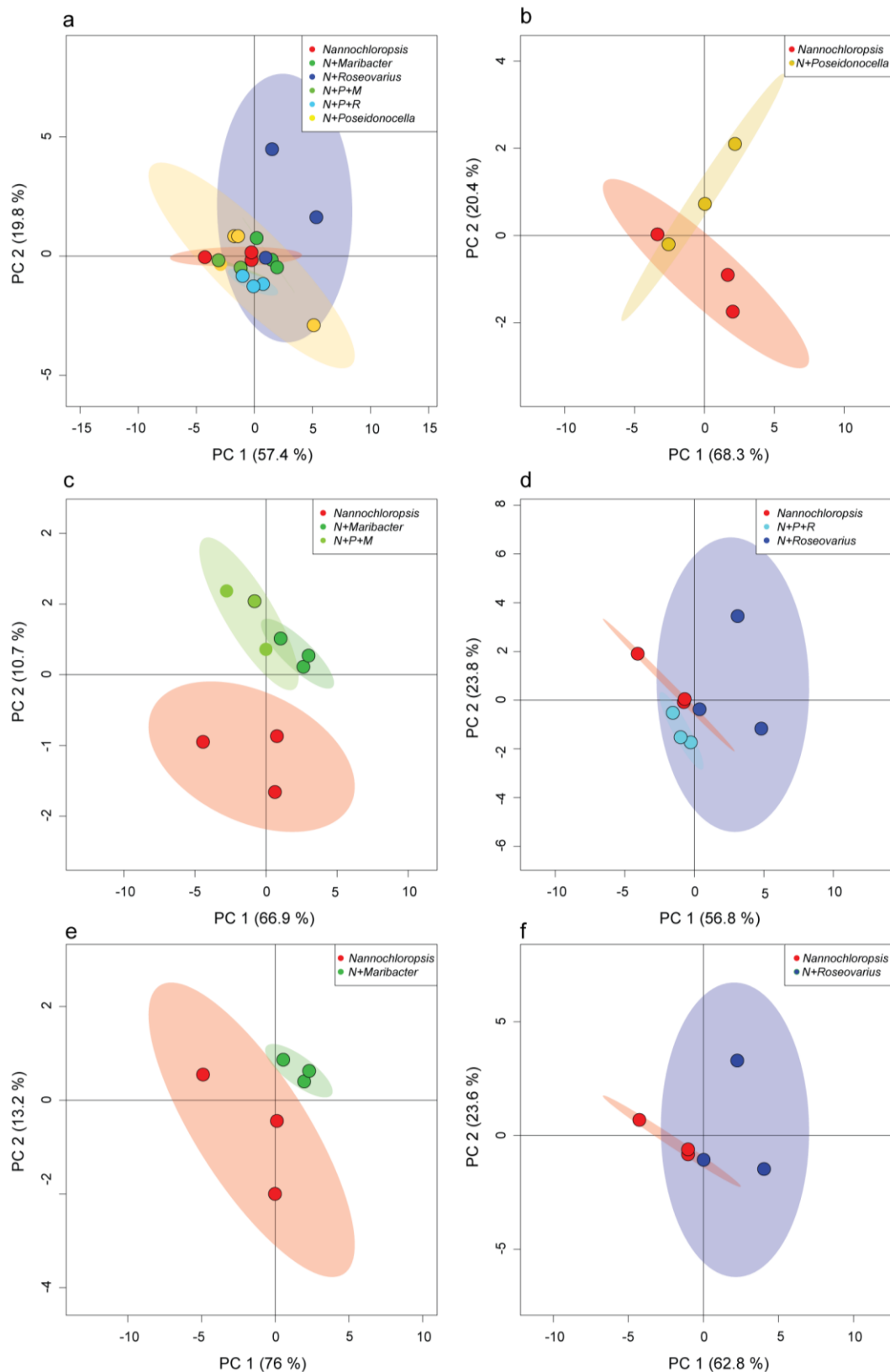


Figure 38: PCA plot of bacterial effect on *Nannochloropsis* endometabolome. PCA analysis (a) between all treatments, between *Nannochloropsis* (red) and (b) *Nannochloropsis* + *Poseidonocella* co-cultivation (yellow), (c) *Nannochloropsis* + *Poseidonocella* + *Maribacter* co-cultivation (light green), (d) *Nannochloropsis* + *Poseidonocella* + *Roseovarius* co-cultivation (light blue), (e) *Nannochloropsis* + *Maribacter* co-cultivation (green) and (f) *Nannochloropsis* + *Roseovarius* co-cultivation (blue).

Looking at PCA plots a and c in Figure 38, we can see that *Roseovarius* sp. is causing a substantial variation between biological replicates, thus highly overlapping with the control. The presence of *Poseidonocella* is reducing this effect, leading to a better clustering and a better separation from the control. When *Nannochloropsis* is grown in presence of *Maribacter* (figure 38b and 38d), the samples are separating better from the control and they are clustering together, with small differences between the treatment with and without *Poseidonocella*. All these results confirm that the effects of bacteria on growth are reflected on a metabolic level.

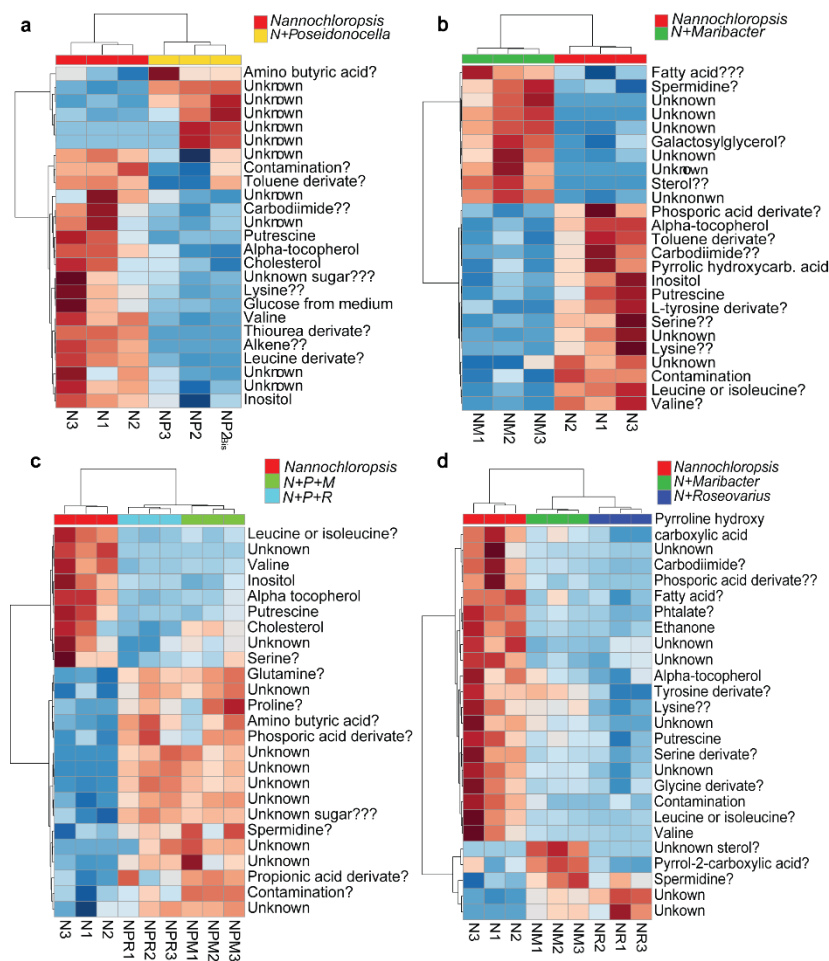


Figure 39: Heatmaps of *Nannochloropsis* endometabolites abundance under different treatments. For two way comparisons, a t-test with $\alpha=0.05$ was used. For multiple comparisons, a two-way ANOVA analysis with adjusted p-value (FDR) cutoff = 0.05 and FisherLSD post-hoc analysis was used. Color code legend is the same as Figure 40. Red metabolites are upregulated, blue are downregulated. Mass spectra were considered identical with a reverse match factor (R Match) >800, tagged with "?" if the RM was between 800 and 700, with "???" if the RM was between 700 and 600 and "?????" if below 600.

We therefore used a t-test for two way comparisons ($\alpha=0.05$) and a two-way ANOVA (adjusted p-value (FDR) cutoff = 0.05 and FisherLSD post-hoc analysis) to highlight the most significant up- and downregulated metabolites in different treatments. As heatmaps in

figure 39 shows, most of the metabolites influenced by bacteria presence or absence are shared among all treatments. Many amino acids (especially aliphatic ones, like valine, leucine, glycine and tyrosine, and charged one, like lysine) were less abundant in presence of bacteria. Also putrescine, a product of amino acid metabolism (Bender, 2012), was upregulated in absence of bacteria, while spermidine (a direct product of putrescine metabolism, Tabor and Tabor, 1976) was higher in presence of bacteria, especially *Maribacter* sp. (Fig 39 c). *Maribacter* is also affecting pyrroline acids derivatives, which are part of proline cycle. Interestingly, the presence of *Poseidonocella* sp. induced a higher production of amino butyric acid, an amino acid which has neurotransmitting functions in vertebrates, and a higher presence of proline and glutamine when other bacteria are present (Figure 39 d). α -tocopherol is always downregulated in presence of bacteria, while sterols exhibit no uniform behavior, sometimes being upregulated (e.g. in presence of *Maribacter*) and sometimes downregulated (e.g. in presence of *Poseidonocella*).

6.2.3 Bacteria isolated from *S. robusta* enhance biofilm formation of *Poseidonocella* sp. on *Nannochloropsis* sp.

Following the studies of Giraldo *et al.*, (submitted) on bacterial-induced biofilm formation in *Nannochloropsis* sp. cultivated in closed bioreactors, we tested if bacteria isolated from *S. robusta* could induce or reduce biofilm formation in the same system. The high throughput biofilm assay established by Giraldo *et al.*, allowed us to test up to 20 different combinations of bacteria and bacteria spent medium co-inoculated with *Nannochloropsis* sp. (the experimental design is shown in figure 36). One-way ANOVA with Bonferroni's correction for multiple comparison was used to test the significance of each treatment compared to the control sample (*Nannochloropsis* sp. alone).

Our experiment confirmed that *Poseidonocella* sp. is inducing biofilm formation when co-cultivated with *Nannochloropsis* sp. ($p=0.025$) (Figure 40). *Roseovarius* sp., *Maribacter* sp. and *Croceibacter* sp. are not inducing significant biofilm formation when they are added to the wells as single strains, but their combination with *Poseidonocella* sp. results in a significant increase of the absorbance of the biofilm, which reaches its maximum in presence of all strains ($OD_{630}=1.2-1.3$, $p < 0.0001$). Interestingly, the most significant effects are seen when bacterial exudates are added to *Poseidonocella* sp. and *Nannochloropsis* sp. co-cultivation.

Glucose and glycerol seem to have a big impact on biofilm formation: *Nannochloropsis sp.* inoculated with f/2 modified medium with glucose and glycerol forms biofilm even without inoculation of bacteria ($p < 0.0001$). The same effect is seen when *Poseidonocella sp.* is added to the well plate.

Since our *Nannochloropsis sp.* cultures are not axenic, it could be that bacteria are taking advantage of the income of fresh carbon resources and they are overgrowing, causing an increase production of biofilm.

However, the effect of residue glucose and glycerol on biofilm formation in co-cultivation of bacteria from *S. robusta*, *Poseidonocella sp.* and *Nannochloropsis* can be excluded, since the spent medium of these bacteria is not triggering any significant biofilm formation (Figure 40).

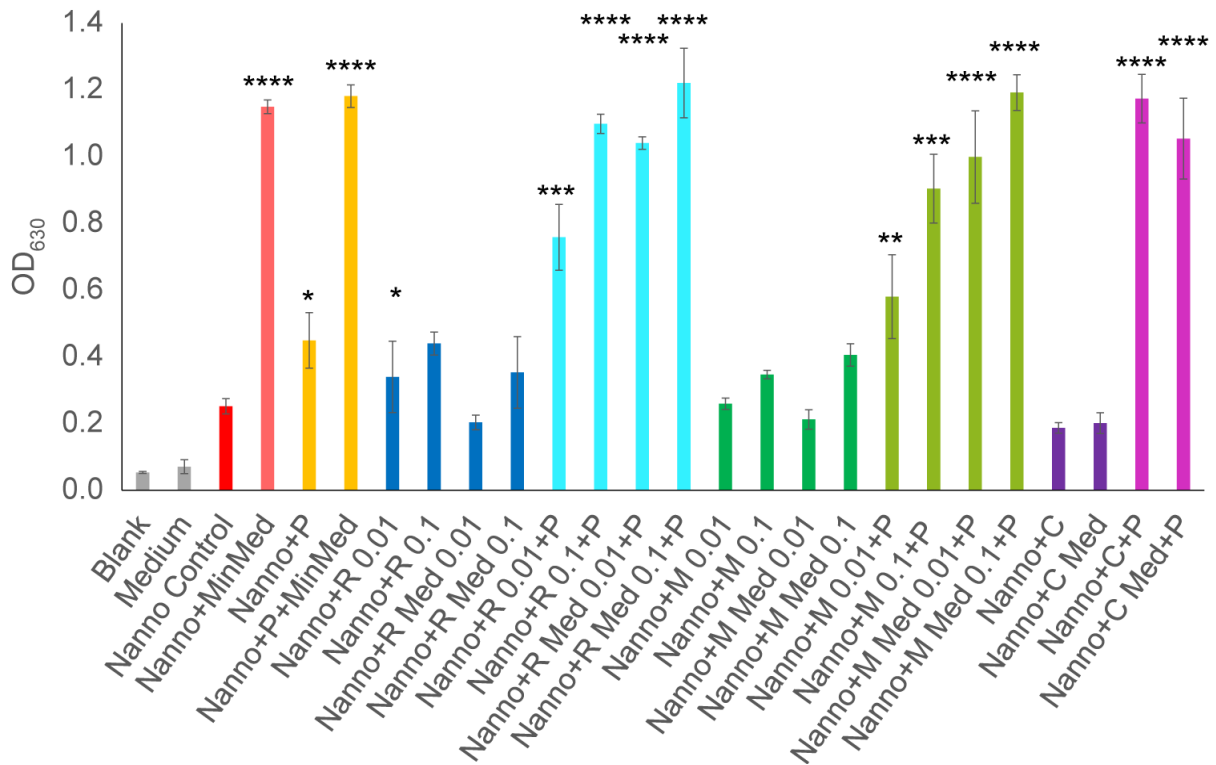


Figure 40: Biofilm formation of *Nannochloropsis sp.* in presence of different bacteria: red indicates controls with no bacteria, orange indicates *Poseidonocella sp.* only, blue *Roseovarius sp.* treatment, light blue *Poseidonocella sp.* + *Roseovarius sp.*, green *Maribacter sp.* treatment, light green *Poseidonocella sp.* + *Maribacter sp.*, purple *Croceibacter sp.* treatments and light purple *Poseidonocella sp.* + *Croceibacter sp.* (experimental design Fig 3). Each treatment was made in triplicates. Data were statistically evaluated with a one-way ANOVA, $\alpha = 0.05$, Bonferroni's correction for multiple comparisons. Asterisks refer to multiple comparisons to *Nannochloropsis sp.* control sample. *Poseidonocella sp.* (P), *Roseovarius sp.* (R), *Maribacter sp.* (M), *Croceibacter* (C). 0.01 and 0.1 are the OD₆₀₀ values for inoculated bacteria. Med stands for bacterial spent medium only. MinMed is the algae growth medium enriched with glucose and glycerol.

6.3. Discussion

Chemically mediated interactions between microalgae and bacteria have been underestimated for a long time, but in the last fifteen years many studies have proved their importance from an ecological and an industrial point of view (Ramanan *et al.*, 2016). A better understanding of microalgae-bacteria interactions could help enhance the production and the quality of microalgal cultivation (Fuentes *et al.*, 2016), as well as the development of new technologies for several industrial applications (Rizwan *et al.*, 2018). Moreover, these inter-kingdom communications are a key to decipher biofilm formation, both from an ecological (Van Colen *et al.*, 2014; Wahl *et al.*, 2012) and industrial perspective (Berner, Heimann, and Sheehan, 2015). Many studies focused on ways to reduce biofilm onset in order to improve microalgal production in photobioreactors (Zerriouh *et al.*, 2017), while other works concentrate their efforts on finding ways to produce stable biofilms, for example to improve wastewater treatment (Gonçalves, Pires and Simões, 2017). The understanding of bacteria-algae interactions can also lead to the development of synthetic microbial communities that are enhancing microalgal production. Microbiome engineering is a relatively novel concept that is attracting growing attention not only from human health research (Foo *et al.*, 2017), plant science (Quiza *et al.*, 2015) and agriculture (Bender, Wagg and van der Heijden, 2016), but also from aquaculture (Charrier *et al.*, 2017). Some studies have tested the effect of indigenous bacteria from wastewater on microalgae growth (Toyama *et al.*, 2018), while other have employed growth-promoting bacteria from plant rhizosphere to improve microalgal productivity in confined environments (Gonzalez and Bashan, 2000).

Following the observation of chapter 4, we decided to test the effect of these bacteria isolated from a natural sample on a different, commercially relevant species belonging to the class of Stramenopile, the oleaginous microalga *Nannochloropsis* sp. This work was done in collaboration with Proviron © (Antwerp, Belgium), a chemical company that since then years has started to invest in microalgal biomass production to create high quality feed for aquaculture. Recently, Giraldo *et al.* (submitted) have found that *Poseidonocella* sp., a gram negative alphaproteobacterium from the Rhodobacteraceae family and phylogenetically close to the *Roseobacter* clade (Romanenko *et al.*, 2012), is inducing biofilm formation in closed bioreactors for *Nannochloropsis* sp. culturing. We therefore tested different bacterial combinations to explore changes in microalgal growth, endometabolome and biofilm

formation in order to understand if an engineered microbiome could enhance biomass productivity while reducing biofouling side effects.

In co-cultivation experiments, we observed different effect of bacteria on *Nannochloropsis* growth (Figure 37). The presence of *Poseidonocella* sp. and *Roseovarius* sp. do not affect *Nannochloropsis* sp. biomass increase until seven days of cultivation. On the other hand, *Maribacter* sp. significantly supports algal growth already 3 days after inoculation. This effect is reduced when *Maribacter* sp. is co-inoculated with *Poseidonocella* sp.: in this treatment the growth is significantly increased only at the end of the seven-day co-cultivation, but the cell density reaches its maximum if compared to all the other conditions. The effects on the non-associated alga are thus different to those on algae with which the bacteria co-exist in nature (Chapter 3). Many studies confirmed that bacteria are able to both support microalgal growth (Seymour *et al.*, 2017), for example by releasing auxins (Amin *et al.*, 2015), and reduce it (Van Tol *et al.*, 2016). Some of them may exhibit a two-faced behaviour, first promoting and then inhibiting algal growth, until becoming pathogenic (Seyedsaymdest *et al.*, 2011). Our work demonstrates that this effect is highly species-specific and it is dependant on both the organisms that are interacting.

To understand if bacteria also have an impact on *Nannochloropsis* sp. endometabolome, we analyzed the different co-cultivations using a GC-MS-based untargeted endometabolomics approach.

Amino acids were the most affected metabolites in *Nannochloropsis* sp. (Figure 39), with many of them being downregulated in the presence of bacterial strains, especially glycine, valine, leucine, isoleucine and tyrosine. Interestingly, glutamate and proline were upregulated in presence of *Poseidonocella* sp. in combination with one of the two bacteria from *S. robusta*. Moreover, *Maribacter* sp. displayed a particular effect on intermediates of the proline cycle: in its presence, pyrrole-2-carboxylic acid is accumulated while pyrroline hydroxycarboxylic acid is decreased. Several studies showed that bacteria have a significant impact on microalgal amino acid metabolism, inducing the production of specific compounds to sustain their own growth (Amin *et al.*, 2015; Chen *et al.*, 2017a; Paul, Matusz, and Pohnert, 2013). This interaction mechanism could be of particular interest for applied purposes, in regard to nutritional value of algae for animal and human consumption (Reboloso-Fuentes *et al.*, 2001). The increase of proline and intermediates of its biosynthetic pathways may suggest a response of the alga to stress, since proline is involved in active response towards toxicity in plants and in some algae (Szabados and Savouré, 2010).

The hypothesis of amino acids breakdown under stress conditions is confirmed by the presence of several degradation byproducts. Spermidine, a polyamine that is a catabolic product of amino acids (especially arginine, Hildebrandt *et al.*, 2015) and putrescine pathway (Tabor and Tabor, 1976) and involved in abiotic stress response in plants (Gupta, Dey, and Gupta, 2013), was higher in *Nannochloropsis* sp. when *Maribacter* sp. was present (Figure 39). Since putrescine was higher in non-treated *Nannochloropsis* sp. cultures, these results show a species-specific stress response of the microalga towards bacteria that involves polyamines. Remarkably, the presence of *Poseidonocella* sp. is increasing the concentration of aminobutyric acid (Figure 39a), another product of amino acids transformation. Among the aminobutyric acids family, γ -aminobutyric acid (GABA) is a fundamental neurotransmitter in mammals and humans (Watanabe *et al.*, 2002) and an important defensive molecule in plants (Gupta *et al.*, 2013) that has been found also in several microalgae (Brown, 1991). A study by Pal *et al.* (2013) correlated the increase of GABA concentration in *Nannochloropsis oculata* to osmotic stress response adaptation. This finding hints to a different effect of *Poseidonocella* sp. on amino acids metabolism and microalgae signaling.

Sterol and fatty acids, two of the main products from *Nannochloropsis* sp., were only slightly influenced by bacteria. Cholesterols levels are higher in microalgal monoculture samples, while *Maribacter* sp. seems to have an enhancing effect on sterols and fatty acid biosynthesis. However, our experimental setup did not show a big influence of bacteria on lipid metabolism. We see clearly that the modulation of growth also goes ahead with the modulation of the cellular metabolism. As demonstrated earlier bacteria have a most pronounced activity on the amino acid content of the algae, confirming the role of these metabolites in cross kingdom nitrogen shuttling (Williams, 2007; Amin *et al.*, 2015). It is important to note that in aquaculture applications not only the growth promoting effect of bacteria but also their putative effect on the concentration of the targeted value product has to be considered. The unbiased metabolomic survey presented here demonstrates that different pathways including amino acid metabolism, lipid and sterol metabolism and saccharide metabolism are influenced by bacteria and most likely cascading effects on targeted value products have to be considered. This consideration is confirmed by the finding that the commercially important α -tocopherol is down regulated in presence of bacteria (Figure 39). *Nannochloropsis* is known to produce Vitamin E in relative high amount depending on nutrient availability and growth stage (Durmaz, 2007), and studies on different

microalgae (Vidoudez and Pohnert, 2012; Mausz and Pohnert, 2015) have shown that its concentration increases during stationary phase as a response to oxidative stress.

All these observations suggest a broad metabolic rewiring of microalgae in presence of bacteria, particularly their stress response.

Finally, bacteria were tested in bioassay to investigate their contribution to biofilm formation of *Nannochloropsis* sp (Figure 40). Although biofilm formation mechanism and dynamics in marine environments are still a subject of intense study, the mostly general accepted theory is that bacteria are initiating biofilm formation by releasing exopolymeric substances (EPS) in the so-called surface conditioning phase (Lorite *et al.*, 2011). EPS are usually composed of exopolysaccharides (40-95%), protein (1-60%), nucleic acids (1-10%) and lipids (1-40%) (Davey and O'toole, 2000; Flemming and Wingender, 2001). These substances create a protecting and resource-rich environment for both bacteria and microalgae (Xiao and Zheng, 2016) and shape multifaceted communities (Bohórquez *et al.*, 2017) that have an important and broad ecological role (Van Colen *et al.*, 2014).

Interestingly, *Maribacter* sp. (or its spent medium) did not significantly increase biofilm formation when co-cultivated with *Nannochloropsis* sp., while *Roseovarius* sp. induced biofilm development only at high cell concentration (Figure 40). However, when these bacteria (or their spent media) were added to microalgal cultures in the presence of *Poseidonocella* sp., biofilm formation was significantly higher as compared to *Nannochloropsis* sp. control cultures and the effect was even larger when compared to the presence of *Poseidonocella* sp. alone. The same promoting effect was seen when only saline medium, enriched in glucose and glycerol, was added to a co-cultivation of *Nannochloropsis* sp. and *Poseidonocella* sp. Glycerol has been used to enhance biomass productivity of *Nannochloropsis* sp. in mixotrophic conditions (Poddar, Sen, and Martin, 2018), while glucose has been recently employed to increase productivity in mixotroph cultivation of *Chlorella vulgaris* on biofilms (Roostaei, Zhang, Gopalakrishnan, and Ochocki, 2018; Ye *et al.*, 2018). Carbon sources (especially glucose) are important to sustain biofilm formation in various bacterial species, such as gram-positive bacteria from the *Bacillales* order (Mhatre, Monterrosa, and Kovács, 2014). Dissolved sugars appear therefore to be a strong trigger for biofilm formation and have to be precisely monitored in closed bioreactor cultures of *Nannochloropsis* sp. in order to prevent unwanted growth of thick biofilm. Further experiments on bacterial exudates, both with fractionation assays and metabolomics approach, will give us more information about putative signaling molecules that are sustaining microalgae growth and biofilm formation. This study already provides new

instruments to control culturing conditions in closed photobioreactors but reducing the manipulation from introduction of bacteria to the application of a pure growth or production stimulator might be an attractive alternative, increasing biomass productivity and reducing contaminations and biofilm formation.

Our study evaluates the opportunity to use bacteria isolated from a natural microalgal species (*Seminavis robusta*) to influence the growth, the metabolome and the biofilm formation of a different, commercially relevant microalgal species (*Nannochloropsis* sp.) in an attempt to design a productive engineered microbiome by microbial transfer. These results demonstrate that further efforts are necessary to study bacteria-algae interactions, using both indigenous and transplanted bacteria, as well as employing –omics approaches (metabolomics, transcriptomics, proteomics) and real-time test in production sites, in order to better understand bacteria-algae interactions and employ them to develop new technological applications.

7. A SPE-based, non-disruptive method to investigate macroalgal surface chemistry⁶

7.1 Introduction

Microbe-microbe communications and the interactions of microscopic organisms with environmental chemical gradients defines a patchy organization of microbial communities, as for example microalgae-bacteria biofilms that are forming on wet surfaces (MacIntyre, Geider, and Miller, 1996). Natural products play a fundamental role in ecological interactions on biotic surfaces under water. Surface metabolites can for example act on the interface of water and macroalgae, corals, sponges and also epilithic and epiphytic biofilms. Such compounds control settling processes, regulate predator/prey relationships, mediate infection processes (Wahl 2009; Dobretsov *et al.*, 2013; da Gama *et al.*, 2014), and may also control competitors by means of allelochemical activity (Gross 2003; Lu *et al.*, 2011; Rasher *et al.*, 2011). Furthermore, regulation of fouling is influenced by these natural products (Dobretsov *et al.*, 2013; da Gama *et al.*, 2014). In the last years, extensive efforts have been done to discover novel antifouling products from algae (Dahms and Dobretsov, 2017) and microbes associated to algal surfaces (Satheesh, Ba-akdah and Al-Sofyani, 2016). However, the study of metabolites released from these patchy environments poses difficult technical challenges. In this chapter, we introduce a novel method to investigate the molecules released from patchy surfaces, focusing on algae-bacteria interactions that happen at the surface of macroalgae. Simple mechanistic considerations suggest that surface metabolites are highly concentrated and thus most active in a very small diffusion-limited laminar-boundary layer of water in the immediate vicinity of the producing organism (Hurd, 2000; Grosser *et al.*, 2012). Knowledge about surface concentrations is thus relevant for the investigation of the ecological role of metabolites (Dworjanyyn *et al.*, 1999, 2006). Nevertheless, until now most investigations on the effect of surface metabolites have been based on bioassays with extracts of whole organisms, or with compounds applied in concentrations found in whole tissue extracts (eg see Hellio *et al.*, 2000). Such experiments do not reflect the real ecological relevance of surface active substances, because only

⁶ This chapter is based on: Cirri, E., Grosser, K., & Pohnert, G. (2016). A solid phase extraction based non-disruptive sampling technique to investigate the surface chemistry of macroalgae. *Biofouling*, 32(2), 145-153. And on: Cirri, E., & Pohnert, G. (2017). Disruption-free solid phase extraction of surface metabolites from macroalgae. *Protocols for Macroalgae Research*, 20, 311-321.

metabolites at the surface or in the immediate vicinity of a producer should be considered (Nylund *et al.*, 2007). The determination of metabolites within the laminar boundary layer around an aquatic organism, a thin film of about 100–200 μm that determines the transition between the surface and the surrounding water, is thus crucial for planning and evaluation of experiments.

Studies performed with resonance Raman microspectroscopy allowed visualization of the gradient of carotenoids in the boundary layer around the macroalgae *Fucus vesiculosus* and *Ulva mutabilis*. A pronounced decline in concentration from up to millimolar values in the immediate vicinity of the algal surface to concentrations below the detection limit at a 100 μm distance was observed (Grosser *et al.*, 2012). However, this elaborate method is limited to a few Raman active metabolites. Most investigations of algal surface chemistry rely on the extraction of secondary metabolites by so-called ‘dipping’ methods (de Nys *et al.*, 1998; Lachnit *et al.*, 2009). Here, algae are immersed in a solvent for a brief period, during which the metabolites are partially extracted from the surface. After concentration in vacuum, the extracts can be analyzed by analytical methods such as gas chromatography-mass spectrometry (GC-MS) and liquid chromatography-mass spectrometry (LC-MS). Although useful, dipping methods are rather problematic since solvent exposure can cause cell lysis and thereby contamination of the surface extract with intracellular metabolites. Algae only tolerate exposure to rather non-polar solvents such as hexane for a few seconds. However, these solvents only extract a very limited range of non-polar metabolites and do not penetrate surface associated water. If solvent mixtures containing methanol are employed, massive damage of the algae can be observed, thereby questioning the validity of results.

To overcome these limitations, a non-destructive, solvent-free and universal method for extracting secondary metabolites from marine macroorganisms based on C18 solid phase extraction principles was developed (Figure 41). The macroalga *Fucus vesiculosus* was used as a model organism for method development. *F. vesiculosus* is a common, well-studied brown alga that can be found at the coasts of the North Sea, the western Baltic Sea, and the Atlantic and Pacific Oceans. Due to its important ecological role, this alga has been the subject of numerous investigations of its chemical defense and antifouling capacity (Lachnit *et al.*, 2009, 2013; Saha *et al.*, 2011, 2012; Rickert *et al.*, 2015). In addition, the green alga *Caulerpa taxifolia* and the red alga *Gracilaria vermiculophylla* were extracted to test the application range of the method, which could be potentially useful to analyze metabolites from other wet surfaces, as epilithic and epiphytic biofilms or underwater technical surfaces colonized by marine organisms.

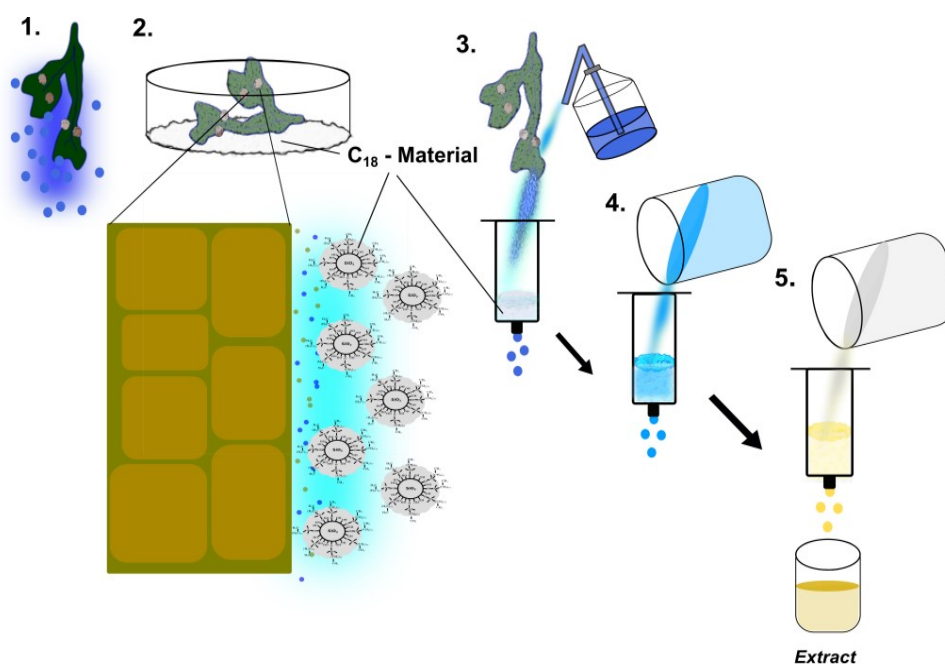


Figure 41: Schematic workflow of the C18 method. (1) Algal fronds are removed from the water and left for 2 min to remove excess water by dripping; (2) fronds are transferred to Petri dishes and covered with absorption material; (3) the C18 material is washed off with excess seawater and collected in an empty solid phase extraction cartridge equipped with a frit; (4) the material is washed with deionized water to remove salts; (5) elution with organic solvents finalizes sample preparation.

7.2 Results

7.2.1 Development of the extraction procedure

The optimum extraction method for surface metabolites is the one that maximizes extraction efficiency while minimizing damage to the alga. The available solvent dipping methods exhibit shortcomings in both respects. Dipping of algae in hexane causes little to no damage of cells, but this highly unpolar solvent allows only extraction of unpolar metabolites (de Nys *et al.*, 1998). Dipping in a mixture of hexane and methanol extracts metabolites with a broader polarity range but causes significant stress (Lachnit *et al.*, 2009; Saha *et al.*, 2011). We therefore developed an extraction method that covers a broad range of metabolites but causes no damage to the algae. This method relies on the absorption capabilities of solid-phase extraction material. By powdering the algal surface with this material, metabolites in the boundary layer around the alga and on its surface can be absorbed (Figure 43). To cover a broad range of metabolites C18-material was selected for method development. Initially, different materials were tested for recovery, purity and ease of handling. Non-encapped silica Gel 100 C18 reversed phase material (100 Å pore size, 40-63 µm particle's dimensions) could be easily handled and was suitable for the extraction of surface

metabolites. However substantial impurities that could not be removed by conditioning interfered with the detection of algal metabolites (Figure S10 in Appendix). Fully endcapped silica Gel 100 C18 reversed phase material (100 Å pore size, 15-25 µm particle's dimensions) was suitable for extraction of surface metabolites exhibiting low background (Figure S11 in appendix) but the very fine powdered material proved to be problematic in the handling (see appendix). The small particles attached poorly to the algal surface and could only be transferred incompletely into the extraction cartridges. Fully endcapped silicaGel 90 C18 material (90 Å pore size, particle's dimensions 40-63 µm, Sigma-Aldrich, Germany) proved to be superior with respect to the low background and the ease of handling (Figure S12).

The different methods for application tested included distribution of the powder with a sieve, dusting the material on the alga and shaking the alga gently in a Petri-dish with silica gel. Even if application using a sieve consumed less material, coverage was higher using the "Petri-dish method" that was further pursued. For *F. vesiculosus* a thallus piece of $36.5 \pm 6.5\text{cm}^2$ proved to be sufficient for the generation of GC-MS and LC-MS samples. However, smaller sample sizes can be used in cases of limitation of biological material since only few microliters are required for chemical analysis. The amount of C18 material recovered in the cartridge, weighted at the end of the experiment after the complete evaporation of the remaining elution solvent, was 0.13 ± 0.01 g. Again, in case of limitation of biological material sensitivity could be increased by more quantitative washing off and recovery of the material. Even if the loss of absorbing material is high, this method gives the most uniform coverage of the alga and allows an easy handling. The incubation time of 60 s represents the best compromise between a good interaction and absorption of metabolites with C18 material and an easy recovery of the powder from the alga.

7.2.2 Microscopic observation

It is essential for a method focused on the determination of surface metabolites that cellular integrity is maintained throughout the entire procedure. Otherwise the overlaying effects of metabolites released from lysed cells would be detected and no estimation of surface concentrations would be possible. To monitor for surface cell integrity, the algal surfaces were documented in microscopic pictures after applying the C18 extraction method for 5, 60 and 300 seconds as indicated above (Figure 42 and Figure S9 in appendix). For comparison, surfaces of algae from the same batch were investigated after applying the "hexane/methanol

"dipping" treatment performed as described in (Lachnit *et al.*, 2009). Additionally, a control group that was taken out of the aquarium for the same time without being extracted was evaluated. Independent of the incubation time with C18 material, visual inspection revealed that surface cells were not damaged or otherwise altered. In strong contrast, even after only 5 seconds of extraction with the "dipping" method, the colour of the *F. vesiculosus* surface changes from the typical yellow-brown to green, which is indicative for damage and pigment loss of the surface cells. Also, fronds of *C. taxifolia* did not show any signs of damage after C18 treatment as examined by light microscopy (Figure S9 in appendix). To visualize dead cells, staining with Evans Blue (Weinberger *et al.*, 2005) and RGB (red, green, blue) evaluation of the recorded microscopic images was carried out. This test confirmed that already after 5 seconds of hexane / methanol dipping, cells were damaged as indicated by a substantial change in red/green ratio, while values did not differ significantly from controls when using the C18 method (Figure 42). Despite its broad application, the Evans Blue staining method is not without problems for the investigation of algal surfaces, since oxidation of the algal pigment after chloroplast rupture cannot be clearly distinguished from the effects of Evans Blue staining.

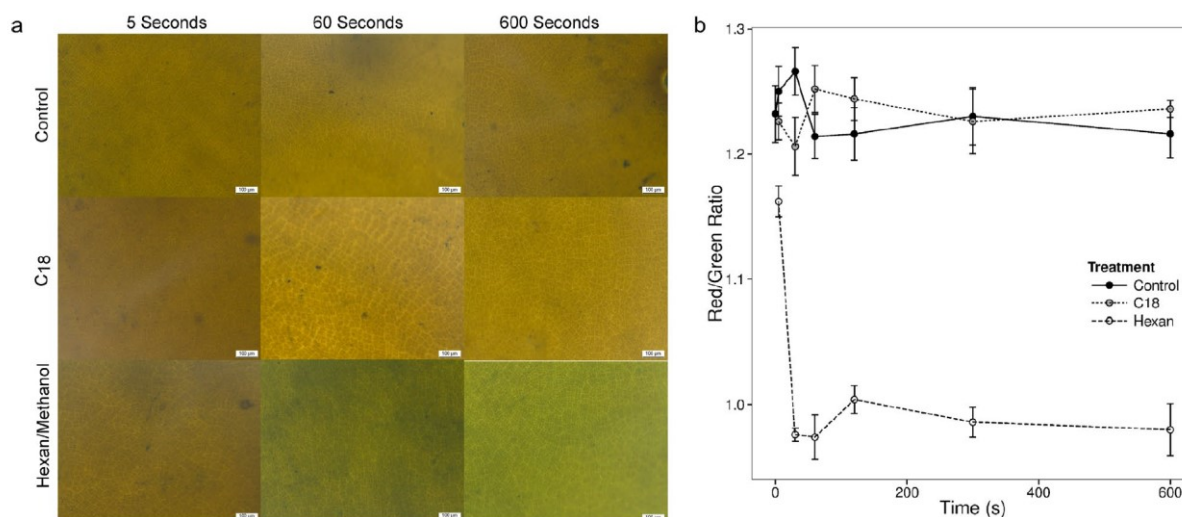


Figure 42: Evaluation of surface damage by different extraction methods. (a) Photographs of *F. vesiculosus* surfaces (scale bars 100 μm). Top row: control after removal from water for 5, 60 and 600 s. Middle row: algae after C18 extraction. Bottom row: after hexane/methanol dipping for the same time spans. (b) Evaluation of cell damage after Evans blue staining by red/green ratio analysis at 5, 30, 60, 120, 300, 600 s exposure to C18 material (gray), hexane/methanol dipping (white) and control (black), ($n = 5 \pm \text{SD}$).

7.2.3 UPLC-MS measurements of extracted metabolites

The methanolic surface extracts resulting from the C18 method can be directly submitted to HPLC or UPLC-MS analysis without any further concentration step. In initial experiments we monitored for the presence of the carotenoid fucoxanthin, a dominant pigment of brown algae such as *Fucus* spp. This metabolite is ideally suitable for method development and comparison since earlier studies using the hexane / methanol dipping method as well as Raman-imaging already indicated that this compound is released from the surface of *Fucus* species (Grosser *et al.*, 2012; Saha *et al.*, 2011). Fucoxanthin was identified in UPLC-MS measurements by comparing its retention time and ESI mass spectrum with a commercial standard ($[M+Na]^+=681$ m/z at 2.43 min). Fucoxanthin can be clearly detected in the samples extracted with the C18 absorbing material.

7.2.4 Quantification of surface metabolites

For quantitative determination, canthaxanthin, another carotenoid pigment that is not found in *F. vesiculosus*, was used as standard. Figure 43 shows the average chromatographic area of fucoxanthin extracted from *F. vesiculosus* with the C18 method in relation to the average chromatographic area of the internal standard canthaxanthin. Values are given for extracts of five specimens, with an average extracted surface of 36.5 ± 6.4 cm^2 . Since extracts were split into two equal parts for GC-MS and LC-MS determination the values determined correspond to an 18.25 cm^2 surface area. The standard deviations of fucoxanthin and canthaxanthin determinations are similar (5.66 and 5.26 of mean peak area). Since canthaxanthin was introduced after the extraction protocol was performed this indicates a very good reproducibility of the extraction procedure. Only minor additional variability in comparison to sample drying, re-dissolution and measurement is introduced by the C18 extraction procedure. The C18 method was compared to the established hexane / MeOH dipping. Recovered fucoxanthin in dipping experiments is significantly higher compared to C18 experiments (Figure 43a and b). This can be due to overall better extraction success, or to contributions of fucoxanthin released by the lysed cells in the hexane / MeOH treatment. An external calibration based on the evaluation of the peak areas of the standard canthaxanthin in relation to areas resulting from different amounts of fucoxanthin (Figure S13 in appendix) allowed estimating the extracted fucoxanthin. Even if quantification is problematic since no reference method for the determination of absolute amounts of surface chemicals is available the procedure allowed the comparison between the extraction success

of this study to other studies in the literature. C18 extraction gives $\sim 1.4 \pm 0.28$ (SD) μg fucoxanthin cm^{-2} while the hexane / methanol dipping recovers absolute amounts of $\sim 22 \pm 18.95$ (SD) μg fucoxanthin cm^{-2} . Previous studies using the dipping method gave similar values ($0.7\text{-}9 \mu\text{g}$ fucoxanthin cm^{-2}) and it can be concluded that algae in our study and the analytical work-flow are matching those in the literature within the margins of error and natural and experimental variability (Saha *et al.*, 2011). The hexane dipping procedure alone did not result in any detectable fucoxanthin (data not shown). It became clear that the absolute values detected using dipping methods are highly dependent on the polarity of the solvent, thus a quantitative comparison of the methods is not advised. It also cannot be finally answered whether the C18 method quantitatively extracts surface metabolites and whether the hexane/methanol overestimates the content due to cell lysis, or whether the C18 method underestimates surface metabolites due to non-quantitative extraction. The reproducibility of the C18 method, however, suggests a highly reliable measurement. The standard deviation of signals in the C18 extract is substantially lower than that in hexane / methanol extracts. Given the facts that the C18-method is by far better reproducible and that it does not introduce cell damage this method has to be considered as superior. Lower recovery is not problematic, since even small thallus fragments provide sufficient extract for the entire analytical process. Extraction and measurement can be easily carried out without additional concentration steps using routine instrumentation.

To test the universal applicability of the C18-method we also investigated two macroalgae with hitherto unknown surface chemistry. No adaptation in the protocol was required for surface extraction of the green alga *Caulerpa taxifolia* and the red alga *Gracilaria vermiculophylla*. In the case of *C. taxifolia*, $45.8 \pm 4.0 \text{ cm}^2$ ($n = 3$) algal surface was extracted without cell damages. LC-MS revealed the presence of caulerpenyne (identified by comparison to authentic material; Jung and Pohnert, 2001). Again, elevated amounts were detected using the hexane / methanol dipping protocol. Since caulerpenyne is a very dominant intracellular metabolite, this elevated value can be interpreted as a result of unwanted extraction of algal cells. Caulerpenyne is involved in chemical defense (Weissflog *et al.*, 2008) and wound closure (Adolph *et al.*, 2005) by the alga. This is the first report demonstrating that caulerpenyne is also present at the surface of the alga (Figure 43c and d) and motivates further investigation of its potential role as surface defense compound or natural anti-fouling metabolite. As with *F. vesiculosus* extracts, hexane / methanol dipping resulted in overall higher caulerpenyne recovery, but also in substantial cell damage (data not shown) and very high standard deviation (Figure 43). Quantitative differences might

again be explained by substantial damage after hexane/methanol extraction, as was observed by visual inspection. Damage was not quantified since a substantial amount of algal material was physically degraded during the dipping procedure. However, a poor extraction efficiency with C18 powder could result in reduced recovery. Finally, initial experiments with *G. vermiculophylla* revealed ion traces corresponding to previously identified oxylipins from whole tissue extracts of the alga (data not shown) (Nylund *et al.*, 2011; Rempt *et al.*, 2012; Jacquemoud and Pohnert, 2015).

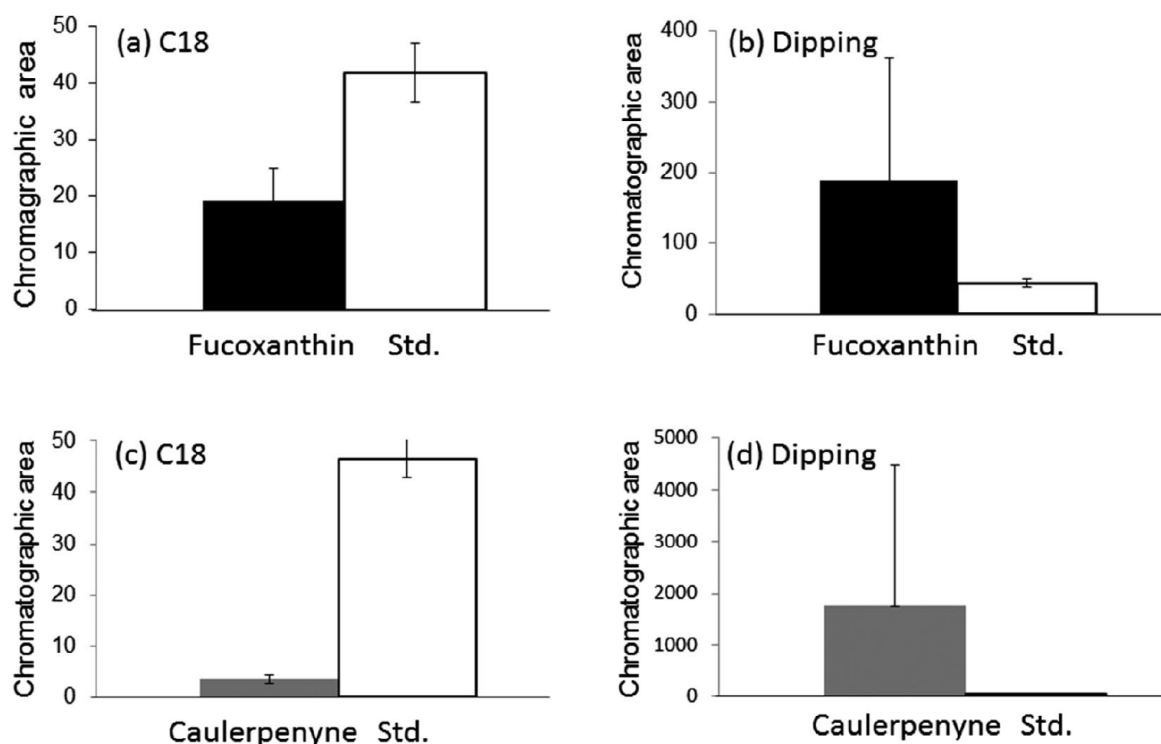


Figure 43: Quantification of extracted compounds from macroalgae. (a, b) Average chromatographic areas of fucoxanthin extracted from *F. vesiculosus* surfaces in relation to cantaxanthin as internal standard (Std): (a) C18 method, $n = 5$, surface extracted = 36.5 ± 6.4 cm²; (b) hexane/methanol dipping method, $n=5$, surface extracted = 29.3 ± 3.0 cm². (c, d) Average chromatographic areas of caulerpenyne extracted from *C. taxifolia* surfaces and cantaxanthin as internal standard: (c) C18 method, $n=3$, mean surface extracted= 45.8 ± 4.0 cm²; (d) hexane/methanol dipping method, $n=3$, mean surface extracted= 36.0 ± 7.3 cm². Note the difference in scale of the y-axis for a, c and b, d.

7.2.5 GC-MS detection of free fatty acids

Since the C18 material is suitable to extract a broad range of non-polar and medium polar compounds, its capability to extract structurally diverse surface metabolites was tested. Since LC-MS techniques do not allow for simple compound identification the exploratory power of GC-MS supported by library identification of metabolites was used to test for additional compound classes picked up by the C18 method. The major metabolites that were extracted

from *F. vesiculosus* surfaces were fatty acids that were transformed by the solvent MeOH to their methyl esters during elution. This transformation was verified by control measurements where EtOH instead of MeOH as elution solvent was used and where ethyl esters instead of methyl esters were detected in the extracts. Characteristic fragments of 79 m/z ($[C_6H_7]^+$ indicative for polyunsaturated fatty acids) and 74 m/z (a McLafferty ion indicative for saturated fatty acids) were detected and structure elucidation was performed by comparison with authentic standards (FAME, Sigma- Aldrich[®], Germany). A representative chromatogram and the assigned metabolites can be found in Figure 44. Fatty acids are common in brown algae (Pereira *et al.*, 2012; Schmid and Stengel, 2015), but were previously never detected as surface metabolites. Their presence in surface extracts can be explained with an active release mechanism of free fatty acids or alternatively with a partial hydrolysis of surface lipids on the surface of the alga. The fact that fatty acids as surface metabolites were overlooked till now might be due to limitations of previous experimental approaches. In accordance, samples that were generated with the hexane / methanol dipping method contained only few fatty acids in trace quantities (GC/MS after derivatisation; data not shown). In addition to free fatty acids, substantial amounts of phytol and a not further identified sterols were found, confirming the broad extraction potential of the C18-method.

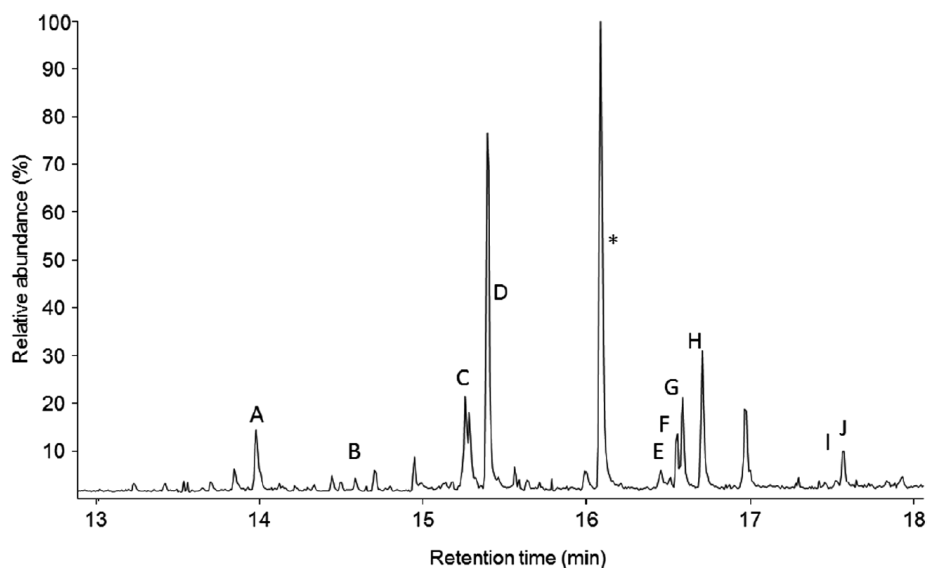


Figure 44: GC-MS run of a C18 extract of *F. vesiculosus* performed with the C18 method and with MeOH as elution solvent. The range of elution of fatty acid methyl esters is shown. A) myristic acid methyl ester (C14:0); B) C15:0; C) C16:1 ((Z)9-hexadecenoic acid (palmitoleic acid) methyl ester); D) C16:0, *phthalate (contamination); E) C18:3 9,12,15-octadecatrienoic acid (α -linolenic acid) methyl ester; F) C18:2 (9,12-octadecadienoic acid (linoleic acid) methyl ester); G) C18:1 (9-octadecenoic acid (oleic acid) methyl ester); H) C18:0 (octadecanoic acid (stearic acid) methyl ester); I) C20:4 (5,8,11,14-eicosatetraenoic acid (arachidonic acid) methyl ester); J) C20:5 (5,8,11,14,17-eicosapentaenoic acid methyl ester). All fatty acid methyl esters were confirmed with synthetic standards.

7.4 Discussion

Investigation of the algal surface chemistry is central for the understanding of ecological interactions on and around these organisms, for example to understand invasion success of allochthon species (Schwartz *et al.*, 2017) or the interaction between algae and epiphytic bacteria (Persson *et al.*, 2011). The search for new, natural and sustainable antifouling compound and biofilm disruptors, as well as the understanding of their mechanism of action, represent another major field of research (Dahms and Dobrestov, 2017; Chen and Qian, 2017). The most commonly used methods involve solvent dipping of the specimens and investigation of the resulting extracts (de Nys *et al.*, 1998; Lachnit *et al.*, 2009). However, these methods pick up compounds in a very limited polarity range and cause substantial damage to the algal tissue. Alternatively elaborate instrumentation as it is required for desorption electrospray MS (Lane *et al.*, 2009) or Raman techniques (Grosser *et al.*, 2012) is needed for surface investigations. The introduced method that is based on covering the algal surface with C18 extraction sorbent and collecting the material for subsequent extraction does not cause stress to the investigated algae. It is universal and suitable for detecting a wide range of natural substances of different polarity. Its ease of handling and the reliable results reflected by low standard deviations make it a universal tool for future investigations, for example to study algal surfaces in different conditions, such as healthy versus infected specimens. Another application could allow to study surface metabolites in presence or absence of epiphytic biofilms (mainly formed by bacteria, cyanobacteria and diatoms) to understand how the surface metabolism of algae is changing and which compounds are important in interactions between biofilm-forming organisms and macroalgae. The method that was validated for algal surface extraction in this study is potentially easily transferred to the investigation of other aquatic organisms and even submerged technical surfaces: for example, the study of molecules released by biofilm colonizing surfaces could expand the understanding about the chemical signaling among bacteria during biofilm formation or employed as biofilm defensive mechanisms, thus leading to new ecological discoveries and technological applications.

8. Conclusive discussion and perspectives

Chemical language is the oldest communication system and its adaptation to diverse environments and ecological conditions, as well as its differentiation in several species, have fascinated many bringing to the foundation of a dedicated branch of science: chemical ecology.

In this thesis, I present the study of the complex inter-kingdom cross-talk between microalgae and bacteria, focusing both on its ecological role and its potential industrial applications. To decipher the molecular mechanisms behind these interactions, I used a combination of physiological assays and modern omics techniques and I was able to identify novel interactions that can help us to better understand the crucial relationships between aquatic microbes that shape Earth's ecosystems.

8.1 New methodologies and –omics techniques to study signalling between marine microorganism

The study of microbial communication has many challenges to face, and this is particularly true for marine chemical ecology (Goullitquer, Potin and Tonon, 2012). The high complexity of the matrix, the dilution of exuded metabolites, the high concentration of salts and the complicated dynamics that regulates marine microbial communities make the isolation and quantification of chemical cues particularly difficult. The detection of secondary metabolites, usually released in small amounts from micro- and macroorganisms, is aided by advanced extraction and enrichment techniques. In case of algal pheromones, for example, a large and dense culture of cells is necessary to isolate more than 100 µg of the active molecule and structurally identify it (Lembke, 2018). Sometimes the extraction techniques are not suitable to generate an extract that can be used to answer a specific ecological question (**Chapter 7**). For example, if we consider the isolation of metabolites that regulate the interactions of macroalgae with other organisms, investigations have been often done using whole cell extractions (Carvalho *et al.*, 2017) and testing the potential antifouling and antibacterial activity of extracted metabolites in bioassay. However, to determine a realistic ecological concentration of such compounds, techniques to extract metabolites released at algal surfaces or biofilm interfaces are necessary (Nylund *et al.*, 2007). The classical “dipping” technique, which involves immersing wet macroalgae in an

organic solvent, is a simple and powerful method for extracting surface metabolites (de Nys *et al.*, 1998; Lachnit *et al.*, 2009). A major drawback of this method is the damage to the algal surface provoked by the solvents. In order to overcome this problem, I developed a non-disruptive technique that use solid-phase extraction principles to extract surface metabolites (**Chapter 7**). The method is fast, easy to handle, does not harm the surface of the alga. From this work I have established a flexible protocol for algal research (Cirri and Pohnert, 2017) can be applied to different macroalgal specimens and potentially to other wet surfaces, as for example epilithic biofilms. By changing the extraction resin, different metabolites can be targeted, from carotenoids to lipids up to polar compounds, like osmolytes and sugars. Moreover, by extracting multiple surfaces in parallel and combine the resin in a single SPE cartridge, the concentration of interesting metabolites can be incremented. A combination of this method with novel sensitive analytical instruments (LC/GC-HR-MS) allows for the detection of known and unknown metabolites excreted at exceedingly low concentrations directly from algal surfaces.

Apart from novel sample preparation techniques and metabolites concentration protocols, a breakthrough in studying algae-bacteria interactions are represented by the introduction of -omics approaches to algal ecology. Transcriptomic analyses allow the identification of an organism's response towards stimuli and its acclimation along time (Jamers, Blust and De Coen, 2009), thus giving useful information about evolutionary adaptation (Caron *et al.*, 2017). Metabolomics approaches gives an important alternative to the bioassay-guided fractionation, overcoming some of the limits of this traditional methodology, like the long preparation time and the risk of losing unstable chemical cues (Kuhlich and Pohnert, 2014). The introduction of highly sensitive high-resolution mass spectrometry techniques (Fuhrer and Zamboni, 2015) and the integration with NMR spectroscopy (Markley *et al.*, 2017) make metabolomics a powerful tool to narrow down the selection of chemical signals or metabolites characteristic for a certain treatment within a short time, thus speeding up the procedure that brings a chemical cue from its extraction to its identification.

The potential information that could be obtained by the integration of these technologies brings new opportunities to systems biology research and many studies have demonstrated the power of omics techniques in marine ecology, for example in the context of nutrient deprivation of diatoms (Allen *et al.*, 2008; Alipanah *et al.*, 2015), viral infection of coccolitophores (Rosenwasser, Mausz *et al.*, 2016) or the influence of bacteria on diatoms (Durham *et al.*, 2015). The application of these approaches is still relatively new and it is yielding an unprecedented number of data. It is therefore crucial to carefully plan a large-

scale multiomics experiment, because the decisions taken during planning large-scale multiomics experiments have a huge impact on data quality. Quality assessment is a pivotal step in omics experiments as it assesses beforehand the possible causes of errors and it helps to minimize them (Dudzic *et al.*, 2018). The use of quality controls, for example, is a powerful approach to control the reproducibility of the measurements, to correct for possible signal drifts within and between analytical batches and control for unwanted variances (Dudzic *et al.*, 2018). In metabolomics, sample stabilization is also crucial in order to prevent the degradation of labile compounds, such as those involved in chemical interactions. Blank samples are fundamental to identify signals coming from impurities coming from the complex marine medium or introduced during the sample preparation procedure. Test measurements are necessary to understand the volume of spent medium (for exometabolomics) or the cell concentrations (for endometabolomics) needed to obtain samples that are not too diluted nor too concentrated. Internal standards for normalization (Sysi-Aho *et al.*, 2007) and retention time index standards for identification (Vinaixa *et al.*, 2016) are additional important tools, considering the high number of unknowns and the big concentration differences in aquatic samples. Also, the decision for the right statistical methods to be applied, even prior to the actual experiment, is crucial to interpret data in a meaningful way (Yi *et al.*, 2016; Kupferschmidt, 2018).

In this thesis, I have adapted transcriptomics and metabolomics methods in order to the effects of bacteria on diatoms and other microalgae. In particular sample preparation was optimized in order to have enough volume to extract a detectable amount of metabolites. Medium blanks were used to remove, during data analysis, all possible interferences coming from artificial sea water. With a combination of transcriptomics, exometabolomics and targeted analysis, it was possible to reconstruct the broad effect of bacterial medium on the metabolism and on sexual reproduction of *Seminavis robusta* (**Chapter 5**). Moreover, by comparing the exudates of control samples (axenic *S. robusta* and bacterial spent medium) to samples of *S. robusta* treated with bacterial spent medium, it was possible to select for potential signaling molecules produced by the bacteria that may induce the rewiring of diatom's metabolism (**Chapter 5**).

Furthermore, by using an endometabolomic approach, a complex metabolic rewiring of *S. robusta* (**Chapter 3**) and *Nannochloropsis* metabolism (**Chapter 6**) in a 7 days co-cultivation with bacteria was observed. In this case, metabolomics gave a snapshot of the effect of bacteria on algae metabolism and it proved to be a powerful tool to assess the quality of algae growth for industrial purposes.

New technologies, like single cell transcriptomics (Sandberg, 2014) and single cell metabolomics (Zenobi, 2013), new tools for the *in-silico* identification of unknown molecules (Blaženović *et al.*, 2018), as well as the implementation of minimum reporting guidelines (Sumner *et al.*, 2007; Considine *et al.*, 2018), will lead aquatic chemical ecology (bacteria-microalgae interaction research included (Cooper and Smith, 2015)) into a new era and will change the perspective of many other applications, like aquatic risk assessment (Brockmeier *et al.*, 2017) and ecotoxicology (Revel, Chatel and Mouneyrac, 2017).

8.2 Understanding metabolic interactions between microalgae and bacteria

In aquatic environments, microbe-microbe interactions define patchy microscale communities which are characterized by gradients of chemical cues (Stocker, 2012). Within these gradients, microbes can select suitable environmental niches, forage on nutrients, find mating partners, defend against predators and interact with other organisms. The phycosphere is one of these microscopic regions rich in organic molecules surrounding algal cells (Bell and Mitchell, 1972). It provides nutrients and protection necessary for the survival and proliferation of microbes in open oceans, benthic zones and freshwater environments. Within this region, algae-bacteria communication takes place and create a complex network of interactions, as explained in chapter 1.2.

In this thesis, I explored the many influences that bacteria have on the model benthic diatom *Seminavis robusta*. I started by testing the effect of different bacterial isolates on algal growth and found that different species have a different impact on it (**Chapter 3**). *Roseovarius* sp. significantly supported diatom proliferation. This effect is not unexpected, since many studies demonstrated that microbes from the *Roseobacter* clade are usually associated to diatoms (Amin *et al.*, 2012) and that many of them are exuding substances that are beneficial for microalgae (Wienhausen *et al.*, 2017). On the other hand, *Croceibacter* sp. did not enhance diatom growth and also didn't decrease cell number after 7 days. This result, which seems to contradict the findings of van Tol *et al.* (2017) of this bacterium on *T. pseudonana*, supports the assumption that the effect of bacteria on algae is species-specific. This hypothesis holds true even more for *Maribacter* sp., a bacterial genus belonging to the *Flavobacteriaceae* (Nedashkovskaya *et al.*, 2004) family. Although being found in association with diatoms, its influence on microalgae has been to date poorly assessed. One study reports its algicidal effect on the ubiquitous diatom *Skeletonema* sp. (Wang *et al.*,

2016a), while other studies show that its presence is essential for the complete morphogenesis of the green macroalga *Ulva mutabilis* (Weiss *et al.*, 2017). In my work, a *Maribacter* sp. showed a mild, positive influence on *S. robusta* growth, thus rising interesting questions about this understudied genus and its effects on algae. Remarkably, the same effect is seen on the commercially relevant microalga *Nannochloropsis* sp. *Maribacter* sp. is supporting the growth of the microalga already during the first days of cultivation (**Chapter 6**) and it is therefore an interesting candidate to be used also in applied aquaculture research.

Novel –omics techniques allowed us to investigate the effect of bacteria on algae at a metabolic level. Metabolomics approaches allow the comprehensive and quantitative investigation all small molecules produced by an organism under a given set of conditions (Fiehn 2002). The endometabolome of *S. robusta* was significantly affected by seven days of co-cultivation with either *Roseovarius* sp. or *Maribacter* sp., while the endometabolome of *Croceibacter* sp. was not affected by tested bacterial associations (**Chapter 3**). Disaccharides are the most abundant metabolites induced by the two bacteria. Sugars are among the compounds that are known to be upregulated in a co-cultivation of *T. pseudonana* and *D. shibae* (Paul, Mausz and Pohnert, 2013), but disaccharides have never been described as induced in microalgae by bacterial influence. These compounds hint to an increased breakdown of polysaccharides in order to face a high requirement of energy (Mausz and Pohnert, 2015). Transcriptomics data obtained after 10 hours of *S. robusta* – bacterial spent medium co-cultivation (**Chapter 5**) showed that oxidative stress response, like tocopherol synthesis and glutathione S-transferase activity, are strongly upregulated in the presence of bacteria, thus hinting to a general stress induced by bacteria on microalgae. However, during stationary phase the higher concentration of unknown sugars and galactosylglycerol in axenic cultures suggest that the absence of bacteria causes even higher level of stress and energy deficiency during stationary phase as already observed in various other studies (Allen *et al.*, 2006.; Vidoudez and Pohnert, 2012; Mausz and Pohnert, 2015). Elevated stress levels are implied also by the higher concentration of α -tocopherol, an important antioxidant employed by algae (Havaux and García-Plazaola, 2014), in axenic cultures compared to xenic ones. These on the first view contradictory results could be explained as a mechanism of adaptation of the alga towards bacteria. *Roseovarius* sp. and *Maribacter* sp. may induce in *S. robusta* an initial strong stress response. After this first interaction, the diatom will likely adapt to the presence of bacteria and start a beneficial communication and interaction. During stationary phase, when resources become scarce,

axenic cultures will face alone this stressful situation, while the non-axenic cultures will benefit from the protection and the fruitful exchange with bacteria, that may partially slow down oxidative and metabolic stress. Detoxification mechanisms of marine bacteria, like ROS scavenging, can increase the fitness and growth rate of microalgae, as in the case of the cyanobacterium *Prochlorococcus* (Morris *et al.*, 2011) or of the arctic diatom *Amphiprora kufferathii* (Hünken *et al.*, 2008). A combination of transcriptomic, endo- and exometabolomic investigations of *S. robusta* sampled at different time points along the growth phases will give more insights to the changes of concentration of these molecules and their regulation. Moreover, specific bioassays to test the effective detoxification mechanisms, for example using flow cytometry experiments (Franklin, Stauber and Lim, 2001) and advance electrobiology techniques (Bailleul *et al.*, 2010b), will help to understand the effect of the presence or absence of bacteria on the photosystem of the diatoms. Additional transcriptomics analysis will also allow to confirm the involvement of cGMP signaling in perception of bacterial exudates. cGMPs are not only involved in diatom mating, as already described by Moeys *et al.*, (2016) and Basu *et al.*, (2018), but they seem to be implicated in recognition of bacterial signal molecules (**Chapter 5**). Up to now, this mode of action was only found in the system *Reugeria pomeroyi* – *Thalassiosira pseudonana* (Durham *et al.*, 2015). Further studies on this process may bring novel understanding in bacteria-diatom recognition mechanisms.

8.3 Physiological and molecular insights into the bacterial effect on sexual reproduction of diatoms

Apart from interspecies communication such as bacteria-algae interactions, intraspecies exchanges of signaling molecules play a fundamental role in maintaining ecological diversity and in assuring the survival of the species (Venuleo, Raven and Giordano, 2017). One of the most important life cycle aspects that is regulated by intraspecies interactions is sexual reproduction. In diatoms, sexual reproduction is a necessary step for population survival, as introduced in chapter 1.1. This process is regulated by chemical signaling, like in the well-study benthic pennate diatom *Seminavis robusta*.

In this thesis, I observed that bacteria associated to *S. robusta* are able to modulate sexual activity and percentage of sexual reproducing cells of the diatom using different strategies. *Maribacter* sp. is negatively influencing *S. robusta* sexual efficiency by reducing the

percentage of gametes and auxospores, while *Roseovarius* sp. is slightly enhancing the auxosporulation process (**Chapter 4**). Transcriptomics investigation and targeted analysis of diproline concentration led me to formulate the hypothesis that *Maribacter* sp. affects intracellular amino acid concentrations by rewiring several metabolic pathways involving glutamate, phenylalanine and tyrosine biosynthesis (**Chapter 5**). This process may reduce the pool of proline, which is hypothesized to be involved in the yet unknown biosynthetic process of diproline (Moeys *et al.*, 2016). A reduction of diproline may therefore lead to a lower sexual efficiency of the diatom (**Chapter 4**). This effect is not present with *Roseovarius* sp., which on the other hand lightly enhances proline synthesis, thus potentially leading to an increased pool of this amino acid that may feed diproline production over a longer time period and increase the reproduction success. These results, together with the evidence of a reduction of diproline concentration in non-axenic cultures compared to axenic ones and the evidence of diproline degradation by bacteria over time (**Chapter 4**) may explain the dramatic drop of the attraction pheromone concentration 12 hours after sexual induction and onset of light, despite the stability of diproline in water (Gillard *et al.*, 2013). These findings, however, do not completely elucidate the reason why bacteria should modulate pheromone systems of algae. This process could be a side effect of other interactions that are more beneficial for the bacteria: for example, the influence of amino acid production could be exploited by bacteria to induce diatoms to release useful resources. The observed upregulation of photosynthetic activity with the consequent consumption of glutamate (necessary for proline synthesis in diatoms) could be an additional defense mechanism of *S. robusta* towards bacteria, a means to overgrow them and preclude a potential swamping effect due to the over-proliferation of bacteria. Such effects have been observed in a relatively short time frame (10 hours of co-incubation) and could give an explanation to the very first stress-response reaction of sexually induced diatoms towards bacteria and to the complete disappearance of the stable diproline after 24 hours of co-incubation.

Another possible explanation could be that bacteria may use diketopiperazines (DKPs), like diproline, as a source of carbon and nitrogen. The presence of DKPs in bacteria culture medium (Tamura *et al.*, 1964) and studies on bacterial degradation of DKPs (Perzborn *et al.*, 2013) support this hypothesis. However, bacterial isolates from *S. robusta* show degradation of diproline only in extremely starved conditions (**Chapter 4**). In a high nutrient medium, as in the productive epilithic biofilms formed by diatoms, bacteria would have enough organic matter to survive without the need of degrading diproline. Nevertheless, the high

concentration of the attraction pheromone found in sexually induced *S. robusta* medium may increase the accessibility of this nutrient and induce the bacteria to degrade it. The decline of diproline over time appears therefore as a combination of influence on metabolic production and active degradation processes from bacteria.

Interestingly, a reduction in SIP⁺ concentration was observed in co-cultures compared to axenic cultures over a growth period of 7 days (**Chapter 3**), and the process was more pronounced in the presence of *Maribacter* sp compared to other bacteria. The identity of this molecule is still unknown. However, it was shown that SIP⁺ contains sulfonated moieties (Moeys *et al.*, 2016) and a putative carbohydrate structure (Lembke doctoral thesis, 2018). The ecological reason behind SIP⁺ degradation is puzzling. Given the fact that many marine bacteria are able to degrade carbohydrates and polysaccharides (Edwards *et al.*, 2010; Buchan *et al.*, 2014), SIP⁺ could be used as an organic source of sulfur and carbon, especially during stationary phase, when inorganic resources are becoming scarce. From the diatom point of view, this mechanism could support algal mate finding by avoiding misguidance towards aged pheromone sources and optimizing the release and production of it by a yet unknown intra- and interspecies signaling cascade.

Taken together, these results rise multiple fascinating questions about a novel inter-kingdom interaction and especially about the role of *Maribacter* sp. as a modulator of microalgal metabolism and pheromone chemistry. Additional experiments will shed light on the hypotheses arising from this thesis. First, higher temporal resolution transcriptomics data are required to study the response of *S. robusta* towards *Maribacter* sp. and *Roseovarius* sp. The structural elucidation of SIPs and subsequent bioassays on bacterial degradation will make us understand why bacteria degrade diatom pheromones, whereas isotope-labelling experiments coupled with high-resolution MS analyses could answer the question of how bacteria consume pheromones and which metabolic pathways are involved. Exometabolomics analysis already suggests the implication of putative signaling molecules released by bacteria, for example methylated nucleobases and furanones (**Chapter 5**). Further investigations on larger volumes of algal and bacteria supernatant, as well as fractionation-guided bioassays, will allow us to identify the molecules that regulate these interactions. These investigations, together with a microbial population diversity study of natural biofilms inhabited by *Seminavis robusta* will expand our understanding of the role of different bacteria and their metabolites in the organization and ecological functions of epipelagic communities.

8.4 From nature to application: microalgae-bacteria interactions in biotechnology

Microalgae-bacteria communication is not only interesting from an ecological point of view, but has recently attracted growing attention from applied and industrial research (Kozuma and Watanabe, 2015).

A fascinating application that has been proposed, but up to now only in few pioneering articles, is the engineering of microbiomes to increase algal cultivation productivity and modulate metabolic production on an industrial level (Charrier *et al.*, 2017). This practice has been investigated and employed to support sustainable agriculture (Quiza, St-Arnaud and Yergeau, 2015; Bender, Wagg and van der Heijden, 2016; del Carmen Orozco-Mosqueda *et al.*, 2018), but to date only few experiments were conducted on microalgae, using plant-growth promoting bacteria to enhance algal biomass increment (Gonzalez and Bashan, 2000). In collaboration with Proviron[®], a chemical company from Belgium that is growing microalgae in closed photobioreactors for aquaculture feeding, I tested the potential effect of bacteria isolated from *S. robusta* on the commercially relevant oleaginous microalga *Nannochloropsis* sp. (**Chapter 6**). I found that *Maribacter* sp. increases algal growth more than other bacterial isolates. This effect is even enhanced in the presence of *Poseidonocella* sp., a species associated to *Nannochloropsis* sp. and isolated from bioreactors by Giraldo *et al.* (submitted). This observation could be supported by metabolomics data: the decreased concentration of α -tocopherol in *Nannochloropsis* sp. cells after 7 days of co-cultivation with *Maribacter* sp. may that the bacterium is protecting the alga from oxidative stress (see chapter 8.1). *Maribacter* sp. is influencing amino acid biosynthesis and degradation of *Nannochloropsis* sp., as shown by the higher concentration of spermidine, a degradation product of amino acids, and the small increase of glutamate and proline intermediates in comparison to the control treatment. The metabolic rewiring could be a strategy used by bacteria to induce the alga to produce compounds useful for its own growth, as observed in other marine microbial consortia (Seymour *et al.*, 2017).

Besides the beneficial effect on algal growth, bacteria are capable of inducing biofilm formation in microalgae (Bruckner *et al.*, 2011). Biofilms are useful for industrial purposes, such as wastewater treatment (Kesaano and Sims, 2014) and aquaculture (Avendaño-Herrera and Riquelme, 2007). More often, biofouling, defined as biofilm formation on technical surfaces, has a negative economic impact on industrial activities (Schultz *et al.*, 2010; Fitridge *et al.*, 2012) and huge investments are needed to reduce it. An alteration in the algal

microbiome may induce biofilm growth and decrease the biomass yield in closed photobioreactor cultivation systems due to reduction of light penetration and increasing contamination (Zerriouh *et al.*, 2017). It is therefore necessary to understand microalgae-bacteria interactions in order to fight harmful biofouling and to design sustainable synthetic microbiomes. The bacteria isolated from *S. robusta* do not induce significant biofilm formation but do enhance biofilm development of *Poseidonocella* sp. (**Chapter 6**). This effect could be due to a synergistic interaction of the bacteria, but more experiments are necessary to prove this hypothesis, to find potential molecules that may trigger biofilm formation. Moreover, the addition of high quantities of carbon sources (like glucose or glycerol) induce significant biofilm production. This information should be taken in consideration, especially when planning to grow algae in mixotrophic conditions.

These preliminary results hint to a promising application of microbiome engineering to closed microalgal cultivation systems and demonstrate that metabolomics is an incredibly useful tool also in applied fields like aquaculture (Alfaro and Young, 2018). However, further tests are needed to elucidate the real potential of synthetic microbiomes. The increasing availability of genomes data of both microalgae and bacteria may lead to a more rational design of the microbiomes (such as metabolic network modeling, and transcriptomic analyses may explain the mechanisms behind the beneficial effect of bacteria on microalgal growth. Different co-cultivation setups, such the dual co-cultivation chambers developed by Paul, Mausz and Pohnert (2015), combined with exometabolomics analysis may lead to the identification of beneficial or harmful molecules produced by bacteria. Finally, flux analyses in pilot closed photobioreactors will test the applicability of this approach on an industrial scale.

9. Materials and methods⁷

9.1. Strains and growth conditions

9.1.1 Strains and general culture conditions

S. robusta strains 85A (MT⁺) and 84A (MT⁻) were obtained from the diatom culture collection of the Belgian Coordinated Collection of Micro-organisms (BCCM/DCG, <http://bccm.belspo.be>). Cultures of both mating types were grown separately under a 12h:12h dark/light regime (light intensity 35 $\mu\text{mol m}^{-2} \text{s}^{-1}$) at 15°C in f/2 medium prepared from Instant Ocean Medium (Instant Ocean, Blacksburg, Virginia, USA) and a mixture of stock solutions following the recipe from Guillard (1962). Axenic cultures were obtained by treating the diatoms every second day for one week with an antibiotic mix (500 $\mu\text{g/mL}$ penicillin, 500 $\mu\text{g/mL}$ ampicillin, 100 $\mu\text{g/mL}$ streptomycin and 50 $\mu\text{g/mL}$ gentamicin). Axenicity of stock cultures was verified before every experiment both by plating a 100 μl aliquot of cultures on DifcoTM Marine Broth Agar and by monitoring the number of SYBR GOLD-stained-bacteria with a BD AccuriTM C6 Plus flow cytometer (modified from Marie *et al.*, 1997). Briefly, 250 μl of cultures were fixed with glutaraldehyde (1% final concentration) for at least 15 minutes in the dark and stained with SYBR GOLD® (10,000 diluted from stock solution) for 10 minutes in the dark. Then samples were measured with a BD AccuriTM C6 flow cytometer with the following settings: 8 μl per samples, 4 $\mu\text{l}/\text{min}$, 3 washing steps between each sample with milliQ water, 3 measurements for each sample. Cultures were considered axenic when no growth of bacteria was observed under the microscope (Figure S1), no colony formation was observed after two weeks of incubation on marine broth agar (Figure S2) and the number of bacteria counted by flow cytometry was $\leq 1\%$ compared to non-axenic cultures (Figure S3).

⁷ All the methods are based on the following publications:

Cirri, E., Grosser, K., & Pohnert, G. (2016). A solid phase extraction based non-disruptive sampling technique to investigate the surface chemistry of macroalgae. *Biofouling*, 32(2), 145-153.

Cirri, E., & Pohnert, G. (2017). Disruption-free solid phase extraction of surface metabolites from macroalgae. *Protocols for Macroalgae Research*, 20, 311-321.

Cirri, E., Vyverman, W., & Pohnert, G. (2018). Biofilm interactions-bacteria modulate sexual reproduction success of the diatom *Seminavis robusta*. *FEMS microbiology ecology*, 94(11).

Cirri, E.*, Giraldo, J.*, Neupane, S., Willems, A., Mangelinckx, S., Roef, L., Vyverman, W., Pohnert, G. Bacteria isolated from *Seminavis robusta* influence growth, biofilm production and the metabolome of *Nannochloropsis* sp. Submitted to *Algal Research*.

Cirri, E.*, De Decker, S.*, Bilcke, G., Osuna, C., Werner, M., Werz, O., Van Delpoole, K., De Veylder, L., Vyverman, W., Pohnert, G. Associated bacteria affect sexual reproduction by altering gene expression and metabolic processes in a biofilm inhabiting diatom. Submitted to *Molecular Ecology*.

Croceibacter sp., *Roseovarius* sp., *Marinobacter* sp., *Maribacter* sp. were isolated from *S. robusta* non axenic cultures of strain 85A. A healthy diatom culture, growing in artificial seawater medium (Tropic Marin® supplemented with Guillard's (F/2) Marine Water Enrichment Solution: Sigma-Aldrich) was suspended and spread-plated on Difco™ Marine Agar. After two to three days of growth, unique colonies were transferred based on morphological characteristics and further purified by repeated plating. DNA was extracted from the pure colonies as follows: cells were lysed with 20 µl of alkaline lyse buffer (0.25% SDS, 0.05M NaOH), heated at 95°C for 15 min. and afterwards cooled on ice. 180 µl of MilliQ water were added and samples were centrifuged at 13000 rpm for 5 min.

Bacterial isolates were identified by partial sequencing of 16S rDNA. Amplification of the 16S rDNA was done using the pA (5'-AGAGTTTGATCCTGGCTCAG-3') (forward, position 8-28) and pH (5'-AAGGAGGTGATCCAGCCGCA-3') (reverse, position 1542-1522) primers (Edwards *et al* 1989). The success of the amplification was verified through gel electrophoresis. The amplicon was purified using a NucleoFast® 96 PCR Cleanup kit (Macherey-Nagel). The sequencing PCR was run using the Big Dye® Terminator cycle sequencing kit (Applied Biosystems) with the primer BKL1 (5'-GTATTA CCG CGG CTG CTG GCA-3'(Cleenwerck *et al* 2007) on the ABI Prism 3130xl Genetic Analyzer (Applied Biosystems). Sequences were aligned and verified using BioNumerics software 5.1 (AppliedMaths, Belgium). Identification was performed using the EzTaxon at <https://www.ezbiocloud.net>. All isolates are stored in the Research collection of the Laboratory of Microbiology, Dept. Biochemistry and Microbiology, Ghent University. Bacterial stock cultures were cryopreserved at -80°C in a 50% glycerol solution and were grown in Difco™ Marine Broth at room temperature for three days before every experiment. *Fucus vesiculosus* was collected on February, April, May and June 2014 in the Kiel Fjord on an easy-to-reach beach (54° 21'36.8" N, 10° 10' 44.0" E). The algae were transported in plastic bags with pulp paper moistened with Baltic sea water at maximum 18°C to the University of Jena. Algae were immediately cleaned with deionized water to reduce epibionts. Then each individual was put into a 7 L aquarium filled with Instant Ocean Medium (Instant Ocean, Blacksburg, Virginia, USA), which was adjusted to the salinity of the Baltic Sea (14-16 PSU). The aquaria were kept in a temperature controlled (15 °C) climate chamber under a constant 14 h / 10 h light / dark regime (light intensity of 65 µmol m⁻² s⁻¹) with aquarium pumps guaranteeing constant ventilation. In the first week, it is necessary to change water every two or three days in order to keep the algae clean, afterwards weekly change of water is required. Under these conditions algae survived in good shape for

three weeks or up to a month. *Caulerpa taxifolia* was obtained by a tropical fish store (Aqua-Reptil-World, Jena, Germany) and transported to the lab in a plastic bag. Algae were washed carefully with deionized water and put into 7 L aquaria filled with Instant Ocean medium adjusted to Mediterranean salinity. Aquaria were aerated with air pumps and kept at room temperature (20-25 °C) with a day / night cycle of 12 h / 12 h and light intensity at the water surface by $40 \mu\text{mol m}^{-2} \text{s}^{-1}$. *Gracilaria vermiculophylla* was collected in the Kiel Fjord (54° 21'36.8" N, 10° 10' 44.0" E) during the last days of April / beginning of May 2014 and transported to Jena in plastic bags with pulp paper moistened with Baltic Sea water. Once in the laboratory, algae were washed carefully with medium and put into 7 L aquaria filled with Instant Ocean Medium (Instant Ocean, Blacksburg, Virginia, USA), which was adjusted to the salinity of the Baltic Sea (14-16 PSU). The aquaria were kept under comparable conditions as those of *C. taxifolia*.

9.2. Co-cultivation of microalgae with isolated bacteria – a metabolomic approach: materials and methods

9.2.1. Growth of *S. robusta* in co-cultivations with isolated bacteria

S. robusta strain 85A (MT⁺) (BCCM: DCG0105) under sexual size threshold (SST= 22.4 μm) was obtained from the diatom culture collection of the Belgian Coordinated Collection of Micro-organisms (BCCM/DCG, <http://bccm.belspo.be>). Diatoms were inoculated in 250 ml f/2 medium in 250 cm² culture flasks (TC Flask T25, Sarstedt®, Nümbrecht, Germany) at an initial cell density of 10^4 cells/ml. Axenic cultures were prepared as explained in Chapter 9.1. *Croceibacter sp.*, *Roseovarius sp.* and *Maribacter sp.* were isolated from *S. robusta* non axenic cultures of strain 85A. The bacteria were grown in 30 mL of marine broth medium for three days. Each bacterial strain culture (2 ml) was transferred into a 2 ml Eppendorf® tube, centrifuged for 3 min. at $6,000 \times g$, washed three times with minimal medium (f/2 medium with 5g/l glucose, 5 ml/l glycerol, 1.5 g/l NH₄NO₃) and transferred to 30 ml of minimal medium. After ten days of growth at room temperature, bacteria were inoculated with the diatoms (initial bacterial cell density = 10^4 cells/ml, initial diatom cell density = 10^3 cells/mL). Each treatment as well as an axenic control was repeated in triplicate. Diatom growth was followed for 7 days by counting the number of cells using a Leica DM IL LED inverted light microscope with a LeicaDFC 280 camera system (Heerbrugg, Switzerland). For each culture flask, 5 pictures were taken and *S. robusta* cells

were counted using ImageJ software (Rasband, 1997). Bacterial growth was followed for seven days by counting bacteria with a BD Accuri™ C6 Plus flow cytometer and by measuring the OD₆₀₀ with a Genesys™ 10S UV-Vis Spectrophotometer (Thermo Fisher Scientific, Bremen, Germany). The growth was statistically analyzed by means of a two-way ANOVA followed by Bonferroni's multiple comparisons tests were performed using GraphPad Prism version 7.00 for Windows (GraphPad Software, La Jolla California USA, www.graphpad.com).

9.2.2. Sample preparation for endo- and pheromone analysis of *S. robusta*

After seven days of co-cultivation, *S. robusta* cells were harvested 3 h after the onset of light to obtain intracellular samples. Therefore, 250 mL of each culture were filtered through GF/C filters (ø 47 mm) at 650 mbar on Nalgene™ reusable bottle top filters units (Thermo Fisher Scientific, Bremen, Germany) connected to sterile 500 mL Duran® bottles (Schott, Jena, Germany). The collected supernatant was stored at 4 °C in the dark until further filtration and extraction. Two filtrations were done in parallel, each filtration took on average 30 min. Cultures that were not extracted were kept under low light and low temperature regime (4 °C) to slow down metabolic processes.

After filtration, the still wet filters were immediately transferred to 25 mL glass beakers. Cells were re-suspended in 2 mL extraction mix (methanol : ethanol : chloroform, 1:3:1, v: v: v) and transferred to 4 mL glass vials. Samples were vortexed for 60 s and kept at -20°C until further processing and analysis.

Supernatant was transferred into Nalgene bottles cleaned with ethanol and distilled water. The bottles were centrifuged for 10 min at 5000 rcf with a Sorvall® Evolution™ RC Superspeed Centrifuge (Thermo Fisher Scientific, Bremen, Germany). The centrifuged supernatant was filtered on GF/F filters (ø 47 mm) at 650 mbar Nalgene™ reusable bottle top filters units (Thermo Fisher Scientific, Bremen, Germany) connected to sterile 500 mL Duran® bottles (Schott, Jena, Germany). Before extraction, 15 nmol of caffeine dissolved in methanol (for HPLC, Sigma-Aldrich, Chromasolv®Plus (≥99.9%)) were added to each sample as internal standard. The filtered supernatants were extracted on 60 mg HLB-SPE cartridges (Oasis®, Waters, Eschborn, Germany) following the manufacturer's instructions. Gentle vacuum was applied to the cartridges with a Visiprep™ SPE Vacuum Manifold (Sigma-Aldrich) to have a flow through of ca. 1 drop per second. The cartridges were eluted

2 times with 1 ml MeOH and the extracts stored at -20 °C until measurement. Medium blanks were (n=4) were prepared in the same way by extracting sterile f/2 medium.

9.2.3. Endometabolite extraction, derivatization and GC-HR-MS measurements

Intracellular samples were thawed and vortexed. 1 mL of *S. robusta* sample and 0.7 mL of *Nannochloropsis* sample were transferred into 1.5 mL centrifuge tubes (Eppendorf, Germany) and 5 µL of 4 mM aqueous ribitol (>99%, Sigma-Aldrich) were added as internal standard (IS). Suspensions were treated for 10 min in an ultrasonic bath (VWR™ Ultrasonic Cleaner), centrifuged (15 min, 30.000 rcf, 4°C), and supernatants were transferred to 1.5 mL glass vials. Samples were evaporated under a stream of nitrogen and dried under vacuum overnight to eliminate the excess of water. Samples were then derivatized with methoxyamine and MSTFA according to Vidoudez and Pohnert (2012). Quality (QC) samples were prepared by pooling 5 µL from each sample and blank samples in one clean vial.

Samples were run in random order with QC every 5 samples for *S. robusta* and every 7 samples for *Nannochloropsis* on a Thermo Scientific™ GC Ultra coupled to a QExactive™ Orbitrap (Thermo Fisher Scientific, Bremen, Germany) equipped with a DB-5ms column (30 m, 0.25 mm internal diameter, 0.25 µm film thickness, 10 m Duraguard pre-column, Phenomenex®). Helium 5.0 (Linde AG, Pullach, Germany) was used as carrier gas with a constant flow of 1 ml min⁻¹. 1 µL of sample was injected in split mode (split ratio 5 for *S. robusta*, 100 for *Nannochloropsis*). The initial oven temperature of 80 °C was held for 2 min, ramped to 120 °C at 2 °C min⁻¹, then to 250 °C at 5 °C min⁻¹ and finally to 320 °C at 10 °C min⁻¹. The final temperature was held for 2 min. The injector temperature was kept at 250 °C during the entire run. All transfer lines were heated at 280 °C, while the ion source was at 300 °C. Electron-impact ionization was carried out at 70 eV. The scanned mass range was between 50 m/z and 600 m/z, at a resolution m/Δm 120,000 full width at half maximum (FWHM) (m/z 200), with automatic gain control (ACG) target 3 × 10⁶, a maximum injection time (IT) of 200 ms.

Data were acquired and processed with the software Xcalibur™ version 4.0.27.19 (Thermo Fisher Scientific, Bremen, Germany).

9.2.4. GC-HR-MS data analysis

Xcalibur™ raw data file were converted to mzXML with the software ProteoWizard v. 3.0.11799 (Chambers *et al.*, 2012) and then uploaded on Workflow4Metabolomics v 3.0 (<http://workflow4metabolomics.org/the-galaxy-environment/>, Giacomoni *et al.*, 2015), an online platform implemented in the Galaxy Environment (Afgan *et al.*, 2018) for pre-processing, analysis and statistics of GC-MS, LC-MS and NMR metabolomics. The GC-MS analysis is based on the R-package metaMS (Wehrens *et al.*, 2014). The important values for features extraction are the following: Full Width at Half Maximum (FWHM) 5, retention time (RT) difference 0.05 min., minimum features 5, similarity threshold 0.7, minimum class fraction 0.1, minimum class size 1.

After the analysis, a table with exact masses, retention times and chromatographic area for each sample was exported for further processing with an in-house R-script (<http://www.R-project.org/>, R Core Team, 2017).

Features were normalized on the internal standard, medium features were deleted from the table and data were then filtered based on QCs coefficient of variation (CV): only features with CV < 35 % were retained (Begley *et al.*, 2009, Dunn *et al.*, 2011). Finally, data were normalized on cell densities.

The obtained .csv table was used to perform statistical analysis with MetaboAnalystR (Chong and Xia, 2018). The data were Pareto scaled to achieve a normal distribution of both features and samples. PCA was performed to detect grouping and outliers in the samples. Significant features were selected by looking at PCAs loading plots and at the results of two-way ANOVA analysis (adjusted p-value (FDR) cutoff = 0.05, FisherLSD post-hoc analysis) were visualized on heatmaps (distance measure = euclidean, clustering algorithm = Ward). After statistical analysis, significant features were manually checked in the chromatogram and identified using the software MS Search (version 2.0 d, NIST) by comparing the spectra with the following library using: NIST 11 library version (mainlib, replib, nist_ri), Golm Metabolome Database libraries T_MSRI_ID (http://csbdb.de/csbdb/dload/dl_msri.html; 2004) and GMD_20111121_VAR5_ALK_MSP (<http://gmd.mpimp-golm.mpg.de/download/>; 2011), and an in-house library (175 compounds from several metabolite classes including algal extracts of *Skeletonema marinoi*, Vidoudez and Pohnert 2012). Mass spectra were considered identical with a reverse match factor (R Match) >800, tagged with "?" if the RM was between 800 and 700, with "???" if the RM was between 700 and 600 and "?????" if below 600. Metabolites with RM < 700 were indicated as putative.

9.2.5. SIP⁺ extraction and UHPLC-HR-MS targeted analysis

Extracellular samples were analyzed for SIP⁺ detection and relative quantification following the method described in Moeys *et al.*, (2016). 1 mL sample was transferred into 1.5 mL glass vials, dried under nitrogen flow and resuspended in 60 μ L of UPLC grade water (...).

Randomized samples were analyzed by UHPLC Dionex UltiMate® 3000 (Thermo Fisher Scientific, Dreieich, Germany), coupled to an ESI-Orbitrap MS Q-Exactive Plus (Thermo Fisher Scientific, Dreieich, Germany).

Liquid chromatography was done with a Kinetex® C18 column (2.1 \times 50 mm, 1.7 μ m, Phenomenex, Torrance, CA, USA). The composition of the mobile phase was set to 100% A (0.1% formic acid and 2% acetonitrile in water) for 0.2 min and ramped to 100% B (0.1% formic acid in acetonitrile) in a linear gradient within 7.8 min. The solvent composition was held at 100% B for 1 min, returned to 100% A in 0.1 min and held at 100% A for 0.9 min. The flow rate was adjusted to 0.4 ml min⁻¹.

Ionization was performed in positive-negative switch mode with a spray voltage of -3.3 kV and a capillary temperature of 360 °C. The sheath gas flow rate was kept at 60 arbitrary units. Nitrogen was used as desolvation gas. The scanned mass range was between m/z 100 and 1,500, at resolution m/ Δ m 280,000 (m/z 200) with automatic gain control (ACG) target 3×10^6 , a maximum injection time (IT) of 200 ms.

MS² experiments were performed by fragmenting the precursor pseudomolecular ion [M-H]⁻ = 842.20 m/z with the following settings: collision energy of 20 eV, resolution m/ Δ m 17,500 (m/z 200), with automatic gain control (ACG) target 3×10^6 , a maximum injection time (IT) of 200 ms.)

The peak area of both SIP⁺ and internal standard were determined with the function Quan Browser included in the software Xcalibur™ version 3.0.63 (Thermo Fisher Scientific, Bremen, Germany) and the software Microsoft Office Excel (Microsoft®, USA). All results were normalized to the number of diatom cells. T-tests and one factor ANOVA with multiple comparisons and Bonferroni's correction were performed with the excel macro Real Statistics Resource Pack software (Release 5.4, copyright (2013 – 2018) Charles Zaiontz. www.real-statistics.com).

9.3. Bacterial modulation of sexual efficiency of the diatom

Seminavis robusta: materials and methods

9.3.1. Bioassay to determine the influence of bacteria on sexual reproduction of *S. robusta*

5 mL of cultures of *S. robusta* strains MT⁺ (strain 85A) and MT⁻ (strain 84A) (10^3 cells/mL), both axenic and non-axenic below the SST (cell size: MT⁺ < 22.4 μ m, MT⁻ < 23.5 μ m) were inoculated in 25 mL f/2 medium in 25 cm² culture flasks (TC Flask T25, Sarstedt[®], Nümbrecht, Germany). Unless otherwise mentioned, cultures were grown for five days to a concentration $\approx 2 \cdot 10^4$ cells/mL. On the fifth day, the cultures were placed in darkness for 24 h to synchronize the cell cycle of the culture in the G1-phase (Gillard, 2013). After cell-cycle synchronization, an aliquot of each mating type culture was transferred and mixed in a 24-well plate (Sarstedt[®], Nümbrecht, Germany) giving approximately 2,000 cells per well (1,000 cells for each mating type). These wells were either used as control or treated with bacteria obtained by the following procedure. Each bacterial strain culture (2 mL) was transferred into a 2 mL Eppendorf[®] tube, centrifuged for 3 min. at $6,000 \times g$, washed three times with minimal medium (f/2 medium with 5g/l glucose, 5 mL/l glycerol, 1.5 g/l NH₄NO₃) and transferred to 30 mL of minimal medium. After ten days of growth at room temperature, different volumes of bacterial cultures were diluted and added to each well containing the algae in order to reach a final OD of 0.005, 0.01, 0.05, and 0.1. For the spent medium bioassays, bacterial cells were filtered on a 0.2 μ m filter before adding the filtrate (spent medium) to the wells. When necessary, each well was filled up to 1.5 mL with fresh f/2 medium. Each condition was repeated in triplicate. The well-plates were placed at 15°C and 35 μ mol.m⁻².s⁻¹ photons and the mating efficiency was established after 24h incubation by counting the number of non-mating cells, mating cells, gametes/zygotes, auxospores using a Leica DM IL LED inverted light microscope with a Leica DFC 280 camera system (Heerbrugg, Switzerland). For each well 9 pictures (approx. 100 cells per picture) were taken and cells were counted using ImageJ software (Rasband, 1997).

9.3.2. Targeted analysis of degradation of natural diproline

Strains 84A and 85A of *S. robusta* were grown for five days and subsequently dark-synchronized in G1-phase of the cell cycle as described above. After 24 hours of darkness,

cultures of the two mating types were mixed, placed in the darkness for 10 additional hours and then exposed to light. To check diproline concentration, the cultures were extracted at different time points after the onset of light (6h, 10h, 13h, 24h) and for each time point two different conditions were tested (axenic versus non-axenic cultures, cell density for both conditions $\approx 5 \cdot 10^4$ cells/mL, $n=3$). The cultures were extracted on 60 mg HLB-SPE cartridges (Oasis®, Waters, Eschborn, Germany) following the manufacturer's instructions. The cartridges were eluted 3 times with 0.5 mL MeOH, the eluate was evaporated to dryness under a stream of nitrogen and dissolved in 50 μ l MeOH. 15nmol of caffeine dissolved in methanol were added to each sample as internal standard. Samples were stored at -20 °C until measurement by GC/MS. In order to exclude degradation of diproline by diatoms, we performed a similar, independent experiment: 6h after the onset of light, 12 cultures (3 for each time point, diatom cell density $\approx 5 \cdot 10^3$ cells/mL) were sterile filtered on GF/D grade microfiber filters (1.2 μ m pore size, Whatman, Maidstone, United Kingdom) to obtain a bacteria-rich, diatom cells-free culture medium containing naturally produced diproline. Then we performed extraction at the same time point as the previous experiment, following the above mentioned procedure.

9.3.3. Degradation of synthetic diproline by isolated bacterial strains

Roseovarius sp., *Maribacter* sp., *Croceibacter* sp. and *Marinobacter* sp. strains were grown in Difco™ Marine Broth at room temperature for three days, to an OD of 1.0-1.2. 30 mL of each culture were centrifuged for 3 min at $6,000 \times g$, washed three times with f/2 medium, diluted to reach an OD ≈ 0.1 -0.3 and then transferred to 30 mL of f/2 medium ($n=3$). After one night at room temperature, synthetic racemic mixture of diproline (prepared following the protocol of Lembke *et al.*, (2018)) was added to a final concentration of 300 nM and incubated for 72 h.

In the second experiment, 2 mL of each culture were transferred into a 2 mL Eppendorf® tube, centrifuged for 3 min at $6,000 \times g$, washed three times with minimal medium (f/2 medium with 5 g/l glucose, 5 mL/l glycerol, 1.5 g/l NH_4NO_3), diluted and transferred to 30 mL of minimal medium ($n=3$). After ten days of growth at room temperature, synthetic diproline was added to a final concentration of 300 nM and incubated for 72 h.

For both experiments, bacteria were removed by centrifugation (3 min at $6,000 \times g$) and filtration using a 2 μ m syringe filter (Sartorius). The sterile supernatant was extracted on

SPE cartridges following the protocol mentioned in the previous section and samples were stored at -20 °C until measurements.

9.3.4. GC-MS measurements of diproline

Diproline was quantified following the method of Gillard (2013). 1 µl of the extract was submitted to analysis on an ISQ Trace GC Ultra GC/MS system (Thermo Fisher, Dreieich, Germany) equipped with a 0.25 µm x 0.25 mm x 30 m DB-5MS + DG column (Agilent, Böblingen, Germany). Helium 5.0 (Linde AG, Pullach, Germany) was used as carrier gas with a constant flow of 1.2 mLmin⁻¹. The split ratio was 1:8. The initial oven temperature of 155 °C was held for 3 min, ramped to 210 °C at 25 °C min⁻¹, then to 255 °C at 7 °C min⁻¹ and finally to 315 °C at 25 °C min⁻¹. The final temperature was held for 3 min. The injector temperature was kept at 300 °C during the entire run. The scanned mass range was between 50 *m/z* and 400 *m/z* with a scan rate of 0.5 scans sec⁻¹ and an inter-scan delay of 0.04 sec. Electron-impact ionization was carried out at 70 eV.

9.3.5. Data analysis, statistics and quantification

For growth curves of *S. robusta* and mating efficiency tests, pictures were taken on an inverted microscope and analyzed with the program ImageJ (Rasband, 1997) using an in-house-built macro that automatically counts vegetative cells. The results were previously compared to manual cell counts to check accuracy and reproducibility. For GC-MS and UPLC-MS measurements, the peak area of both diproline and internal standard were determined with the function Quan Browser included in the software Xcalibur™ version 3.0.63 (Thermo Fisher Scientific, Bremen, Germany) and the software Microsoft Office Excel (Microsoft®, USA). All results were normalized to the number of diatom cells.

Two-way ANOVA followed by Bonferroni's multiple comparisons tests were performed using GraphPad Prism version 7.00 for Windows (GraphPad Software, La Jolla California USA, www.graphpad.com). T-tests were done with the excel macro Real Statistics Resource Pack software (Release 5.4, copyright (2013 – 2018) Charles Zaiontz. www.real-statistics.com).

9.4 Molecular insights into bacterial effect on sexual reproduction of *Seminavis robusta*: materials and methods

9.4.1 Cultivation of *S. robusta* and associated bacteria

S. robusta strains 85A (MT+) (BCCM: DCG0105) and 84A (MT-) (BCCM: DCG0104) were obtained from the diatom culture collection of the Belgian Coordinated Collection of Micro-organisms (BCCM/DCG, <http://bccm.belspo.be>). Cultures of both mating types were grown separately under a 12h:12h dark/light regime (cool white light at an intensity of 50 $\mu\text{mol m}^{-2} \text{s}^{-1}$) at 18°C in Guillard's f/2 medium. This medium was prepared by autoclaving 34.5 g/l Tropic Marin® BIO-ACTIF sea salt (Tropic Marin®, Wartenberg, Germany) and supplementing it with 20 ml/l Guillard's (f/2) Marine Water Enrichment Solution (Sigma-Aldrich). Axenic cultures were prepared following chapter 9.1.

Stock cultures of *Roseovarius* sp. and *Maribacter* sp. isolated from *S. robusta* were grown in Difco™ Marine Broth medium at room temperature for three days before the experiment. Then 25 ml of the bacterial culture was transferred to a 50 ml Falcon tube, centrifuged for 3 min. at $6,000 \times g$, washed three times with minimal medium (F/2 medium with 5 g/l glucose, 5 ml/l glycerol, 1.5 g/l NH_4NO_3) and transferred to 500 ml of minimal medium. The cultures were grown for 10 days at room temperature until they reached an $\text{OD}_{600} = 0.1$ (measured with a Shimadzu® UV-1601 spectrophotometer) before being sterile-filtered to harvest sterile bacterial spent medium.

9.4.2 Harvesting of MT⁺ medium

S. robusta strain 85A (MT+) was grown at 18°C in CELLSTAR® Standard Cell Culture Flasks with a 175 cm² surface area, filled with 200 mL Guillard's F/2 medium under 12h:12h dark:light regime (50 $\mu\text{mol m}^{-2} \text{s}^{-1}$ photons of cool white light). As a proxy for the biomass in the flasks, we measured the minimum fluorescence value (F₀) after 15 minutes of dark-adaptation. Pulse-Amplitude-Modulation (PAM) fluorimetry measurements were performed using a MAXI Imaging PAM Fluorimeter, M-series (Waltz, Effeltrich, Germany), equipped with an IMAG-K4 camera and mounted with an IMAG-MAX/F filter. F₀ was measured using the following software settings: intensity 7, gain 3 and damping 2. When the culture reached an F₀-value of ≈ 0.35 , the medium was harvested, sterile-filtered using GF/F filters (\varnothing 47 mm) on Nalgene™ reusable bottle top filters units (Thermo Fisher Scientific, Bremen, Germany) connected to sterile 250 mL Duran® bottles (Schott, Jena, Germany),

aliquoted in 50 mL Falcon tubes and stored at -20°C until usage. In total, 12 culture flasks (2,4 L SIP⁺-containing medium) were harvested.

9.4.3 Induction of sexuality in *S. robusta* and treatment with bacterial medium

S. robusta strain 84A (MT⁻) was grown at 18°C in CELLSTAR® Standard Cell Culture Flasks with a 175 cm² surface area, filled with 200 mL Guillard's f/2 medium under 12h:12h dark:light regime (50 μmol m⁻² s⁻¹ photons of cool white light). For biomass assessment, we measured the minimal fluorescence value (F₀) after 15 minutes of dark adaptation, as described above. Once the cultures reached an F₀-value of ≈0.3, the culture medium was renewed and the flasks were placed in complete darkness at 18°C for 24h to synchronize the cell cycle in G₁-phase (Moeys *et al.*, 2016). After 21h of darkness, sexuality was induced in MT⁻ cultures by removing 20 mL medium and replacing it with 20 mL SIP⁺-containing medium to end up with a final dilution of 1:10 SIP⁺. Also after 21h of darkness, bacterial spent medium was added to the flasks, diluted to a volume equivalent to the volume of a full bacterial culture at OD₆₀₀=0.05, the cell density at which the effects on sexual reproduction of these bacteria were shown (Chapter 4). Addition of SIP⁺ and/or bacterial spent medium was done in a dark room to prevent progression through the cell cycle. Control cultures, where no SIP⁺ or bacterial spent medium was added, were also moved to the dark room and back to avoid any differences in light treatment between control and treatment cultures. After addition of SIP⁺ and/or bacterial spent medium, the cultures were placed in complete darkness at 18°C for another 3h before the light was switched on (50 μmol m⁻² s⁻¹ photons). All six treatments (control, SIP⁺-treated, *Roseovarius* sp. -treated, *Maribacter* sp.-treated, SIP⁺ + *Roseovarius* sp.-treated and SIP⁺ + *Maribacter* sp.-treated) were cultured and harvested in five replicates.

9.4.4 Cell harvesting for RNA extraction

After 10h of light, 150 mL of the medium was poured over a GF/C filter (ø 47 mm) at 650 mbar on Nalgene™ reusable bottle top filters units (Thermo Fisher Scientific, Bremen, Germany) connected to sterile 250 mL Duran® bottles (Schott, Jena, Germany) without disturbing the cells. The filtrate was used for exometabolome extraction. The cells were then scraped from the surface of the culture flasks using a cell scraper and homogenized in the remaining medium (50 mL) by shaking. 10 mL of the cell suspension was used for flow

cytometry analysis, while the remaining 40 mL of the suspension was used for RNA extraction.

9.4.5 Cell cycle analysis using flow cytometry

Of each harvested culture, 10 mL was isolated in a 15 mL falcon. The samples were centrifuged for 5 minutes at 2000 rcf. The cells were fixated by resuspending the pellet in 10 mL ice cold 75% ethanol. Samples were stored in the dark at 4°C until analysis.

Fixated cultures were centrifuged for 5 minutes at 3000 rpm, after which the supernatant was replaced with 2 mL ice cold 75% ethanol. 1mL of each sample was transferred to a 1.5mL tube and washed 3 times with PBS buffer to remove all remaining ethanol. The fixed cells were treated with 1µg/mL RNase A for 20 min at 37 °C and afterwards stained with SYBR green (1x concentration, Life Technologies) in the dark for 20 min.

Samples were filtered through a cell strainer with pore size of 70 µm before feeding into the flow cytometer. Flow cytometry was carried out on a Bio-Rad S3e cell sorter (Bio-Rad Laboratories, Inc, Hercules, California), collecting 10 000 for each sample and gating in the FSC and SSC channel. An unstained control sample was run first to localize the cell population. After running the samples, G1 and G2 peaks were visually selected using ProSort 1.5 (Bio-Rad Laboratories, Inc.).

Data analysis was carried out in R (v3.4.3, <http://www.R-project.org/>, R Core team, 2017). Since the data is proportional in nature, we adopted a generalized linear model with binomial distribution and logit link using the R glm function to assess significance for the effect of SIP and bacterial exudates. Post-hoc tests comparing all combinations of treatments were carried out using the glht function from the Multcomp package (Hothorn, Bretz and Westfall, 2008).

9.4.6 RNA extraction and quality assessment

The cells for RNA extraction (40 mL suspension, see above) were harvested by filtration over a Versapor filter (3 µm pore size, 25mm diameter, PALL). Immediately after filtration, the filters were put in Eppendorf tubes, flash-frozen in liquid nitrogen and stored at -80°C until RNA extraction.

RNA was extracted from all samples (6 treatments, 5 replicates each) using the RNeasy® Plant Mini Kit (Qiagen). First, 1 ml RLT buffer and 10 µl β-mercaptoethanol were added to the Eppendorf tube containing the frozen filter. The cells were removed from the filter by

pipetting up and down and using the pipet tip to scrape the filter. The filter was removed and silicon carbide beads (1 mm, BioSpec) were added to the Eppendorf tube. The cells were lysed by silicon carbide beads beating on a beating mill (Retsch, 3 x 1 min. at frequency 20 Hz, with 30 sec. on ice in between each run). The lysate was then transferred to a QIAshredder spin column (RNeasy® kit) and the manufacturer's instructions were followed from there. An on-column DNase treatment was performed using the RNase-free DNase set (Qiagen) according to the manufacturer's instructions.

RNA quality was evaluated by spectrophotometry (Nanodrop™) and Bioanalyzer (Agilent Technologies). For each treatment, the three replicates with the highest quality (high 260/230- and 280/260 ratio's and high RIN-value) were selected for library preparation and sequencing.

9.4.7 RNA sequencing and transcriptomic analysis

The 18 sequencing libraries were prepared using Illumina® TruSeq Stranded mRNA kit. The libraries were sequenced (2x75 bp) in one Illumina® NextSeq 500 H150 run. Library preparation and sequencing were performed by VIB Nucleomics Core (VIB, Leuven).

Paired-end reads were quality-trimmed using FastQ Quality Filter from the FastX Toolkit v. 0.0.13 (http://hannonlab.cshl.edu/fastx_toolkit/index.html) using the following settings: -q 28, -p 30. Using the Salmon software tool in quasi-mapping mode (Patro *et al.*, 2017), the quality-trimmed reads were mapped to an annotated genes model assembly of *S. robusta*. To generate the annotated assembly, Illumina paired-end reads and PacBio long reads were combined in a hybrid assembly approach and gene models were annotated using expression data as training for the BRAKER1 (Hoff *et al.*, 2016) pipeline. Next, functional annotations for the *Seminavis robusta* gene models were determined using three different strategies: i) InterProScan v5.3 (Jones *et al.*, 2014) was run to scan protein sequences for matches against the InterPro protein signature databases; ii) eggNOG-mapper (Huerta-Cepas *et al.*, 2017) was executed with DIAMOND mapping mode, based on eggNOG 4.5 orthology data (Huerta-Cepas *et al.*, 2016); iii) AnnoMine (Vandepoele *et al.*, 2013) was employed to retrieve consensus gene functional annotation from protein similarity searches (using DIAMOND v0.9.9.110 maximum (Buchfink *et al.*, 2015), e-value 10e-05 against Swiss-Prot (Bairoch and Apweiler, 2000) database). Gene Ontology terms were retrieved from the results of the eggNOG-mapper.

The transcript-level abundances generated with Salmon were imported into R (v.3.4.4) and aggregated to gene level counts using the tximport package (Soneson, Love and Robinson 2015). Genes with low overall counts (counts-per-million (CPM) < 1 in at least three samples) were removed from the libraries because they have little power for detecting differential expression. Differences in sequencing depth and RNA population were corrected using a weighted trimmed mean of the log expression ratios (TMM) normalization (Robinson and Oshlack, 2010). Preliminary differences between expression profiles of different samples were explored with multi-dimensional scaling (MDS) plots based on the top 500 genes, generated using the plotMDS function included in the EdgeR package.

Differential expression (DE) analysis was performed using the R package edgeR 3.20.9 (Robinson *et al.*, 2010). Negative binomial generalized linear models (GLMs) were fitted to model read counts for each gene in each sample and a dispersion parameter which accounts for variability between biological replicates was calculated (Lun *et al.*, 2016). For differential expression analysis, 9 comparisons (contrasts) were defined (SIP vs C, M vs C, R vs C, SIP+M vs SIP, SIP+R vs SIP, SIP+R vs R, SIP+M vs M, SIP+M vs SIP+R, see Fig 1 for experimental setup). A gene was considered differentially expressed if the false discovery rate (FDR) adjusted p-values were below 0.01 and the absolute log₂ fold-change (LFC) was equal or greater than 1. To confirm GTP specificity of the putative guanylate cyclases, a multiple sequence alignment was carried out in MEGA 7 (Kumar, Stecher and Tamura, 2016) to check the presence of guanylate cyclase specific motifs (Winger *et al.*, 2008).

For genes differentially expressed in one specific contrast, Gene Ontology enrichment for single comparisons was determined using a gene set enrichment approach (GSEA) as implemented in CAMERA (Wu and Smyth, 2012), included in the R package limma v.3.34.9 (Ritchie *et al.*, 2015). Redundant GO terms were removed using REVIGO (<http://revigo.irb.hr/>, Supek *et al.*, 2011) using a low similarity value of 0.5. GO enrichment of genes that were differentially expressed in multiple contrasts was performed using Fisher's exact test and the 'weight' algorithm for GO group scoring as implemented in TopGO (Alexa and Rahnenfuhrer, 2018). Venn Diagrams were generated with the R package VennDiagram v. 1.6.20 and with the web based application Venny v. 2.1 (Oliveros, 2007-2015, <http://bioinfogp.cnb.csic.es/tools/venny/index.html>).

9.4.8 Exometabolome extraction

150 mL of filtered medium from each culture flasks was transferred to sterile and cleaned 250 mL Erlenmeyer flasks, which were covered immediately with aluminum foil and cooled down to 4 °C before solid phase extraction. *Roseovarius* sp. and *Maribacter* sp. spent medium (n=4, diluted to an equivalent OD₆₀₀=0.05 with minimal medium) were prepared and stored in the same way. Before extraction, 15 nmol of caffeine dissolved in methanol (HPLC grade, Sigma-Aldrich, Chromasolv®Plus (≥99.9%)) were added to each sample as an internal standard. The medium was extracted on 60 mg Oasis® HLB-SPE cartridges (Waters, Eschborn, Germany), following the manufacturer's instructions. Gentle vacuum was applied to the cartridges with a Visiprep™ SPE Vacuum Manifold (Sigma-Aldrich) to have a flow-through of ca. 1 drop per second. The cartridges were eluted three times with 1 mL of methanol. The 3 ml of eluate were stored in 4 mL vial glass at -80 °C until further analysis. Medium blanks (n=3) were prepared in the same way by extracting sterile F/2 medium. 1.5 ml of the eluate from each sample was transferred to a clean vial, evaporated under a stream of nitrogen and dissolved in 50 µl of methanol. Two quality control (QC) samples were prepared by pooling 5µl from each sample in one clean vial.

9.4.9 UHPLC-MS measurements

After randomizing the order of the samples and including QC samples every 7 samples, 5 µl of each sample were analyzed by UHPLC Dionex UltiMate® 3000 (Thermo Fisher Scientific, Dreieich, Germany), coupled to an ESI-Orbitrap MS Q-Exactive Plus (Thermo Fisher Scientific, Dreieich, Germany).

Liquid chromatography was performed on an Accucore® C18 column (2.1 × 100 mm, 2.6 µm particle size, Thermo Scientific, Dreieich, Germany). The composition of the mobile phase was set to 100% A (0.1% HCOOH and 2% ACN in H₂O) for 0.2 min and ramped to 100% B (0.1% HCOOH in ACN) in a linear gradient within 9 min. The solvent composition was held at 100% B for 4 min, returned to 100% A in 0.1 min and held at 100% A for 0.9 min. The flow rate ramped from 0.4 ml min⁻¹ to 0.7 ml min⁻¹ from 0.5 min to 13.5 min.

Ionization was performed with a spray voltage of 3 kV and a capillary temperature of 360 °C. Nitrogen was used as desolvation gas.

For monitoring, the scanned mass range was between 100 and 1 500 *m/z*, at a resolution *m/Δm* 280 000 full width at half maximum (FWHM) (*m/z* 200) in positive mode, with automatic gain control (ACG) target 3×10^6 , a maximum injection time (IT) of 200 ms.

For compound identification, full-scan MS/data dependent MS/MS (ddMS²) experiment was performed on QC samples. Each experiment was composed of one full MS and up to five ddMS². The five ions with the most intense signal detected in the full MS scan (intensity threshold 1.6×10^5) produced a specific MS/MS spectrum. For full MS, the settings were the ones described above, while for the data dependent MS/MS the settings were the following: positive mode with a resolution of $m/\Delta m$ 35 000 and an ACG target 1×10^5 , a maximum IT of 50 ms, a stepped normalized collision energy (NCE, 15, 30, 45), an isolation window of 0.4 m/z .

All data was acquired and processed with the software XcaliburTM version 3.0.63 (Thermo Fisher Scientific, Bremen, Germany).

9.4.10 LC-HR-MS data analysis

XcaliburTM raw data file were imported into Thermo Compound Discoverer 2.1.0.398 (Thermo Fisher Scientific, Bremen, Germany) and analyzed following a standard pipeline for untargeted metabolomics for high resolution spectra. The important values for features extraction are the following: precursor ion deviation 5 ppm, maximum retention time shift 0.5 min., signal to noise threshold (S/N) 3, minimum peak intensity for peak selection 1×10^6 au, retention time shift for grouping 0.5 min., relative intensity tolerance for isotope search 30%. The exact masses of unknown compounds found in the samples were compared to online databases (PubChem, ChemSpider, mzCloud) and to an in-house library of 650 natural compounds (mass tolerance = 5 ppm) for identification.

After the analysis, a table with putative compound names and the molecular formula, exact masses, retention times and chromatographic area for each sample was exported for further processing. All features found in the medium blank samples were removed from the samples. Data were then filtered based on QCs coefficient of variation (CV): only features with CV < 20% were retained (Dunn *et al.*, 2011).

Finally, data were normalized on diatom cell densities and Pareto scaled to obtain normally distributed data. The obtained .csv Table was used to perform statistical analysis with MetaboAnalystR (Chong and Xia, 2018). PCA was performed to detect grouping and outliers in the samples. Significant features were selected from the results of two-way ANOVA analysis (FDR adjusted p-value cutoff = 0.05, FisherLSD post-hoc analysis), which were visualized by heatmaps (distance measure = euclidean, clustering algorithm = Ward).

After statistical analysis, significant features were selected in the Thermo Compound Discoverer molecule list and exported to SIRIUS v. 4.0 (Böcker *et al.*, 2008) to confirm features identity. Defaults settings for Orbitrap High Resolution Mass Spectrometry were used (ppm=5), choosing all the possible adducts as candidates. CSI:FingerID (Dührkop *et al.*, 2015) was used for compound structure evaluation, using a PubMed as spectral database.

9.4.11 Oxylipins measurements

Targeted detection of oxylipins was based on a method by Rettner *et al.*, (2018). Briefly, measurements were performed on a Shimadzu[®] LC-20AD HPLC equipped with a Shimadzu[®] SIL-20AC autoinjector (Shimadzu, Kyoto, JP) and coupled with a QTrap[®] 5500 (ABSciex, Framingham, MA). The column used was a BEH[®] C18 (2.1x100 mm, 1.7 μ m, 130 Å, Aquity, Milford, US) kept at 50 °C (ThermaSphere TS-130; Phenomenex, Torrance, CA).

The QTrap 5500 was operated in negative ionization mode only using scheduled or unscheduled multiple reaction monitoring (MRM). The scheduled MRM window was 60 s, and each oxylipin parameter was optimized individually (CE, EP, DP, CXP). The investigated oxylipins are the same analyzed by Rettner *et al.* (2018). Following instrument settings were used: curtain gas 35, collision gas medium (MRM); ion spray voltage -4000, temperature 500 °C, ion source gas 1 and 2 40. Solvent used were A: 100 % H₂O + 0.01 % CH₃COOH and B: 100 % CH₃OH + 0.01 % CH₃COOH with a solvent flow 0.3 ml*min⁻¹. Injection volumes 10 μ L. The gradient started at 42% B, ramped at 86% B at 12.5 min, then 98% B at 15.5 min, returned to 42% B in 0.5 min and re-equilibrated for 1 min. Manual integration of corresponding peaks were enabled by Analyst software version 1.6. To confirm their presence in all samples, arachidonic acid and 15-HETE (Hydroxyeicosatetraenoic acid) were additionally measured in negative mode on a UHPLC Dionex UltiMate[®] 3000 (Thermo Fisher Scientific, Dreieich, Germany), coupled to an ESI-Orbitrap MS Q-Exactive Plus (Thermo Fisher Scientific, Dreieich, Germany), following the method mentioned in the previous paragraph. Identity of the compounds was confirmed by comparison with an external standard.

GC-MS measurements and quantification of diproline

Diproline analysis and quantification were performed in the same way as explained in par. 9.3.4 and 9.3.5.

9.5. From ecology to applied research: effect of bacteria on a commercial microalga: materials and methods

9.5.1. *Nannochloropsis* sp. cultivation and co-cultivation with isolated bacteria from *S. robusta*

The microalga *Nannochloropsis* sp., strain CCAP211/78 was obtained from the Culture Collection of Algae and Protozoa (CCAP, United Kingdom). It was cultivated in 100 ml of saline medium (Fret *et al.*, 2017) in 250 cm² culture flasks (Greiner bio-one) in a cultivation chamber at 20°C. The light irradiation was 70 $\mu\text{mol} \cdot \text{m}^{-2} \cdot \text{s}^{-1}$ and applied from cool fluorescent light source in day-night cycles of 16:8. The cultures were agitated twice a day to avoid precipitation of algal cells.

Poseidonocella sp. was isolated as described in Giraldo *et al.*, (under submission). It was grown in 50 mL saline medium enriched with 20 mM of glucose in 100 mL flasks (Greiner bio-one).

Croceibacter sp., *Roseovarius* sp. and *Maribacter* sp. isolated from *S. robusta* were grown in 30 mL of marine broth medium for three days. Afterwards, the cultures were transferred to 50 mL Falcon tubes, centrifuged for 3 min. at 6,000 \times g, washed three times with 10 mL minimal medium (f/2 medium with 5g/l glucose, 5 ml/l glycerol, 1.5 g/l NH₄NO₃) and transferred to 100 mL of minimal medium in 250 cm² culture flasks (TC Flask T25, Sarstedt®, Nümbrecht, Germany). After ten days of growth at room temperature bacteria reached an OD₆₀₀ of \approx 0.3-0.4 and were ready for inoculation.

Nannochloropsis sp. (initial OD₆₃₀=0.620 \pm 0.050) was inoculated with *Poseidonocella*, *Roseovarius* sp. and *Maribacter* sp. to reach a final OD₆₀₀=0.1 for each strain. Six co-cultivation were established: *Nannochloropsis* sp. + *Poseidonocella* sp., *Nannochloropsis* sp. + *Roseovarius* sp., *Nannochloropsis* sp. + *Maribacter* sp., *Nannochloropsis* sp. + *Poseidonocella* sp. + *Maribacter* sp. (N+P+M) and *Nannochloropsis* sp. + *Poseidonocella* sp., + *Roseovarius* sp. (N+P+R). Each treatment was repeated in triplicates.

The growth of *Nannochloropsis* sp. was estimated by daily measurements of OD₆₃₀ (maximum chlorophyll concentration, Kandilian *et al.*, 2013) and OD₇₅₀ (total algae biomass, Griffiths *et al.*, 2011) during 7 days using a Cary 50 UV-Visible spectrophotometer (Agilent Technologies).

The growth at both wavelength was statistically analyzed by means of a two-way ANOVA followed by Bonferroni's multiple comparisons tests were performed using GraphPad Prism

version 7.00 for Windows (GraphPad Software, La Jolla California USA, www.graphpad.com).

9.5.2. Sample preparation for endometabolomics of *Nannochloropsis* sp.

After seven days of co-cultivation, *Nannochloropsis* co-cultivation were extracted. 45 mL of each cultures were transferred to a 50 mL Falcon tubes and centrifuged in a Sigma® 4K15 centrifuge at 3500 rcf for 15 min. Afterwards, the supernatant was discarded and the cell pellet was immediately frozen in liquid nitrogen and stored at -80 °C until extraction. To extract the endometabolite, samples were thawed, vortexed and cells were re-suspended in 2 mL extraction mix (methanol : ethanol : chloroform, 1:3:1, v: v: v) and transferred to 4 mL glass vials. Samples were vortexed for 60 s and kept at -20°C until further processing and analysis.

9.5.3. Extraction, derivatization, GC-HR-MS measurements and data analysis

GC-HR-MS sample preparation, measurements and data analysis were done as explained in par. 9.2.3 - 9.2.5.

9.5.4. *Nannochloropsis* sp. biofilm formation assay

Biofilm formation assays were performed in flat bottomed 96-well plates (Sarstedt) that were inoculated with *Nannochloropsis* sp. and different bacteria. Each well was inoculated with 150 µL of algae suspension with an $OD_{630} = 1.50 \pm 0.05$ and $OD_{750} 1.40 \pm 0.05$. *Poseidonocella* sp. and *Croceibacter* sp. were inoculated at a final OD_{600} of 0.1, *Roseovarius* sp. and *Maribacter* sp. were inoculated at final OD_{600} of 0.1 and 0.01. Spent medium of each bacterial strain was obtained after centrifuging 5 mL of each bacteria at 5000 rpm for 5 minutes. Supernatants were separated and filtered (0.2 µm Supor® Membrane, PALL® Acrodisc® 32mm) to obtained sterile supernatant. Sterile supernatant was added to well plates to reach for each strain an equivalent OD_{600} as mentioned before. Volumes were adjusted to 250 µL with glucose free f/2 medium. In total, 20 treatments were tested in triplicates (see figure 38 in chapter 6 for experimental setup summary).

Initial absorbance of well plates was measured with a Cytation 3™ plate reader (BioTek® instruments, Winooski, VT) using Gen5™ software. For each well, average absorbance at 630 nm and 750 nm was calculated from nine equidistant measurements points. Afterwards,

plates were incubated for 10 days at 20°C, with a light irradiation of $30 \mu\text{mol} \cdot \text{m}^{-2} \cdot \text{s}^{-1}$ in day-night cycles of 16:8 h. After the incubation, the medium and non-adherent cells were removed by manual pipetting and biofilm absorbance was measured at 630 nm and 750 nm using the same parameter as reported above.

Biofilm absorbance measurements were compared by means of a one-way ANOVA followed by a Bonferroni post-hoc test for multiple comparisons ($p < 0.05$) using GraphPad Prism version 7.00 for Windows (GraphPad Software, La Jolla California USA, www.graphpad.com).

9.6. A SPE based non-disruptive method to investigate macroalgal surface chemistry: materials and methods

9.6.1. Materials

All reagents used were of analytical grade or superior purity. The absorption material used was a fully endcapped silica Gel 90 C18 material (pore size 90 Å, particle's dimensions 40-63 μm , Sigma-Aldrich, Germany). For collection of absorption material, empty 6 mL polypropylene columns with PE frits (CHROMABOND, Germany) were used. HPLC-grade methanol and ethanol (Sigma-Aldrich) were used for elution. Standards of fucoxanthin, canthaxanthin and FAME (fatty acid methyl esters) were purchased from Sigma-Aldrich.

9.6.2. Method development

Before extraction, algae ($n=5$) were taken out of the tanks and hanged on clamps for ca. 2 minutes, in order to let most of the water drop off. This resulted in *wet algal* surfaces with comparable amounts of surface water. Algae should not be blotted dry to avoid removal of the water in the laminar layer of the thalli. Meanwhile, the C18 absorbing material ($0.51 \text{ g} \pm 0.01 \text{ g}$, $n=5$, weighted with a Kern ALJ 220-4 balance) was spread in 58 cm^2 Petri dishes. Then $36.5 \pm 6.5 \text{ cm}^2$ fragments of *F. vesiculosus* were laid into the petri dishes and, after closing, the dishes were gently shaken for ca 10 seconds, in order to obtain a full and uniform coverage of the algal surface with the absorption material (the entire procedure is illustrated in Figure 41). The extracted surface was determined by taking photos of the algae after the treatment and analyzing the images with the software ImageJ (Rasband 1994-2014). Due to the humidity of the algal surfaces C18 material that got into contact with it remained attached to the surface. The exceeding material remaining in the petri dish (ca. 0.4 g) did not contain

any detectable surface metabolites (verified by UPLC/MS of blank samples) and could be discarded. After covering with C18 material, the algae were left for 60 s in the Petri dishes without moving them. This incubation time was optimized for recovery of fucoxanthin in several experiments (20 to 300 s). Subsequently, the algae were rinsed with an excess of artificial sea water to wash off the C18 material. The material was directly collected, with the help of a plastic funnel, into an empty solid phase extraction (SPE) cartridge to which vacuum was applied (ca. 550 Torr). The C18 absorption material settles at the bottom of the cartridge and attention must be paid not to dry the powder. The funnel and the C18 material were washed three times with 10 mL deionized water, in order to remove salts and to recover all the C18 material. Metabolites adsorbed on the C18 material were eluted with 3 x 0.5 mL of MeOH. The extracts were combined and splitted in two equal samples for UPLC-MS and GC-MS investigations. UPLC-MS samples 200 μ L were supplemented with canthaxanthin (stock solution = 500 nM in MeOH) as internal standard. The extracts were then dried under a stream of nitrogen. UPLC-MS samples were taken up in 200 μ L of methanol and GC-MS samples in 100 μ L of methanol. At this stage samples can be stored at -20°C until further measurements.

After extraction algae were observed under a confocal light microscope (BX40, Olympus, Japan) to verify cellular integrity.

9.6.3. UPLC-MS measurements

After solid phase extraction, the samples were analyzed with UPLC-MS and GC-MS. 10 μ L of samples were analysed by UHPLC (Waters® ACQUITY UPLC-MS system, Massachusetts, USA) coupled with a Micromass® Q-ToF micro ESI-TOF mass spectrometer. The chromatographic separation was done on a BEH C18 column from Waters (2.1 mm \times 50 mm, particle size 1.7 μ m). The eluents were A: water (UPLC-MS grade, Biosolv) with 0.1% formic acid (v/v) and B: acetonitrile (UPLC-MS grade, Biosolv) with 0.1% formic acid (v/v). The flow rate was 0.6 mL/min and the equilibration time 1 min. The gradient started with 50 % B and was ramped within 4 min to 100 % B and held for 1.5 min. As wash step the polarity of the eluent was increased until 6 min (5 % B) and held for 0.5 min. The solvent returned to 50 % B in 1 min. The injection volume was of, by means of an autosampler. A commercial fucoxanthin standard (5 μ M in 100 μ L of MeOH) was used for identification of the algal metabolite.

9.6.4. Calibration curve for UPLC-MS measurements

To prepare the external calibration curve (Fig S13) using the ratio of peak areas of fucoxanthin and cantaxanthin, 0,66 mg of fucoxanthin (purity $\geq 95\%$, Sigma Aldrich©, Germany) were weighted and dissolved in 10 mL methanol in order to obtain a 100 μM stock solution. From this stock, several dilutions at different concentration were prepared (1 μM , 750 nM, 500 nM, 250 nM, 100 nM). 10 μL of a 20 μM canthaxanthin (analytical standard grade, Sigma Aldrich©, Germany) solution in methanol were added to 190 μL of each sample in order to have a final concentration of 1 μM of canthaxanthin. After this, every point of the curve was measured 3 times using the UPLC-MS method described above.

9.6.5. GC-MS measurements

Samples used for GC-MS analysis were derivatized as described above. 1 μL of sample was injected in splitless mode (injector temperature = 250 °C) in a Trace GC-ULTRA system (Thermo Scientific® (Massachusetts, USA) coupled to a Thermo Scientific® ISQ EI-mass spectrometer, equipped with a quadrupole analyzer. The column used was an Agilent® Durabond DB5MS (30 m length, 0.250 mm diameter, 0.25 μm internal film). Helium 5.0 (Linde AG, Pullach, Germany) was used as carrier gas with a constant flow of 1.2 mL min⁻¹. The temperature program started at 60°C (held for 4 min) and was ramped at 15°C min⁻¹ to 300°C (held for 5 min).

References

1. Abinandan, S., Subashchandrabose, S. R., Venkateswarlu, K., & Megharaj, M. (2018). Nutrient removal and biomass production: advances in microalgal biotechnology for wastewater treatment. *Critical reviews in biotechnology*, 38(8), 1244-1260.
2. Adams, E., Blass, D. A., Harford, J. B., and Adams, J. A. (1978). Bacterial utilization of cyclo (glycyl-L-prolyl). *Experientia*, 34(5), 579-580.
3. Adolph, S., Jung, V., Rattke, J., and Pohnert, G. (2005). Wound closure in the invasive green alga *Caulerpa taxifolia* by enzymatic activation of a protein cross-linker. *Angewandte Chemie International Edition*, 44(18), 2806-2808.
4. Afgan, E., Baker, D., Batut, B., van den Beek, M., Bouvier, D., Čech, M., ... Blankenberg, D. (2018). The Galaxy platform for accessible, reproducible and collaborative biomedical analyses: 2018 update. *Nucleic Acids Research*, 46(W1), W537–W544.
5. Aiyar, P., Schaeme, D., García-Altres, M., Flores, D. C., Dathe, H., Hertweck, C., ... and Mittag, M. (2017). Antagonistic bacteria disrupt calcium homeostasis and immobilize algal cells. *Nature Communications*, 8(1), 1756.
6. Ajimura, M., Leem, S. H., and Ogawa, H. (1993). Identification of new genes required for meiotic recombination in *Saccharomyces cerevisiae*. *Genetics*, 133(1), 51-66.
7. Akbar, M. A., Ahmad, A., Usup, G., and Bunawan, H. (2018). Current knowledge and recent advances in marine dinoflagellate transcriptomic research. *Journal of Marine Science and Engineering*, 6(1), 13.
8. Alexa, A., & Rahnenführer, J. (2009). Gene set enrichment analysis with topGO. *Bioconductor Improv*, 27.
9. Alfaro, A. C., and Young, T. (2018). Showcasing metabolomic applications in aquaculture: A review. *Reviews in Aquaculture*, 10(1), 135-152.
10. Aline, R. F., Reeves, C. D., Russo, A. F., & Volcani, B. E. (1984). Role of silicon in diatom metabolism: cyclic nucleotide levels, nucleotide cyclase, and phosphodiesterase activities during synchronized growth of *Cylindrotheca fusiformis*. *Plant Physiology*, 76(3), 674-679.

11. Allen, A. E., LaRoche, J., Maheswari, U., Lommer, M., Schauer, N., Lopez, P. J., ... and Bowler, C. (2008). Whole-cell response of the pennate diatom *Phaeodactylum tricornutum* to iron starvation. *Proceedings of the National Academy of Sciences*.
12. Almeida, E., Diamantino, T. C., & de Sousa, O. (2007). Marine paints: The particular case of antifouling paints. *Progress in Organic Coatings*, 59(1), 2–20.
13. Amato, A., Sabatino, V., Nylund, G. M., Bergkvist, J., Basu, S., Andersson, M. X., ... and Ferrante, M. I. (2018). Grazer-induced transcriptomic and metabolomic response of the chain-forming diatom *Skeletonema marinoi*. *The ISME Journal*, 12(6), 1594.
14. Amin, S.A., Green, D.H., Hart, M.C., Kupper, F.C., Sunda, W.G., Carrano, C.J. (2009). Photolysis of iron-siderophore chelates promotes bacterial-algal mutualism. *Proceedings of the National Academy of Sciences* 106: 17071-17076.
15. Amin, S. A., Parker, M. S., and Armbrust, E. V. (2012). Interactions between diatoms and bacteria. *Microbiology and Molecular Biology Reviews*, 76(3), 667-684.
16. Amin, S. A., Hmelo, L. R., Van Tol, H. M., Durham, B. P., Carlson, L. T., Heal, K. R., Morales, R. L., Berthiaume, C. T., Parker, M. S., Djunaedi, B., Ingalls, A. E., Parsek, M.R., Moran, M. A. and Armbrust, E. V. (2015). Interaction and signaling between a cosmopolitan phytoplankton and associated bacteria. *Nature*, 522(7554), 98.
17. Amsler, C.D., and Iken, K.B. (2001) Chemokinesis and chemotaxis in marine bacteria and algae. In: McClintock J. B. BBJ (ed) *Marine Chemical Ecology*. CRC Press, p 413–430
18. Amsler, C. D. (2008). *Algal chemical ecology* (Vol. 468). Berlin: Springer.
19. Andreae, M. O. (1990). Ocean-atmosphere interactions in the global biogeochemical sulfur cycle. *Marine Chemistry*, 30, 1-29.
20. Armbrust, E. V., Berges, J. A., Bowler, C., Green, B. R., Martinez, D., Putnam, N. H., ... & Brzezinski, M. A. (2004). The genome of the diatom *Thalassiosira pseudonana*: ecology, evolution, and metabolism. *Science*, 306(5693), 79-86.
21. Armbrust, E. V. (2009). The life of diatoms in the world's oceans. *Nature*, 459(7244), 185.
22. Arora, N., Pienkos, P. T., Pruthi, V., Poluri, K. M., and Guarnieri, M. T. (2018). Leveraging algal omics to reveal potential targets for augmenting TAG accumulation. *Biotechnology advances*.

23. Azam, F., and Malfatti, F. (2007). Microbial structuring of marine ecosystems. *Nature Reviews Microbiology*, 5(10), 782.
24. Bach, L. T., Mackinder, L. C., Schulz, K. G., Wheeler, G., Schroeder, D. C., Brownlee, C., and Riebesell, U. (2013). Dissecting the impact of CO₂ and pH on the mechanisms of photosynthesis and calcification in the coccolithophore *Emiliana huxleyi*. *New Phytologist*, 199(1), 121-134.
25. Badri, D. V., Weir, T. L., van der Lelie, D., and Vivanco, J. M. (2009). Rhizosphere chemical dialogues: plant–microbe interactions. *Current Opinion in Biotechnology*, 20(6), 642-650.
26. Bahn, Y. S., Xue, C., Idnurm, A., Rutherford, J. C., Heitman, J., and Cardenas, M. E. (2007). Sensing the environment: lessons from fungi. *Nature Reviews Microbiology*, 5(1), 57.
27. Bahnson, B. J., Anderson, V. E., and Petsko, G. A. (2002). Structural mechanism of enoyl-CoA hydratase: three atoms from a single water are added in either an E1cb stepwise or concerted fashion. *Biochemistry*, 41(8), 2621-2629.
28. Bailleul, B., Cardol, P., Breyton, C., & Finazzi, G. (2010a). Electrochromism: a useful probe to study algal photosynthesis. *Photosynthesis Research*, 106(1-2), 179.
29. Bailleul, B., Rogato, A., De Martino, A., Coesel, S., Cardol, P., Bowler, C., ... and Finazzi, G. (2010b). An atypical member of the light-harvesting complex stress-related protein family modulates diatom responses to light. *Proceedings of the National Academy of Sciences*, 201007703.
30. Bairoch, A., and Apweiler, R. (2000). The SWISS-PROT protein sequence database and its supplement TrEMBL in 2000. *Nucleic Acids Research*, 28(1), 45-48.
31. Bantscheff, M., Schirle, M., Sweetman, G., Rick, J., and Kuster, B. (2007). Quantitative mass spectrometry in proteomics: a critical review. *Analytical and Bioanalytical Chemistry*, 389(4), 1017-1031.
32. Barah, P., and Bones, A. M. (2014). Multidimensional approaches for studying plant defence against insects: from ecology to omics and synthetic biology. *Journal of Experimental Botany*, 66(2), 479-493.
33. Barofsky, A., Vidoudez, C., and Pohnert, G. (2009). Metabolic profiling reveals growth stage variability in diatom exudates. *Limnology and Oceanography: Methods*, 7(6), 382-390.

34. Barranguet, C., Veuger, B., Van Beusekom, S. A., Marvan, P., Sinke, J. J., and Admiraal, W. (2005). Divergent composition of algal-bacterial biofilms developing under various external factors. *European Journal of Phycology*, 40(1), 1-8.
35. Barton, N. H., Briggs, D. E. G., Eisen, J. A., Goldstein, D. B., and Patal, N. H. (2007). Evolution Cold Spring Harbor Laboratory Press. *New York, NY*.
36. Barupal, D. K., Fan, S., and Fiehn, O. (2018). Integrating bioinformatics approaches for a comprehensive interpretation of metabolomics datasets. *Current Opinion in Biotechnology*, 54, 1-9.
37. Basu, S., Patil, S., Mapleson, D., Russo, M. T., Vitale, L., Fevola, C., Maumus, F., Casotti, R., Mock, T., Caccamo, M., Montresor, M. and Ferrante, M. E. (2017). Finding a partner in the ocean: molecular and evolutionary bases of the response to sexual cues in a planktonic diatom. *New Phytologist*, 215(1), 140-156.
38. Baudino, S., Lucas, C., and Smadja, C. (2016). Omics in Chemical Ecology. *Chemical Ecology*, 117-137.
39. Beale, S. I. (1995). Biosynthesis and structures of porphyrins and hemes. *In Anoxygenic photosynthetic bacteria* (pp. 153-177). Springer, Dordrecht.
40. Begg, G. S., Cook, S. M., Dye, R., Ferrante, M., Franck, P., Lavigne, C., ... and Quesada, N. (2017). A functional overview of conservation biological control. *Crop Protection*, 97, 145-158.
41. Behringer, G., Ochsenkühn, M. A., Fei, C., Fanning, J., Koester, J. A., & Amin, S. A. (2018). Bacterial communities of diatoms display strong conservation across strains and time. *Frontiers in Microbiology*, 9, 659.
42. Belchik, S. M., and Xun, L. (2011). S-glutathionyl-(chloro) hydroquinone reductases: a new class of glutathione transferases functioning as oxidoreductases. *Drug Metabolism Reviews*, 43(2), 307-316.
43. Beliaev, A. S., Romine, M. F., Serres, M., Bernstein, H. C., Linggi, B. E., Markillie, L. M., ... and Pinchuk, G. E. (2014). Inference of interactions in cyanobacterial–heterotrophic co-cultures via transcriptome sequencing. *The ISME Journal*, 8(11), 2243.
44. Bell, W., and Mitchell, R. (1972). Chemotactic and growth responses of marine bacteria to algal extracellular products. *The Biological Bulletin*, 143(2), 265-277.
45. Bender, D. A. (2012). The metabolism of “surplus” amino acids. *British Journal of Nutrition*, 108(S2), S113-S121.

46. Bender, S. F., Wagg, C., and van der Heijden, M. G. (2016). An underground revolution: biodiversity and soil ecological engineering for agricultural sustainability. *Trends in Ecology and Evolution*, 31(6), 440-452.
47. Bergström, G. (2007). Chemical ecology= chemistry + ecology! *Pure and Applied Chemistry*, 79(12), 2305-2323.
48. Berner, F., Heimann, K., & Sheehan, M. (2015). Microalgal biofilms for biomass production. *Journal of Applied Phycology*, 27(5), 1793–1804.
49. Bhaskar, P. V., and Bhosle, N. B. (2005). Microbial extracellular polymeric substances in marine biogeochemical processes. *Current Science*, 45-53.
50. Blanton, H. L., Radford, S. J., McMahan, S., Kearney, H. M., Ibrahim, J. G., and Sekelsky, J. (2005). REC, *Drosophila* MCM8, drives formation of meiotic crossovers. *PLoS genetics*, 1(3), e40.
51. Blaženović, I., Kind, T., Ji, J., and Fiehn, O. (2018). Software tools and approaches for compound identification of lc-ms/ms data in metabolomics. *Metabolites*, 8(2), 31.
52. Blunt, J. W., Copp, B. R., Keyzers, R. A., Munro, M. H., and Prinsep, M. R. (2013). Marine natural products. *Natural Product Reports*, 30(2), 237-323.
53. Böcker, S., Letzel, M. C., Lipták, Z., and Pervukhin, A. (2008). SIRIUS: decomposing isotope patterns for metabolite identification. *Bioinformatics*, 25(2), 218-224.
54. Boerjan, B., Cardoen, D., Verdonck, R., Caers, J., and Schoofs, L. (2012). Insect omics research coming of age. *Canadian Journal of Zoology*, 90(4), 440-455.
55. Bohman, B., Flematti, G. R., Barrow, R. A., Pichersky, E., and Peakall, R. (2016). Pollination by sexual deception—it takes chemistry to work. *Current Opinion in Plant Biology*, 32, 37-46.
56. Bohórquez, J., McGenity, T. J., Papaspyrou, S., García-Robledo, E., Corzo, A., & Underwood, G. J. C. (2017). Different Types of Diatom-Derived Extracellular Polymeric Substances Drive Changes in Heterotrophic Bacterial Communities from Intertidal Sediments. *Frontiers in Microbiology*, 8, 245.
57. Boland, W., Pohnert, G., and Maier, I. (1995). Pericyclic reactions in nature: spontaneous Cope rearrangement inactivates algae pheromones. *Angewandte Chemie International*, 34(15), 1602-1604.
58. Bondoc, K. G. V., Heuschele, J., Gillard, J., Vyverman, W., and Pohnert, G. (2016). Selective silicate-directed motility in diatoms. *Nature Communications*, 7, 10540.

59. Bondoc, K. G. V., Lembke, C., Vyverman, W., and Pohnert, G. (2018a). Selective chemoattraction of the benthic diatom *Seminavis robusta* to phosphate but not to inorganic nitrogen sources contributes to biofilm structuring. *MicrobiologyOpen*, e00694.
60. Bondoc, K. G. V., Lembke, C., Lang, S. N., Germerodt, S., Schuster, S., Vyverman, W., and Pohnert, G. (2018b). Decision-making of the benthic diatom *Seminavis robusta* searching for inorganic nutrients and pheromones. *The ISME Journal*, 1.
61. Bowler, C., Allen, A. E., Badger, J. H., Grimwood, J., Jabbari, K., Kuo, A., ... and Rayko, E. (2008). The *Phaeodactylum* genome reveals the evolutionary history of diatom genomes. *Nature*, 456(7219), 239.
62. Bowler, C., De Martino, A., and Falciatore, A. (2010). Diatom cell division in an environmental context. *Current Opinion in Plant Biology*, 13(6), 623-630.
63. Brockmeier, E. K., Hodges, G., Hutchinson, T. H., Butler, E., Hecker, M., Tollefsen, K. E., ... and Colbourne, J. (2017). The role of omics in the application of adverse outcome pathways for chemical risk assessment. *Toxicological Sciences*, 158(2), 252-262.
64. Bromke, M. A. (2013). Amino acid biosynthesis pathways in diatoms. *Metabolites*, 3(2), 294-311.
65. Brown, M. R. (1991). The amino-acid and sugar composition of 16 species of microalgae used in mariculture. *Journal of Experimental Marine Biology and Ecology*, 145(1), 79-99.
66. Brown, M. R. (2002). Nutritional value and use of microalgae in aquaculture. *Avances en Nutrición Acuícola VI. Memorias del VI Simposium Internacional de Nutrición Acuícola*, 3, 281-292.
67. Bruckner, C. G., Bahulikar, R., Rahalkar, M., Schink, B., & Kroth, P. G. (2008). Bacteria associated with benthic diatoms from Lake Constance: phylogeny and influences on diatom growth and secretion of extracellular polymeric substances. *Applied And Environmental Microbiology*, 74(24), 7740-7749.
68. Bruckner, C. G., Rehm, C., Grossart, H. P., and Kroth, P. G. (2011). Growth and release of extracellular organic compounds by benthic diatoms depend on interactions with bacteria. *Environmental Microbiology*, 13(4), 1052-1063.
69. Buchan, A., LeCleir, G. R., Gulvik, C. A., and González, J. M. (2014). Master recyclers: features and functions of bacteria associated with phytoplankton blooms. *Nature Reviews Microbiology*, 12(10), 686.

70. Buchfink, B., Xie, C., and Huson, D. H. (2014). Fast and sensitive protein alignment using DIAMOND. *Nature Methods*, 12(1), 59.
71. Buhmann, M. T., Schulze, B., Förderer, A., Schleheck, D., and Kroth, P. G. (2016). Bacteria may induce the secretion of mucin-like proteins by the diatom *Phaeodactylum tricornutum*. *Journal of Phycology*, 52(3), 463-474.
72. Butenandt, V. A. (1959). Über den sexual-lockstoff des seidenspinners *Bombyx mori*. *Reindarstellung und konstitution*. *Z. Naturforschung*, b, 14, 283.
73. Calatrava, V., Hom, E. F., Llamas, Á., Fernández, E., and Galván, A. (2018). OK, thanks! A new mutualism between *Chlamydomonas* and methylobacteria facilitates growth on amino acids and peptides. *FEMS Microbiology Letters*, 365(7), fny021.
74. Calder, P. C. (2011). Fatty acids and inflammation: the cutting edge between food and pharma. *European Journal of Pharmacology*, 668, S50-S58.
75. Caron, D. A., Alexander, H., Allen, A. E., Archibald, J. M., Armbrust, E. V., Bachy, C., ... and Heidelberg, K. B. (2017). Probing the evolution, ecology and physiology of marine protists using transcriptomics. *Nature Reviews Microbiology*, 15(1), 6.
76. Carpenter, L. J., Archer, S. D., and Beale, R. (2012). Ocean-atmosphere trace gas exchange. *Chemical Society Reviews*, 41(19), 6473-6506.
77. Carvalho, A. P., Batista, D., Dobretsov, S., and Coutinho, R. (2017). Extracts of seaweeds as potential inhibitors of quorum sensing and bacterial growth. *Journal of Applied Phycology*, 29(2), 789-797.
78. Chambers, M. C., Maclean, B., Burke, R., Amodei, D., Ruderman, D. L., Neumann, S., ... Mallick, P. (2012). A cross-platform toolkit for mass spectrometry and proteomics. *Nature Biotechnology*, 30(10), 918-20.
79. Charrier, B., Abreu, M. H., Araujo, R., Bruhn, A., Coates, J. C., De Clerck, O., ... Wichard, T. (2017). Furthering knowledge of seaweed growth and development to facilitate sustainable aquaculture. *New Phytologist*, 216(4), 967-975.
80. Chauton, M. S., Winge, P., Brembu, T., Vadstein, O., and Bones, A. M. (2013). Gene regulation of carbon fixation, storage, and utilization in the diatom *Phaeodactylum tricornutum* acclimated to light/dark cycles. *Plant Physiology*, 161(2), 1034-1048.
81. Chen, L., and Qian, P. Y. (2017a). Review on molecular mechanisms of antifouling compounds: an update since 2012. *Marine Drugs*, 15(9), 264.
82. Chen, T., Zhao, Q., Wang, L., Xu, Y., and Wei, W. (2017b). Comparative metabolomic analysis of the green microalga *Chlorella sorokiniana* cultivated in the

- single culture and a consortium with bacteria for wastewater remediation. *Applied Biochemistry and Biotechnology*, 183(3), 1062-1075.
83. Cheng, J., Li, K., Zhu, Y., Yang, W., Zhou, J., and Cen, K. (2017). Transcriptome sequencing and metabolic pathways of astaxanthin accumulated in *Haematococcus pluvialis* mutant under 15% CO₂. *Bioresource Technology*, 228, 99-105.
84. Chepurnov, V. A., Mann, D. G., Vyverman, W., Sabbe, K., and Danielidis, D. B. (2002). Sexual reproduction, mating system, and protoplast dynamics of *Seminavis* (Bacillariophyceae). *Journal of Phycology*, 38(5), 1004-1019.
85. Chepurnov, V. A., Mann, D. G., Sabbe, K. and Vyverman, W. Experimental studies on sexual reproduction in diatoms. *International Review of Cytology* 237, 91-154 (2004).
86. Chepurnov, V. A., Mann, D. G., Von Dassow, P., Vanormelingen, P., Gillard, J., Inzé, D., ... and Vyverman, W. (2008). In search of new tractable diatoms for experimental biology. *BioEssays*, 30(7), 692-702.
87. Chew, K. W., Yap, J. Y., Show, P. L., Suan, N. H., Juan, J. C., Ling, T. C., ... and Chang, J. S. (2017). Microalgae biorefinery: high value products perspectives. *Bioresource Technology*, 229, 53-62.
88. Cho, J. Y. (2012). Algicidal activity of marine *Alteromonas* sp. KNS-16 and isolation of active compounds. *Bioscience, Biotechnology, and Biochemistry*, 76(8), 1452-1458.
89. Chong, J., Xia, J., and Stegle, O. (2018). MetaboAnalystR: an R package for flexible and reproducible analysis of metabolomics data. *Bioinformatics*, 1, 2.
90. Christie-Oleza, J. A., Sousoni, D., Lloyd, M., Armengaud, J., and Scanlan, D. J. (2017). Nutrient recycling facilitates long-term stability of marine microbial phototroph–heterotroph interactions. *Nature Microbiology*, 2(9), 17100.
91. Cirri, E., & Pohnert, G. (2017). Disruption-free solid phase extraction of surface metabolites from macroalgae. *Protocols for Macroalgae Research*, 20, 311-321.
92. Cleenwerck, I., Camu, N., Engelbeen, K., De Winter, T., Vandemeulebroecke, K., De Vos, P., and De Vuyst, L. (2007). *Acetobacter ghanensis* sp. nov., a novel acetic acid bacterium isolated from traditional heap fermentations of Ghanaian cocoa beans. *International Journal of Systematic and Evolutionary Microbiology*, 57(7), 1647-1652.
93. Coale, K. H., Johnson, K. S., Fitzwater, S. E., Gordon, R. M., Tanner, S., Chavez, F. P., ... and Steinberg, P. (1996). A massive phytoplankton bloom induced by an

- ecosystem-scale iron fertilization experiment in the equatorial Pacific Ocean. *Nature*, 383(6600), 495.
94. Cohen, N. R., Gong, W., Moran, D. M., McIlvin, M. R., Saito, M. A., and Marchetti, A. (2018). Transcriptomic and proteomic responses of the oceanic diatom *Pseudo-nitzschia granii* to iron limitation. *Environmental Microbiology*, 20(8), 3109-3126.
 95. Cole, J. J. (1982). Interactions between bacteria and algae in aquatic ecosystems. *Annual Review of Ecology and Systematics*, 13(1), 291-314.
 96. Coleman, A. W., Jaenicke, L., and Starr, R. C. (2001). Genetics and sexual behavior of the pheromone producer *Chlamydomonas allensworthii* (Chlorophyceae). *Journal of Phycology*, 37(2), 345-349.
 97. Considine, E. C., Thomas, G., Boulesteix, A. L., Khashan, A. S., and Kenny, L. C. (2018). Critical review of reporting of the data analysis step in metabolomics. *Metabolomics*, 14(1), 7.
 98. Cook, S. M., Khan, Z. R., and Pickett, J. A. (2007). The use of push-pull strategies in integrated pest management. *Annual Review of Entomology*, 52.
 99. Cooper, M. B., and Smith, A. G. (2015). Exploring mutualistic interactions between microalgae and bacteria in the omics age. *Current Opinion in Plant Biology*, 26, 147-153.
 100. Courant, F., Martzloff, A., Rabin, G., Antignac, J. P., Le Bizec, B., Giraudeau, P., ... and Grizeau, D. (2013). How metabolomics can contribute to bio-processes: a proof of concept study for biomarkers discovery in the context of nitrogen-starved microalgae grown in photobioreactors. *Metabolomics*, 9(6), 1286-1300.
 101. Crenn, K., Duffieux, D., & Jeanthon, C. (2018). Bacterial epibiotic communities of ubiquitous and abundant marine diatoms are distinct in short-and long-term associations. *Frontiers in Microbiology*, 9.
 102. Croft, M. T., Lawrence, A. D., Raux-Deery, E., Warren, M. J., and Smith, A. G. (2005). Algae acquire vitamin B 12 through a symbiotic relationship with bacteria. *Nature*, 438(7064), 90.
 103. Crowley, S., O'Gara, F., O'Sullivan, O., Cotter, P., & Dobson, A. (2014). Marine *Pseudovibrio* sp. as a novel source of antimicrobials. *Marine drugs*, 12(12), 5916-5929.
 104. Cushnie, T. T., & Lamb, A. J. (2005). Antimicrobial activity of flavonoids. *International journal of antimicrobial agents*, 26(5), 343-356

105. da Gama, B. A., Plouguerné, E., and Pereira, R. C. (2014). The antifouling defence mechanisms of marine macroalgae. In *Advances in Botanical Research* (Vol. 71, pp. 413-440). Academic Press.
106. Dahms, H., and Dobretsov, S. (2017). Antifouling compounds from marine macroalgae. *Marine Drugs*, 15(9), 265.
107. Dang, H., and Lovell, C. R. (2016). Microbial surface colonization and biofilm development in marine environments. *Microbiology and Molecular Biology Reviews*, 80(1), 91-138.
108. Dar, M. I., Naikoo, M. I., Rehman, F., Naushin, F., & Khan, F. A. (2016). Proline Accumulation in Plants: Roles in Stress Tolerance and Plant Development. In *Osmolytes and Plants Acclimation to Changing Environment: Emerging Omics Technologies* (pp. 155–166). New Delhi: Springer India.
109. Davey, M. E., & O’toole, G. A. (2000). Microbial biofilms: from ecology to molecular genetics. *Microbiology and Molecular Biology Reviews : MMBR*, 64(4), 847–67.
110. David Morgan, E. (2009). Trail pheromones of ants. *Physiological entomology*, 34(1), 1-17.
111. De Decker, S., Vanormelingen, P., Pinseel, E., Sefbom, J., Audoor, S., Sabbe, K., and Vyverman, W. (2018). Incomplete reproductive isolation between genetically distinct sympatric clades of the pennate model diatom *Seminavis robusta*. *Protist*, 169(4), 569-583.
112. De Nys, R., Dworjanyn, S. A., and Steinberg, P. D. (1998). A new method for determining surface concentrations of marine natural products on seaweeds. *Marine Ecology Progress Series*, 162, 79-87.
113. De Troch, M., Vergaerde, I., Cnudde, C., Vanormelingen, P., Vyverman, W., and Vincx, M. (2012). The taste of diatoms: the role of diatom growth phase characteristics and associated bacteria for benthic copepod grazing. *Aquatic Microbial Ecology*, 67(1), 47-58.
114. De-Bashan, L. E., Hernandez, J. P., Morey, T., and Bashan, Y. (2004). Microalgae growth-promoting bacteria as “helpers” for microalgae: a novel approach for removing ammonium and phosphorus from municipal wastewater. *Water Research*, 38(2), 466-474.

115. del Carmen Orozco-Mosqueda, M., del Carmen Rocha-Granados, M., Glick, B. R., & Santoyo, G. (2018). Microbiome engineering to improve biocontrol and plant growth-promoting mechanisms. *Microbiological Research*, 208, 25-31.
116. Demidchik, V., Maathuis, F., & Voitsekhovskaja, O. (2018). Unravelling the plant signalling machinery: an update on the cellular and genetic basis of plant signal transduction. *Functional Plant Biology*, 45(2), 1-8.
117. Dicke, M., and Sabelis, M. W. (1988). Infochemical terminology: based on cost-benefit analysis rather than origin of compounds?. *Functional Ecology*, 131-139.
118. Dobretsov, S., Abed, R. M., and Teplitski, M. (2013). Mini-review: Inhibition of biofouling by marine microorganisms. *Biofouling*, 29(4), 423-441.
119. Dong, H. P., Dong, Y. L., Cui, L., Balamurugan, S., Gao, J., Lu, S. H., and Jiang, T. (2016). High light stress triggers distinct proteomic responses in the marine diatom *Thalassiosira pseudonana*. *BMC Genomics*, 17(1), 994.
120. Drebes, G. (1977). *Sexuality*. In: Werner D (ed.). *The Biology of Diatoms*. Oxford: Blackwell Scientific Publications, 250–283.
121. Duarte, C. M., Holmer, M., Olsen, Y., Soto, D., Marbà, N., Guiu, J., ... and Karakassis, I. (2009). Will the oceans help feed humanity?. *BioScience*, 59(11), 967-976.
122. Dudzik, D., Barbas-Bernardos, C., García, A., and Barbas, C. (2018). Quality assurance procedures for mass spectrometry untargeted metabolomics. A review. *Journal of Pharmaceutical and Biomedical Analysis*, 147, 149-173.
123. Dührkop, K., Shen, H., Meusel, M., Rousu, J., & Bocker, S. (2015). Searching molecular structure databases with tandem mass spectra using CSI:FingerID. *Procedure of National Academy of Science*, 112(41), 12580-12585.
124. Dulac, C., and Torello, A. T. (2003). Molecular detection of pheromone signals in mammals: from genes to behaviour. *Nature Reviews Neuroscience*, 4(7), 551.
125. Dunn, W. B., Broadhurst, D., Begley, P., Zelena, E., Francis-McIntyre, S., Anderson, N., Brown, M., Knowles, J. D., Halsall, A., Haselden, J.N., Nicholls, A. W., Wilson, I. D., Kell, D. B., Goodacre, R. (2011). Procedures for large-scale metabolic profiling of serum and plasma using gas chromatography and liquid chromatography coupled to mass spectrometry. *Nature Protocols*, 6(7), 1060.
126. Dunstan, G. A., Volkman, J. K., Barrett, S. M., Leroi, J. M., & Jeffrey, S. W. (1993). Essential polyunsaturated fatty acids from 14 species of diatom (Bacillariophyceae). *Phytochemistry*, 35(1), 155-161.

127. Durham, B. P., Sharma, S., Luo, H., Smith, C. B., Amin, S. A., Bender, S. J., ... and Armbrust, E. V. (2015). Cryptic carbon and sulfur cycling between surface ocean plankton. *Proceedings of the National Academy of Sciences*, 112(2), 453-457.
128. Durham, B. P., Dearth, S. P., Sharma, S., Amin, S. A., Smith, C. B., Campagna, S. R., ... and Moran, M. A. (2017). Recognition cascade and metabolite transfer in a marine bacteria-phytoplankton model system. *Environmental Microbiology*, 19(9), 3500-3513.
129. Durmaz, Y. (2007). Vitamin E (α -tocopherol) production by the marine microalgae *Nannochloropsis oculata* (Eustigmatophyceae) in nitrogen limitation. *Aquaculture*, 272(1-4), 717-722.
130. Dworjanyn, S. A., De Nys, R., and Steinberg, P. D. (1999). Localisation and surface quantification of secondary metabolites in the red alga *Delisea pulchra*. *Marine Biology*, 133(4), 727-736.
131. Dworjanyn, S., T. Wright, J., A. Paul, N., De Nys, R., and D. Steinberg, P. (2006). Cost of chemical defence in the red alga *Delisea pulchra*. *Oikos*, 113(1), 13-22.
132. Dyhrman, S. T., Jenkins, B. D., Rynearson, T. A., Saito, M. A., Mercier, M. L., Alexander, H., ... and Wu, Z. (2012). The transcriptome and proteome of the diatom *Thalassiosira pseudonana* reveal a diverse phosphorus stress response. *PLoS One*, 7(3), e33768.
133. Edwards, J. L., Smith, D. L., Connolly, J., McDonald, J. E., Cox, M. J., Joint, I., ... and McCarthy, A. J. (2010). Identification of carbohydrate metabolism genes in the metagenome of a marine biofilm community shown to be dominated by Gammaproteobacteria and Bacteroidetes. *Genes*, 1(3), 371-384.
134. Edwards, U., Rogall, T., Blöcker, H., Emde, M., and Böttger, E. C. (1989). Isolation and direct complete nucleotide determination of entire genes. Characterization of a gene coding for 16S ribosomal RNA. *Nucleic Acids Research*, 17(19), 7843-7853.
135. Ekblom, R., and Galindo, J. (2011). Applications of next generation sequencing in molecular ecology of non-model organisms. *Heredity*, 107(1), 1.
136. Erb, M. (2018). Plant defenses against herbivory: closing the fitness gap. *Trends in Plant Science*, 23(3), 187-194.
137. Fabre, J.-H. (1918). *Social Life in the Insect World*, Fisher Unwin, London.
138. Fabris, M., Matthijs, M., Carbonelle, S., Moses, T., Pollier, J., Dasseville, R., ... and Goossens, A. (2014). Tracking the sterol biosynthesis pathway of the diatom *Phaeodactylum tricorutum*. *New Phytologist*, 204(3), 521-535.

139. Falkowski, P. G. (1994). The role of phytoplankton photosynthesis in global biogeochemical cycles. *Photosynthesis research*, 39(3), 235-258.
140. Feldmesser, E., Rosenwasser, S., Vardi, A., and Ben-Dor, S. (2014). Improving transcriptome construction in non-model organisms: integrating manual and automated gene definition in *Emiliana huxleyi*. *BMC genomics*, 15(1), 148.
141. Ferris, P. J., Waffenschmidt, S., Umen, J. G., Lin, H., Lee, J. H., Ishida, K., ... and Goodenough, U. W. (2005). Plus and minus sexual agglutinins from *Chlamydomonas reinhardtii*. *The Plant Cell*, 17(2), 597-615.
142. Fiehn, O. (2002). Metabolomics—the link between genotypes and phenotypes. In *Functional genomics* (pp. 155-171). Springer, Dordrecht.
143. Fitridge, I., Dempster, T., Guenther, J., & de Nys, R. (2012). The impact and control of biofouling in marine aquaculture: a review. *Biofouling*, 28(7), 649–669.
144. Flemming, H. C., & Wingender, J. (2001). Relevance of microbial extracellular polymeric substances (EPSs)--Part I: Structural and ecological aspects. *Water Science and Technology: A Journal of the International Association on Water Pollution Research*, 43(6), 1–8.
145. Foo, J. L., Ling, H., Lee, Y. S., and Chang, M. W. (2017). Microbiome engineering: Current applications and its future. *Biotechnology Journal*, 12(3), 1600099.
146. Foster, R. A., Kuypers, M. M., Vagner, T., Paerl, R. W., Musat, N., and Zehr, J. P. (2011). Nitrogen fixation and transfer in open ocean diatom–cyanobacterial symbioses. *The ISME journal*, 5(9), 1484.
147. Franklin, N. M., Stauber, J. L., and Lim, R. P. (2001). Development of flow cytometry-based algal bioassays for assessing toxicity of copper in natural waters. *Environmental Toxicology and Chemistry*, 20(1), 160-170.
148. Frenkel, J., Vyverman, W., and Pohnert, G. (2014a). Pheromone signaling during sexual reproduction in algae. *The Plant Journal*, 79(4), 632-644.
149. Frenkel, J., Wess, C., Vyverman, W., & Pohnert, G. (2014b). Chiral separation of a diketopiperazine pheromone from marine diatoms using supercritical fluid chromatography. *Journal of Chromatography B*, 951, 58-61.
150. Fret, J., Roef, L., Blust, R., Diels, L., Tavernier, S., Vyverman, W., & Michiels, M. (2017). Reuse of rejuvenated media during laboratory and pilot scale cultivation of *Nannochloropsis* sp. *Algal Research*, 27, 265–273.

151. Fuentes, J. L., Garbayo, I., Cuaresma, M., Montero, Z., González-del-Valle, M., and Vilchez, C. (2016). Impact of microalgae-bacteria interactions on the production of algal biomass and associated compounds. *Marine drugs*, *14*(5), 100.
152. Fuhrer, T., and Zamboni, N. (2015). High-throughput discovery metabolomics. *Current Opinion in Biotechnology*, *31*, 73-78.
153. Gebser, B., and Pohnert, G. (2013). Synchronized regulation of different zwitterionic metabolites in the osmoadaptation of phytoplankton. *Marine Drugs*, *11*(6), 2168-2182.
154. Giacomoni, F., Le Corguille, G., Monsoor, M., Landi, M., Pericard, P., Petera, M., ... Caron, C. (2015). Workflow4Metabolomics: a collaborative research infrastructure for computational metabolomics. *Bioinformatics*, *31*(9), 1493–1495.
155. Gillard, J., Devos, V., Huysman, M. J., De Veylder, L., D'hondt, S., Martens, C., ... and Inzé, D. (2008). Physiological and transcriptomic evidence for a close coupling between chloroplast ontogeny and cell cycle progression in the pennate diatom *Seminavis robusta*. *Plant Physiology*, *148*(3), 1394-1411.
156. Gillard, J., Frenkel, J., Devos, V., Sabbe, K., Paul, C., Rempt, M., ... and Vyverman, W. (2013). Metabolomics enables the structure elucidation of a diatom sex pheromone. *Angewandte Chemie International Edition*, *52*(3), 854-857.
157. Gilles, R., Gilles, C., and Jaenicke, L. (1984). Pheromone-binding and matrix-mediated events in sexual induction of *Volvox carteri*. *Zeitschrift für Naturforschung C*, *39*(6), 584-592.
158. Goncalves, E. C., Wilkie, A. C., Kirst, M., and Rathinasabapathi, B. (2016). Metabolic regulation of triacylglycerol accumulation in the green algae: identification of potential targets for engineering to improve oil yield. *Plant Biotechnology Journal*, *14*(8), 1649-1660.
159. Gonçalves, A. L., Pires, J. C., and Simões, M. (2017). A review on the use of microalgal consortia for wastewater treatment. *Algal Research*, *24*, 403-415.
160. Gonzalez, L. E., & Bashan, Y. (2000). Increased growth of the microalga *Chlorella vulgaris* when coimmobilized and cocultured in alginate beads with the plant-growth-promoting bacterium *Azospirillum brasilense*. *Applied and Environmental Microbiology*, *66*(4), 1527-1531.
161. Goodacre, R., Vaidyanathan, S., Dunn, W. B., Harrigan, G. G., and Kell, D. B. (2004). Metabolomics by numbers: acquiring and understanding global metabolite data. *Trends in Biotechnology*, *22*(5), 245-252.

162. Goulitquer, S., Potin, P., and Tonon, T. (2012). Mass spectrometry-based metabolomics to elucidate functions in marine organisms and ecosystems. *Marine Drugs*, 10(4), 849-880.
163. Grandclément, C., Tannières, M., Moréra, S., Dessaux, Y., and Faure, D. (2015). Quorum quenching: role in nature and applied developments. *FEMS Microbiology Reviews*, 40(1), 86-116.
164. Gregory, W. (1857). XXXI.—On New Forms of Marine Diatomaceæ, found in the Firth of Clyde and in Loch Fine. *Earth and Environmental Science Transactions of The Royal Society of Edinburgh*, 21(4), 473-542.
165. Griffiths, M. J., Garcin, C., van Hille, R. P., & Harrison, S. T. L. (2011). Interference by pigment in the estimation of microalgal biomass concentration by optical density. *Journal of Microbiological Methods*, 85(2), 119–123.
166. Gross, E. M. (2003). Allelopathy of aquatic autotrophs. *Critical Reviews in Plant Sciences*, 22(3-4), 313-339.
167. Grossart, H. P., Levold, F., Allgaier, M., Simon, M., and Brinkhoff, T. (2005). Marine diatom species harbour distinct bacterial communities. *Environmental Microbiology*, 7(6), 860-873.
168. Grossart, H. P., and Simon, M. (2007). Interactions of planktonic algae and bacteria: effects on algal growth and organic matter dynamics. *Aquatic Microbial Ecology*, 47(2), 163-176.
169. Grosser, K., Zedler, L., Schmitt, M., Dietzek, B., Popp, J., and Pohnert, G. (2012). Disruption-free imaging by Raman spectroscopy reveals a chemical sphere with antifouling metabolites around macroalgae. *Biofouling*, 28(7), 687-696.
170. Grozea, C. M., and Walker, G. C. (2009). Approaches in designing non-toxic polymer surfaces to deter marine biofouling. *Soft Matter*, 5(21), 4088-4100.
171. Guarnieri, M. T., and Pienkos, P. T. (2015). Algal omics: unlocking bioproduct diversity in algae cell factories. *Photosynthesis Research*, 123(3), 255-263.
172. Güell, M., Yus, E., Lluch-Senar, M., and Serrano, L. (2011). Bacterial transcriptomics: what is beyond the RNA hori-z-ome?. *Nature Reviews Microbiology*, 9(9), 658.
173. Guillard, R. R., and Ryther, J. H. (1962). Studies of marine planktonic diatoms: I. *Cyclotella nana* Hustedt, and *Detonula confervacea* (Cleve) Gran. *Canadian Journal of Microbiology*, 8(2), 229-239.

174. Gupta, K., Dey, A., & Gupta, B. (2013). Plant polyamines in abiotic stress responses. *Acta Physiologiae Plantarum*, 35(7), 2015–2036.
175. Ha, T. S. (2009). Odorant and pheromone receptors in insects. *Frontiers in cellular neuroscience*, 3, 10.
176. Haines, K. C., and Guillard, R. R. (1974). Growth of vitamin b12-requiring marine diatoms in mixed laboratory cultures with vitamin B12-producing marine bacteria. *Journal of Phycology*, 10(3), 245-252.
177. Hallmann, A., Godl, K., Wenzl, S., and Sumper, M. (1998). The highly efficient sex-inducing pheromone system of *Volvox*. *Trends in Microbiology*, 6(5), 185-189.
178. Hallmann, A. (2011). Evolution of reproductive development in the volvocine algae. *Sexual Plant Reproduction*, 24(2), 97-112.
179. Hamm, C. E., Merkel, R., Springer, O., Jurkojc, P., Maier, C., Prechtel, K., and Smetacek, V. (2003). Architecture and material properties of diatom shells provide effective mechanical protection. *Nature*, 421(6925), 841.
180. Harun, R., Singh, M., Forde, G. M., and Danquah, M. K. (2010). Bioprocess engineering of microalgae to produce a variety of consumer products. *Renewable and Sustainable Energy Reviews*, 14(3), 1037-1047.
181. Havaux, M., and García-Plazaola, J. I. (2014). Beyond non-photochemical fluorescence quenching: the overlapping antioxidant functions of zeaxanthin and tocopherols. In *Non-Photochemical Quenching and Energy Dissipation in Plants, Algae and Cyanobacteria* (pp. 583-603). Springer, Dordrecht.
182. Haynes, K. F., and Yeargan, K. V. (1999). Exploitation of intraspecific communication systems: illicit signalers and receivers. *Annals of the Entomological Society of America*, 92(6), 960-970.
183. Haynes, K., Hofmann, T. A., Smith, C. J., Ball, A. S., Underwood, G. J., and Osborn, A. M. (2007). Diatom-derived carbohydrates as factors affecting bacterial community composition in estuarine sediments. *Applied and Environmental Microbiology*, 73(19), 6112-6124.
184. Hellio, C., Bremer, G., Pons, A. M., Le Gal, Y., and Bourgougnon, N. (2000). Inhibition of the development of microorganisms (bacteria and fungi) by extracts of marine algae from Brittany, France. *Applied Microbiology and Biotechnology*, 54(4), 543-549.
185. Helliwell, K. E., Pandhal, J., Cooper, M. B., Longworth, J., Kudahl, U. J., Russo, D. A., ... and Wright, P. C. (2018). Quantitative proteomics of a B12-dependent alga

- grown in coculture with bacteria reveals metabolic tradeoffs required for mutualism. *New Phytologist*, 217(2), 599-612.
186. Helsper, J. P., and Loewus, F. A. (1982). Metabolism of l-Threonic Acid in *Rumex x acutus* L. and *Pelargonium crispum* (L.) L'Hér. *Plant Physiology*, 69(6), 1365-1368.
187. Hennon, G. M., Ashworth, J., Groussman, R. D., Berthiaume, C., Morales, R. L., Baliga, N. S., Orellana M. V. and Armbrust, E. V. (2015). Diatom acclimation to elevated CO₂ via cAMP signaling and coordinated gene expression. *Nature Climate Change*, 5(8), 761.
188. Hildebrandt, T. M., Nunes Nesi, A., Araújo, W. L., & Braun, H.-P. (2015). Amino acid catabolism in plants. *Molecular Plant*, 8(11), 1563–1579.
189. Hiltner L. (1904). Über neuere Erfahrungen und Probleme auf die Gebiete der Bodenbakteriologie unter besonderer Berücksichtigung der Gründüngung und Brache. *Arb DLG* 98:59–78.
190. Hoff, K. J., Lange, S., Lomsadze, A., Borodovsky, M., & Stanke, M. (2016). BRAKER1: Unsupervised RNA-Seq-Based Genome Annotation with GeneMark-ET and AUGUSTUS. *Bioinformatics*, 32, 767-769.
191. Hollants, J., Leliaert, F., De Clerck, O., and Willems, A. (2013). What we can learn from sushi: a review on seaweed–bacterial associations. *FEMS Microbiology Ecology*, 83(1), 1-16.
192. Holzinger, A., and Pichrtová, M. (2016). Abiotic stress tolerance of charophyte green algae: new challenges for omics techniques. *Frontiers in Plant Science*, 7, 678.
193. Hook, S. E., and Osborn, H. L. (2012). Comparison of toxicity and transcriptomic profiles in a diatom exposed to oil, dispersants, dispersed oil. *Aquatic Toxicology*, 124, 139-151.
194. Horgan, R. P., and Kenny, L. C. (2011). ‘Omic’ technologies: genomics, transcriptomics, proteomics and metabolomics. *The Obstetrician and Gynaecologist*, 13(3), 189-195.
195. Horňák, K., Kasalický, V., Šimek, K., and Grossart, H. P. (2017). Strain-specific consumption and transformation of alga-derived dissolved organic matter by members of the Limnohabitans-C and Polynucleobacter-B clusters of Betaproteobacteria. *Environmental Microbiology*, 19(11), 4519-4535.

196. Horton, P., and Ruban, A. (2004). Molecular design of the photosystem II light-harvesting antenna: photosynthesis and photoprotection. *Journal of Experimental Botany*, 56(411), 365-373.
197. Howse, P., Stevens, J. M., and Jones, O. T. (2013). *Insect pheromones and their use in pest management*. Springer Science and Business Media.
198. Hothorn, T., Bretz, F., & Westfall, P. (2008). Simultaneous inference in general parametric models. *Biom J*, 50, 346-363. doi: 10.1002/bimj.200810425
199. Hu, C. A., Delauney, A. J., and Verma, D. P. (1992). A bifunctional enzyme (delta 1-pyrroline-5-carboxylate synthetase) catalyzes the first two steps in proline biosynthesis in plants. *Proceedings of the National Academy of Sciences*, 89(19), 9354-9358.
200. Hu, J., Nagarajan, D., Zhang, Q., Chang, J. S., and Lee, D. J. (2018). Heterotrophic cultivation of microalgae for pigment production: A review. *Biotechnology Advances*, 36(1), 54-67.
201. Hubbard, P. (2015). Pheromones in marine fish with comments on their possible use in aquaculture. *Fish Pheromones and Related Cues*, 1, 237-253.
202. Huerta-Cepas, J., Szklarczyk, D., Forslund, K., Cook, H., Heller, D., Walter, M. C., ... and Jensen, L. J. (2015). eggNOG 4.5: a hierarchical orthology framework with improved functional annotations for eukaryotic, prokaryotic and viral sequences. *Nucleic Acids Research*, 44(D1), D286-D293.
203. Huerta-Cepas, J., Forslund, K., Coelho, L. P., Szklarczyk, D., Jensen, L. J., von Mering, C., and Bork, P. (2017). Fast genome-wide functional annotation through orthology assignment by eggNOG-mapper. *Molecular Biology and Evolution*, 34(8), 2115-2122.
204. Hulatt, C. J., Wijffels, R. H., Bolla, S., & Kiron, V. (2017). Production of fatty acids and protein by nanochloropsis in flat-plate photobioreactors. *PLoS One*, 12(1), e0170440.
205. Hünken, M., Harder, J., and Kirst, G. O. (2008). Epiphytic bacteria on the Antarctic ice diatom *Amphiprora kufferathii* Manguin cleave hydrogen peroxide produced during algal photosynthesis. *Plant Biology*, 10(4), 519-526.
206. Hurd, C. L. (2000). Water motion, marine macroalgal physiology, and production. *Journal of Phycology*, 36(3), 453-472.

207. Hutchinson, G. E. (1961). The paradox of the plankton. *The American Naturalist*, 95(882), 137-145.
208. Huysman, M. J., Vyverman, W., and De Veylder, L. (2013). Molecular regulation of the diatom cell cycle. *Journal of Experimental Botany*, 65(10), 2573-2584.
209. Ianora, A., Bentley, M. G., Caldwell, G. S., Casotti, R., Cembella, A. D., Engström-Öst, J., ... and Paldavičienė, A. (2011). The relevance of marine chemical ecology to plankton and ecosystem function: an emerging field. *Marine Drugs*, 9(9), 1625-1648.
210. Isner, J. C., and Maathuis, F. J. (2018). cGMP signaling in plants: from enigma to main stream. *Functional Plant Biology*, 45(2), 93-101.
211. Jacquemoud, D., and Pohnert, G. (2015). Extraction and analysis of oxylipins from macroalgae illustrated on the example *Gracilaria vermiculophylla*. In *Natural products from marine algae* (pp. 159-172). Humana Press, New York, NY.
212. Jamers, A., Blust, R., and De Coen, W. (2009). Omics in algae: paving the way for a systems biological understanding of algal stress phenomena?. *Aquatic Toxicology*, 92(3), 114-121.
213. Ji, X., Jiang, M., Zhang, J., Jiang, X., & Zheng, Z. (2018). The interactions of algae-bacteria symbiotic system and its effects on nutrients removal from synthetic wastewater. *Bioresource Technology*, 247, 44–50.
214. Johnson, W. M., Soule, M. C. K., and Kujawinski, E. B. (2016). Evidence for quorum sensing and differential metabolite production by a marine bacterium in response to DMSP. *The ISME Journal*, 10(9), 2304.
215. Johnston, A. W., Green, R. T., and Todd, J. D. (2016). Enzymatic breakage of dimethylsulfoniopropionate—a signature molecule for life at sea. *Current Opinion in Chemical Biology*, 31, 58-65.
216. Jones, C. S., and Mayfield, S. P. (2012). Algae biofuels: versatility for the future of bioenergy. *Current Opinion in Biotechnology*, 23(3), 346-351.
217. Jones, P., Binns, D., Chang, H. Y., Fraser, M., Li, W., McAnulla, C., ... and Pesseat, S. (2014). InterProScan 5: genome-scale protein function classification. *Bioinformatics*, 30(9), 1236-1240.
218. Jung, V., and Pohnert, G. (2001). Rapid wound-activated transformation of the green algal defensive metabolite caulerpenyne. *Tetrahedron*, 57(33), 7169-7172.
219. Jüttner, F., and Müller, H. (1979). Excretion of octadiene and octatrienes by a freshwater diatom. *Naturwissenschaften*, 66(7), 363-364.

220. Kandilian, R., Lee, E., & Pilon, L. (2013). Radiation and optical properties of *Nannochloropsis oculata* grown under different irradiances and spectra. *Bioresource Technology*, 137, 63–73.
221. Kanzaki, H., Oda, S., Kobayashi, A., and Kawazu, K. (1997). Microbial hydrolysis of diketopiperazines: different types of diketopiperazine-assimilating bacteria. *Journal of Fermentation and Bioengineering*, 83(4), 386-388.
222. Karlson, P. and Lüscher, M. (1959). ‘Pheromones’: a new term for a class of biologically active substances. *Nature* 183, 55.
223. Kazamia, E., Czesnick, H., Nguyen, T. T. V., Croft, M. T., Sherwood, E., Sasso, S., ... and Smith, A. G. (2012). Mutualistic interactions between vitamin B12-dependent algae and heterotrophic bacteria exhibit regulation. *Environmental Microbiology*, 14(6), 1466-1476.
224. Kazamia, E., Helliwell, K. E., Purton, S., and Smith, A. G. (2016). How mutualisms arise in phytoplankton communities: building eco-evolutionary principles for aquatic microbes. *Ecology Letters*, 19(7), 810-822.
225. Kell, D. B., Kaprelyants, A. S., and Grafen, A. (1995). Pheromones, social behaviour and the functions of secondary metabolism in bacteria. *Trends in Ecology and Evolution*, 10(3), 126-129.
226. Keller, N. P., Turner, G., and Bennett, J. W. (2005). Fungal secondary metabolism—from biochemistry to genomics. *Nature Reviews Microbiology*, 3(12), 937.
227. Kesaano, M., and Sims, R. C. (2014). Algal biofilm based technology for wastewater treatment. *Algal Research*, 5, 231-240.
228. Kolas, N. K., and Cohen, P. E. (2004). Novel and diverse functions of the DNA mismatch repair family in mammalian meiosis and recombination. *Cytogenetic and Genome Research*, 107(3-4), 216-231.
229. Koo, A. J. (2018). Metabolism of the plant hormone jasmonate: a sentinel for tissue damage and master regulator of stress response. *Phytochemistry Reviews*, 17(1), 51-80.
230. Kouzuma, A., & Watanabe, K. (2015). Exploring the potential of algae/bacteria interactions. *Current Opinion in Biotechnology*, 33, 125–129.
231. Krell, A., Funck, D., Plettner, I., John, U., and Dieckmann, G. (2007). Regulation of proline metabolism under salt stress in the psychrophilic diatom *Fragilariopsis cylindrus* (Bacillariophyceae) 1. *Journal of Phycology*, 43(4), 753-762.

232. Krohn-Molt, I., Alawi, M., Förstner, K. U., Wiegandt, A., Burkhardt, L., Indenbirken, D., ... and Streit, W. R. (2017). Insights into microalga and bacteria interactions of selected phycosphere biofilms using metagenomic, transcriptomic, and proteomic approaches. *Frontiers in Microbiology*, 8, 1941.
233. Kubanek, J., Hicks, M. K., Naar, J., and Villareal, T. A. (2005). Does the red tide dinoflagellate *Karenia brevis* use allelopathy to outcompete other phytoplankton?. *Limnology and Oceanography*, 50(3), 883-895.
234. Kuczynska, P., Jemiola-Rzeminska, M., & Strzalka, K. (2015). Photosynthetic pigments in diatoms. *Marine Drugs*, 13(9), 5847.
235. Kumar, S., Stecher, G., and Tamura, K. (2016). MEGA7: molecular evolutionary genetics analysis version 7.0 for bigger datasets. *Molecular Biology and Evolution*, 33(7), 1870-1874.
236. Kupferschmidt, K. (2018). A recipe for rigor. *Science*, 361, 6408, 1192-1193.
237. Lachnit, T., Wahl, M., and Harder, T. (2009). Isolated thallus-associated compounds from the macroalga *Fucus vesiculosus* mediate bacterial surface colonization in the field similar to that on the natural alga. *Biofouling*, 26(3), 247-255.
238. Lachnit, T., Fischer, M., Künzel, S., Baines, J. F., and Harder, T. (2013). Compounds associated with algal surfaces mediate epiphytic colonization of the marine macroalga *Fucus vesiculosus*. *FEMS Microbiology Ecology*, 84(2), 411-420.
239. Landa, M., Blain, S., Christaki, U., Monchy, S., and Obernosterer, I. (2016). Shifts in bacterial community composition associated with increased carbon cycling in a mosaic of phytoplankton blooms. *The ISME Journal*, 10(1), 39.
240. Landa, M., Burns, A. S., Roth, S. J., and Moran, M. A. (2017). Bacterial transcriptome remodeling during sequential co-culture with a marine dinoflagellate and diatom. *The ISME Journal*, 11(12), 2677.
241. Lane, A. L., Nyadong, L., Galhena, A. S., Shearer, T. L., Stout, E. P., Parry, R. M., ... and Kubanek, J. (2009). Desorption electrospray ionization mass spectrometry reveals surface-mediated antifungal chemical defense of a tropical seaweed. *Proceedings of the National Academy of Sciences*, 106(18), 7314-7319.
242. Larranaga, P., Calvo, B., Santana, R., Bielza, C., Galdiano, J., Inza, I., ... and Robles, V. (2006). Machine learning in bioinformatics. *Briefings in bioinformatics*, 7(1), 86-112.

243. Lauritano, C., Orefice, I., Procaccini, G., Romano, G., and Ianora, A. (2015). Key genes as stress indicators in the ubiquitous diatom *Skeletonema marinoi*. *BMC Genomics*, *16*(1), 411.
244. Leach, J. E., Triplett, L. R., Argueso, C. T., and Trivedi, P. (2017). Communication in the phytobiome. *Cell*, *169*(4), 587-596.
245. Leal, W. S. (2017). Reverse chemical ecology at the service of conservation biology. *Proceedings of the National Academy of Sciences*, 201717375.
246. Lee, J. J. L., Chen, L., Shi, J., Trzcinski, A., and Chen, W. N. (2014). Metabolomic profiling of *Rhodospiridium toruloides* grown on glycerol for carotenoid production during different growth phases. *Journal of Agricultural and Food Chemistry*, *62*(41), 10203-10209.
247. Legrand, C., Rengefors, K., Fistarol, G. O., and Graneli, E. (2003). Allelopathy in phytoplankton-biochemical, ecological and evolutionary aspects. *Phycologia*, *42*(4), 406-419.
248. Lehtonen, J., and Whitehead, M. R. (2014). Sexual deception: Coevolution or inescapable exploitation?. *Current Zoology*, *60*(1), 52-61.
249. Lembke, C (2018). Chemical ecology of diatom mate finding: pheromone elucidation and perception. Doctoral thesis, Friedrich-Schiller-Universität Jena.
250. Lembke, C., Stettin, D., Speck, F., Ueberschaar, N., De Decker, S., Vyverman, W., and Pohnert, G. (2018). Attraction pheromone of the benthic diatom *Seminavis robusta*: studies on structure-activity relationships. *Journal of Chemical Ecology*, *44*(4), 354-363.
251. Lenihan-Geels, G., Bishop, K. S., & Ferguson, L. R. (2013). Alternative sources of omega-3 fats: can we find a sustainable substitute for fish? *Nutrients*, *5*(4), 1301–15.
252. Lépinay, A., Turpin, V., Mondeguer, F., Grandet-Marchant, Q., Capiiaux, H., Baron, R., and Lebeau, T. (2018). First insight on interactions between bacteria and the marine diatom *Haslea ostrearia*: Algal growth and metabolomic fingerprinting. *Algal Research*, *31*, 395-405.
253. Levitan, O., Dinamarca, J., Zelzion, E., Lun, D. S., Guerra, L. T., Kim, M. K., ... and Falkowski, P. G. (2015). Remodeling of intermediate metabolism in the diatom *Phaeodactylum tricorutum* under nitrogen stress. *Proceedings of the National Academy of Sciences*, *112*(2), 412-417.

254. Li, J., Han, D., Wang, D., Ning, K., Jia, J., Wei, L., ... and Hu, Q. (2014). Choreography of transcriptomes and lipidomes of *Nannochloropsis* reveals the mechanisms of oil synthesis in microalgae. *The Plant Cell*, tpc-113.
255. Li, S., Xu, J., Chen, J., Chen, J., Zhou, C., and Yan, X. (2014). The major lipid changes of some important diet microalgae during the entire growth phase. *Aquaculture*, 428, 104-110.
256. Lian, J., Wijffels, R. H., Smidt, H., & Sipkema, D. (2018). The effect of the algal microbiome on industrial production of microalgae. *Microbial Biotechnology*, 11(5), 806–818.
257. Libbrecht, M. W., and Noble, W. S. (2015). Machine learning applications in genetics and genomics. *Nature Reviews Genetics*, 16(6), 321.
258. Liggi, S., Hinz, C., Hall, Z., Santoru, M. L., Poddighe, S., Fjeldsted, J., ... and Griffin, J. L. (2018). KniMet: a pipeline for the processing of chromatography–mass spectrometry metabolomics data. *Metabolomics*, 14(4), 52.
259. Lima-Mendez, G., Faust, K., Henry, N., Decelle, J., Colin, S., Carcillo, F., ... and Bittner, L. (2015). Determinants of community structure in the global plankton interactome. *Science*, 348(6237), 1262073.
260. Liu, X., Ser, Z., and Locasale, J. W. (2014). Development and quantitative evaluation of a high-resolution metabolomics technology. *Analytical Chemistry*, 86(4), 2175-2184.
261. Liu, L., Pohnert, G., and Wei, D. (2016). Extracellular metabolites from industrial microalgae and their biotechnological potential. *Marine Drugs*, 14(10), 191.
262. Liu, J., Song, Y., and Qiu, W. (2017). Oleaginous microalgae *Nannochloropsis* as a new model for biofuel production: review and analysis. *Renewable and Sustainable Energy Reviews*, 72, 154-162.
263. Lommer, M., Specht, M., Roy, A. S., Kraemer, L., Andreson, R., Gutowska, M. A., ... and Beiko, R. G. (2012). Genome and low-iron response of an oceanic diatom adapted to chronic iron limitation. *Genome Biology*, 13(7), R66.
264. Longhurst, A., Sathyendranath, S., Platt, T., and Caverhill, C. (1995). An estimate of global primary production in the ocean from satellite radiometer data. *Journal of Plankton Research*, 17(6), 1245-1271.
265. Lorite, G. S., Rodrigues, C. M., de Souza, A. A., Kranz, C., Mizaikoff, B., & Cotta, M. A. (2011). The role of conditioning film formation and surface chemical changes

- on *Xylella fastidiosa* adhesion and biofilm evolution. *Journal of Colloid and Interface Science*, 359(1), 289–295.
266. Loureiro, R., Gachon, C. M., and Rebours, C. (2015). Seaweed cultivation: potential and challenges of crop domestication at an unprecedented pace. *New Phytologist*, 206(2), 489-492.
267. Lu, H., Xie, H., Gong, Y., Wang, Q., & Yang, Y. (2011). Secondary metabolites from the seaweed *Gracilaria lemaneiformis* and their allelopathic effects on *Skeletonema costatum*. *Biochemical Systematics and Ecology*, 39(4-6), 397-400.
268. Lu, H., Qu, G., Qi, X., Lu, L., Tian, C., and Ma, Y. (2013). Transcriptome analysis of *Chlamydomonas reinhardtii* during the process of lipid accumulation. *Genomics*, 101(4), 229-237.
269. Lun, A. T., Chen, Y., and Smyth, G. K. (2016). It's DE-licious: a recipe for differential expression analyses of RNA-seq experiments using quasi-likelihood methods in edgeR. In *Statistical Genomics* (pp. 391-416). Humana Press, New York, NY.
270. Lüring, M., and Scheffer, M. (2007). Info-disruption: pollution and the transfer of chemical information between organisms. *Trends in Ecology and Evolution*, 22(7), 374-379.
271. MacIntyre, H. L., Geider, R. J., & Miller, D. C. (1996). Microphytobenthos: the ecological role of the “secret garden” of unvegetated, shallow-water marine habitats. I. Distribution, abundance and primary production. *Estuaries*, 19(2), 186-201.
272. Maher, C. A., Kumar-Sinha, C., Cao, X., Kalyana-Sundaram, S., Han, B., Jing, X., ... and Chinnaiyan, A. M. (2009). Transcriptome sequencing to detect gene fusions in cancer. *Nature*, 458(7234), 97.
273. Maheswari, U., Mock, T., Armbrust, E. V., and Bowler, C. (2008). Update of the Diatom EST Database: a new tool for digital transcriptomics. *Nucleic acids research*, 37(suppl_1), D1001-D1005.
274. Maier, I., Müller, D. G., Schmid, C., Boland, W., and Jaenicke, L. (1988). Pheromone receptor specificity and threshold concentrations for spermatozoid release in *Laminaria digitata*. *The Science of Nature*, 75(5), 260-263.
275. Malviya, S., Scalco, E., Audic, S., Vincent, F., Veluchamy, A., Poulain, J., ... and Zingone, A. (2016). Insights into global diatom distribution and diversity in the world's ocean. *Proceedings of the National Academy of Sciences*, 201509523.

276. Mann, D. G., and Vanormelingen, P. (2013). An inordinate fondness? The number, distributions, and origins of diatom species. *Journal of Eukaryotic Microbiology*, 60(4), 414-420.
277. Marie, D., Partensky, F., Jacquet, S., and Vaultot, D. (1997). Enumeration and cell cycle analysis of natural populations of marine picoplankton by flow cytometry using the nucleic acid stain SYBR Green I. *Applied and Environmental Microbiology*, 63(1), 186-193.
278. Markley, J. L., Brüschweiler, R., Edison, A. S., Eghbalnia, H. R., Powers, R., Raftery, D., and Wishart, D. S. (2017). The future of NMR-based metabolomics. *Current Opinion in Biotechnology*, 43, 34-40.
279. Martin, G. J., Hill, D. R., Olmstead, I. L., Bergamin, A., Shears, M. J., Dias, D. A., ... and Callahan, D. L. (2014). Lipid profile remodeling in response to nitrogen deprivation in the microalgae *Chlorella* sp.(Trebouxiophyceae) and *Nannochloropsis* sp.(Eustigmatophyceae). *PLoS One*, 9(8), e103389.
280. Martin-Platero, A. M., Cleary, B., Kauffman, K., Preheim, S. P., McGillicuddy, D. J., Alm, E. J., and Polz, M. F. (2018). High resolution time series reveals cohesive but short-lived communities in coastal plankton. *Nature Communications*, 9(1), 266.
281. Mausz, M. A., and Pohnert, G. (2015). Phenotypic diversity of diploid and haploid *Emiliania huxleyi* cells and of cells in different growth phases revealed by comparative metabolomics. *Journal of Plant Physiology*, 172, 137-148.
282. McKusick, V. A., and Ruddle, F. H. (1987). A new discipline, a new name, a new journal. *Genomics*, 1.
283. Mendes, R., Garbeva, P., and Raaijmakers, J. M. (2013). The rhizosphere microbiome: significance of plant beneficial, plant pathogenic, and human pathogenic microorganisms. *FEMS microbiology reviews*, 37(5), 634-663.
284. Merchant, S. S., Kropat, J., Liu, B., Shaw, J., and Warakanont, J. (2012). TAG, You're it! *Chlamydomonas* as a reference organism for understanding algal triacylglycerol accumulation. *Current Opinion in Biotechnology*, 23(3), 352-363.
285. Meyer, N., Bigalke, A., Kaulfuß, A., and Pohnert, G. (2017). Strategies and ecological roles of algicidal bacteria. *FEMS Microbiology Reviews*, 41(6), 880-899.
286. Meyer, N., Rettner, J., Werner, M., Werz, O., Pohnert, G. (2018). Algal oxylipins mediate the resistance of diatoms against algicidal bacteria. *Marine Drugs*, 16, 486.

287. Mhatre, E., Monterrosa, R. G., & Kovács, Á. T. (2014). From environmental signals to regulators: Modulation of biofilm development in Gram-positive bacteria. *Journal of Basic Microbiology*, 54(7), 616–632.
288. Miller, M. B., and Bassler, B. L. (2001). Quorum sensing in bacteria. *Annual Reviews in Microbiology*, 55(1), 165-199.
289. Misra, B. B., and van der Hooft, J. J. (2016). Updates in metabolomics tools and resources: 2014–2015. *Electrophoresis*, 37(1), 86-110.
290. Mock, T., Samanta, M. P., Iverson, V., Berthiaume, C., Robison, M., Holtermann, K., ... and Kallas, T. (2008). Whole-genome expression profiling of the marine diatom *Thalassiosira pseudonana* identifies genes involved in silicon bioprocesses. *Proceedings of the National Academy of Sciences*, 105(5), 1579-1584.
291. Moerdijk-Poortvliet, T. C., Beauchard, O., Stal, L. J., and Boschker, H. T. (2018). Production and consumption of extracellular polymeric substances in an intertidal diatom mat. *Marine Ecology Progress Series*, 592, 77-95.
292. Moeys, S., Frenkel, J., Lembke, C., Gillard, J. T., Devos, V., Van den Berge, K., Bouillon, B., Huysman, M. J. J., De Decker, S., Scharf, J., Bones, A., Brembu, T., Winge, P., Sabbe, K., Vuylsteke, M., Clement, L., De Veylder, L., Pohnert, G. and Vyverman, W. (2016). A sex-inducing pheromone triggers cell cycle arrest and mate attraction in the diatom *Seminavis robusta*. *Scientific Reports*, 6, 19252.
293. Moore, E. R., Bullington, B. S., Weisberg, A. J., Jiang, Y., Chang, J., and Halsey, K. H. (2017). Morphological and transcriptomic evidence for ammonium induction of sexual reproduction in *Thalassiosira pseudonana* and other centric diatoms. *PLoS One*, 12(7), e0181098.
294. Morozova, O., and Marra, M. A. (2008). Applications of next-generation sequencing technologies in functional genomics. *Genomics*, 92(5), 255-264.
295. Morris, J. J., Johnson, Z. I., Szul, M. J., Keller, M., and Zinser, E. R. (2011). Dependence of the cyanobacterium *Prochlorococcus* on hydrogen peroxide scavenging microbes for growth at the ocean's surface. *PLoS One*, 6(2), e16805.
296. Mühlenbruch, M., Grossart, H. P., Eigemann, F., and Voss, M. (2018). Mini-review: Phytoplankton-derived polysaccharides in the marine environment and their interactions with heterotrophic bacteria. *Environmental Microbiology*, 20(8), 2671-2685.
297. Müller, D. G., Jaenicke, L., Donike, M., and Akintobi, T. (1971). Sex attractant in a brown alga: chemical structure. *Science*, 815-817.

298. Müller, D. G. (1972). Chemotaxis in brown algae. *Naturwissenschaften*, 59(4), 166-166.
299. Natrah, F. M. I., Bossier, P., Sorgeloos, P., Yusoff, F. M., & Defoirdt, T. (2014). Significance of microalgal-bacterial interactions for aquaculture. *Reviews in Aquaculture*, 6(1), 48–61.
300. Nedashkovskaya, O. I., Kim, S. B., Han, S. K., Lysenko, A. M., Rohde, M., Rhee, M. S., ... and Bae, K. S. (2004). *Maribacter* gen. nov., a new member of the family Flavobacteriaceae, isolated from marine habitats, containing the species *Maribacter sedimenticola* sp. nov., *Maribacter aquivivus* sp. nov., *Maribacter orientalis* sp. nov. and *Maribacter ulvicola* sp. nov. *International Journal of Systematic and Evolutionary Microbiology*, 54(4), 1017-1023.
301. Needham, D. M., Fichot, E. B., Wang, E., Berdjeb, L., Cram, J. A., Fichot, C. G., and Fuhrman, J. A. (2017). Dynamics of finely resolved, abundant symbiotic marine plankton and other interacting microbes via automated high-frequency sampling. *bioRxiv*, 216978.
302. Nelson, D. M., Tréguer, P., Brzezinski, M. A., Leynaert, A., and Quéguiner, B. (1995). Production and dissolution of biogenic silica in the ocean: revised global estimates, comparison with regional data and relationship to biogenic sedimentation. *Global Biogeochemical Cycles*, 9(3), 359-372.
303. Nylund, G. M., Gribben, P. E., de Nys, R., Steinberg, P. D., and Pavia, H. (2007). Surface chemistry versus whole-cell extracts: antifouling tests with seaweed metabolites. *Marine Ecology Progress Series*, 329, 73-84.
304. Nylund, G. M., Weinberger, F., Rempt, M., and Pohnert, G. (2011). Metabolomic assessment of induced and activated chemical defence in the invasive red alga *Gracilaria vermiculophylla*. *PLoS One*, 6(12), e29359.
305. Nymark, M., Valle, K. C., Brembu, T., Hancke, K., Winge, P., Andresen, K., ... and Bones, A. M. (2009). An integrated analysis of molecular acclimation to high light in the marine diatom *Phaeodactylum tricornutum*. *PLoS One*, 4(11), e7743.
306. Oliveros, J.C. (2007-2015) Venny. An interactive tool for comparing lists with Venn's diagrams. <http://bioinfogp.cnb.csic.es/tools/venny/index.html>
307. Patro, R., Duggal, G., Love, M. I., Irizarry, R. A., & Kingsford, C. (2017). Salmon provides fast and bias-aware quantification of transcript expression. *Nature methods*, 14, 417. doi: 10.1038/nmeth.4197

308. Paerl, H. W., and Pinckney, J. L. (1996). A mini-review of microbial consortia: their roles in aquatic production and biogeochemical cycling. *Microbial Ecology*, 31(3), 225-247.
309. Paerl, R. W., Bouget, F. Y., Lozano, J. C., Vergé, V., Schatt, P., Allen, E. E., ... & Azam, F. (2017). Use of plankton-derived vitamin B1 precursors, especially thiazole-related precursor, by key marine picoeukaryotic phytoplankton. *The ISME journal*, 11(3), 753.
310. Pal, D., Khozin-Goldberg, I., Didi-Cohen, S., Solovchenko, A., Batushansky, A., Kaye, Y., ... Boussiba, S. (2013). Growth, lipid production and metabolic adjustments in the euryhaline eustigmatophyte *Nannochloropsis oceanica* CCALA 804 in response to osmotic downshift. *Applied Microbiology and Biotechnology*, 97(18), 8291–8306.
311. Palenik, B., Grimwood, J., Aerts, A., Rouzé, P., Salamov, A., Putnam, N., ... and Zhou, K. (2007). The tiny eukaryote *Ostreococcus* provides genomic insights into the paradox of plankton speciation. *Proceedings of the National Academy of Sciences*, 104(18), 7705-7710.
312. Paul, C., Barofsky, A., Vidoudez, C., and Pohnert, G. (2009). Diatom exudates influence metabolism and cell growth of co-cultured diatom species. *Marine Ecology Progress Series*, 389, 61-70.
313. Paul, C., and Pohnert, G. (2011). Interactions of the algicidal bacterium *Kordia algicida* with diatoms: regulated protease excretion for specific algal lysis. *PLoS One*, 6(6), e21032.
314. Paul, C., Mausz, M. A., and Pohnert, G. (2013). A co-culturing/metabolomics approach to investigate chemically mediated interactions of planktonic organisms reveals influence of bacteria on diatom metabolism. *Metabolomics*, 9(2), 349-359.
315. Paul, C., and Pohnert, G. (2013). Induction of protease release of the resistant diatom *Chaetoceros didymus* in response to lytic enzymes from an algicidal bacterium. *PLoS One*, 8(3), e57577.
316. Paul, V. J., and Ritson-Williams, R. (2008). Marine chemical ecology. *Natural Product Reports*, 25(4), 662-695.
317. Paul, V. J., Ritson-Williams, R., and Sharp, K. (2011). Marine chemical ecology in benthic environments. *Natural Product Reports*, 28(2), 345-387.
318. Pei, G., Li, X., Liu, L., Liu, J., Wang, F., Chen, L., and Zhang, W. (2017). De novo transcriptomic and metabolomic analysis of docosaheptaenoic acid (DHA)-producing

- Crypthecodinium cohnii* during fed-batch fermentation. *Algal Research*, 26, 380-391.
319. Pereira, H., Barreira, L., Figueiredo, F., Custódio, L., Vizetto-Duarte, C., Polo, C., ... and Varela, J. (2012). Polyunsaturated fatty acids of marine macroalgae: potential for nutritional and pharmaceutical applications. *Marine Drugs*, 10(9), 1920-1935.
320. Peršoh, D. (2015). Plant-associated fungal communities in the light of meta'omics. *Fungal Diversity*, 75(1), 1-25.
321. Persson, F., Svensson, R., Nylund, G. M., Fredriksson, N. J., Pavia, H., and Hermansson, M. (2011). Ecological role of a seaweed secondary metabolite for a colonizing bacterial community. *Biofouling*, 27(6), 579-588.
322. Perzborn, M., Syldatk, C., and Rudat, J. (2013). Enzymatical and microbial degradation of cyclic dipeptides (diketopiperazines). *AMB Express*, 3(1), 51.
323. Piomelli, D. (1993). Arachidonic acid in cell signaling. *Current Opinion in Cell Biology*, 5(2), 274-280.
324. Poddar, N., Sen, R., & Martin, G. J. O. (2018). Glycerol and nitrate utilisation by marine microalgae *Nannochloropsis salina* and *Chlorella* sp. and associated bacteria during mixotrophic and heterotrophic growth. *Algal Research*, 33, 298–309.
325. Pohnert, G., and Boland, W. (1997). Pericyclic reactions in nature: synthesis and Cope rearrangement of thermolabile bis-alkenylcyclopropanes from female gametes of marine brown algae (Phaeophyceae). *Tetrahedron*, 53(40), 13681-13694.
326. Pohnert, G. (2002). Phospholipase A2 activity triggers the wound-activated chemical defense in the diatom *Thalassiosira rotula*. *Plant physiology*, 129, 103-111. doi: 10.1104/pp.010974
327. Pohnert, G., and Boland, W. (2002). The oxylipin chemistry of attraction and defense in brown algae and diatoms. *Natural Product Reports*, 19(1), 108-122.
328. Pohnert, G. (2004). Chemical defense strategies of marine organisms. In *The Chemistry of Pheromones and Other Semiochemicals I* (pp. 179-219). Springer, Berlin, Heidelberg.
329. Poirier, I., Pallud, M., Kuhn, L., Hammann, P., Demortiere, A., Jamali, A., ... and Bertrand, M. (2018). Toxicological effects of CdSe nanocrystals on the marine diatom *Phaeodactylum tricorutum*: The first mass spectrometry-based proteomic approach. *Ecotoxicology and Environmental Safety*, 152, 78-90.

330. Pokrzywinski, K. L., Tilney, C. L., Warner, M. E., and Coyne, K. J. (2017). Cell cycle arrest and biochemical changes accompanying cell death in harmful dinoflagellates following exposure to bacterial algicide IRI-160AA. *Scientific reports*, 7, 45102.
331. Poulin, R. X., and Pohnert, G. (2018a). Simplifying the complex: metabolomics approaches in chemical ecology. *Analytical and Bioanalytical Chemistry*, 1-7.
332. Poulin, R. X., Poulson-Ellestad, K. L., Roy, J. S., and Kubanek, J. (2018b). Variable allelopathy among phytoplankton reflected in red tide metabolome. *Harmful Algae*, 71, 50-56.
333. Poulin, R. X., Hogan, S., Poulson-Ellestad, K. L., Brown, E., Fernández, F. M., and Kubanek, J. (2018c). *Karenia brevis* allelopathy compromises the lipidome, membrane integrity, and photosynthesis of competitors. *Scientific Reports*, 8(1), 9572.
334. Poulson-Ellestad, K. L., Harvey, E. L., Johnson, M. D., and Mincer, T. J. (2016). Evidence for strain-specific exometabolomic responses of the coccolithophore *Emiliania huxleyi* to grazing by the dinoflagellate *Oxyrrhis marina*. *Frontiers in Marine Science*, 3, 1.
335. Pregitzer, P., Schubert, M., Breer, H., Hansson, B. S., Sachse, S., and Krieger, J. (2012). Plant odorants interfere with detection of sex pheromone signals by male *Heliothis virescens*. *Frontiers in Cellular Neuroscience*, 6, 42.
336. Prince, E. K., Poulson, K. L., Myers, T. L., Sieg, R. D., and Kubanek, J. (2010). Characterization of allelopathic compounds from the red tide dinoflagellate *Karenia brevis*. *Harmful Algae*, 10(1), 39-48.
337. Quijano, C., Trujillo, M., Castro, L., and Trostchansky, A. (2016). Interplay between oxidant species and energy metabolism. *Redox Biology*, 8, 28-42.
338. Quiza, L., St-Arnaud, M., and Yergeau, E. (2015). Harnessing phytomicrobiome signaling for rhizosphere microbiome engineering. *Frontiers in Plant Science*, 6, 507.
339. R Development Core Team (2008). R: A language and environment for statistical computing. R Foundation for Statistical Computing, Vienna, Austria.
340. Raina, J. B., Clode, P. L., Cheong, S., Bougoure, J., Kilburn, M. R., Reeder, A., ... and Tapiolas, D. (2017). Subcellular tracking reveals the location of dimethylsulfoniopropionate in microalgae and visualises its uptake by marine bacteria. *Elife*, 6, e23008.

341. Ramanan, R., Kim, B. H., Cho, D. H., Oh, H. M., and Kim, H. S. (2016). Algae–bacteria interactions: evolution, ecology and emerging applications. *Biotechnology advances*, 34(1), 14-29.
342. Rampen, S. W., Abbas, B. A., Schouten, S., & Sinninghe Damste, J. S. (2010). A comprehensive study of sterols in marine diatoms (Bacillariophyta): Implications for their use as tracers for diatom productivity. *Limnology and Oceanography*, 55(1), 91–105.
343. Rasband, W. (1994-2018). ImageJ, US National Institutes of Health, Bethesda, MD, USA. Available from: <http://imagej.nih.gov/ij/>
344. Rasher, D. B., Stout, E. P., Engel, S., Kubanek, J., and Hay, M. E. (2011). Macroalgal terpenes function as allelopathic agents against reef corals. *Proceedings of the National Academy of Sciences*, 201108628.
345. Raven, J. A., and Beardall, J. (2003). Carbohydrate metabolism and respiration in algae. In *Photosynthesis in algae* (pp. 205-224). Springer, Dordrecht.
346. Ray, J. L., Althammer, J., Skaar, K. S., Simonelli, P., Larsen, A., Stoecker, D., ... and Frischer, M. (2016). Metabarcoding and metabolome analyses of copepod grazing reveal feeding preference and linkage to metabolite classes in dynamic microbial plankton communities. *Molecular Ecology*, 25(21), 5585-5602.
347. Reboloso-Fuentes, M. M., Navarro-Pérez, A., García-Camacho, F., Ramos-Miras, J. J., & Guil-Guerrero, J. L. (2001). Biomass nutrient profiles of the microalga *Nannochloropsis*. *Journal of Agricultural and Food Chemistry*, 49(6), 2966–72.
348. Remmers, I. M., D'Adamo, S., Martens, D. E., de Vos, R. C., Mumm, R., America, A. H., ... and Lamers, P. P. (2018). Orchestration of transcriptome, proteome and metabolome in the diatom *Phaeodactylum tricornutum* during nitrogen limitation. *Algal Research*, 35, 33-49.
349. Rempt, M., Weinberger, F., Grosser, K., and Pohnert, G. (2012). Conserved and species-specific oxylipin pathways in the wound-activated chemical defense of the noninvasive red alga *Gracilaria chilensis* and the invasive *Gracilaria vermiculophylla*. *Beilstein Journal of Organic Chemistry*, 8, 283.
350. Rettner, J., Werner, M., Meyer, N., Werz, O., and Pohnert, G. (2018). Survey of the C20 and C22 oxylipin family in marine diatoms. *Tetrahedron Letters*, 59(9), 828-831.
351. Revel, M., Chatel, A., & Mouneyrac, C. (2017). Omics tools: New challenges in aquatic nanotoxicology?. *Aquatic Toxicology*, 193, 72-85.

352. Rickert, E., Karsten, U., Pohnert, G., and Wahl, M. (2015). Seasonal fluctuations in chemical defenses against macrofouling in *Fucus vesiculosus* and *Fucus serratus* from the Baltic Sea. *Biofouling*, 31(4), 363-377.
353. Riemann, L., Steward, G. F., and Azam, F. (2000). Dynamics of bacterial community composition and activity during a mesocosm diatom bloom. *Applied and Environmental Microbiology*, 66(2), 578-587.
354. Ritchie, M. E., Phipson, B., Wu, D., Hu, Y., Law, C. W., Shi, W., & Smyth, G. K. (2015). limma powers differential expression analyses for RNA-sequencing and microarray studies. *Nucleic acids research*, 43, e47-e47.
355. Rizwan, M., Mujtaba, G., Memon, S. A., Lee, K., and Rashid, N. (2018). Exploring the potential of microalgae for new biotechnology applications and beyond: a review. *Renewable and Sustainable Energy Reviews*, 92, 394-404.
356. Robinson, M. D., McCarthy, D. J., & Smyth, G. K. (2010). edgeR: a Bioconductor package for differential expression analysis of digital gene expression data. *Bioinformatics*, 26(1), 139-140.
357. Robinson, M. D., and Oshlack, A. (2010). A scaling normalization method for differential expression analysis of RNA-seq data. *Genome Biology*, 11(3), R25.
358. Romanenko, L. A., Tanaka, N., Svetashev, V. I., & Kalinovskaya, N. I. (2012). *Poseidonocella pacifica* gen. nov., sp. nov. and *Poseidonocella sedimentorum* sp. nov., novel alphaproteobacteria from the shallow sandy sediments of the Sea of Japan. *Archives of Microbiology*, 194(2), 113–121.
359. Roostaei, J., Zhang, Y., Gopalakrishnan, K., & Ochocki, A. J. (2018). Mixotrophic Microalgae Biofilm: A Novel Algae Cultivation Strategy for Improved Productivity and Cost-efficiency of Biofuel Feedstock Production. *Scientific Reports*, 8(1), 12528.
360. Rosa, G. J., de Leon, N., and Rosa, A. (2017). A review of microarray experimental design strategies for genetical genomics studies. *Physiological Genomics*.
361. Rosenwasser, S., Mausz, M. A., Schatz, D., Sheyn, U., Malitsky, S., Aharoni, A., ... and Pohnert, G. (2014). Rewiring host lipid metabolism by large viruses determines the fate of *Emiliana huxleyi*, a bloom-forming alga in the ocean. *The Plant Cell*, tpc-114.
362. Round, F.E., Mann, D. G., Crawford, R. M. (1990). *The Diatoms: Biology and Morphology of the Genera*. Cambridge Univ. Press.

363. Saha, M., Rempt, M., Grosser, K., Pohnert, G., and Weinberger, F. (2011). Surface-associated fucoxanthin mediates settlement of bacterial epiphytes on the rockweed *Fucus vesiculosus*. *Biofouling*, 27(4), 423-433.
364. Saha, M., Rempt, M., Gebser, B., Grueneberg, J., Pohnert, G., and Weinberger, F. (2012). Dimethylsulphopropionate (DMSP) and proline from the surface of the brown alga *Fucus vesiculosus* inhibit bacterial attachment. *Biofouling*, 28(6), 593-604.
365. Sandberg, R. (2014). Entering the era of single-cell transcriptomics in biology and medicine. *Nature Methods*, 11(1), 22.
366. Santucci, A., Bernardini, G., Braconi, D., Petricci, E., and Manetti, F. (2017). 4-hydroxyphenylpyruvate dioxygenase and its inhibition in plants and animals: small molecules as herbicides and agents for the treatment of human inherited diseases. *Journal of Medicinal Chemistry*, 60(10), 4101-4125.
367. Sapp, M., Schwaderer, A. S., Wiltshire, K. H., Hoppe, H. G., Gerdt, G., and Wichels, A. (2007). Species-specific bacterial communities in the phycosphere of microalgae?. *Microbial Ecology*, 53(4), 683-699.
368. Sapriel, G., Quinet, M., Heijde, M., Jourdain, L., Tanty, V., Luo, G., ... and Lopez, P. J. (2009). Genome-wide transcriptome analyses of silicon metabolism in *Phaeodactylum tricornerutum* reveal the multilevel regulation of silicic acid transporters. *PloS One*, 4(10), e7458.
369. Satheesh, S., Ba-akdah, M. A., and Al-Sofyani, A. A. (2016). Natural antifouling compound production by microbes associated with marine macroorganisms: A review. *Electronic Journal of Biotechnology*, 19(3), 26-35.
370. Sato, S., Beakes, G., Idei, M., Nagumo, T., and Mann, D. G. (2011). Novel sex cells and evidence for sex pheromones in diatoms. *PloS One*, 6(10), e26923.
371. Scalco, E., Stec, K., Iudicone, D., Ferrante, M. I. and Montresor, M. (2014). The dynamics of sexual phase in the marine diatom *Pseudo-nitzschia multistriata* (Bacillariophyceae). *Journal of Phycology*, 50, 817-828.
372. Scalco, E., Amato, A., Ferrante, M. I., and Montresor, M. (2016). The sexual phase of the diatom *Pseudo-nitzschia multistriata*: cytological and time-lapse cinematography characterization. *Protoplasma*, 253(6), 1421-1431.
373. Schatz, D., Rosenwasser, S., Malitsky, S., Wolf, S. G., Feldmesser, E., and Vardi, A. (2017). Communication via extracellular vesicles enhances viral infection of a cosmopolitan alga. *Nature Microbiology*, 2(11), 1485.

374. Schatz, D., & Vardi, A. (2018). Extracellular vesicles—new players in cell–cell communication in aquatic environments. *Current Opinion in Microbiology*, *43*, 148-154.
375. Schellenberger Costa, B., Jungandreas, A., Jakob, T., Weisheit, W., Mittag, M., and Wilhelm, C. (2012). Blue light is essential for high light acclimation and photoprotection in the diatom *Phaeodactylum tricornutum*. *Journal of Experimental Botany*, *64*(2), 483-493.
376. Schmid, M., and Stengel, D. B. (2015). Intra-thallus differentiation of fatty acid and pigment profiles in some temperate Fucales and Laminariales. *Journal of Phycology*, *51*(1), 25-36.
377. Schnurr, P. J., and Allen, D. G. (2015). Factors affecting algae biofilm growth and lipid production: a review. *Renewable and Sustainable Energy Reviews*, *52*, 418-429.
378. Schubert, O. T., Röst, H. L., Collins, B. C., Rosenberger, G., and Aebersold, R. (2017). Quantitative proteomics: challenges and opportunities in basic and applied research. *Nature Protocols*, *12*(7), 1289.
379. Schultz, M. P., Bendick, J. A., Holm, E. R., & Hertel, W. M. (2010). Economic impact of biofouling on a naval surface ship. *Biofouling*, *27*.
380. Schulz, S., Kubanek, J., and Piel, J. (2015). Chemical Ecology. *Natural Product Reports*, *32*(7), 886-887.
381. Schwartz, N., Rohde, S., Dobretsov, S., Hiromori, S., and Schupp, P. J. (2017). The role of chemical antifouling defence in the invasion success of *Sargassum muticum*: A comparison of native and invasive brown algae. *PloS One*, *12*(12), e0189761.
382. Scognamiglio, M., D'Abrosca, B., Esposito, A., and Fiorentino, A. (2015). Metabolomics: an unexplored tool for allelopathy studies. *Journal of Allelochemical Interactions*, *1*, 9-23.
383. Segev, E., Wyche, T. P., Kim, K. H., Petersen, J., Ellebrandt, C., Vlamakis, H., ... and Kolter, R. (2016). Dynamic metabolic exchange governs a marine algal-bacterial interaction. *Elife*, *5*, e17473.
384. Sekimoto, H. (2017). Sexual reproduction and sex determination in green algae. *Journal of Plant Research*, *130*(3), 423-431.
385. Seyedsayamdost, M. R., Case, R. J., Kolter, R., and Clardy, J. (2011). The Jekyll-and-Hyde chemistry of *Phaeobacter gallaeciensis*. *Nature Chemistry*, *3*(4), 331.

386. Seymour, J. R., Ahmed, T., and Stocker, R. (2009). Bacterial chemotaxis towards the extracellular products of the toxic phytoplankton *Heterosigma akashiwo*. *Journal of Plankton Research*, 31(12), 1557-1561.
387. Seymour, J. R., Simó, R., Ahmed, T., and Stocker, R. (2010). Chemoattraction to dimethylsulfoniopropionate throughout the marine microbial food web. *Science*, 329(5989), 342-345.
388. Seymour, J. R., Amin, S. A., Raina, J. B., and Stocker, R. (2017). Zooming in on the phycosphere: the ecological interface for phytoplankton–bacteria relationships. *Nature Microbiology*, 2(7), 17065.
389. Seymour, J. R., and Raina, J. B. (2018). Swimming in the sea: chemotaxis by marine bacteria. *Microbiology Australia*.
390. Shapiro, E., Biezuner, T., and Linnarsson, S. (2013). Single-cell sequencing-based technologies will revolutionize whole-organism science. *Nature Reviews Genetics*, 14(9), 618.
391. Sheehan, D., Meade, G., and Foley, V. M. (2001). Structure, function and evolution of glutathione transferases: implications for classification of non-mammalian members of an ancient enzyme superfamily. *Biochemical Journal*, 360(1), 1-16.
392. Shi, L., and Tu, B. P. (2015). Acetyl-CoA and the regulation of metabolism: mechanisms and consequences. *Current Opinion in Cell Biology*, 33, 125-131.
393. Shrestha, R. P., Tesson, B., Norden-Krichmar, T., Federowicz, S., Hildebrand, M., and Allen, A. E. (2012). Whole transcriptome analysis of the silicon response of the diatom *Thalassiosira pseudonana*. *BMC Genomics*, 13(1), 499.
394. Sies, H., Berndt, C., and Jones, D. P. (2017). Oxidative stress. *Annual Review of Biochemistry*, 86, 715-748.
395. Singh, R. P., and Reddy, C. R. K. (2016). Unraveling the functions of the macroalgal microbiome. *Frontiers in Microbiology*, 6, 1488.
396. Sison-Mangus, M. P., Jiang, S., Tran, K. N., and Kudela, R. M. (2014). Host-specific adaptation governs the interaction of the marine diatom, *Pseudo-nitzschia* and their microbiota. *The ISME Journal*, 8(1), 63.
397. Smith, D. J., & Underwood, G. J. C. (1998). Exopolymer production by intertidal epipelagic diatoms. *Limnology and Oceanography*, 43(7), 1578–1591.
398. Smith, S. R., Gle, C., Abbriano, R. M., Traller, J. C., Davis, A., Trentacoste, E., . . . Hildebrand, M. (2016). Transcript level coordination of carbon pathways during

- silicon starvation-induced lipid accumulation in the diatom *Thalassiosira pseudonana*. *New Phytologist*, 210.
399. Smriga, S., Fernandez, V. I., Mitchell, J. G., and Stocker, R. (2016). Chemotaxis toward phytoplankton drives organic matter partitioning among marine bacteria. *Proceedings of the National Academy of Sciences*, 113(6), 1576-1581.
400. Sommer, U. (Ed.). (2012). *Plankton ecology: succession in plankton communities*. Springer Science and Business Media.
401. Soneson, C., Love, M. I., and Robinson, M. D. (2015). Differential analyses for RNA-seq: transcript-level estimates improve gene-level inferences. *F1000Research*, 4.
402. Sonnenschein, E. C., Syit, D. A., Grossart, H. P., and Ullrich, M. S. (2012). Chemotaxis of *Marinobacter adhaerens* and its impact on attachment to the diatom *Thalassiosira weissflogii*. *Applied and Environmental Microbiology*, 78(19), 6900-6907.
403. Sorensen, P. W., and Wisenden, B. D. (Eds.). (2015). *Fish pheromones and related cues*. John Wiley and Sons.
404. Stahl, A., and Ullrich, M. S. (2016). Proteomics analysis of the response of the marine bacterium *Marinobacter adhaerens* HP15 to the diatom *Thalassiosira weissflogii*. *Aquatic Microbial Ecology*, 78(2), 65-79.
405. Stal, L. J., and De Brouwer, J. F. C. (2003). Biofilm formation by benthic diatoms and their influence on the stabilization of intertidal mudflats. *Berichte-Forschungszentrum Terramare*, 12, 109-111.
406. Starling, E. H. (1905). The Croonian Lectures. *Lancet*, 26, 579-583.
407. Stock, W., Pinseel, E., Decker, S., Seftom, J., Blommaert, L., Chepurnova, O., ... and Vyverman, W. (2018). Expanding the toolbox for cryopreservation of marine and freshwater diatoms. *Scientific Reports*, 8(1), 4279.
408. Stocker, R. (2012). Marine microbes see a sea of gradients. *Science*, 338(6107), 628-633.
409. Su, Y., Wang, J., Shi, M., Niu, X., Yu, X., Gao, L., ... and Zhang, W. (2014). Metabolomic and network analysis of astaxanthin-producing *Haematococcus pluvialis* under various stress conditions. *Bioresource Technology*, 170, 522-529.
410. Suleiman, M., Zecher, K., Yücel, O., Jagmann, N., and Philipp, B. (2016). Interkingdom cross-feeding of ammonium from marine methylamine-degrading

- bacteria to the diatom *Phaeodactylum tricornutum*. *Applied and Environmental Microbiology*, AEM-01642.
411. Sumner, L. W., Amberg, A., Barrett, D., Beale, M. H., Beger, R., Daykin, C. A., ... and Hankemeier, T. (2007). Proposed minimum reporting standards for chemical analysis. *Metabolomics*, 3(3), 211-221.
412. Sumper, M., and Kröger, N. (2004). Silica formation in diatoms: the function of long-chain polyamines and silaffins. *Journal of Materials Chemistry*, 14(14), 2059-2065.
413. Sun, M., Yang, Z., and Wawrik, B. (2018). Metabolomic fingerprints of individual algal cells using the single-probe mass spectrometry technique. *Frontiers in plant science*, 9.
414. Supek, F., Bošnjak, M., Škunca, N., and Šmuc, T. (2011). REVIGO summarizes and visualizes long lists of gene ontology terms. *PloS One*, 6(7), e21800.
415. Sysi-Aho, M., Katajamaa, M., Yetukuri, L., and Orešič, M. (2007). Normalization method for metabolomics data using optimal selection of multiple internal standards. *BMC Bioinformatics*, 8(1), 93.
416. Szabados, L., & Savouré, A. (2010). Proline: a multifunctional amino acid. *Trends in Plant Science*, 15(2), 89–97.
417. Tabor, C. W., & Tabor, H. (1976). 1,4-Diaminobutane (Putrescine), Spermidine, and Spermine. *Annual Review of Biochemistry*, 45(1), 285–306.
418. Tada, Y., Nakaya, R., Goto, S., Yamashita, Y., and Suzuki, K. (2017). Distinct bacterial community and diversity shifts after phytoplankton-derived dissolved organic matter addition in a coastal environment. *Journal of Experimental Marine Biology and Ecology*, 495, 119-128.
419. Tamura, S., Suzuki, A., Aoki, Y., and Otake, N. (1964). Isolation of several diketopiperazines from peptone. *Agricultural and Biological Chemistry*, 28(9), 650-652.
420. Tanaka, T., Maeda, Y., Veluchamy, A., Tanaka, M., Abida, H., Maréchal, E., ... and Yoshino, T. (2015). Oil accumulation by the oleaginous diatom *Fistulifera solaris* as revealed by the genome and transcriptome. *The Plant Cell*, tpc-114.
421. Tang, X., He, L. Y., Tao, X. Q., Dang, Z., Guo, C. L., Lu, G. N., and Yi, X. Y. (2010). Construction of an artificial microalgal-bacterial consortium that efficiently degrades crude oil. *Journal of Hazardous Materials*, 181(1-3), 1158-1162.

422. Teeling, H., Fuchs, B. M., Becher, D., Klockow, C., Gardebrecht, A., Bennke, C. M., ... Amann, R. (2012). Substrate-Controlled Succession of Marine Bacterioplankton Populations Induced by a Phytoplankton Bloom. *Science*, 336(6081), 608–611.
423. Teeling, H., Fuchs, B. M., Bennke, C. M., Krueger, K., Chafee, M., Kappelmann, L., ... and Lucas, J. (2016). Recurring patterns in bacterioplankton dynamics during coastal spring algae blooms. *Elife*, 5, e11888.
424. Teplitski, M., Chen, H., Rajamani, S., Gao, M., Merighi, M., Sayre, R. T., ... and Bauer, W. D. (2004). *Chlamydomonas reinhardtii* secretes compounds that mimic bacterial signals and interfere with quorum sensing regulation in bacteria. *Plant Physiology*, 134(1), 137-146.
425. Thume, K., Gebser, B., Chen, L., Meyer, N., Kieber, D. J., and Pohnert, G. (2018). The metabolite dimethylsulfoxonium propionate extends the marine organosulfur cycle. *Nature*, 563(7731), 412.
426. Tian, C.F., Garnerone, A.M., Mathieu-Demazière, C., Masson-Boivin, C., Batut, J. (2012). Plant-activated bacterial receptor adenylate cyclases modulate epidermal infection in the *Sinorhizobium meliloti*–*Medicago symbiosis*. *Proceedings of the National Academy of Sciences*, 201120260.
427. Titelman, J., Varpe, Ø., Eliassen, S., and Fiksen, Ø. (2007). Copepod mating: chance or choice?. *Journal of Plankton Research*, 29(12), 1023-1030.
428. Hothorn, T., Bretz, F., & Westfall, P. (2008). Simultaneous inference in general parametric models. *Biometrical journal*, 50(3), 346-363.
429. Toseland, A. D. S. J., Daines, S. J., Clark, J. R., Kirkham, A., Strauss, J., Uhlig, C., ... and Mock, T. (2013). The impact of temperature on marine phytoplankton resource allocation and metabolism. *Nature Climate Change*, 3(11), 979.
430. Toyama, T., Kasuya, M., Hanaoka, T., Kobayashi, N., Tanaka, Y., Inoue, D., ... and Mori, K. (2018). Growth promotion of three microalgae, *Chlamydomonas reinhardtii*, *Chlorella vulgaris* and *Euglena gracilis*, by in situ indigenous bacteria in wastewater effluent. *Biotechnology for Biofuels*, 11(1), 176.
431. Tréguer, P. J., and De La Rocha, C. L. (2013). The world ocean silica cycle. *Annual Review of Marine Science*, 5, 477-501.
432. Trezzini, G. F., Horrichs, A., and Somssich, I. E. (1993). Isolation of putative defense-related genes from *Arabidopsis thaliana* and expression in fungal elicitor-treated cells. *Plant Molecular Biology*, 21(2), 385-389.

433. Tsuchikane, Y., Fukumoto, R. H., Akatsuka, S., Fujii, T., and Sekimoto, H. (2003). Sex pheromones that induce sexual cell division in the *Closterium peracerosum–strigosum–littorale* complex (charophyta) 1. *Journal of Phycology*, 39(2), 303-309.
434. Tsuchikane, Y., Fujii, T., Ito, M., and Sekimoto, H. (2005). A sex pheromone, protoplast release-inducing protein (PR-IP) inducer, induces sexual cell division and production of PR-IP in *Closterium*. *Plant and Cell Physiology*, 46(9), 1472-1476.
435. Tzin, V., and Galili, G. (2010). The biosynthetic pathways for shikimate and aromatic amino acids in *Arabidopsis thaliana*. *The Arabidopsis book/American Society of Plant Biologists*, 8.
436. Unfried, F., Becker, S., Robb, C. S., Hehemann, J. H., Markert, S., Heiden, S. E., ... & Avcı, B. (2018). Adaptive mechanisms that provide competitive advantages to marine bacteroidetes during microalgal blooms. *The ISME journal*, 12(12), 2894.
437. Urano, K., Kurihara, Y., Seki, M., and Shinozaki, K. (2010). ‘Omics’ analyses of regulatory networks in plant abiotic stress responses. *Current Opinion in Plant Biology*, 13(2), 132-138.
438. Van Colen, C., Underwood, G. J., Serôdio, J., & Paterson, D. M. (2014). Ecology of intertidal microbial biofilms: mechanisms, patterns and future research needs. *Journal of Sea Research*, 92, 2-5.
439. Van der Meij, A., Worsley, S. F., Hutchings, M. I., and van Wezel, G. P. (2017). Chemical ecology of antibiotic production by actinomycetes. *FEMS Microbiology Reviews*, 41(3), 392-416.
440. Vandepoele, K., Van Bel, M., Richard, G., Van Landeghem, S., Verhelst, B., Moreau, H., ... and Piganeau, G. (2013). pico-PLAZA, a genome database of microbial photosynthetic eukaryotes. *Environmental Microbiology*, 15(8), 2147-2153.
441. Van Hummel, H. C. (1975). Chemistry and biosynthesis of plant galactolipids. In *Fortschritte der Chemie Organischer Naturstoffe/Progress in the Chemistry of Organic Natural Products* (pp. 267-295). Springer, Vienna.
442. van Tol, H. M., Amin, S. A., and Armbrust, E. V. (2017). Ubiquitous marine bacterium inhibits diatom cell division. *The ISME Journal*, 11(1), 31.
443. Vanni, M. J., and Findlay, D. L. (1990). Trophic cascades and phytoplankton community structure. *Ecology*, 71(3), 921-937.

444. Vanstechelman, I., Sabbe, K., Vyverman, W., Vanormelingen, P., and Vuylsteke, M. (2013). Linkage mapping identifies the sex determining region as a single locus in the pennate diatom *Seminavis robusta*. *PLoS One*, 8(3), e60132.
445. Venuleo, M., Raven, J. A., & Giordano, M. (2017). Intraspecific chemical communication in microalgae. *New Phytologist*, 215(2), 516-530.
446. Verheggen, F. J., Haubruge, E., and Mescher, M. C. (2010). Alarm pheromones—chemical signaling in response to danger. In *Vitamins and Hormones* (Vol. 83, pp. 215-239). Academic Press.
447. Vidoudez, C., and Pohnert, G. (2012). Comparative metabolomics of the diatom *Skeletonema marinoi* in different growth phases. *Metabolomics*, 8(4), 654-669.
448. Vinaixa, M., Schymanski, E. L., Neumann, S., Navarro, M., Salek, R. M., and Yanes, O. (2016). Mass spectral databases for LC/MS-and GC/MS-based metabolomics: state of the field and future prospects. *TrAC Trends in Analytical Chemistry*, 78, 23-35.
449. Von Dassow, P., Ogata, H., Probert, I., Wincker, P., Da Silva, C., Audic, S., ... and de Vargas, C. (2009). Transcriptome analysis of functional differentiation between haploid and diploid cells of *Emiliana huxleyi*, a globally significant photosynthetic calcifying cell. *Genome Biology*, 10(10), R114.
450. Wahl, M. (2009). Epibiosis. In *Marine hard bottom communities* (pp. 61-72). Springer, Berlin, Heidelberg.
451. Wang, Z., Gerstein, M., and Snyder, M. (2009). RNA-Seq: a revolutionary tool for transcriptomics. *Nature Reviews Genetics*, 10(1), 57.
452. Wang, J., Cao, S., Du, C., and Chen, D. (2013). Underwater locomotion strategy by a benthic pennate diatom *Navicula* sp. *Protoplasma*, 250(5), 1203-1212.
453. Wang, H., Tomasch, J., Jarek, M., and Wagner-Döbler, I. (2014). A dual-species co-cultivation system to study the interactions between Roseobacters and dinoflagellates. *Frontiers in Microbiology*, 5, 311.
454. Wang, H., Butt, L., Rooks, P., Khan, F., Allen, M. J., and Ali, S. T. (2016a). Characterisation of algicidal bacterial exometabolites against the lipid-accumulating diatom *Skeletonema* sp. *Algal Research*, 13, 1-6.
455. Wang, H., Hill, R. T., Zheng, T., Hu, X., and Wang, B. (2016b). Effects of bacterial communities on biofuel-producing microalgae: stimulation, inhibition and harvesting. *Critical Reviews in Biotechnology*, 36(2), 341-352.

456. Wasternack, C. (2007). Jasmonates: an update on biosynthesis, signal transduction and action in plant stress response, growth and development. *Annals of botany*, 100, 681-697.
457. Watanabe, M., Maemura, K., Kanbara, K., Tamayama, T., & Hayasaki, H. (2002). GABA and GABA receptors in the central nervous system and other organs. *International Review of Cytology*, 213, 1–47.
458. Weber, H. (2002). Fatty acid-derived signals in plants. *Trends in plant science*, 7(5), 217-224.
459. Wehrens, R., Weingart, G., & Mattivi, F. (2014). metaMS: An open-source pipeline for GC–MS-based untargeted metabolomics. *Journal of Chromatography B*, 966, 109–116.
460. Weinberger, F., Leonardi, P., Miravalles, A., Correa, J. A., Lion, U., Kloareg, B., and Potin, P. (2005). Dissection of two distinct defense-related responses to agar oligosaccharides in *Gracilaria chilensis* (Rhodophyta) and *Gracilaria conferta* (Rhodophyta). *Journal of Phycology*, 41(4), 863-873.
461. Weiss, A., Costa, R., and Wichard, T. (2017). Morphogenesis of *Ulva mutabilis* (Chlorophyta) induced by *Maribacter* species (Bacteroidetes, Flavobacteriaceae). *Botanica Marina*, 60(2), 197-206.
462. Weissflog, J., Adolph, S., Wiesemeier, T., and Pohnert, G. (2008). Reduction of herbivory through wound-activated protein cross-linking by the invasive macroalga *Caulerpa taxifolia*. *ChemBioChem*, 9(1), 29-32.
463. Wertheim, B., van Baalen, E. J. A., Dicke, M., and Vet, L. E. (2005). Pheromone-mediated aggregation in nonsocial arthropods: an evolutionary ecological perspective. *Annual Reviews Entomology*, 50, 321-346.
464. Westerhoff, H. V., and Palsson, B. O. (2004). The evolution of molecular biology into systems biology. *Nature biotechnology*, 22(10), 1249.
465. Wienhausen, G., Noriega-Ortega, B. E., Niggemann, J., Dittmar, T., and Simon, M. (2017). The exometabolome of two model strains of the Roseobacter group: a marketplace of microbial metabolites. *Frontiers in Microbiology*, 8, 1985.
466. Williams, P. (2007). Quorum sensing, communication and cross-kingdom signalling in the bacterial world. *Microbiology*, 153(12), 3923–3938.
467. Winck, F. V., Melo, D. O. P., and Barrios, A. F. G. (2013). Carbon acquisition and accumulation in microalgae *Chlamydomonas*: Insights from “omics” approaches. *Journal of Proteomics*, 94, 207-218.

468. Winger, J. A., Derbyshire, E. R., Lamers, M. H., Marletta, M. A., and Kuriyan, J. (2008). The crystal structure of the catalytic domain of a eukaryotic guanylate cyclase. *BMC structural biology*, 8(1), 42.
469. Winkler, H. (1920). Verbreitung und ursache der parthenogenesis im pflanzen-und tierreiche. Fisher Verlag, Jena.
470. Windler, M., Leinweber, K., Bartulos, C. R., Philipp, B., and Kroth, P. G. (2015). Biofilm and capsule formation of the diatom *Achnantheidium minutissimum* are affected by a bacterium. *Journal of Phycology*, 51(2), 343-355.
471. Wishkerman, A., and Arad, S. (2017). Production of silver nanoparticles by the diatom *Phaeodactylum tricornutum*. In *Nanotechnology VIII* (Vol. 10248, p. 102480W). International Society for Optics and Photonics.
472. Woodley, S. K. (2010). Pheromonal communication in amphibians. *Journal of Comparative Physiology A*, 196(10), 713-727.
473. Worden, A. Z., Follows, M. J., Giovannoni, S. J., Wilken, S., Zimmerman, A. E., & Keeling, P. J. (2015). Rethinking the marine carbon cycle: Factoring in the multifarious lifestyles of microbes. *Science*, 347(6223), 1257594–1257594.
474. Wördenweber, R., Rokitta, S. D., Heidenreich, E., Corona, K., Kirschhöfer, F., Fahl, K., ... and Mussnug, J. H. (2018). Phosphorus and nitrogen starvation reveal life-cycle specific responses in the metabolome of *Emiliana huxleyi* (Haptophyta). *Limnology and Oceanography*, 63(1), 203-226.
475. Wu, D., Smyth, G.K. (2012) Camera: a competitive gene set test accounting for inter-gene correlation. *Nucleic Acids Research*, 40(17):e133.
476. Xiao, R., & Zheng, Y. (2016). Overview of microalgal extracellular polymeric substances (EPS) and their applications. *Biotechnology Advances*, 34(7), 1225–1244.
477. Xing, G., Yuan, H., Yang, J., Li, J., Gao, Q., Li, W., and Wang, E. (2018). Integrated analyses of transcriptome, proteome and fatty acid profilings of the oleaginous microalga *Auxenochlorella protothecoides* UTEX 2341 reveal differential reprogramming of fatty acid metabolism in response to low and high temperatures. *Algal Research*, 33, 16-27.
478. Yaakob, Z., Ali, E., Zainal, A., Mohamad, M., & Takriff, M. S. (2014). An overview: biomolecules from microalgae for animal feed and aquaculture. *Journal of Biological Research-Thessaloniki*, 21(1), 6.
479. Yadav, S. P. (2007). The wholeness in suffix-omics, -omes, and the word om. *Journal of Biomolecular Techniques: JBT*, 18(5), 277.

480. Yang, C., Fang, S., Chen, D., Wang, J., Liu, F., and Xia, C. (2016). The possible role of bacterial signal molecules N-acyl homoserine lactones in the formation of diatom-biofilm (*Cylindrotheca* sp.). *Marine Pollution Bulletin*, 107(1), 118-124.
481. Yao, S., Lyu, S., An, Y., Lu, J., Gjermansen, C., & Schramm, A. (2019). Microalgae–bacteria symbiosis in microalgal growth and biofuel production: a review. *Journal of Applied Microbiology*, 126(2), 359-368.
482. Ye, Y., Huang, Y., Xia, A., Fu, Q., Liao, Q., Zeng, W., ... Zhu, X. (2018). Optimizing culture conditions for heterotrophic-assisted photoautotrophic biofilm growth of *Chlorella vulgaris* to simultaneously improve microalgae biomass and lipid productivity. *Bioresource Technology*, 270, 80–87.
483. Yee, M. S.-L., Khiew, P.-S., Chiu, W. S., Tan, Y. F., Kok, Y.-Y., & Leong, C.-O. (2016). Green synthesis of graphene-silver nanocomposites and its application as a potent marine antifouling agent. *Colloids and Surfaces B: Biointerfaces*, 148, 392–401.
484. Yew, J. Y., and Chung, H. (2015). Insect pheromones: An overview of function, form, and discovery. *Progress in Lipid Research*, 59, 88-105.
485. Yi, L., Dong, N., Yun, Y., Deng, B., Ren, D., Liu, S., and Liang, Y. (2016). Chemometric methods in data processing of mass spectrometry-based metabolomics: A review. *Analytica Chimica Acta*, 914, 17-34.
486. Zebelo, S. A., and Maffei, M. E. (2014). Role of early signaling events in plant–insect interactions. *Journal of Experimental Botany*, 66(2), 435-448.
487. Zenobi, R. (2013). Single-cell metabolomics: analytical and biological perspectives. *Science*, 342(6163), 1243259.
488. Zerriouh, O., Reinoso-Moreno, J. V., López-Rosales, L., Cerón-García, M. D. C., Sánchez-Mirón, A., García-Camacho, F., & Molina-Grima, E. (2017). Biofouling in photobioreactors for marine microalgae. *Critical reviews in biotechnology*, 37(8), 1006-1023.
489. Ziegler, T. A., and Forward, R. B. (2007). Larval release behaviors in the Caribbean spiny lobster, *Panulirus argus*: Role of peptide pheromones. *Journal of Chemical Ecology*, 33(9), 1795-1805.
- 490.

Appendix

Supporting informations chapter 3 – Co-cultivation of microalgae with isolated bacteria – a metabolomic approach

Supporting informations chapter 4 – Bacterial modulation of sexual efficiency of the diatom *Seminavis robusta*

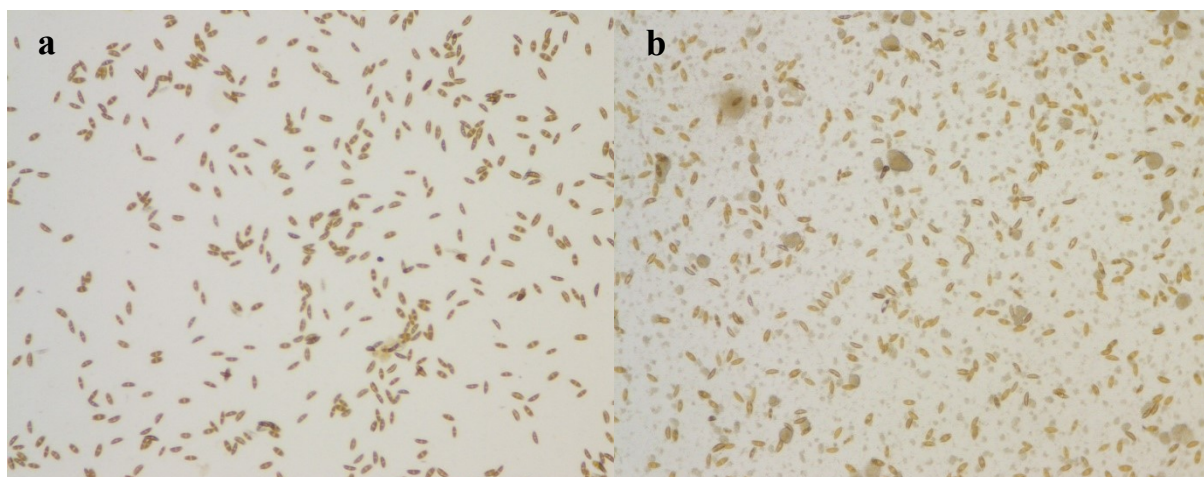


Figure S1. a) Axenic culture b) non-axenic culture of *S. robusta* 5 days after inoculation. Formation of biofilms and bacterial aggregates is absent in axenic cultures compared to non-axenic ones.

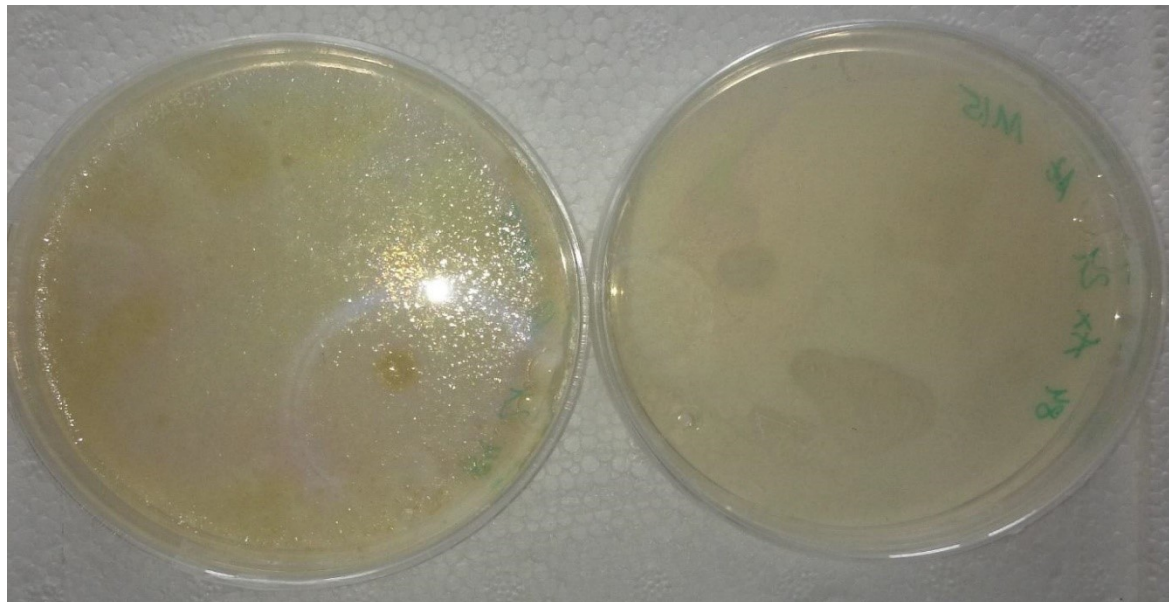


Figure S2. Assessment of axenicity with agar plates: 100 μ l of non-axenic (left) and axenic (right) cultures were plated on marine broth agar plates. Cultures were considered axenic when there was no colony formation after two weeks of growth

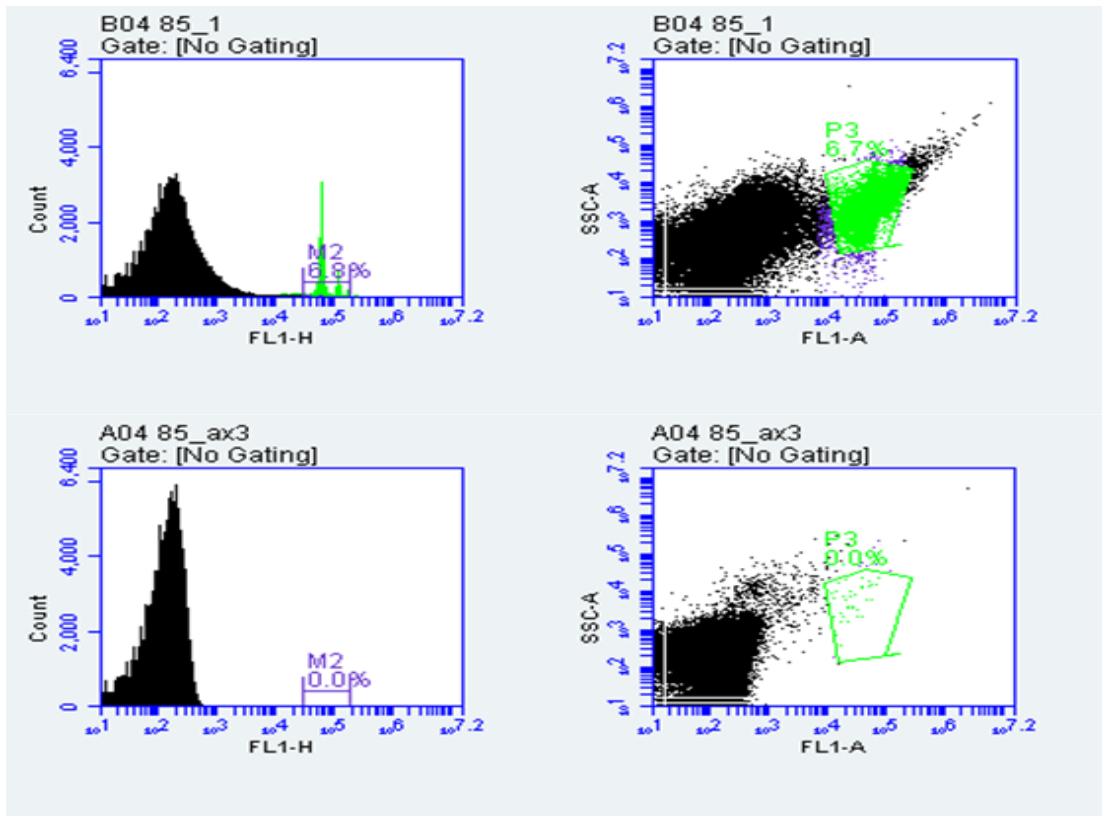


Figure S3. Assessment of axenicity via flow cytometry. Upper figures: non axenic cultures; lower figures: axenic cultures. Cultures were considered axenic if the numbers of events/mL (number of cells) in the gate M2 was below 1% compared to the non-axenic cultures.

<i>Croceibacter</i> spent medium effect									
	OD=0.05			OD=0.01			OD=0.005		
	Mean	Variance	Pval	Mean	Variance	Pval	Mean	Variance	Pval
Non Mating	72.31%	0.048%	0.00040	68.27%	0.160%	0.02110	64.35%	0.012%	>0.9999
Non Mating Control	62.61%	0.018%		62.61%	0.018%		62.61%	0.018%	
Mating	11.06%	0.030%	<0.0001	4.01%	0.024%	0.04340	1.15%	0.003%	>0.9999
Mating Control	1.59%	0.002%		1.59%	0.002%		1.59%	0.002%	
Gam/Zyg	9.43%	0.014%	0.01300	9.24%	0.071%	0.01090	17.56%	0.026%	>0.9999
Gam/Zyg Control	16.32%	0.079%		16.32%	0.079%		16.32%	0.079%	
Auxo	7.20%	0.004%	0.00020	18.48%	0.262%	>0.9999	16.94%	0.031%	0.70130
Auxo Control	19.48%	0.023%		19.48%	0.023%		19.48%	0.023%	
<i>Roseovarius</i> spent medium effect									
	OD=0.05			OD=0.01			OD=0.005		
	Mean	Variance	Pval	Mean	Variance	Pval	Mean	Variance	Pval
Non Mating	63.89%	0.003%	>0.9999	61.45%	0.016%	0.94198	62.89%	0.034%	0.78100
Non Mating Control	62.61%	0.018%		62.61%	0.018%		62.61%	0.018%	
Mating	1.09%	0.002%	0.38230	0.00%	0.000%	0.00060	0.00%	0.000%	0.00060
Mating Control	1.59%	0.002%		1.59%	0.002%		1.59%	0.002%	
Gam/Zyg	10.63%	0.051%	0.07590	12.64%	0.040%	0.37430	14.56%	0.118%	>0.9999
Gam/Zyg Control	16.32%	0.079%		16.32%	0.079%		16.32%	0.079%	
Auxo	24.39%	0.030%	0.00890	25.91%	0.012%	0.00120	22.56%	0.045%	0.11460
Auxo Control	19.48%	0.023%		19.48%	0.023%		19.48%	0.023%	
<i>Marinobacter</i> spent medium effect									
	OD=0.05			OD=0.01			OD=0.005		
	Mean	Variance	Pval	Mean	Variance	Pval	Mean	Variance	Pval
Non Mating	79.70%	0.101%	0.00100	78.10%	0.119%	0.00222	63.28%	0.799%	>0.9999
Non Mating Control	62.61%	0.018%		62.61%	0.018%		62.61%	0.018%	
Mating	9.24%	0.001%	<0.0001	1.78%	0.003%	>0.9999	0.35%	0.001%	0.01130
Mating Control	1.59%	0.002%		1.59%	0.002%		1.59%	0.002%	
Gam/Zyg	6.05%	0.132%	0.00220	5.81%	0.000%	0.02266	14.78%	0.136%	>0.9999
Gam/Zyg Control	16.32%	0.079%		16.32%	0.079%		16.32%	0.079%	
Auxo	5.01%	0.033%	0.00200	14.31%	0.122%	0.16290	21.60%	0.303%	>0.9999
Auxo Control	19.48%	0.023%		19.48%	0.023%		19.48%	0.023%	
<i>Maribacter</i> spent medium effect									
	OD=0.05			OD=0.01			OD=0.005		
	Mean	Variance	Pval	Mean	Variance	Pval	Mean	Variance	Pval
Non Mating	79.77%	0.08%	0.00210	66.11%	0.325%	>0.9999	71.19%	0.842%	0.13060
Non Mating Control	62.61%	0.02%		62.61%	0.018%		62.61%	0.018%	
Mating	4.75%	0.10%	0.04770	0.80%	0.010%	>0.9999	0.55%	0.002%	>0.9999
Mating Control	1.59%	0.00%		1.59%	0.002%		1.59%	0.002%	
Gam/Zyg	7.96%	0.11%	0.02988	8.72%	0.126%	0.09360	10.37%	0.402%	0.24170
Gam/Zyg Control	16.32%	0.08%		16.32%	0.079%		16.32%	0.079%	
Auxo	7.52%	0.01%	0.00220	24.37%	0.146%	0.27050	17.89%	0.414%	>0.9999
Auxo Control	19.48%	0.02%		19.48%	0.023%		19.48%	0.023%	

ST2: Statistical evaluation of bacterial medium effect on *S. robusta* sexual reproduction efficiency. Two-way ANOVA, $\alpha=0.05$, Bonferroni's correction for multiple comparisons. Color code as in Figure 1: blue for non-mating cells, red for mating cells, green for gamets/zygotes, purple for auxospores.

Supporting informations chapter 5 – Molecular insights into the bacterial effect on sexual reproduction of *S. robusta*

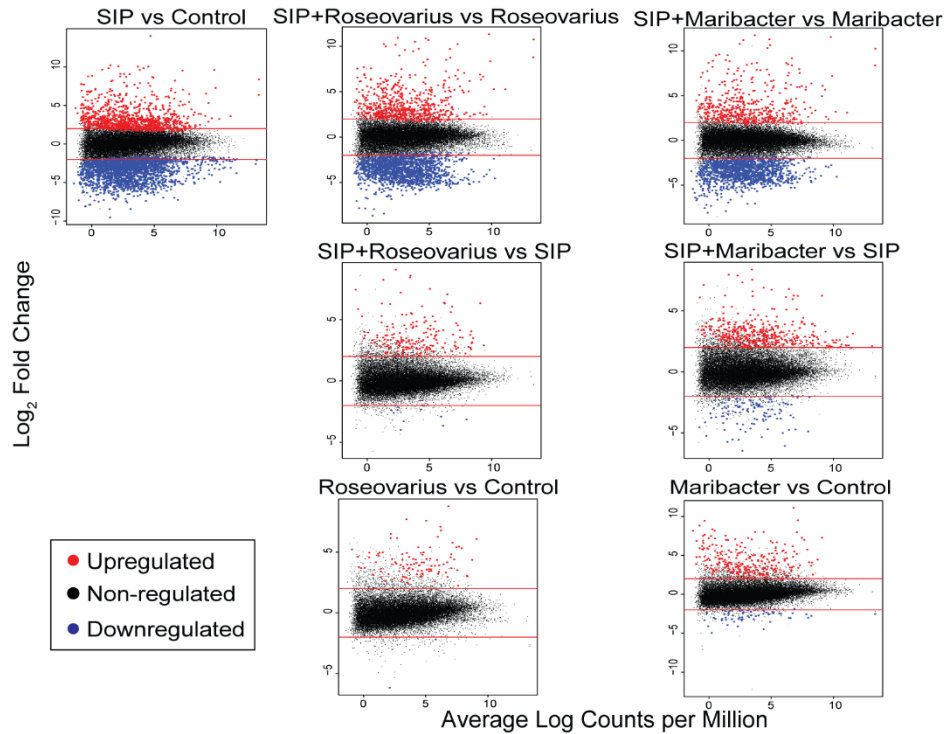


Figure S4: Mean-difference plot of \log_2 fold change versus the average \log_2 -count per millions in different comparisons of different treatments.

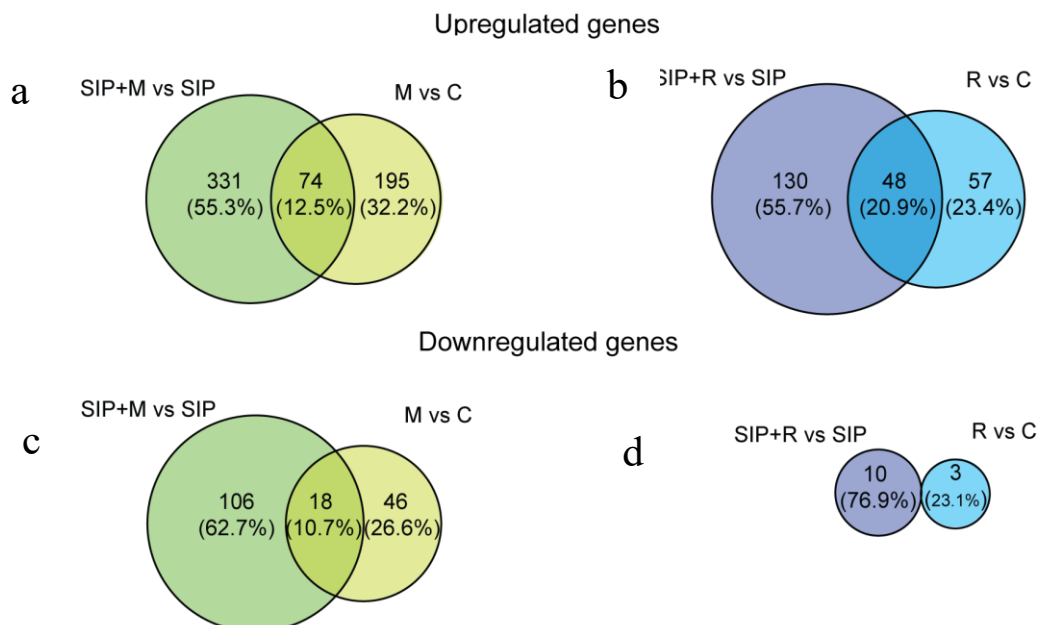


Figure S5: Venn diagrams of up- (a and b) and downregulated (b and c) *S. robusta* genes under bacterial influence. a) and c) refers to SIP+ induced treatment versus non-induced treatments in presence of *Maribacter* sp. medium, b) and d) to SIP+ induced treatment versus non-induced treatments in presence of *Roseovarius* sp. medium.

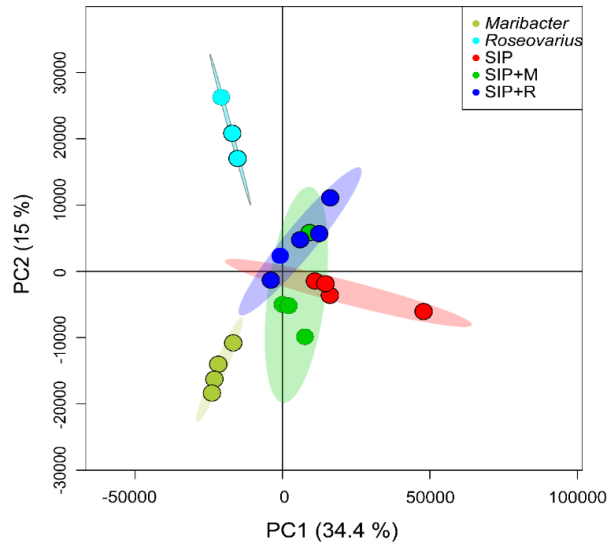


Figure S6: PCA of exometabolome samples of SIP⁺-induced cultures and bacteria spent medium. Each dot represent a sample for each treatment. Red dots are axenic induced cultures, green dots are induced cultures treated with *Maribacter* sp. medium, blue dots are induced cultures treated with *Roseovarius* sp. medium, light blue dots are spent medium from *Roseovarius* sp. cultures and light green dots are spent medium from *Maribacter* sp.

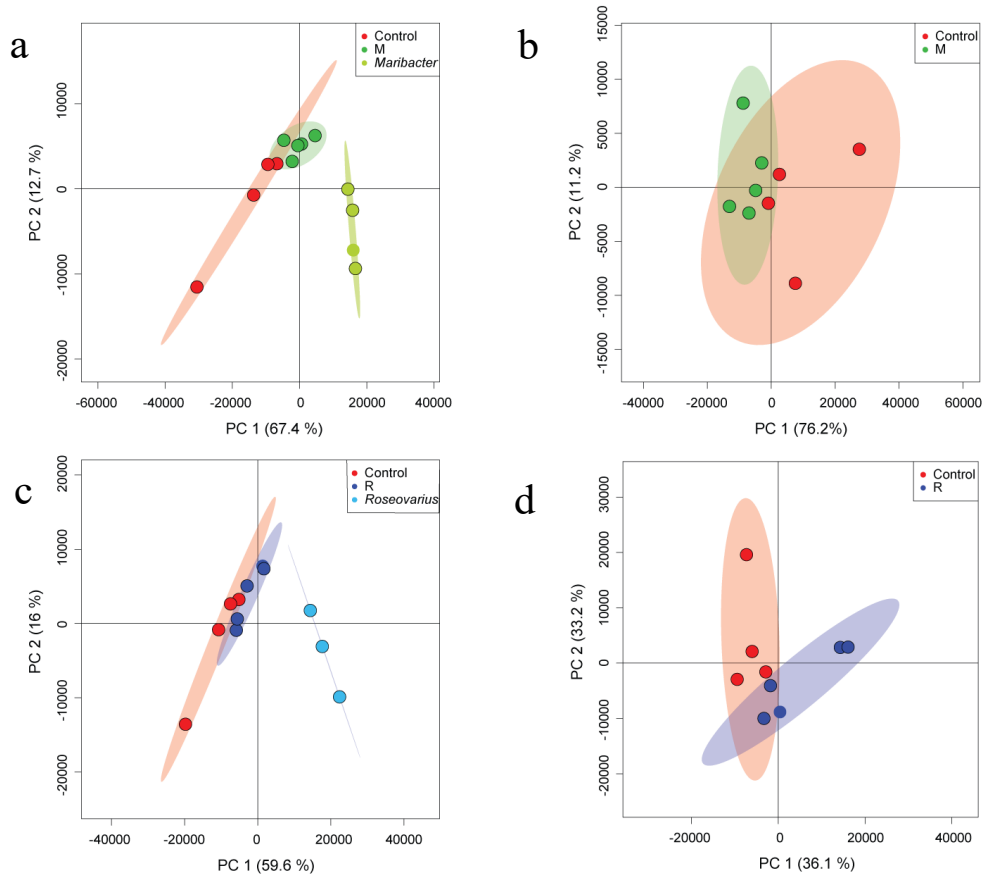


Figure S7: PCA of exometabolome samples of non-induced cultures and bacteria spent medium. a) PCA of axenic control, axenic control + *Maribacter* sp. spent medium (M) treatment and *Maribacter* sp. exudates, b) PCA of axenic control and axenic control + *Maribacter* sp. spent medium (M) with subtraction of features from *Maribacter* sp. exudates, c) PCA of axenic control, axenic control + *Roseovarius* sp. spent medium (R) and *Roseovarius* sp. exudates, d) PCA of axenic control and axenic control + *Roseovarius* sp. spent medium (R) with subtraction of features from *Roseovarius* sp. exudates.

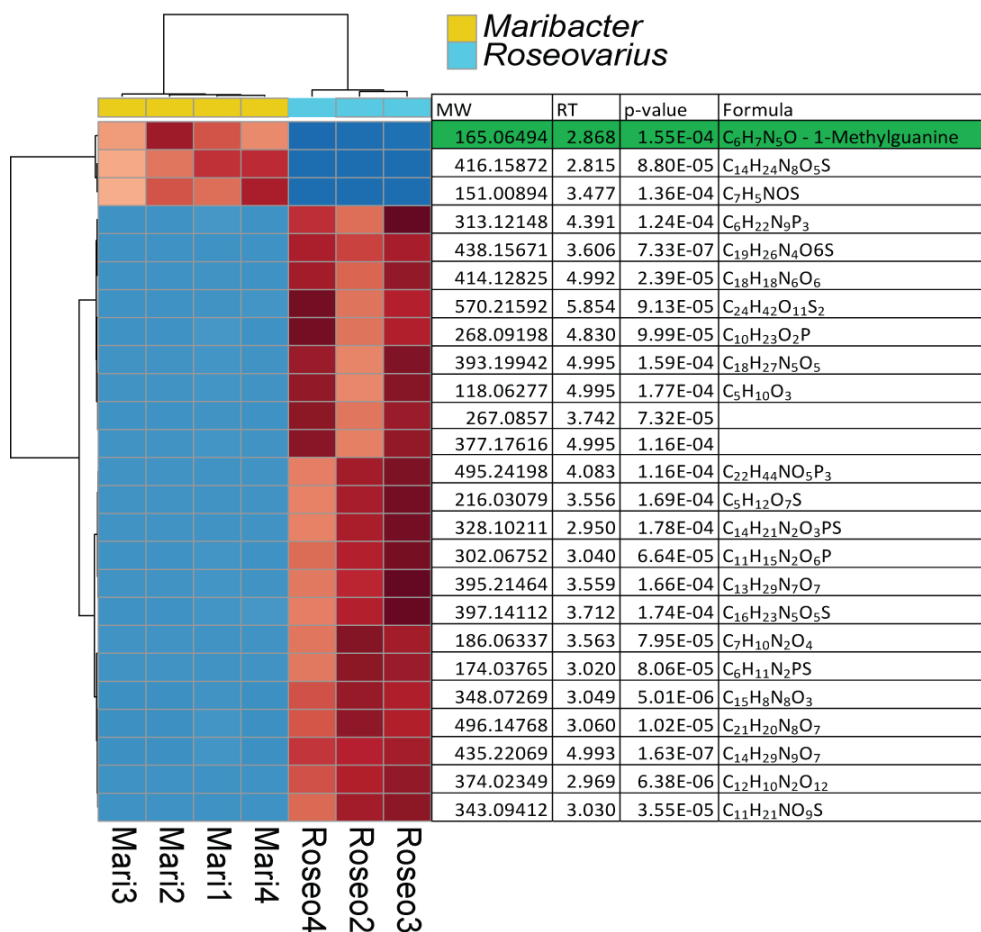


Figure S8: Heatmaps of up- and downregulated exometabolites from *Maribacter* sp. spent medium and *Roseovarius* sp. spent medium. Significance evaluated with a t-Test ($\alpha=0.05$), hierarchical clustering is based on Euclidean distances and using Ward's method. Red is for upregulated metabolites, blue is for downregulated metabolites.

GO ID	GO Function	Genes	p-value
Biological function			
GO:0034394	protein localization to cell surface	2	2.20E-03
GO:0006805	xenobiotic metabolic process	3	2.90E-03
GO:0042049	cellular acyl-CoA homeostasis	1	6.00E-03
GO:0007225	patched ligand maturation	1	6.00E-03
GO:0070859	positive regulation of bile acid biosynthesis	1	1.19E-02
GO:0015864	pyrimidine nucleoside transport	1	1.19E-02
Molecular function			
GO:0010181	FMN binding	2	4.40E-04
GO:0015389	pyrimidine- and adenine-specific:sodium symporter activity	1	5.57E-03
GO:0030248	cellulose binding	1	5.57E-03
GO:0009976	tocopherol cyclase activity	1	5.57E-03
GO:0015390	purine-specific nucleoside:sodium symporter activity	1	5.57E-03
GO:0016162	cellulose 1,4-beta-cellobiosidase activity	1	5.57E-03
GO:0008123	cholesterol 7-alpha-monooxygenase activity	1	1.11E-02
GO:0008127	quercetin 2,3-dioxygenase activity	1	1.11E-02
GO:0004313	[acyl-carrier-protein] S-acetyltransferase activity	1	1.11E-02

ST4: Upregulated pathways elicited by *Roseovarius* sp. medium in SIP⁺-induced cultures (SIP+R vs SIP).

GO ID	GO Function	Genes	p-value
Biological function			
GO:0006572	tyrosine catabolic process	2	7.10E-07
GO:0006559	L-phenylalanine catabolic process	2	1.30E-06
GO:0010188	response to microbial phytotoxin	1	3.10E-04
GO:0048830	adventitious root development	1	3.10E-04
GO:0001560	regulation of cell growth by extracellular stimulus	1	6.10E-04
GO:0009684	indoleacetic acid biosynthetic process	1	6.10E-04
GO:1902000	homogentisate catabolic process	1	9.20E-04
GO:0010189	vitamin E biosynthetic process	1	1.53E-03
GO:0006527	arginine catabolic process	1	1.84E-03
GO:0046689	response to mercury ion	1	3.68E-03
GO:0019761	glucosinolate biosynthetic process	1	3.68E-03
GO:0006103	2-oxoglutarate metabolic process	1	3.99E-03
GO:0042538	hyperosmotic salinity response	1	3.99E-03
GO:0009064	glutamine family amino acid metabolic process	2	7.84E-03
GO:0006094	gluconeogenesis	1	1.13E-02
GO:0004838	L-tyrosine:2-oxoglutarate aminotransferase activity	1	3.70E-04
GO:0080108	S-alkylthiohydroximate lyase activity	1	3.70E-04
GO:0033855	nicotianamine aminotransferase activity	1	3.70E-04
GO:0004121	cystathionine beta-lyase activity	1	1.11E-03
GO:0004334	fumarylacetoacetase activity	1	1.11E-03

ST5: Downregulated pathways triggered by *Roseovarius* sp. medium in SIP⁺-induced cultures (SIP+R vs SIP).

Gene ID	logFC	PValue	FDR	Annotation	EggNogg
Sro54_g031900	7.44	5.86E-05	1.63E-02	of fatty acids protein 1	fatty acid elongase
Sro434_g142030	4.85	3.46E-04	4.73E-02	Probable LIM domain-containing serine/threonine-protein kinase DDB	protein kinase kinase kinase
Sro2017_g311180	4.51	1.96E-04	3.63E-02	-	Inherit from NOG: Low-co2 inducible protein
Sro123_g059760	4.08	5.75E-05	1.63E-02	-	gluconolactonase (EC 3.1.1.17)
Sro1984_g309320	3.79	3.39E-04	4.72E-02	CRAL-TRIO lipid binding domain	-
Sro1006_g230290	3.77	1.67E-04	3.42E-02	helicase PIF1	PIF1 5'-to-3' DNA helicase homolog (S. cerevisiae)
Sro2734_g335850	3.76	5.03E-05	1.48E-02	Heat shock 70 kDa protein (Fragment)	heat shock protein
Sro1178_g249460	3.71	1.83E-04	3.59E-02	-	Enzyme of the cupin superfamily
Sro535_g161880	3.70	2.84E-04	4.31E-02	Peroxisomal membrane protein 2	peroxisomal membrane protein
Sro58_g033810	3.66	2.60E-04	4.10E-02	Low temperature requirement A	-
Sro396_g134350	3.53	1.79E-04	3.57E-02	Arf GTPase activating protein	-
Sro244_g097220	3.52	3.21E-05	1.12E-02	quercetin 2,3-dioxygenase PA2418	pinin (iron-binding nuclear protein)
Sro11_g008460	3.48	2.67E-04	4.13E-02	AdipoR/Haemolysin-III-related	-
Sro1157_g247380	3.35	3.02E-04	4.50E-02	ATP carrier protein 1	carrier protein
Sro896_g217300	3.22	2.41E-04	4.02E-02	Short-chain dehydrogenase TIC 32, chloroplastic	Dehydrogenase
Sro20_g014010	3.21	2.51E-04	4.08E-02	fatty acid desaturase A	Fatty acid desaturase
Sro686_g187010	3.16	3.37E-04	4.72E-02	-	Domain of unknown function (DUF1996)
Sro2020_g311370	3.14	6.12E-05	1.68E-02	monoxygenase	Monoxygenase
Sro324_g117530	3.11	3.07E-04	4.50E-02	Alpha/Beta hydrolase fold	-
Sro311_g114370	3.07	3.47E-04	4.73E-02	-	Inherit from ascNOG: Methyltransferase
Sro355_g125030	3.01	4.24E-05	1.31E-02	Vesicle transport protein GOT1B	golgi transport
Sro1264_g257350	2.84	1.91E-04	3.63E-02	-	Serine threonine kinase with two-component sensor domain
Sro1003_g229980	2.83	3.05E-04	4.50E-02	-	ANK
Sro585_g170970	2.82	3.40E-04	4.72E-02	GTPase Era	-
Sro1496_g277480	2.76	9.81E-05	2.32E-02	SET domain	-
Sro380_g130620	2.73	3.16E-04	4.56E-02	GAP domain, ANK repeat and PH domain-containing protein 2	ArfGAP with dual PH domains
Sro649_g181180	2.71	2.36E-04	4.02E-02	Polyubiquitin (Fragment)	ubiquitin
Sro373_g129060	2.68	1.81E-04	3.59E-02	Cytochrome P450	-
Sro113_g056150	2.67	2.08E-04	3.72E-02	Pick C1-like protein 1	patched domain containing
Sro437_g142800	2.63	1.88E-04	3.63E-02	Monoglyceride lipase	Monoglyceride lipase
Sro4_g003650	2.60	2.66E-04	4.13E-02	-	Transcriptional regulator
Sro180_g078830	2.59	3.06E-04	4.50E-02	Mycocerosic acid synthase-like polyketide synthase	fatty acid synthase
Sro686_g187020	2.53	1.94E-04	3.63E-02	Leucine-rich repeat domain superfamily	-
Sro327_g118400	2.42	1.29E-05	6.22E-03	Transmembrane 9 superfamily	transmembrane 9 superfamily
Sro3_g002520	2.40	1.91E-04	3.63E-02	-	fatty acid desaturase family protein
Sro1330_g263400	2.38	1.69E-04	3.43E-02	FKBP-type 22 kDa peptidyl-prolyl cis-trans isomerase	Peptidyl-prolyl cis-trans isomerase
Sro505_g156100	2.36	2.64E-04	4.13E-02	Failed axon connections homolog	failed axon connections homolog (Drosophila)
Sro613_g175560	2.32	2.72E-04	4.17E-02	D-alanine-D-alanyl carrier protein ligase	PKS_AT
Sro301_g112010	2.29	3.23E-04	4.60E-02	guanosine(18)-2'-O-methyltransferase	mitochondrial rRNA methyltransferase 1 homolog (S. cerevisiae)
Sro549_g164610	2.28	1.40E-04	3.00E-02	-	-
Sro54_g031760	2.27	2.29E-04	3.93E-02	Endonuclease Muts2 (Fragment)	DNA mismatch repair protein
Sro49_g028680	2.21	2.54E-04	4.08E-02	Probable nucleoredoxin 1	nucleoredoxin-like
Sro1006_g230310	2.20	2.46E-04	4.06E-02	S-transferase omega-like 2	glutathione Stransferase
Sro1542_g281060	2.16	4.07E-05	1.31E-02	-	-
Sro1695_g291810	2.11	2.21E-04	3.84E-02	of very long chain fatty acids protein 4	fatty acid elongase
Sro2358_g324650	2.09	3.26E-04	4.60E-02	-	reductase

ST7: Upregulated genes elicited by *Roseovarius* sp. medium in SIP⁺-induced cultures (SIP+R vs SIP).

Supporting informations chapter 6 – From ecology to applied research: effect of bacteria on a commercial microalga

Supporting informations chapter 7– A SPE based non-disruptive method to investigate macroalgal surface chemistry

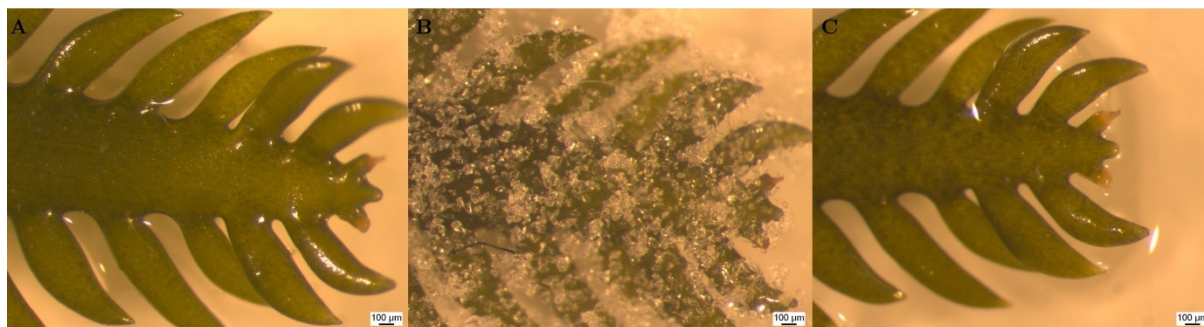


Figure S9: Microscopic prove of non-disruptive effect of C18 material on *Caulerpa taxifolia* surface. The pictures (light microscopy) show a *Caulerpa taxifolia* fronds before (left), during (center) and after a 1 min treatment with C18 material. No major tissue lysing was observed after extraction treatment.

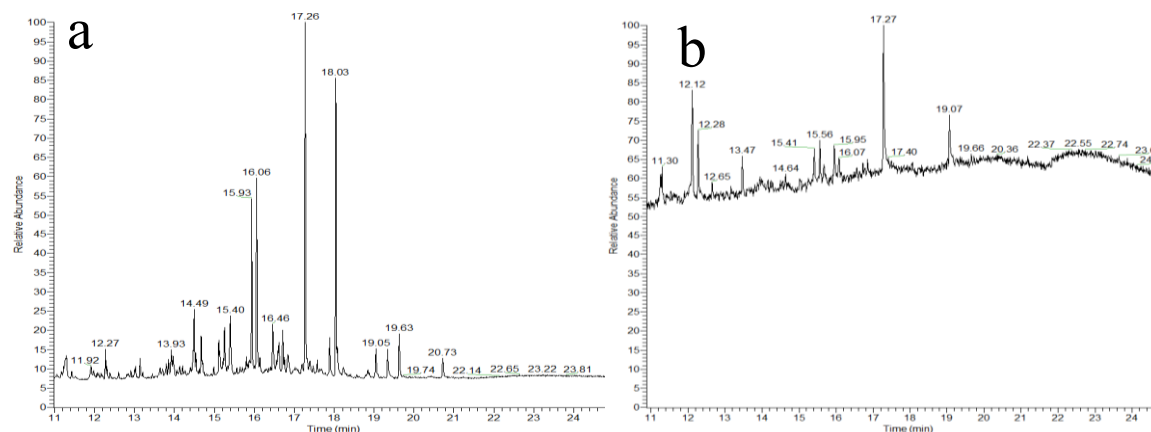


Figure S10: GC/MS profiles of C18 material (non endcapped) blank a) before and b) after conditioning with eluting solvent. Not-endcapped silica Gel 100 C18 reversed phase material (100 Å pore size, 40-63 µm particle's dimensions, Sigma-Aldrich©, Germany) was suitable for extracting fucoxanthin but was not suitable for GC-MS measurements. Some intense peaks of impurities between 14.5 and 18 min interfered with signals from the samples. These peaks cannot be completely removed even after excess conditioning of the powder with the extracting solvent.

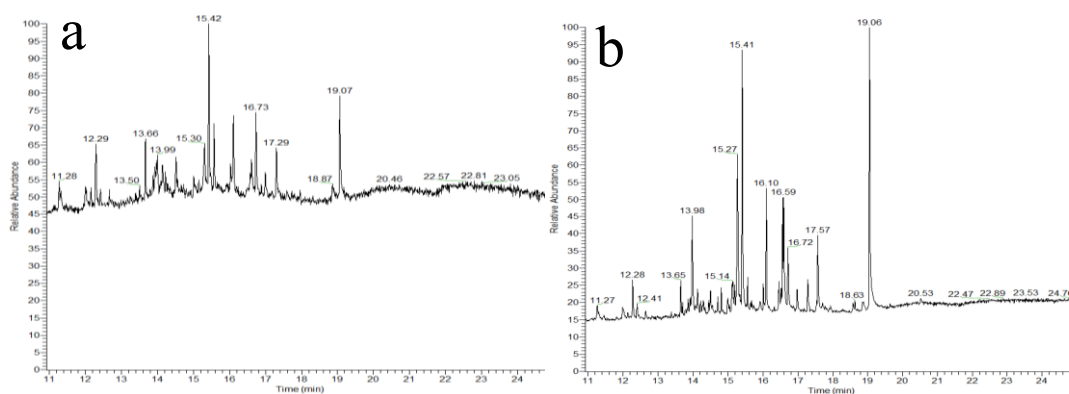


Figure S11: GC/MS profiles of silica Gel 100. a) blank b) extract of *Fucus vesiculosus*. Fully endcapped silica Gel 100 C18 reversed material (100 Å pore size, 15-25 µm particle's dimensions, Sigma-Aldrich®, Germany) was suitable for extraction of surface metabolites (Figures S2 and S3). Contaminants did not substantially interfere with measurements, since the total ion current (TIC) of the blank was lower than the one of the samples and background subtraction was possible. However, silica Gel 100 was not further considered because of problems in the handling due to the very small size of the particles. The fine dust hardly stuck to the surface of the algae and could not be transferred quantitatively into the SPE cartridge.

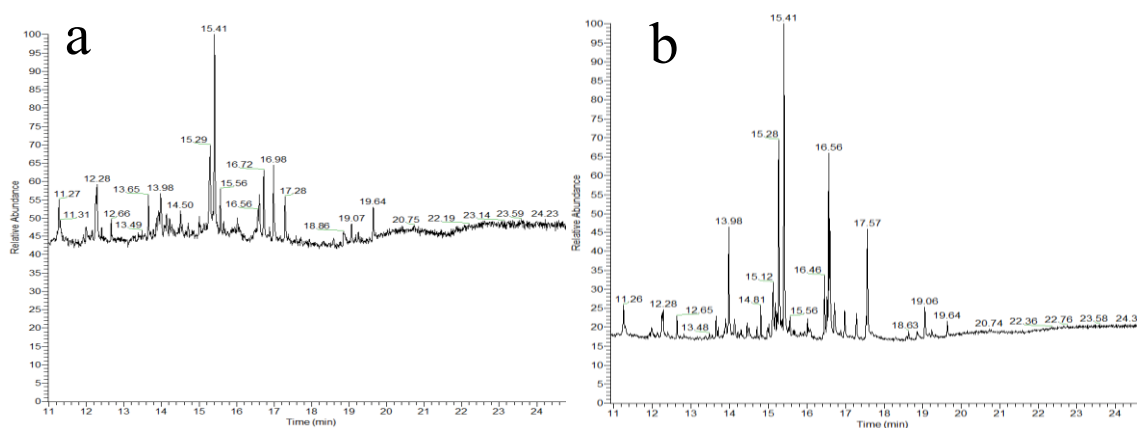


Figure S12: GC/MS profiles of silica Gel 90. a) blank b) extract of *Fucus vesiculosus*.

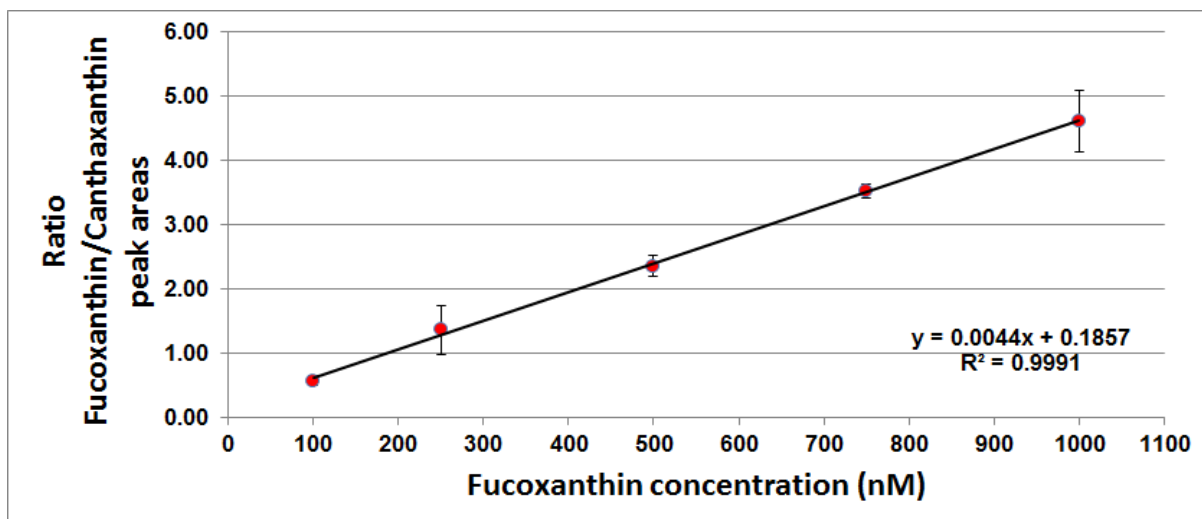


Figure S13: Calibration curve for quantitative determination of the fucoxanthin content in surface metabolites extracts. To prepare the external calibration curve, 0.66 mg of fucoxanthin (purity $\geq 95\%$, Sigma Aldrich©, Germany) were weighted and dissolved in 10 mL methanol in order to obtain a 100 μM stock solution. Five dilutions at different concentration were prepared (1 μM , 750 nM, 500 nM, 250 nM, 100 nM). 10 μL of a 20 μM canthaxanthin (analytical standard grade, Sigma Aldrich©, Germany) solution in methanol were added to 190 μL of each sample in order to have a final concentration of 1 μM of canthaxanthin. Every point of the curve was measured 3 times with the UPLC-MS method developed for surface extraction.

Acknowledgments

“It’s a long way to the top, if you wanna rock ‘n’ roll”. I think this immortal principle from AC/DC can be easily applied also to a PhD. Three years of ups and downs, of doubts and celebrations, of (rare but important) successes and (much more frequent but fundamental) difficulties. If I think about myself, I cannot even realize how many things changed in this time. Three and a half years ago, I moved to another country, I said goodbye to friends, family, important relationships, I started struggling with a new culture and a new language, signed up for a Marie Curie PhD with a lot of expectations but without really knowing what was going to happen. And damn! Here we are, I am writing the acknowledgments of my PhD thesis, I have had countless experiences and travelled like never before in my life, I even learned how to ride a bike and how to speak that (sometimes still) complicated language! I have rediscovered myself, met my inner demons, fought (and still fighting) with some of them and made peace with some other, learned which are my strengths and, more importantly, my limits.

A long adventure, a long ride, that would have been much more difficult and darker without an amazing number of travel companions. During these years, I have met a lot of beautiful, amazing new people, I have strengthened the bond with old friends, I have rediscovered the meaning of friendship and love. So, I am sorry guys, but you deserve this long, cheesy, multilingual acceptance speech! I hope not to forget someone. If I do, forgive me!

First of all, I would like to thank my supervisor, Georg. You accepted this random Italian student in your group not once, but twice! You believed in me and in my capabilities when I didn’t, you gave me the opportunity to do this wonderful experience. Your support in all my decisions, the freedom you gave me to develop my work, my personality, my decision in what to do and where to go are invaluable.

I would like also to thank Prof. Wim Vyverman for hosting me in his group in Gent and giving me the opportunity to setup a stimulating experiment that lead to a fruitful and exciting collaboration.

Thanks also to Proviron and especially to Luc Roef for hosting me for a short stay in Antwerp which turned out to be an interesting collaboration and a pleasant time of research and

Thanks also to all the collaborators that contributed to the writing of manuscripts, for their patience and their proofreading. Thanks to Conny and Remington for proofreading this

Thesis. Many thanks to Anne, Jasmin and especially Sandesh for their work and the help they gave me in the most time consuming projects.

Und was wäre Wissenschaft und Forschung ohne tolle Kollegen und eine schöne Arbeitsatmosphäre?

Ich danke allen den ehemaligen und aktuellen Arbeitsgruppenmitgliedern, weil die Arbeit und das Leben ohne euch viel weniger interessant und lustig gewesen wären.

Also vielen Dank an Marino, dass er mit mir nur auf Deutsch mit viel Geduld gesprochen hat, an Hannes, für die technische Unterstützung, für die Witze, für die gute und schlechte Laune, an Marcel, für alle die tollen Konzerten, die wir zusammen besucht haben. And thanks also to Michiel and Iannis, that most of the times joined us. Danke Tim für die grandiosen Metal-Konzerten und für die stimulierende Gespräche über Musik, Filme, Pop-Kultur und Wissenschaft. Danke Daniel für die Zusammenarbeit mit dem GC und für die Möglichkeit an deinem Rollenspiel (kurz) teilzunehmen, danke Nils für deine wissenschaftlichere Präzision und deine Begeisterung für die Natur und für Italien. Danke Tini und Karen, weil wir immer das „Seminavis-team“ bleiben werden. Danke Franzi, Arite, Michael, Julia, Stefan, Marine, Simona, Frieder, Anne, Michiel, Iannis, Nico. Thanks also to the newcomers Remington and Carlos, for showing me different ways to work in research. Vielen Dank Kathleen, weil du eine echte, gute Freundin bist und wir haben viel zusammen verbracht. Und du hast noch mir (zusammen mit Conny) gelehrt, wie man Fahrrad fährt, wenn ich geglaubt hatte, dass es einfach unmöglich war!

Und ein großer, riesiger Dank an Conny. Du warst eine gute Kollegin, eine witzige und verrückte „Labor-Buddy“, eine nette Deutschlehrerin, aber du bist überhaupt eine wertvolle, vertraute Freundin, und ich bin froh, dass du trotz der Entfernung noch hier bist.

Thanks to Lydia, because you are the “buddy” with whom you made dirty jokes and good, loud laugh, but also the shoulder where to cry and the one who’s always ready to give a precious advice. Grazie a Gianmaria: abbiamo iniziato insieme, abbiamo viaggiato insieme e ne abbiamo passate tante, ma non ti ho mai detto che senza di te il laboratorio sarebbe stato un posto più difficile da vivere. Grazie per le discussioni scientifiche, le chiacchierate a cuore aperto e la pazienza nel sopportare le mie improvvise e indesiderate incursioni nel tuo ufficio.

Thanks to all Prof. Vyverman group, the “Sterre Crew”, for the productive scientific discussion, the dirty jokes, the parties, the beers, the hard work and the great fun, the

beautiful memories of Gent. Thanks to Evelin, Ilse, Olga, Heidi, Kenny, Renaat, Willem, Lucas, Gust, Koen, Eli (the adopted ALFFy), Andrea and most of all to Sam de Decker, who is not only a precious, professional, talented and enthusiastic scientific collaborator, but also an amazing person, always ready to help other people, to interact with joy and happiness. You gave me much more than you think (and sorry that I cannot make right now one of those dirty, politically incorrect jokes, but this is an official document, man!).

A great thank you goes to Dr. Claire Gachon, for her enormous and continuous effort to create and maintain the ITN Marie Curie Network “ALFF: Algae Microbiome, Friends or Foes”, a European project that did not only generate great science and allowed me to travel in many different, beautiful countries, but that also created a group of amazing human beings that are not only colleagues, but friends. So thanks to Shu Min, Shri, Andrea, Frederik, Hetty, Johannes, Noreen, Miriam. And especially thanks to Freddie, for the great scientific collaboration, the fine drinks and nice events in Gent, the talks in German, to Kathryn, for being always enthusiastic, strong, empathic, to Javier, for the fruitful work in Proviron, the great week in Antwerp, the many parties, the amazing shared experiences and memories, to Lachy, for being a brilliant scientist, always ready to help and discuss, and moreover for being a deep, sensitive person.

E adesso alcuni ringraziamenti in italiano. Prima di tutto, alla mia famiglia di Jena, con cui ho condiviso tante avventure. Grazie a Simona per essere una amica schietta e genuina, sempre pronta a dare consiglio, che è sempre stata presente, soprattutto nei periodi più bui. Grazie a Fabiana, perché abbiamo davvero ballato di tutto insieme e mi hai donato sorrisi anche nei momenti difficili. Grazie a Federica, che è stata qui poco ma in un momento cruciale della mia vita. Grazie a Vincenza, perché dire che sia una persona unica, in ogni senso immaginabile, è usare un eufemismo. Grazie a quei pazzi di Frank, Giacomo, Sebastian, Mara. E soprattutto grazie a Lucia, compagna di mille esperienze che non è scomparsa quando è andata via da Jena, ma anzi è diventata parte integrante del mio mondo. Perché l'amicizia abbatte ogni distanza fisica.

Grazie alla redazione de “Lo Spazio Bianco” e al gruppo dei “True Believers”, la famiglia con cui condividere il mio grande amore per il fumetto, che mi ha insegnato il valore (e il piacere) del lavoro di squadra, dandomi la possibilità di migliorare le mie doti di “giornalista per hobby” e di realizzare un piccolo sogno.

Grazie ai miei amici di università con cui sono sempre in contatto, grazie a Chiara per avermi ospitato a Gent per due mesi, grazie a Riccardo per i fondamentali aggiornamenti semestrali. Grazie a Giulia. Grazie ancora a Costanza, perché senza un tuo consiglio questa avventura

non sarebbe nemmeno iniziata. Grazie a Roberto, compagno dell'avventura in terra teutonica, visitatore a Jena e visitato a Bochum, felice incontro casuale nella stazione di Bruxelles, bussola etica e politica, sfida costante alla mia capacità argomentativa. Grazie a Andrea (lo Sciarra), Luca (Luiso) e Renato, perché le Screaming Monkeys vivono sempre e riunirle nell'occasione di un matrimonio è stato fantastico. Grazie soprattutto alla famiglia del Cubo, una stanza ormai non più fisica, ma che sopravvive nel cuore e negli affetti. Grazie a Sara, Dario, a Pippo, a Ciccio (visitatore inaspettato in questa cittadina sperduta nel cuore di Germania), a Matteo "Bartolo" Bartolini. Grazie a Matteoandrea "Luche" Lucherelli, per la pazienza nell'ascoltare i miei scazzi o le mie paturnie, il supporto costante e l'amicizia profonda che si rinforza con gli anni, nonostante ci dividano un migliaio di chilometri (spero di non essere stato troppo sdolcinato, che hai pure il diabete e ci resti secco!). E grazie a Matteo "Bessi" Bessi. Grazie per aprire sempre le mie fastidiose note vocali (un centinaio e più negli ultimi tre anni?), per ascoltare ogni mia storia e ogni mio sbotto, per aprirti a tua volta con me, per essere (scemo?) come me e migliore di me in tante cose. Per essere un amico vero.

E grazie agli amici che sono il pilastro del mio mondo, quelli che ci sono da sempre e sempre ci saranno: grazie Greta, Federico, Andrea, Chiara, Mattia (ti aspetto per un'altra visita!). Grazie a quelli che ci sono stati e sono stati trascinati via dai flussi tortuosi e tormentati di questa esperienza. Scusatemi per i miei errori e i miei egoismi, e vi auguro una vita piena di felicità e bellezza.

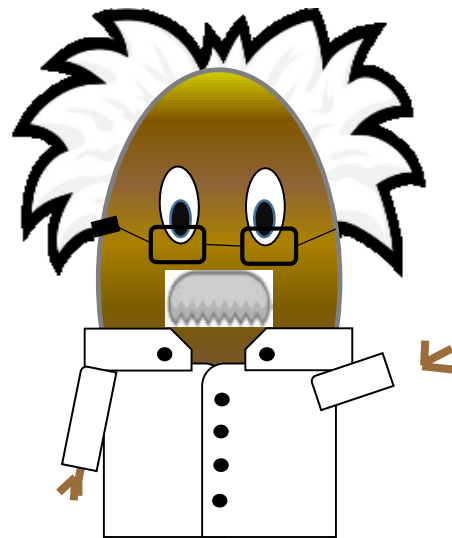
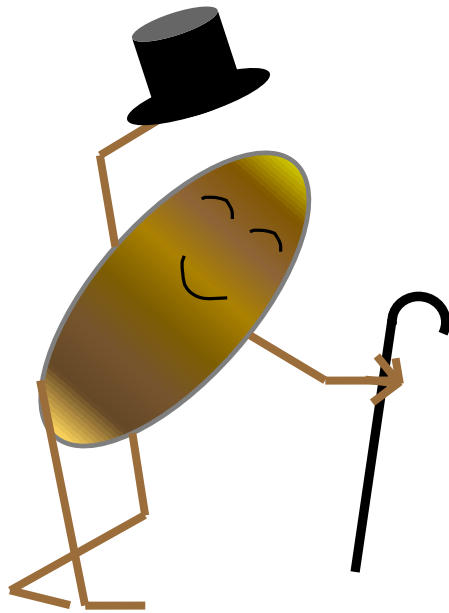
E ancora un grazie enorme, che si ripete ormai ad ogni mio singolo traguardo, grande o piccolo che sia. Un grazie alle due persone che ci sono sempre state, che mi hanno sostenuto e mi sostengono sempre, che hanno appoggiato la mia scelta di partire, con sentimenti contrastanti di orgoglio e di dispiacere nel vedere un figlio diventare grande e andarsene lontano. Ogni passo che ho fatto l'ho potuto fare grazie a voi. Ogni vostro insegnamento vive in me. Grazie mamma e grazie babbo.

E infine grazie a te, che sei entrata nella mia vita quando pensavo che non ci fosse posto per niente se non per me stesso e il mio senso di inadeguatezza. Hai guardato attraverso un muro di autocommiserazione e hai visto qualcosa che ti è piaciuto e ti ha incuriosito, chissà come mai. E io ho contraccambiato lo sguardo, ed è stato come vedere il sole per la prima volta dopo tanti giorni di nuvole e di pioggia. Con il tuo entusiasmo e la tua forza incrollabile, la tua pazienza e la tua sensibilità, la tua dolcezza e il tuo saper ascoltare, hai preso la mia vita e ne hai fatto qualcosa di nuovo, di più luminoso e leggero. Abbiamo fatto tanti passi insieme

in poco tempo, come se fosse l'evoluzione più naturale, l'unica strada possibile. Ho trovato un'amica, una complice, un appiglio solido come roccia. E adesso so di essere arrivato finalmente a casa. Casa mia sei tu. Spero di essere lo stesso per te. Per ogni nuovo passo che faremo insieme. Grazie Francesca.

And so, this is it. Thanks for being here, all of you.

See You Space Cowboy(s).



Curriculum vitae

Personal informations

Name: Emilio Cirri
Date of birth: 22/01/1990
Place of birth: Florence (IT)
Nationality: Italian
E-Mail: emilio.cirri@gmail.com

Academic experience

02/07/2015 – 02/07/2018 PhD Candidate at Friedrich Schiller University of Jena in the Institute for Analytic and Inorganic Chemistry as part of the ITN Marie Project Horizon 2020 “ALFF: Algae Microbiome ,Friends or Foes”

02/07/2014 – 24/07/2014 ERASMUS project at Friedrich Schiller University of Jena in the Institute for Analytic and Inorganic Chemistry, Prof. Pohnert working group

2012-2014 M. Sc. in analytical and environmental chemistry at Università degli studi di Firenze

2009-2012 B. Sc. in chemistry at Università degli studi di Firenze

2004-2009 Liceo Scientifico Niccolò Copernico

Research visit

02/2018 Research stay at Proviron, Antwerp, Belgium

01/2018-02/2018 Research stay at University of Gent, Belgium, Group of Protistology and aquatic ecology, Prof. Wim Vyverman

05/2017-07/2017 Research stay at University of Gent, Belgium, Group of Protistology and aquatic ecology, Prof. Wim Vyverman

Teaching and technical experience

2015 - 2018 Operation and maintenance of GC system (FID, TOF, Quad), FSU Jena, Germany

2015-2017 Supervision of hands-on course on GC and GC-MS analysis, FSU Jena, Germany

11/09/2017-15/09/2017 Organization and supervision of international COST Action workshop "Crossing the kingdoms: Macroalgae-bacteria interactions promoting algal growth and development", FSU Jena, Germany

19/09/2016 - 23/09/16 Organization and supervision of international Marie Curie ITN ALFF workshop "Deciphering symbiotic interactions with metabolomics", FSU Jena, Germany

Further working experience

01/03/2015 – 01/06/2015 Laboratory technician at Bluclad S.r.l., Prato, Italy

Scientific conferences, oral and poster presentations

23/08/2015 - 28/08/2015 6th European Phycological Conference, London, United Kingdom

9/10/2015 50th PhD workshop “Naturstoffe:Chemie, Biologie und Ökologie”, Würzburg, Germany

13/10/2016 -16/10/2016 VAAM, Annual Conference of the Association for General and Applied Microbiology, Jena, Germany – Poster Presentation

29/10/2016 – 30/10/2016 3rd International Workshop on Image-based Systems Biology, Jena, Germany

14/10/2016 52th PhD workshop “Naturstoffe:Chemie, Biologie und Ökologie”, Halle, Germany – Oral presentation

20/03/2017 – 23/03/2017 MiCom Conference 2017, Jena, Germany – Poster presentation

13/08/2017 – 19/08/2017 11th International Phycological Conference, Szczecin, Poland – Oral presentation

11/09/2017 – 15/09/2017 Phycomorph workshop "Crossing the kingdoms: Deciphering seaweed substances and bacteria interactions promoting algal growth and development", Jena, Germany – Oral Presentation

17/09/2017 – 20/09/2017 58th Conference of the Czech Phycological Society, Ostrava, Czech Republic – Oral Presentation

19/03/2018 – 22/03/2018 MiCom 2018, Jena – Oral Presentation

14/05/2018 – 18/05/2018 Young algaeers symposium, Oban, Scotland

24/03/2018 – 28/03/2018 14th International Conference of the Metabolomics Society, Seattle, United States – Travel Award and Best Oral Talk award

Workshops

7/09/2015 - 11/09/2015 ALFF Workshop - “Algal culturing: from the field to the lab”, Station Biologique de Roscoff, France.

22/02/2016 – 26/02/2016 ALFF Workshop – “Entrepreneurship and industrial development”, Lisbon, Portugal

19/09/2016 - 23/09/2016	ALFF Workshop - "Deciphering symbiotic interactions with metabolomics", FSU Jena, Germany
14/02/2017 – 16/02/2016	ALFF Mid Term Review Meeting, UKON, Konstanz, Germany
3/07/2017 – 7/07/2017	ALFF Workshop – Bioinformatics, VIB, Gent, Belgium
20/09/2017 – 22/09/2017	ALFF Workshop - “Eukaryotic diversity, phylogeny, and evolution“, University of Ostrava, Ostrava, Czech Republic
14/05/2018 – 18/05/2018	ALFF Workshop - Algal Research for Policy-Making and Biotech (ARPMB), SAMS, Oban, Scotland

List of publications

1. Cirri, E., Grosser, K., and Pohnert, G. (2016). A solid phase extraction based non-disruptive sampling technique to investigate the surface chemistry of macroalgae. *Biofouling*, 32(2), 145-153.
2. Cirri, E., and Pohnert, G. (2017). Disruption-free solid phase extraction of surface metabolites from macroalgae. *Protocols for Macroalgae Research*, 20, 311-321.
3. Cirri, E., Vyverman, W., and Pohnert, G. (2018). Biofilm interactions—bacteria modulate sexual reproduction success of the diatom *Seminavis robusta*. *FEMS microbiology ecology*, 94(11), fiy161.
4. Cirri, E., and Pohnert, G. Algae-bacteria interactions that balance the planktonic microbiome. *The New Phytologist*. Under revision.
5. Cirri, E.*, De Decker, S.*, Bilcke, G., Osuna, C., Werner, M., Werz, O., Van Delpoole, K., De Veylder, L., Vyverman, W., Pohnert, G. Associated bacteria affect sexual reproduction by altering gene expression and metabolic processes in a biofilm inhabiting diatom. Submitted to *Molecular Ecology*.
6. Cirri, E.*, Giraldo, J.*, Neupane, S., Willems, A., Mangelinckx, S., Roef, L., Vyverman, W., Pohnert, G. Bacteria isolated from *Seminavis robusta* influence growth, biofilm production and the metabolome of *Nannochloropsis* sp. Submitted to *Algal Research*.
7. Stock, F.*, Cirri, E.*, Nuwanthi, S., Uberschaar, N., Mangelinckx, S, Pohnert, G., Vyverman, W. Sampling, separation and quantification of N-acyl homoserine lactones from intertidal biofilms. In preparation.

*Authors equally contributed to the publication

Manuscripts 1, 2, 3, 4 and 5 were adapted and used for this thesis.

Emilio Cirri

Jena,

Selbstständigkeitserklärung

Hiermit erkläre ich, dass ich die vorliegende Arbeit selbstständig und unter Verwendung der angegebenen Hilfsmittel, persönlichen Mitteilungen, und Quellen angefertigt habe.

Emilio Cirri

Jena, den